MECHANISM AND FUNCTION OF ALDOSTERONE INDUCTION OF ENDOTHELIN-1 IN RENAL COLLECTING DUCT CELLS

By

LISA REBECCA STOW

A DISSERTATION PRESENTED TO THE GRADUATE SCHOOL
OF THE UNIVERSITY OF FLORIDA IN PARTIAL FULFILLMENT
OF THE REQUIREMENTS FOR THE DEGREE OF
DOCTOR OF PHILOSOPHY

UNIVERSITY OF FLORIDA

2009

To my hero, my grandfather, George C. Stow

ACKNOWLEDGMENTS

I would like to express my gratitude to my doctoral mentor, Dr. Charles Wingo, for his guidance during my dissertation work. Thank you for your commitment to my education. I would also like to express my gratitude to the members of my dissertation committee, Dr. Brian Cain, Dr. Chris Baylis, and Dr. Peter Sayeski. Their advice was crucial in the development and success of this project.

I would also like to thank the American Heart Association for awarding me with a predoctoral fellowship that funded a major portion of my dissertation work. I would also like to thank the other members of my lab including Dr. Michelle Gumz for her support and friendship. A special "thank you" goes to Ms. Jeanette Lynch for the many hours of technical assistance during the majority of the animal studies presented here. I also thank Ms. Alicia Rudin and Ms. Megan Greenlee for their technical support and friendship.

I would not have made it to the finish line without the love and support of my friends and family. Thank you Mom, for being my best friend and my biggest fan. Another big thanks goes to my fiancé, Dr. Marc Bailly, for his encouragement and love. Marc is also a scientist and has given me a tremendous amount of scientific and moral support. Marc was also kind enough to assist me in the preparation of the figures that appear in this document. Thank you!

But most of all, I want to thank my grandfather, George C. Stow. I admired my grandfather greatly and I have chosen to dedicate my dissertation to him for many reasons. He was a World War II veteran that enlisted as a paratrooper in the United States Army. This decision caused him to leave his family, forfeit his admission to medical school and ultimately left him a wounded veteran. The title "American hero" is used so often that it almost seems cliché. However, when I think of the sacrifice my grandfather made to save the lives of others I realize that it was nothing short of heroic. Without the selfless bravery of men and women like

my grandfather I may not have had the opportunity to live a free and peaceful life, nor may I had the opportunity to pursue a doctorate of philosophy in science. For these reasons, I am forever grateful.

I knew my grandfather as a patient and quiet man. He had the kind of wisdom that could only be acquired through decades of experience. He was an avid reader, a wine enthusiast, a dog lover and a gardener. He was also a chemist. In many ways, it was his infectious passion for knowledge and his inquisitive appreciation of the natural world inspired me to pursue a scientific career. In an effort to share with me some of his knowledge, my grandfather gave me many books. He would write inspiring messages and quotes from famous philosophers inside the cover of each book to encourage me to seek an education, believe in myself and follow my dreams. It is only now that I truly appreciate how amazing of a gift it is to have his words of advice in indelible ink inside books filled with information he thought was interesting or valuable.

I will always be grateful for the lessons my grandfather taught me. He will always be my hero and the greatest man I've ever known. Although he is no longer with us, I hope that somehow, someway I made him proud today.

TABLE OF CONTENTS

LIST OF TABLES

LIST OF FIGURES

Abstract of Dissertation Presented to the Graduate School
of the University of Florida in Partial Fulfillment of the
Requirements for the Degree of Doctor of Philosophy

MECHANISM AND FUNCTION OF ALDOSTERONE INDUCTION OF ENDOTHELIN-1 IN THE RENAL COLLECTING DUCT

By

Lisa Stow

December 2009

Chair: Charles S. Wingo
Major: Medical Sciences
Concentration: Physiology and Pharmacology

This dissertation will focus on the function and mechanism of interaction between two hormones that regulate renal sodium transport; aldosterone and endothelin-1 (ET-1). Data presented in this work demonstrate that the ET-1 peptide was stimulated by aldosterone in rat inner medulla *in vivo* and the ET-1 gene (*edn1*) was stimulated by aldosterone in acutely isolated rat inner medullary collecting duct cells *ex vivo* and in mouse cortical, outer medullary, and inner medullary collecting duct cells *in vitro*. Mechanistic studies revealed that aldosterone directed the transcription of the *edn1* promoter through two hormone response elements that bound both the mineralocorticoid receptor (MR) and the glucocorticoid receptor (GR). These hormone receptors mediated the association of chromatin remodeling complexes, histone modification, and RNA polymerase II at the *edn1* promoter. A synthetic glucocorticoid was able to replicate aldosterone action on *edn1* through the exclusive action of GR. Preliminary functional studies indicated that *edn1* knockdown altered normal mRNA expression patterns for two aldosterone response genes, *sgk1* and *scnn1a*. Direct interaction between aldosterone and ET-1 has important implications for renal and cardiovascular function.

CHAPTER 1
INTRODUCTION AND OVERVIEW

The Kidneys

General Functions

The kidneys are a pair of highly specialized organs that filter the blood and produce urine. Because of their function, the kidneys receive an impressive 1700 liters (L) per day of blood or roughly 20 percent (%) of the cardiac output (Williams and Leggett, 1989). Proper renal function is essential for numerous processes including fluid and electrolyte homeostasis, acid-base balance, maintenance of systemic arterial blood pressure, and excretion of metabolic waste and toxic bioactive substances (Brenner and Rector, 2008).

The human body is continuously accumulating metabolic waste products such as urea, uric acid, and creatinine. These waste products, along with other toxic substances, are removed from the circulation by the kidneys or the liver. The kidney is a vital organ and patients in kidney failure cannot live without blood or peritoneal dialysis or renal transplantation that facilitates the removal of these toxic waste products. Other functions of the kidneys include bioactive metabolism and gluconeogenesis (Marsenic, 2009). The kidneys participate in several biosynthetic pathways including the synthesis of active vitamin D (1,25-dihydroxyvitamin D3) (Dusilova-Sulkova, 2009; Michigami, 2007) and the production of erythropoietin (Jacobson et al., 1957; Lemke and Muller, 1989). Erythropoietin is an important hormone that stimulates the bone marrow to increase red blood cell production, which is known as erythropoesis. Indeed, anemia is often present in patients in renal failure.

The kidneys possess transport mechanisms for various mineral ions, organic ions, amino acids and metabolites (Brenner and Rector, 2008). Renal transport mechanisms also play a fundamental role in the maintenance of water (H_2O) and sodium (Na^+) homeostasis. H_2O and

Na^+ balance is ultimately important due to the direct impact on extracellular fluid volume and blood pressure. The work presented in this dissertation will focus on the function and mechanism of interaction between two hormones that affect blood pressure through the regulation of renal Na^+ transport, aldosterone and endothelin-1 (ET-1).

The Role of the Kidneys in Blood Pressure Control

The kidneys participate in several integrated physiological mechanisms that modulate blood pressure. Ultimately, these renal mechanisms converge on one of the two key factors that determine blood pressure, cardiac output and systemic vascular resistance (Guyton, 1981; Luetscher et al., 1973). The kidneys produce various vasoactive substances that modulate total vascular resistance such as prostaglandins (Schulz et al., 1995), nitric oxide (Ito, 1995), ET-1 (Kohan and Fiedorek, 1991), and angiotensin II (Ang II). The kidneys also control mechanisms that determine the concentration of potassium (K^+) in the body, and K^+ participates in the repolarization of the myocardium to ensure normal cardiac contractile function (Walker et al., 1964). However, the kidneys primarily function in the maintenance of blood pressure by controlling blood volume, which is a primary determinant of cardiac output. The kidneys control blood volume through the regulation of Na^+ and H_2O homeostasis. The following sections will present the anatomy of the kidney followed by a discussion of the important transport processes for Na^+ and H_2O that occur in the different regions of the kidney.

Gross Anatomy

The kidneys are located in the retroperitoneal cavity and normally receive blood flow from a single renal artery. A bisected kidney is divided into two distinct regions: the renal cortex and the renal medulla (Figure 1-1, left panel). In humans, the medulla is organized into 8-18 conical masses referred to as renal pyramids that each extend toward the renal pelvis to form a papilla (Preuss, 1993). In comparison, many small laboratory animals including rodents have kidneys

with only one renal pyramid and one papilla (Dunn, 1949). Blood flow from the renal artery passes into smaller lobar arteries and eventually flows into a capillary bed known as a glomerulus. The glomerular capillary bed is unique because it has both upstream and downstream resistance vessels known as afferent and efferent arterioles. Each glomerulus represents a single filtration unit of the kidney and is located inside a structure called the Bowman's capsule. Together, the glomerulus and Bowman's capsule comprise a structure known as the renal corpuscle. Blood plasma is filtered across the glomerulus and the primary filtrate collects in the Bowman's space where it flows into the lumen of the nephron and the adjoining tubule structure called the collecting duct. The nephron and collecting duct receive blood flow from peritubular capillaries. In humans, collecting ducts drain into funnel-like calyces that surround each of the renal pyramids. In unipapillated animals, collecting ducts drain directly into the renal pelvis. The final filtered product is the urinary output, which exits each kidney through a ureter that connects to the urinary bladder.

The Nephron and Collecting Duct System

The primary glomerular filtrate contains electrolytes, organic ions, glucose, amino acids, vitamins, and other small proteins that must be reabsorbed back into the circulation. This process of selective reabsorption occurs along the length of the nephron and collecting duct, which is comprised of a single epithelial cell layer that participates in the selective transport of water, electrolytes, and organic solutes. Each human kidney contains about one million nephrons (Gumz et al., 2009c; Preuss, 1993). In comparison, a rat kidney contains approximately 30,000 nephrons (Corman et al., 1985).

Each nephron includes a renal corpuscle, the proximal tubule, thin descending limb, thick ascending limb, distal tubule, and connecting tubule (Figure 1-1, right panel). The initial region of the nephron is called the proximal convoluted tubule, which connects to the proximal straight

tubule typically at the corticomedullary junction before transitioning into the loop of Henle. Mammalian kidneys have nephrons with both long and short loops of Henle depending on the location of the originating glomerulus (Brenner and Rector, 2008). The majority of nephrons in humans and rodents have short loops of Henle with a thin limb that curves back into the thick ascending limb in the outer medulla. Alternatively, long nephrons typically originate from juxtamedullary glomeruli and have a descending thin limb that extends deep into the inner medulla. These inner medullary thin limbs eventually transition into a thin ascending limb and subsequently a thick ascending limb of Henle in the outer medulla. The thick ascending limb returns the filtrate back into the cortex where specialized macula densa cells of the tubule run adjacent with the source glomerulus at a specialized region called the juxtaglomerular apparatus. Following the juxtaglomerular apparatus, the cortical thick ascending limb has an abrupt transition to the distal convoluted tubule and subsequently the connecting segment, the terminal region of the nephron. Each nephron drains into a collecting duct system that consists of cortical, outer medullary, and inner medullary collecting ducts. Collecting ducts have a different embryonic origin than the nephron, however they are also composed of a single epithelial cell layer involved in tubular transport. The collecting duct epithelium is composed of two major cell types known as principal cells and intercalated cells (Madsen et al., 1988). Each cell type has distinct functional and morphological properties. Intercalated cells have a low cellular profile in the tubule lumen and are thought to mediate transport involved in acid-base balance (Clapp et al., 1987). Principal cells are tall with relatively few organelles and function in Na^+ and H_2O reabsorption. The following sections will focus on how the kidneys regulate Na^+ homeostasis starting with the formation of the glomerular ultrafiltrate and continuing with a detailed description of Na^+ transport mechanisms in different regions in the tubule.

Formation of the Tubular Ultrafiltrate

Tubular transport is highly dependent on the composition and the rate of formation of the primary filtrate entering the nephron. This initial filtrate is formed by a process called glomerular filtration, which is the movement of blood plasma across the glomerular capillary wall into the Bowman's space (Thomson and Blantz, 2008). Three adjacent layers form the filtration barrier: the fenestrated endothelium of the glomerular capillary, the glomerular basement membrane, and the slit diaphragm of the surrounding podocytes (Haraldsson et al., 2008; Jarad and Miner, 2009). This filtration barrier has both charge and size selective properties that restrict the passage of molecules that are too negatively charged or larger than 8 nanometers (nm). As a result, the normal filtration barrier is completely impermeable to molecules larger than 70 kilodaltons (kDa), whereas molecules smaller than 7 kDa are freely filtered. Substances between 7 and 70 kDa or 4 and 8 nm in diameter have variable filterability (Haraldsson and Jeansson, 2009). For example, albumin has molecular weight of 66 kDa and a diameter of 7 nm, however, less than 0.02% of albumin is filtered due to its negative charge (Jarad and Miner, 2009). In contrast, mineral ions and organic solutes are small and freely filtered irrespective of their charge.

The concentration of freely filtered substances, like Na^+, in the primary ultrafiltrate is called the filtered load and is directly proportional to glomerular filtration rate (GFR). The tubule reabsorbs approximately the same percentage of filtered Na^+ in a process referred to as glomerulotubular balance. Consequently, changes in GFR are reflected by changes in net Na^+ excretion. Neurohumoral factors that control GFR also influence Na^+ homeostasis and will be discussed in further detail in the section **Regulation of Renal Sodium Transport**.

Primary determinants of GFR include the permeability of the glomerular capillaries, the glomerular filterable surface area, and the net filtration pressure (Brenner and Rector, 2008).

The product of glomerular capillary permeability (i.e., hydraulic conductivity) and the effective filtration surface area is known as the glomerular ultrafiltration coefficient (K_f). Net filtration pressure is determined is the sum of hydrostatic pressures (P) and oncotic pressures (π) on either side of the glomerular filtration barrier known as Starling forces (Starling, 1899). Net hydrostatic and oncotic pressures are determined by the difference between the pressure in the glomerular capillary (P_{GC} or π_{GC}) and the pressure in the tubule (P_T or π_T). Taken together, GFR is calculated for each nephron by the following equation: $GFR = K_f * [(P_{GC} - P_T) - (\pi_{GC} - \pi_T)]$ (Brenner and Rector, 2008).

GFR is tightly maintained in a healthy individual and GFR measurement is the most important clinical indicator of renal function (Brenner and Rector, 2008). The glomerulus possesses both upstream (afferent) and downstream (efferent) vascular resistance vessels to autoregulate glomerular perfusion pressure and maintain a relatively constant GFR over a large range of arterial blood pressures (Cupples, 2007; Haraldsson et al., 2008). A normal GFR is 125 ml/min or 180 L/day (Brenner and Rector, 2008). At this rate, a human would excrete their entire blood volume in a matter of minutes. However, an average person produces only 1 L/day of urine (Brenner and Rector, 2008). This means that the renal nephrons and collecting ducts have the daunting task to reabsorb greater than 99% or 179 L of tubular fluid everyday.

Mechanisms of Renal Sodium Transport

Na^+ constitutes over 90% of the osmotically active solute in the blood plasma and extracellular fluid (140 milliequivalents (mEq)/L) (Gumz et al., 2009c). Consequently, the reabsorption of Na^+ is critical to the maintenance of extracellular fluid volume and blood pressure. This process of Na^+ reabsorption occurs along the length of the nephron and collecting duct and is summarized in Table 1-1 (Gumz et al., 2009c). The universal driving force for Na^+ reabsorption is generated by the activity of the basolateral Na^+/K^+ adenosine triphosphatase

pump (Na^+/K^+-ATPase). For every ATP three Na^+ ions are pumped into the interstitial fluid in exchange for two K^+ ions pumped into the cell. This uneven stoichiometry produces an intracellular negative charge and contributes to the generation of the electrochemical gradient that favors Na^+ reabsorption. However, the net transport of Na^+ is accompanied by an anion and a water molecule and is therefore, electro-neutral. The major anions coupled to Na^+ are chloride (Cl^-) and bicarbonate (HCO_3^-), which are present in the extracellular fluid at 110 and 24 mEq/L, respectively (Eaton and Pooler, 2004). The kidneys typically reabsorb between 96% and greater than 99% of the filtered Na^+. The vast majority of this Na^+ is reabsorbed in the proximal tubule and thick ascending limb of Henle; while less than 10% of the total filtered load of Na^+ is reabsorbed in the distal nephron and collecting duct. Relatively small changes in Na^+ reabsorption can lead to large changes fluid transport and a concomitant increase or decrease in extracellular fluid volume. Therefore, the transport mechanisms in the distal nephron and collecting duct are ideal targets for controlling the "fine-tuning" of Na^+ reabsorption. Indeed, most hormonal, paracrine and neuronal regulatory mechanisms converge on this region of the tubule to achieve homeostatic adjustments in Na^+ balance.

Sodium Transport in the Proximal Tubule

The proximal tubule is responsible for reabsorbing the bulk of the glomerular ultrafiltrate including greater than 60% of Na^+, 80% of HCO_3^- and virtually all of the organic compounds that are filtered at the glomerulus (Brenner and Rector, 2008). To accommodate this immense transport capacity, proximal tubule cells have apical microvilli that increase the absorptive surface area and give the cells their characteristic "brush border." As depicted in Figure 1-2, proximal tubule cells have both active transcellular and passive paracellular Na^+ transport mechanisms. The transcellular electrochemical gradient favors Na^+ reabsorption, and Na^+ absorption transport is often coupled to the movement of glucose, amino acids, phosphate,

sulfate, and organic molecules including lactate, acetoacetate, β-hydroxybutyrate, and tricarboxylic acid cycle intermediates such as α-ketoglutarate, succinate and citrate. However, the predominant mechanism for Na^+ reabsorption in the proximal tubule is via apical Na^+/H^+ exchange (NHE) (Burckhardt et al., 2002).

The activity of NHE results in the reabsorption of one Na^+ ion in exchange for the extrusion of one H^+ into the lumen (Figure 1-2). Intracellular Na^+ ions are then pumped back into the interstitial space by basolateral Na^+/ K^+-ATPase and Na^+/ HCO_3^- -cotransport (NBC). In fact, proximal tubule Na^+ reabsorption is closely associated with net HCO_3^- reabsorption and is important for proper acid-base balance. As shown in Figure 1-2, tubular (type IV) and cytosolic (type II) carbonic anhydrases link transport by apical NHE to basolateral NBC and result in net reabsorption of $NaHCO_3$.

The tight junctions of the proximal tubule are particularly permeable to Na^+ and Cl^- ions. In the early proximal tubule the lumen has a net negative charge. This negative potential difference between the lumen and interstitial fluid drives the paracellular movement of Cl^- from the tubule lumen to the interstitium. As a result of luminal Cl^- removal, the lumen potential difference changes from negative to positive in the mid- to late- portions of the proximal tubule. Under these conditions the electrical gradient drives paracellular diffusion of Na^+ ions. In addition, the removal of $NaHCO_3$ from the tubular lumen serves to increase the concentration of luminal Cl^- and shifts the concentration gradient for Cl^- and the electrical gradient for Na^+ to favor passive paracellular reabsorption in the late proximal tubule.

Sodium Transport in the Limb of Henle

The loop of Henle participates in the renal countercurrent system, which functions to concentrate the urinary output. To generate the countercurrent system the descending and ascending limbs of Henle transport water and electrolytes in separate regions. This unique

property of the loop of Henle generates a hypertonic medullary interstitium; which, in turn, determines the capacity of downstream water transport in the collecting duct and the overall urinary concentrating ability of the kidney.

The majority of the transport in the thin limb of Henle is passive. As tubular fluid moves from the proximal tubule to the thin descending limb the epithelial tight junctions become less permeable to Na^+ and Cl^-. However, these cells are particularly permeable to H_2O and facilitate passive H_2O reabsorption. Consequently, the osmolality of the tubular fluid progressively increases as it moves toward the renal papillary tip. In contrast to the descending limb, the thin ascending limb has low H_2O permeability, but a very large Na^+ and Cl^- permeability. Consequently, Na^+ and Cl^- are passively reabsorbed along the ascending thin limb. Although the electrolyte transport in the thin ascending limb participates in the countercurrent multiplier, the overall quantity of Na^+ reabsorbed in this region remains relatively small. The majority of Na^+ reabsorbed in the loop of Henle takes place in the thick ascending limb.

The thick ascending limb is responsible for reabsorbing greater than 25% of the filtered load of Na^+ through both active transport and passive paracellular diffusion (Figure 1-3) (Gumz et al., 2009c). Active Na^+ transport in these cells is coupled to the reabsorption of K^+ and Cl^- via the action of the electro-neutral Na^+-K^+-2Cl^--cotransporter (NKCC2) (Gamba et al., 1994). Reabsorbed Na^+ is pumped across the basolateral membrane by the ubiquitous Na^+/K^+-ATPase. Basolateral Cl^- channels (ClC-Kb) facilitate electrogenic Cl^- efflux into the interstitial fluid (Estevez et al., 2001). Additionally, the electrogenic Cl^- gradient is used to cotransport Cl- and K^+ on a basolateral K^+/Cl^- symporter (KCC) (Greger, 1985). The activity of NKCC2 is dependent on K^+ recycling at the apical membrane via ROMK channels (Wang, 2006). In addition, apical K^+ recycling via ROMK, in combination with basolateral ClC-Kb channels,

generates a lumen positive charge. This positive transepithelial potential difference serves to drive a significant amount of passive paracellular diffusion of Na^+. Loss of function of NKCC2, ROMK, or CIC-Kb results in Bartter's syndrome, which is characterized by chronic Na^+ wasting, hypokalemia and hypovolemia with activation of renin and aldosterone without hypertension (Lang et al., 2005; Unwin and Capasso, 2006).

In addition to mediating bulk Na^+ reabsorption, the thick ascending limb also mediates tubuloglomerular feedback (TGF) in specialized macula densa cells in the cortical thick ascending limb (Schnermann, 1998). Furthermore, the thick ascending limb also has an important role to generate a medullary osmotic gradient that is required to concentrate the urinary output (Gottschalk and Mylle, 1958). Similar to the thin ascending limb, the thick ascending limb remains impermeable to H_2O. As a result, active NaCl reabsorption via NKCC2 causes the luminal fluid to become hypotonic, which is a key determinant of downstream H_2O transport in the collecting duct (Sands and Layton, 2009). A larger medullary osmotic gradient decreases the osmolality of the tubular fluid leaving the thick ascending limb and proportionally increases downstream H_2O reabsorption in the collecting duct. Pharmacological blockade of NKCC2 with furosemide or bumetanide prevents the generation of the medullary osmotic gradient and reduces downstream H_2O transport leading to a diuresis. Clinically, these inhibitors are referred to as "loop diuretics" (Shankar and Brater, 2003).

Sodium Transport in the Distal Convoluted Tubule

By the time the filtrate enters the distal convoluted tubule greater than 90% of the filtered Na^+ has been reabsorbed (Gumz et al., 2009c). The role of the distal convoluted tubule, along with the downstream connecting segment and collecting duct system, is to reabsorb the precise amount of remaining Na^+ to maintain whole body Na^+ and fluid homeostasis. Not surprisingly,

Na^+ transport processes in these regions of the renal tubule are subject to numerous regulatory factors (Bhalla and Hallows, 2008; Meneton et al., 2004; Zeidel, 1993).

The major Na^+ transport mechanism in the distal convoluted tubule is the apical Na^+/Cl^- cotransporter (NCC) (Figure 1-4) (Gamba et al., 1994; Gumz et al., 2009c). Reabsorbed Na^+ is pumped through the basolateral Na^+/K^+-ATPase, while Cl^- exits via KCC or basolateral Cl^- channels. Blockade of NCC with thiazide diuretics, a first line treatment for clinical hypertension, results in an increase in excretion of Na^+ and H_2O in the urine, processes referred to as natriuresis and diuresis, respectively (Salvetti and Ghiadoni, 2006). Evidence also exists that the distal convoluted tubule expresses other Na^+ reabsorptive mechanisms such as apical NHE2 (Chambrey et al., 1998) and apical epithelial Na^+ channels (ENaC) (Loffing et al., 2000). ENaC is an important target of aldosterone, a mineralocorticoid hormone that acts to increase Na^+ reabsorption and blood pressure, and will be discussed in further detail below.

Sodium Transport in the Collecting Duct

The collecting duct is the terminal site for regulated fluid and electrolyte transport by the kidney. The collecting duct is composed of principal cells and intercalated cells that each specialize in different types of solute transport. Na^+ transport occurs in principal cells and is primarily mediated by apical ENaC and the basolateral Na^+/K^+-ATPase pump (Figure 1-5) (Loffing et al., 2000; Masilamani et al., 1999). In the collecting duct principal cell, H_2O is also transported and occurs almost exclusively through the coordinated action of apical and basolateral aquaporin (AQP) channels (Nielsen et al., 2002). The apical AQP isoform is AQP2 and the basolateral AQP isoforms include both AQP3 and AQP4. Most notably, the expression of apical AQP2 is directly controlled by antidiuretic hormone (ADH, also known as arginine vasopressin). ADH is formed in the hypothalamus and transported to the pituitary gland where it is released in response to hyperosmolality, hypotension, hypovolemia, and other factors such as

angiotensin II (Ang II) (von Bohlen und Halbach and Albrecht, 2006). Following release, ADH activates vasopressin 2 (V_2) receptors in the collecting duct that mediate the insertion of AQP2 channels into the apical membrane. The basolateral exit pathway for H_2O is mediated by AQP3 and AQP4 channels (Nielsen et al., 2002).

Collecting duct Na^+ transport also influences the transport of K^+ and Cl^-. In the traditional view, net Na^+ reabsorption generates a lumen negative potential difference to drive paracellular Cl^- reabsorption in addition to active Cl^- transport in adjacent intercalated cells. This lumen-negative potential difference promotes luminal K^+ secretion via apical K^+ channels (Koeppen et al., 1983; Sansom et al., 1984; Stokes, 1981). However, Cl^- reabsorption can occur in the absence of basolateral Na^+/K^+-ATPase activity, which is required to maintain the lumen negative potential difference that drives Cl^- transport in the classical model (Wingo, 1989a, b; Zhou et al., 1998). Moreover, the electro-neutral apical secretory pathway for K^+ is highly dependent on Cl^- and is consistent with the actions of an apical K^+/Cl^- cotransporter (Wingo, 1989b) (Figure 1-5).

The movement of Na^+ through ENaC is passive as the ion moves down its electrochemical gradient generated by the basolateral Na^+/K^+-ATPase pump. ENaC is a heterotrimeric membrane channel consisting of α, β, and γ subunits transcribed from three individual genes, *scnn1a*, *scnn1b* and *scnn1g*, respectively (Bhalla and Hallows, 2008). The importance of ENaC is emphasized by fact that activating mutations in the genes that encode for βENaC or γENaC (*scnn1b* or *scnn1g*) result in a severe hypertensive phenotype called Liddle's syndrome (Lang et al., 2005; Martinez-Aguayo and Fardella, 2009). In contrast, inactivating mutations in αENaC, βENaC, or γENaC (*scnn1a*, *scnn1b*, or *scnn1g*) cause pseudohypoaldosteronism type I, which is a severe Na^+ wasting syndrome associated with hyperkalemia and metabolic acidosis (Riepe, 2009). Undoubtedly, renal Na^+ transport and blood pressure are closely related. In the collecting

duct, the expression of αENaC (*scnn1a*) represents the rate-limiting step for forming an active channel. However, ENaC is further regulated by mechanisms that control the channel activity as well as the cellular localization and proteasomal degradation of ENaC.

Regulation of Renal Sodium Transport and Blood Pressure

Compounds that inhibit renal Na^+ transport represent a major class of antihypertensive drugs. In fact, hypertensive drugs are the most commonly prescribed drugs in the world as hypertension is estimated to affect over 1 billion people worldwide (Kearney et al., 2005). Although cardiovascular and renal control of blood pressure has been described, the mechanisms driving hypertension are poorly understood. Indeed, greater than 90% of hypertensive patients are diagnosed with essential hypertension, for which there is no known cause (Binder, 2007). Most of the known etiologies of hypertension such as renovascular disease, hyperaldosteronism and gene mutations, converge on the kidney. Indeed, most forms of chronic kidney disease regardless of the primary etiology result in secondary hypertension. Not surprisingly, the numerous hormonal, neuronal, and paracrine mechanisms that modulate renal Na^+ transport are of particular importance for blood pressure control. Aberrations in any of these mechanisms can lead to pathological changes in blood pressure. A relationship between systemic arterial pressure and renal Na^+ excretion also exists and is known as the phenomenon of pressure natriuresis (Guyton, 1991). Normally, an increase in arterial blood pressure ultimately results in an increase urinary H_2O and Na^+ excretion that minimizes the increase in blood pressure (Guyton et al., 1972). In general, small changes in total body Na^+ content can lead to large changes in extracellular fluid volume and blood pressure. Consequently, most factors that control Na^+ balance affect renal Na^+ absorption mechanisms in the distal nephron and collecting duct.

Glomerular Filtration Rate

When GFR changes the kidney responds by adjusting the net rate of Na^+ excretion. This phenomenon is defined as glomerulotubular balance. Changes in GFR are achieved by alterations in factors that affect either glomerular ultrafiltration coefficient (K_f) or the net filtration pressure (Brenner and Rector, 2008; Vallon, 2003). Glomerular mesangial cells have the ability to influence K_f due to their intrinsic contractile properties. Increased mesangial tone can result in a decrease in glomerular filtration surface area and a consequent decrease in GFR. The inverse is also true, and factors that relax mesangial cells can result in an increase in GFR and net Na^+ filtration. A change in net glomerular filtration pressure is typically a consequence of a change in P_{GC} due to afferent and efferent arteriole vascular resistances. However, the control of GFR through the modulation of arteriole vascular tone is complex. For example, preferential vasoconstriction of the efferent arteriole can lead to an increase in P_{GC} and GFR. Conversely, vasoconstriction of the afferent arteriole or both the afferent and efferent arterioles results in a decreased P_{GC} and a decrease in GFR.

The control of both K_f and arteriole vascular tone is dynamic and involves various signaling molecules. The sympathetic nervous system plays an important role in controlling arteriole vascular tone. In fact, endogenous catecholamines, (norepinephrine, epinephrine, and dopamine) have important roles in both the tonic and phasic regulation of renal vascular tone. Norepinephrine, along with Ang II and ET-1, all result in potent vasoconstriction of both afferent and efferent arterioles. Consequently, these factors lead to a decrease in GFR and Na^+ and fluid retention. Ang II and ET-1 preferentially constrict the efferent arteriole. Factors that decrease the vascular tone of both arterioles include nitric oxide, dopamine, acetylcholine, prostaglandin E2, and prostacyclin. Furthermore, some hormones such as bradykinin and adenosine have no reported effects on the afferent arteriole while they selectively relax the efferent arteriole. Under

these conditions, net glomerular filtration pressure will decrease due to decreased hydrostatic pressures in the glomerular capillaries.

Tubuloglomerular Feedback

Another important feature of renal Na^+ transport is the process by which an individual nephron autoregulates its own blood flow and GFR. This process is called tubuloglomerular feedback (TGF) and occurs in the juxtaglomerular apparatus that is composed of specialized macula densa cells, extra-glomerular mesangial cells, and specialized renin-secreting cells of the afferent arteriole. Macula densa cells sense the composition of the filtrate delivered to the distal nephron by sensing the transport of ions through the apical NKCC2. A change in transport at the macula densa results in inverse changes on renin release and GFR. In the current model (Vallon, 2003), an increase in NKCC2 activity results in an increase in adenosine production and consequent adenosine A1 receptor activation on the adjacent extra-glomerular mesangial cells. This is followed by an increase in intracellular calcium and calcium currents that inhibit the release of renin and vasoconstriction of the afferent arteriole. The latter effect immediately decreases RBF and GFR. The secretion of renin activates the renin-angiotensin system and results in decreased Na^+ excretion as discussed in detail below.

Natriuretic Signals

Various natriuretic signals act in the kidney including nitric oxide, prostaglandin and natriuretic peptides. Brain natriuretic peptide and atrial natriuretic peptide are produced by the heart and have both vascular and tubular action in the kidney (Martinez-Rumayor et al., 2008). These peptides act to vasodilate the afferent arteriole to increase GFR as well as inhibit classical Na^+ retaining mechanisms such as renin release and Ang II production. Other hormones that have reported natriuretic properties include glucagon (Gutzwiller et al., 2006), progesterone (Oparil et al., 1975), and parathyroid hormone (Agus et al., 1973).

Antinatriuretic Signals

Antinatriuretic signals act to increase renal Na^+ reabsorption. The most important hormone pathway is the renin-angiotensin pathway and the consequent induction of aldosterone. These hormones will be described in detail below. Other well-known hormones that stimulate Na^+ reabsorption include cortisol, estrogen, growth hormone, thyroid hormone and insulin. Net Na^+ reabsorption in the collecting duct can also be stimulated indirectly by ADH; a hormone that acts to increase the H_2O permeability of the cortical and medullary collecting ducts and decrease net renal H_2O excretion. Notably, ADH and aldosterone act in coordination to preserve blood volume and blood pressure during volume depletion.

Renin-Angiotensin-Aldosterone System

A central theme in the regulation of renal Na^+ balance and blood pressure is the activation of the renin-angiotensin-aldosterone system. Indeed, the vast majority of inheritable monogenetic hypertension results from a defect in this pathway (Martinez-Aguayo and Fardella, 2009). The two major effectors of this pathway are aldosterone and Ang II. Ang II is the biologically active eight amino acid peptide that mediates an increase in blood pressure through its action on the vasculature as well as renal epithelium. Renin is a monospecific aspartyl proteolytic enzyme that is synthesized and secreted from specialized afferent arteriole cells of the juxtaglomerular apparatus. Renin is responsible for the conversion of angiotensinogen into the ten amino acid peptide angiotensin I (Ang I). Angiotensin converting enzyme (ACE) then converts Ang I into Ang II. ACE is predominantly localized to the lungs; however, it is also widely expressed on the luminal surface of vascular endothelial cells. The later enzymatic reaction occurs freely, consequently the synthesis and secretion of renin is the rate-limiting step in the production of Ang II. Renin is released in response to various stimuli including a decrease in afferent arteriole pressure and a decrease in NaCl delivery to the macula densa (via TGF).

Ang II has multiple actions that modulate renal Na^+ excretion and increase blood pressure. Ang II binds to angiotensin 1 (AT1) receptors to produce potent vasoconstriction of both afferent and efferent arterioles, as well as systemic resistance vessels (Mehta and Griendling, 2007). AT1 receptor activation is also indicated in Ang II-dependent cardiac remodeling. Furthermore, Ang II acts on the brain to stimulate ADH release from the pituitary gland, as well as to stimulate thirst centers. Ang II further potentiates the vasoconstrictive effect by stimulating norepinephrine release from sympathetic nerves. In fact, AT1 receptor blockers (ARBs) and ACE inhibitors are two major classes of antihypertensive drugs that are used clinically (Izzo et al., 2008). Ang II also has a well-known and very important role in stimulating the adrenal cortex to release aldosterone, a steroid hormone with important actions to control renal Na^+ transport and fluid homeostasis (Blair-West et al., 1963; Ganong et al., 1966).

The Aldosterone System

Aldosterone was originally identified in the early 1950s as key physiological hormone that participates in the conservation of salt and minerals; hence the name "mineralocorticoid" (Grundy et al., 1952; Simpson SA, 1953). In addition to Ang II, aldosterone is released in response so several other stimuli including stimulation by pituitary hormone and adenocorticotropic hormone (ACTH) (Romero et al., 2007; Spat and Hunyady, 2004). Once released, aldosterone acts on certain polarized epithelial cells, including the principal cells of the distal nephron and collecting duct, to increase Na^+ reabsorption. In general, the action of aldosterone is mediated through the mineralocorticoid receptor (MR); a ligand-dependent transcription factor responsible for orchestrating the transcription of genes involved in transepithelial Na^+ transport (Fuller, 2004). The response to aldosterone is generally biphasic characterized by both an early and late response (Gaeggeler et al., 2005). The early response is predominantly transcriptional, whereas the late response involves an increase in Na^+ transport. In

addition, several lines of evidence suggest that aldosterone can also mediate rapid, non-genomic effects via second messenger pathways that may or may not involve the activation of MR (Boldyreff and Wehling, 2003a; Harvey et al., 2008). The net effect of aldosterone is to couple the apical reabsorption of Na^+ by ENaC to the basolateral Na^+/K^+-ATPase. Indeed, increased plasma concentrations of circulating aldosterone can lead to inappropriate Na^+ retention and hypertension.

Classical Aldosterone Targets

A basic model of aldosterone action is shown in Figure 1-6. Aldosterone binds to and activates cytoplasmic MR. Ligand binding leads to a conformational change in MR and the release of chaperone heat shock proteins. This ligand-dependent conformation also reveals multiple nuclear localization signals and causes the receptor to undergo nuclear translocation and binding to the deoxyribonucleic acid (DNA) sequence of target genes to stimulate or repress transcription. Classical aldosterone induced genes include *scnn1a* (αENaC) (Sayegh et al., 1999), *atp1a1* (Na^+/K^+-ATPase α1) (Kolla et al., 1999), and *sgk1* (serum- and glucocorticoid- regulated kinase-1) (Loffing et al., 2001; Webster et al., 1993). Increasing the expression levels of ENaC and Na^+/K^+-ATPase will increase a cell's capacity to mediate electrogenic Na^+ transport.

Sgk1 is a serine/threonine kinase that is homologous to protein kinase B/Akt kinases and it is highly conserved across mammalian species (McCormick et al., 2005). Sgk1 functions to enhance Na^+ transport positively regulates the apical localization of ENaC and stimulates the channel open probability (Vallon and Lang, 2005). A major function of Sgk1 is to mediate the phosphorylation of ubiquitin ligase neural precursor cell-expressed developmentally downregulated (gene 4) protein (Nedd4-2) (Debonneville et al., 2001; Flores et al., 2005) (Figure 1-6). Nedd4-2 binds to and ubiquitinylates ENaC, which negatively controls ENaC surface expression and causes rapid ENaC turnover. However, phosphorylation of Nedd4-2 by Sgk1

creates a docking site for 14-3-3 adaptor protein and prevents Nedd4-2 from binding ENaC by steric hindrance. Blocking Nedd4-2 precludes ENaC ubiquitinylation, internalization, and degradation. Indeed, aldosterone stimulation results in enhanced apical membrane expression of all three ENaC subunits (Masilamani et al., 1999).

The Mineralocorticoid Receptor

Aldosterone action is predominantly mediated through MR at the level of transcription (Arriza et al., 1987). MR is a member of the nuclear receptor family that includes the estrogen, progesterone, androgen, and glucocorticoid receptor (GR). The MR gene (*nr3c2*) has eight coding exons and two untranslated exons. The first two exons are alternatively spliced from exon 1α or 1β (Arriza et al., 1987) (Figure 1-7). The gene codes for a 107 kDa protein with four distinct functional domains including an N-terminal domain (NTD), a DNA binding domain (DBD), a hinge region, and a ligand binding domain (LBD) (Figure 1-7). This structure is highly homologous to the well-characterized GR (Arriza et al., 1987) (Figure 1-9).

The action of MR is consistent with classical steroid receptors (Beato and Klug, 2000). In the absence of ligand, MR is located in the cytoplasm and is stabilized in an inactive conformation through the interaction of the LBD with several heat shock proteins (HSPs). Aldosterone binding leads to a conformational change in MR structure that causes the HSPs to be released and nuclear localization signals to be revealed. Aldosterone-bound receptors are transported into the nucleus as dimers where they bind directly to specific DNA regions known as hormone response elements (HREs). The DBD is 66 amino acids long and is highly conserved (>90% homology) among steroid receptors. This domain contains two zinc fingers that facilitate binding to an imperfect palindrome that is classically represented as the consensus sequence: 5'-GGTACAnnnTGTTCT-3' (Beato, 1989).

The hinge region is responsible for the interaction of the NTD and the LBD. Disruption of the interface between the NTD and LBD by spironolactone, an MR antagonist, prevents MR activity and demonstrates the functional importance of this interaction (Rogerson et al., 2003). The NTD is the only domain that displays a significant amount of diversity between steroid receptors. However, it is highly evolutionarily conserved across species (Pascual-Le Tallec and Lombès, 2005) indicating that the NTD houses important activation functions specific to MR. The NTD contains two transactivation domains (AF1a and AF1b) (Pascual-Le Tallec and Lombès, 2005) and numerous modification sites (Figure 1-7). AF1a and AF1b transactivation functions are generally thought to be ligand-independent, but recent evidence has revealed mineralocorticoid-selective AF1 activity as well.

The LBD also has a transactivation domain, AF2, which is formed and activated in a ligand-dependent, but not ligand-specific manner (i.e. both mineralocorticoids and glucocorticoids can activate AF2). The functional importance of AF2 is evident in patients suffering from type I pseudohypoaldosteronism due to naturally occurring missense mutations in the LBD (Pascual-Le Tallec and Lombès, 2005). AF2 is highly conserved among steroid receptors and is capable of interacting with several transcriptional coactivators, including the steroid receptor coactivator-1 (SRC-1). SRC-1 mediates the formation of the transcriptional preinitiation complex by the sequential recruitment of SWI/SNF chromatin remodeling complexes, histone-methyltransferases including CARM1 and PRTM1, and the histone acetylase cyclic adenosine monophosphate (cAMP) response element binding protein-binding protein (CBP/p300) (Li et al., 2005; Pascual-Le Tallec and Lombès, 2005).

Ligand specificity of the mineralocorticoid receptor

MR can bind both mineralocorticoids and glucocorticoids with approximately the same affinity (K_D = 0.5 nM and 0.7 nM, respectively) (Arriza et al., 1987). Na^+-transporting epithelia

confer aldosterone-selective MR activity largely by expression of 11β-hydroxysteroid dehydrogenase type II (11βHSD-2), which converts cortisol into inactive cortisone (Whorwood et al., 1994). Naturally occurring defects in 11βHSD-2 activity leads to Apparent Mineralocorticoid Excess, a syndrome characterized by severe hypertension (Mune et al., 1995). This disease exemplifies the importance of 11βHSD-2 in protecting MR from spurious glucocorticoid activation. Although mineralocorticoids and glucocorticoids have similar K_Ds for MR, glucocorticoids have different transactivation activities than mineralocorticoids. Moreover, despite their similar structures, mineralocorticoids and glucocorticoids induce ligand-specific conformational changes in the LBD, which alters the interaction between the NTD and LBD (Lombes et al., 1994). Compared to cortisol, aldosterone induces a stronger interaction between the NTD and LBD of MR (Rogerson and Fuller, 2003). Recently, it was discovered that these ligand-specific conformational changes extend to the AF1a domain of the NTD. Aldosterone, but not cortisol, causes an exclusive interaction of AF1a and ribonucleic acid (RNA) helicase A (RHA) (Kitagawa et al., 2002). Furthermore, aldosterone-specific recruitment of RHA leads to the association of CBP, which has intrinsic histone acetyltransferase activity. The selective association of a CBP may result in aldosterone-specific changes in chromatin structure, and this potential mechanism of aldosterone-mediated transcription should be investigated further.

Ligand promiscuity and overlap of nuclear receptors

It is well accepted that mineralocorticoid responsive cells of the distal nephron and collecting duct inactivate glucocorticoid ligands by 11βHSD-2. However, these cells express the glucocorticoid receptor (GR) (Todd-Turla et al., 1993) and the role of GR is not well defined in 11βHSD-2 expressing cells. MR is highly homologous to the glucocorticoid receptor (GR) (Figure 1-9). Not surprisingly, aldosterone is also able to bind GR with a slightly lower affinity than it binds to MR (K_D = 14-60 nM) (Arriza et al., 1987). MR and GR have overlapping DNA

target genes and the two receptors can heterodimerize to mediate transcription of certain genes (Gaeggeler et al., 2005; Ou et al., 2001). In fact, both MR and GR are able to stimulate Na^+ transport in IMCD cells (Husted et al., 1990). It is possible that aldosterone action is mediated through both MR and GR in mineralocorticoid-responsive cells such as collecting duct cells (Figure 1-10).

However, the diversity in MR and GR NTDs suggests that they have different transactivation functions and may interact with different transcriptional coactivators. To date, the only known MR-specific coactivator is the elongation factor ELL. ELL binds directly to the NTD of MR and mediates potent AF1b transactivation (Pascual-Le Tallec and Lombès, 2005). Interestingly, ELL strongly represses the transactivation of GR, and ELL may play an important role in preventing illicit GR-mediated transcription of mineralocorticoid target genes (Pascual-Le Tallec et al., 2005). Taken together, a specific interaction between MR and GR has the potential to stimulate or repress transcription of target genes in a different manner than either receptor acting as an individual homodimer. Clearly, the differences in aldosterone-specific MR and GR transactivation are functionally important and warrant further investigation.

Hormone Response Elements

In general, steroid hormone receptors bind to DNA as dimers and the corresponding DNA element consists of two 'half-sites' in which each receptor interacts with the DNA. This is reflected in the fact that efficient HREs often consist of multiple binding sites. Moreover, half-site orientation is known to affect both hormone receptor binding and activity (Geserick et al., 2005). The human αENaC gene (*scnn1a*) contains two putative HREs; one with half-sites arranged as direct-repeats and the other as an imperfect palindrome. Only the palindromic HRE was capable of stimulating transcription as demonstrated by deletion analysis (Sayegh et al., 1999). GR is known to bind to the DNA as a homodimer in a "head-to-head" orientation that

favors dimerization on an inverted repeat (Luisi et al., 1991) (Figure 1-11). However variations in half-site spacing and orientation are common (Aumais et al., 1996).

Emerging Aldosterone Targets

Because of aldosterone's physiological role in Na^+ balance, its mechanism of action has been extensively studied. Recent reports have identified several novel transcriptional targets of aldosterone. For example, microarray analysis identified the glucocorticoid-induced leucine zipper protein (*gilz*) as an aldosterone-induced transcript (Soundararajan et al., 2005). The protein Gilz was later shown to induce Na^+ transport in Xenopus oocytes and renal epithelial cells. Fakitsas et al. performed a microarray analysis on dissected CCD segments from mice treated with aldosterone for one hour (Fakitsas et al., 2007). Three novel aldosterone-induced transcripts were identified, which included the gene encoding for the protein-related to DAN and Cerberus, activating transcription factor 3, and ubiquitin-specific protease 2-45 (Usp2-45). Subsequent experiments showed that Usp2-45 stimulated a Na^+ current in Xenopus oocytes and renal epithelial cells. It was further demonstrated that Usp2-45 "de-represses" ENaC by removing the ubiquitin groups added by the ubiquitin ligase neural precursor cell-expressed developmentally downregulated gene 4 protein (Nedd4-2). Gumz et al. used microarray to identify early aldosterone response genes in IMCD cells at 1 h (Gumz et al., 2003). This approach identified several novel aldosterone-stimulated genes including connective tissue growth factor, period 1 (*per1*), and endothelin-1 (*edn1*). Interestingly, Per1 was recently shown to regulate both the tonic and aldosterone-dependent expression of *scnn1a* (αENaC) messenger RNA (mRNA) in collecting duct cells (Gumz et al., 2009b). Of particular interest was the induction of *edn1*. The *edn1* gene encodes for preproendothelin-1, the precursor to ET-1. ET-1 plays a complex role in regulating vascular tone and fluid homeostasis (see below).

Demonstration of an interaction between aldosterone and ET-1 would have a significant impact on vascular and renal physiology.

The Endothelin-1 System

ET-1 was discovered in 1985 by Hickey and colleagues as an endothelium-secreted peptide that induced prolonged vasoconstriction (Hickey et al., 1985). The gene product of ET-1 is a 212 amino acid prepropeptide that must undergo several enzymatic cleavages to form the biologically active, 21 amino acid peptide (Figure 1-12). The final cleavage step is mediated by endothelin converting enzymes (ECE-1 and ECE-2), which cleave Big ET-1 (1-38 amino acids) to ET-1 (1-21 amino acids). ECE-1 and ECE-2 are integral membrane metalloproteases that have distinct functional characteristics. ECE-1 is an extracellular integral membrane protein and rapidly converts exogenous Big ET-1 to ET-1. Conversely, ECE-2 is active in acidic environments and does not convert exogenous Big ET-1 efficiently; suggesting that ECE-2 functions primarily intracellularly (Emoto and Yanagisawa, 1995). Cardiovascular production of ET-1 occurs primarily in endothelial cells, but has also been demonstrated in vascular smooth muscle and epicardial cells. ET-1 mediates both autocrine and paracrine signaling through two ET-1 receptor subtypes, ET_A and ET_B (Figure 1-13). ET_A receptors are localized to vascular smooth muscle and mediate vasoconstriction, proliferation, and hypertrophy (Davenport, 2002; Molenaar et al., 1993) (Figure 1-13). ET_B receptors are localized to endothelial cells where they mediate vasodilation by the release of nitric oxide and prostacyclin (D'Orleans-Juste et al., 2002; Edwards et al., 1992; Vassileva et al., 2003) (Figure 1-13). However, there is also evidence that ET_B receptors located on vascular smooth muscle mediate vasoconstriction (Davenport et al., 1993; Just et al., 2004), signifying the existence of cell-specific signal transduction pathways and emphasizing the paracrine nature of ET-1 signaling.

Systemic ET-1 System

Intravenous injection of ET-1 leads to transient hypotension followed by a sustained increase in arterial pressure (Clavell et al., 1995). ET_A antagonism attenuates the increase in blood pressure, indicating predominant ET_A-mediated vasoconstriction. Conversely, ET_B antagonism abolishes the transient depressor response and exacerbates the pressor response, which indicates that ET_B receptors are largely responsible for vasodilation. ET_B also functions as a clearance receptor, and ET_B antagonism results in an increase in circulating ET-1 levels. Consequently, the increase in blood pressure in the presence of systemic ET_B antagonism may result from reduced ET_B-mediated vasodilation or enhanced ET_A-mediated vasoconstriction. High doses of exogenous ET-1 are also associated with antidiuresis and antinatriuresis, whereas, low doses of ET-1 leads to transient natriuresis and diuresis, suggesting that ET-1 plays an important role in modulating renal function (Clavell et al., 1995).

The Renal ET-1 System

As depicted in Figure 1-14, the kidney is both a functional target and source of ET-1. In fact, the highest concentration of ET-1 in the body has been consistently localized to the inner medulla (Kitamura et al., 1990; Pupilli et al., 1994). Within the inner medulla, both IMCDs and vasa recta endothelial cells are known to produce ET-1 (Chen et al., 1993; Kohan and Fiedorek, 1991; Pupilli et al., 1994). *In vivo* data also demonstrates ET-1 synthesis in the glomeruli, proximal tubules, juxtaglomerular cells, medullary thick ascending limb, cortical collecting duct (CCD) and outer medullary collecting duct (OMCD) (Battistini et al., 2006; Kotelevtsev and Webb, 2001; Lehrke et al., 2001). Expression of ET-1 receptor subtypes largely parallels ET-1 synthesis, with the highest concentration in the inner medulla (Battistini et al., 2006; Wendel et al., 2006). In addition, ET_B receptors are more numerous than ET_A receptors and are the predominant receptor subtype in the human kidney (Pupilli et al., 1994). ET_B receptors are

expressed in proximal tubules, collecting ducts, peritubular capillaries, vasa recta, glomeruli, and both afferent and efferent arterioles (Battistini et al., 2006; Davenport et al., 1993; Gellai et al., 1994; Kohan et al., 1992; Wendel et al., 2006). ET_A receptors are abundantly expressed in the cortical vasculature including the arcuate arteries and both afferent and efferent arterioles, but expression has also been identified in mesangial cells, descending vasa recta, and, to a lesser extent, renal tubule cells (Battistini et al., 2006; Inscho et al., 2005; Kuc and Davenport, 2004; Wendel et al., 2006).

The heterogeneous population of ET_A and ET_B receptors demonstrates that ET-1 has a complex role in the kidney. Evidence exists for ET-1 mediating effects on renal hemodynamics (Inscho et al., 2005), Na^+ and water homeostasis (Kohan, 2006), and acid-base balance (Khanna et al., 2005). To add to the complexity, the effect of ET-1 depends on its dose and source. A high dose of exogenous ET-1 causes profound cortical vasoconstriction of afferent and efferent arterioles, arcuate arteries and mesangial cells. This vasoconstriction is largely attributed to the activation of ET_A receptors. However, there are conflicting reports regarding the role of the ET_B receptor in vasoconstriction of the afferent arteriole (Baylis, 1999; Inscho et al., 2005). As a result of cortical vasoconstriction, renal blood flow (RBF) and GFR subsequently decrease and antidiuresis and antinatriuresis are observed as secondary changes (Clavell et al., 1995; Katoh et al., 1990). In contrast to cortical action, ET-1 results in medullary vasodilation, even at doses capable of inducing cortical vasoconstriction (Vassileva et al., 2003). Medullary vasodilation is mediated by ET_B receptors and functions through the production of nitric oxide and prostaglandins (Chou and Porush, 1995; Pollock and Pollock, 2008). Interestingly, low doses of ET-1 lead to transient natriuresis and diuresis by a mechanism that is also attributed to ET_B receptors (Clavell et al., 1995). Vasodilation of the inner medulla will increase medullary blood

flow and result in enhanced Na^+ excretion (Cowley, 1997). However, in addition to vasodilatory mechanisms, ET-1 can mediate direct effects on Na^+ and water transport.

ET-1 in Renal Water Transport

ET-1 controls water transport by modulating ADH responsiveness of the collecting duct. Oishi et al. originally demonstrated that ET-1 inhibits ADH-stimulated water permeability in isolated perfused IMCD segments (Oishi et al., 1991). The decrease in water permeability results from ET_B-mediated inhibition of adenylate cyclase and cAMP accumulation (Kohan, 1993). However, the most unambiguous evidence for ET-1's role in modulating ADH action comes from a series of collecting duct *edn1* and *etar* knockout mice. The *edn1* or *etar* genes were selectively knocked out in principal cells of the collecting duct with a cre recombinase driven by the aquaporin-2 promoter (Stricklett et al., 1999). Collecting duct cell *edn1* knockout mice exhibit enhanced ADH sensitivity (Ge et al., 2005a). Consequently, these mice demonstrate a reduced ability to excrete an acute water load, exhibit a higher increase in ADH-stimulated cAMP, and have lower levels of circulating ADH. In contrast, collecting duct *etar* knock out mice demonstrate an enhanced ability to excrete an acute water load as a result of blunted ADH activity (Ge et al., 2005b). Taken together, collecting duct derived ET-1 acts to inhibit ADH responsiveness through the ET_B receptor; whereas, ET_A receptors stimulate ADH responsiveness.

Interestingly, extracellular hypertonicity stimulates ET-1 release from IMCD cells. An increase in medullary tonicity occurs during antidiuresis when medullary ADH levels are elevated. This suggests that ET-1 is stimulated to mediate a negative feedback mechanism on water reabsorption. Likewise, increased tubule and vasa recta flow rate occur during salt and water loading. Although it has not been directly observed in tubules or vasa recta, increased flow rate and shear stress stimulate the release of ET-1 from many vascular and nonvascular cell

types (Kohan, 2006). Moreover, increased IMCD shear stress results in the release of nitric oxide (Cai et al., 2000) and may be a downstream product of ET-1 synthesis. Thus, ET-1 is stimulated under several conditions where water flux is maximal and suggests that ET-1 mediates an important negative feedback loop on water reabsorption.

ET-1 in Renal Sodium Transport

In 1993, Tomita et al. demonstrated that ET-1 reversibly inhibited H_2O and Cl^- transport in isolated CCD (Tomita et al., 1993). Mounting evidence exists that ET_B receptors promote natriuresis by direct inhibition of ENaC activity through a mechanism mediated, at least in part, by nitric oxide and Src kinases (Gilmore et al., 2001). Using a patch-clamp technique, Gallego et al. demonstrated that ET-1 inhibited amiloride-sensitive Na^+ transport in an ET_B dependent manner (Gallego and Ling, 1996). Moreover, ET-1 inhibits medullary thick ascending limb Cl^- transport via an ET_B-mediated increase in endothelial nitric oxide synthase (eNOS) expression and release of nitric oxide (Herrera and Garvin, 2004). In the IMCD, ET-1 is able to stimulate eNOS (Ye et al., 2003), nitric oxide (Schneider et al., 2008), cyclic guanosine monophosphate (cGMP) (Edwards et al., 1992), and inhibit Na^+/K^+-ATPase via cyclooxygenase metabolites (Zeidel et al., 1989).

Russell et al. demonstrated that Big ET-1 binds to the glomeruli, distal tubules, collecting ducts, and endothelial cells in human kidneys (Russell et al., 1998). In contrast to ET-1, systemic infusion of Big ET-1 at high doses leads to profound natriuresis, diuresis, and sustained vasoconstriction (Hoffman et al., 2000). This observation likely results from local conversion of Big ET-1 to ET-1 by ECE-1 and reflects ET-1 production *de novo*.

Renal ET-1 Mediated Natriuresis in Experimental Models

Medullary ET-1 is reduced in several models of experimental hypertension including spontaneously hypertensive, Dahl S, and Prague hypertensive rats (Kohan, 2006). However, the

importance of ET_B-mediated natriuresis was originally revealed in studies conducted on spotting lethal (sl) ET_B deficient rats. Homozygous spotting lethal rats have a naturally occurring 301 bp deletion in *etbr* that leads to aganglionic megacolon and mortality shortly after birth. Gariepy and colleagues rescued the fatal phenotype in the enteric system by a dopamine hydroxylase promoter (Gariepy et al., 2000). Rescued spotting lethal rats exhibit low renin salt-sensitive hypertension and do not demonstrate an acute depressor response to systemic ET-1 injection. These rats also have higher levels of circulating ET-1 presumably as a result of decreased ET_B clearance. As mentioned previously, in the absence of ET_B receptors levels of ET-1 can accumulate in the circulation leading to the activation of vascular ET_A receptors and vasoconstriction. In addition, rescued spotting lethal rats have enhanced ET_A-mediated sympathetic tone that was also implicated in the observed increase in blood pressure (Ohkita et al., 2005). However, selective ET_A antagonism only partially decreased blood pressure; whereas, treatment with the ENaC inhibitor, amiloride, led to the complete normalization of blood pressure. This data strongly supports the role of ET_B-mediated inhibition of ENaC.

However, the most definitive evidence of ET_B-mediated natriuresis comes from collecting duct cell specific *edn1*, *etar* and *etbr* knockout mice. Collecting duct *edn1* knockout mice are hypertensive on a normal NaCl diet (Ahn et al., 2004). These mice are also salt-sensitive as demonstrated by their reduced ability to excrete Na^+ in the presence of a NaCl challenge. Treatment with amiloride corrected the inappropriate Na^+ retention and normalized the blood pressure. Clearly, collecting duct derived ET-1 plays an important role in inhibiting Na^+ reabsorption. Collecting duct ET_B knockout mice also develop hypertension due to impaired Na^+ excretion, but to a lesser extent than collecting duct ET-1 knockout mice (Ge et al., 2006). This indicates that ET_B receptors located on the collecting duct are functionally important in

mediating Na^+ excretion, but surrounding ET_B receptors likely compensate by producing nitric oxide which is readily membrane permeable and can rapidly diffuse into neighboring cells. In contrast to ET-1 and ET_B, collecting duct ET_A knockout mice exhibit normal Na^+ excretion on both a normal and high NaCl diet (Ge et al., 2005). Collectively, these data unambiguously establishes the role for collecting duct ET-1 and ET_B receptors in modulating transepithelial Na^+ transport in the collecting duct.

Regulation of the Renal ET-1 System.

ET-1 has well defined effects to promote Na^+ excretion and many components of the medullary ET-1 system are upregulated in response to a high NaCl diet, including ET-1, ECE-1, and ET_B (Fattal et al., 2004; Herrera and Garvin, 2005; Tsai et al., 2006; Vassileva et al., 2003). These observations provide direct evidence for a physiological role of ET-1-mediated Na^+ excretion. Furthermore, Herrera and colleagues demonstrated that a high salt diet increases medullary osmolality and stimulates eNOS expression in the medullary thick ascending limb by an ET-1 and ET_B mediated pathway (Herrera and Garvin, 2005). Stimulation of eNOS will increase levels of nitric oxide and inhibit Na^+ transport. In addition, hypertonicity also stimulates ET-1 synthesis and release from the IMCD (Herrera and Garvin, 2005; Kohan and Padilla, 1993). In normal humans, plasma ET-1 is not affected by dietary salt intake, but urinary ET-1, a marker of renal-derived ET-1 (Serneri et al., 1995), positively correlates with Na^+ excretion and urinary volume (Modesti et al., 1998). These data suggests that renal ET-1 may participate in normal natriuretic processes in a healthy humans.

There is also extensive literature demonstrating the functional regulation of the renal ET-1 system in response to mineralocorticoid-induced hypertension. Medullary ET-1, ECE-1, and ET_B expression are upregulated in the pre-hypertensive and hypertensive deoxycorticosterone acetate (DOCA)- salt treated rat (Hsieh et al., 2000; Pollock et al., 2000; Tostes et al., 2000).

Furthermore, blockade of ET_B in DOCA-salt sensitive hypertensive animals exacerbates the increase in blood pressure and impairs Na^+ excretion. These observations indicate that the upregulation of ET-1, ECE-1, and ET_B is a compensatory mechanism that should reduce systemic arterial pressure and promote Na^+ excretion.

Interaction Between Aldosterone and Endothelin-1

As mentioned in **Emerging Aldosterone Targets** section, the ET-1 gene (*edn1*) has been identified as an aldosterone response gene in IMCD cells *in vitro* (Gumz et al., 2003). This observation is of particular interest because aldosterone and ET-1 have well defined and opposing action on Na^+ transport in the collecting duct. A possible explanation for this observation is that ET-1 triggers a negative feedback loop on aldosterone-mediated Na^+ reabsorption. This hypothesis is in agreement with the previous observations that DOCA-salt hypertensive rats upregulate their medullary ET-1/ET_B pathway as a compensatory mechanism (Hsieh et al., 2000). As noted below, there is a considerable body of literature linking ET-1 and ET_B signaling to a negative feedback mechanism that inhibits aldosterone action.

The only documented negative feedback loop on aldosterone action involves the activation of extracellular receptor kinases (ERK1/2) by epidermal growth factor (EGF) and its receptor (EGFR). In renal collecting duct cells, EGF inhibits amiloride-sensitive Na^+ reabsorption through activation of ERK1/2 (Shen and Cotton, 2003). Aldosterone stimulates EGF-EGFR-ERK1/2 signaling cascade in principal cells, and functional patch clamp data demonstrates that this signaling cascade serves as negative feedback to control aldosterone-induced Na^+ reabsorption (Grossmann et al., 2004a). There are four observations directly linking ET-1/ET_B signaling to ERK1/2 activation. First, ET-1 stimulates EGFR transactivation and downstream ERK1/2 activation in several cell models (Grantcharova et al., 2006; Portik-Dobos et al., 2006). In vascular smooth muscle, ET_B receptors demonstrate a distinct biphasic pattern of ERK1/2

activation (Grantcharova et al., 2006). The second phase of ERK activation involves EGFR transactivation and is dependent on the extracellular N-terminal domain of ET_B (Grantcharova et al., 2002). Second, ET_B receptors stimulate G proteins-$G_{\beta/\gamma}$ and downstream activation of ERK2 in kidney cells (Aquilla et al., 1996). Third, blocking ERK activation with pertussis toxin preferentially inhibits ET_B, but not ET_A mediated-intracellular calcium signaling (Saita et al., 1997). This demonstrates that known ET_B action is mediated through ERK activation. Finally, protein kinase C (PKC)-mediated activation of ERK1/2 in distal tubule cells leads to the targeted degradation of ENaC. This is of particular interest because ET-1 stimulates PKC to modulate ADH activity in the same region of the nephron. Taken together, ET_B has several direct links to the only known negative feedback loop on aldosterone action. However, it still remains to be determined if medullary ET_B receptors stimulate directly EGF-EGFR-ERK1/2 signal transduction in the collecting duct to mediate inhibition of aldosterone.

Summary

Hypertension is a leading risk factor for cardiovascular disease, the leading cause of death. However, the molecular mechanisms driving hypertension are not well defined, as more than 95% of hypertensive patients have no known etiology. However, it is known is that Na^+ reabsorption by the distal nephron and collecting duct plays a pivotal role in determining extracellular fluid volume and blood pressure, and this process is stimulated by the mineralocorticoid hormone, aldosterone. Currently, a negative feedback loop on aldosterone action in the kidney has not been defined.

Gumz et al. has reported that aldosterone stimulated the *edn1* mRNA and ET-1 protein in mIMCD-3 cells in vitro (Gumz et al., 2003). ET-1 has a direct inhibition of amiloride-sensitive Na^+ transport through ENaC in collecting duct cells. Moreover, collecting duct-specific gene knockout mice have revealed an important role for ET-1 in salt-sensitive hypertension. The

overarching hypothesis of this dissertation is that aldosterone-stimulated *edn1* mediates a negative feedback loop on aldosterone-stimulated Na^+ transport in the renal collecting duct. The scientific objectives of this dissertation were to 1) characterize aldosterone- and age-dependent ET-1 expression in the kidney *in vivo*, 2) determine if collecting duct cells were the target cell type for aldosterone-dependent *edn1* stimulation, 3) characterize the mechanism of aldosterone induction of *edn1* in target epithelial collecting duct cells, and 4) evaluate the role of *edn1* in aldosterone-dependent gene expression.

Initial whole animal experiments revealed that important aldosterone-dependent gene expression occurred in the renal inner medulla, as well as the known aldosterone-responsive regions of the kidney; the cortex and outer medulla. Furthermore, ET-1 peptide levels positively correlated with age and plasma aldosterone concentrations in the inner medulla, but not the cortex. Collecting duct cells were verified as the target cell type for aldosterone action on the *edn1* gene. *In vitro* reporter assays were not capable of reproducing the endogenous gene activity. However, evaluation of the endogenous gene revealed aldosterone-dependent association of MR and GR with the *edn1* promoter. Further analysis of the *edn1* promoter revealed at least two HREs each that differed from the classical HRE sequence. The synthetic glucocorticoid dexamethasone confirmed the role of GR in modulating *edn1* transcription. In fact, dexamethasone action on the collecting duct mimicked aldosterone in that every aldosterone-response gene investigated was stimulated. Finally, blocking *edn1* mRNA expression caused alterations in the aldosterone-target genes *scnn1a* and *sgk1* in the presence or absence of hormone. Taken together, these studies presented in this dissertation clearly demonstrate that aldosterone activates both MR and GR to drive the transcription of *edn1* in collecting duct cells and that the role of *edn1* expression has a direct effect on ENaC.

Table 1-1. Sodium transport mechanisms in the nephron and collecting duct*

Tubule Segment	% Filtered Na^+ Reabsorbed	Molecular Mechanism
Proximal tubule	65%	Na^+/H^+ exchanger (NHE), other Na^+/anion exchangers, Na^+-cotransporters, and paracellular diffusion
Thick ascending limb of Henle	25%	$Na^+/K^+/2Cl^-$ cotransporter (NKCC2)
Distal convoluted tubule	5 – 7%	Na^+/Cl^- cotransporter (NCC) and the epithelial Na^+ channel (ENaC)
Collecting duct	1 – 3%	ENaC

*Adapted from (Gumz, Stow et al., 2009b)

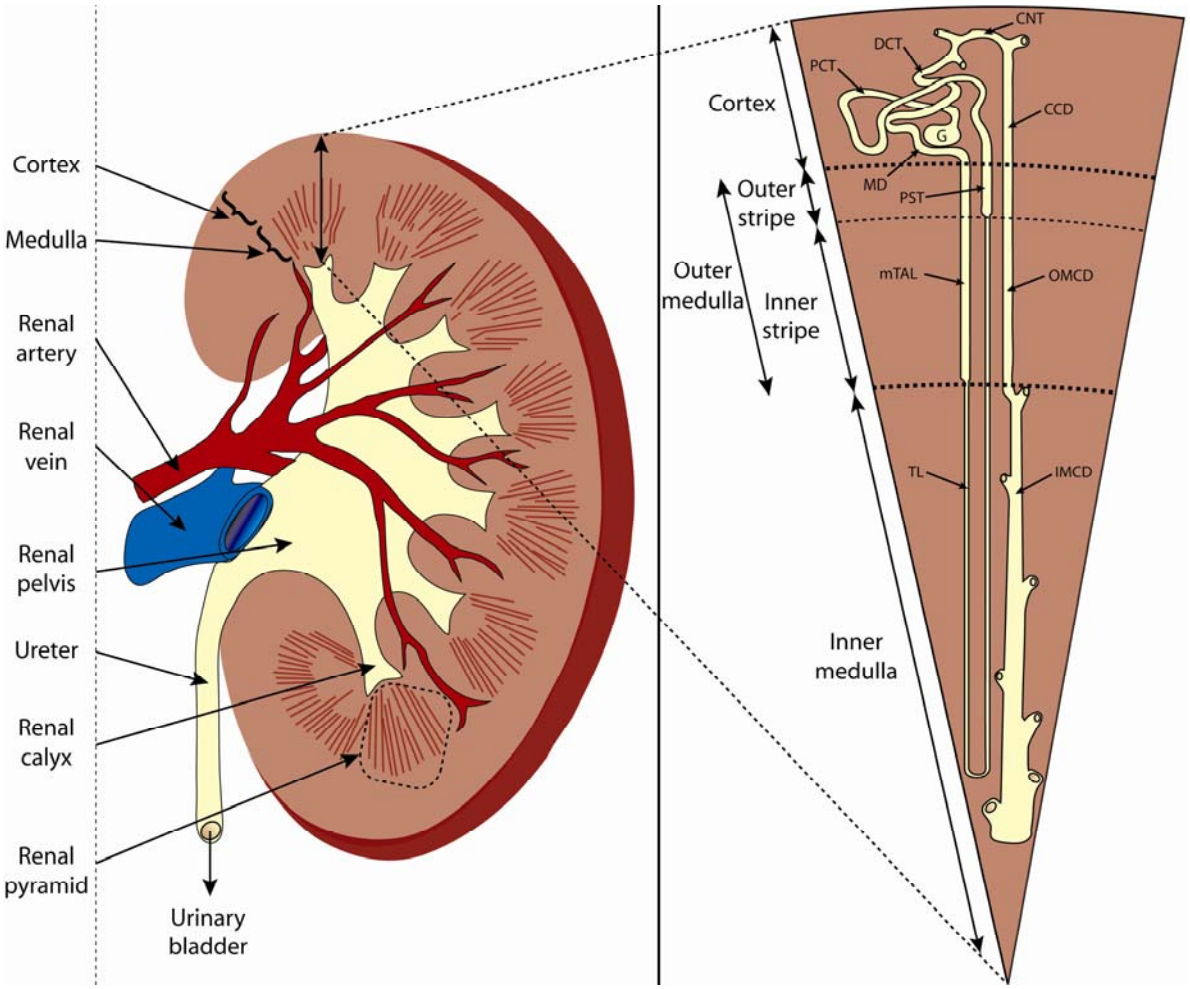

Figure 1-1. Diagram of the bisected kidney and tubule. (Left panel) Cross sectional view of the kidney indicating the major anatomical features. (Right panel) Enlargement of a typical long-looped nephron and collecting duct indicating the basic morphological features and regional boundaries. G: glomerulus, PCT: proximal convoluted tubule, PST: proximal straight tubule, TL: thin limb of Henle, mTAL: medullary thick ascending limb of Henle, DCT: distal convoluted tubule, MD: macula densa, CNT: connecting segment, CCD: cortical collecting duct, OMCD: outer medullary collecting duct, IMCD: inner medullary collecting duct.

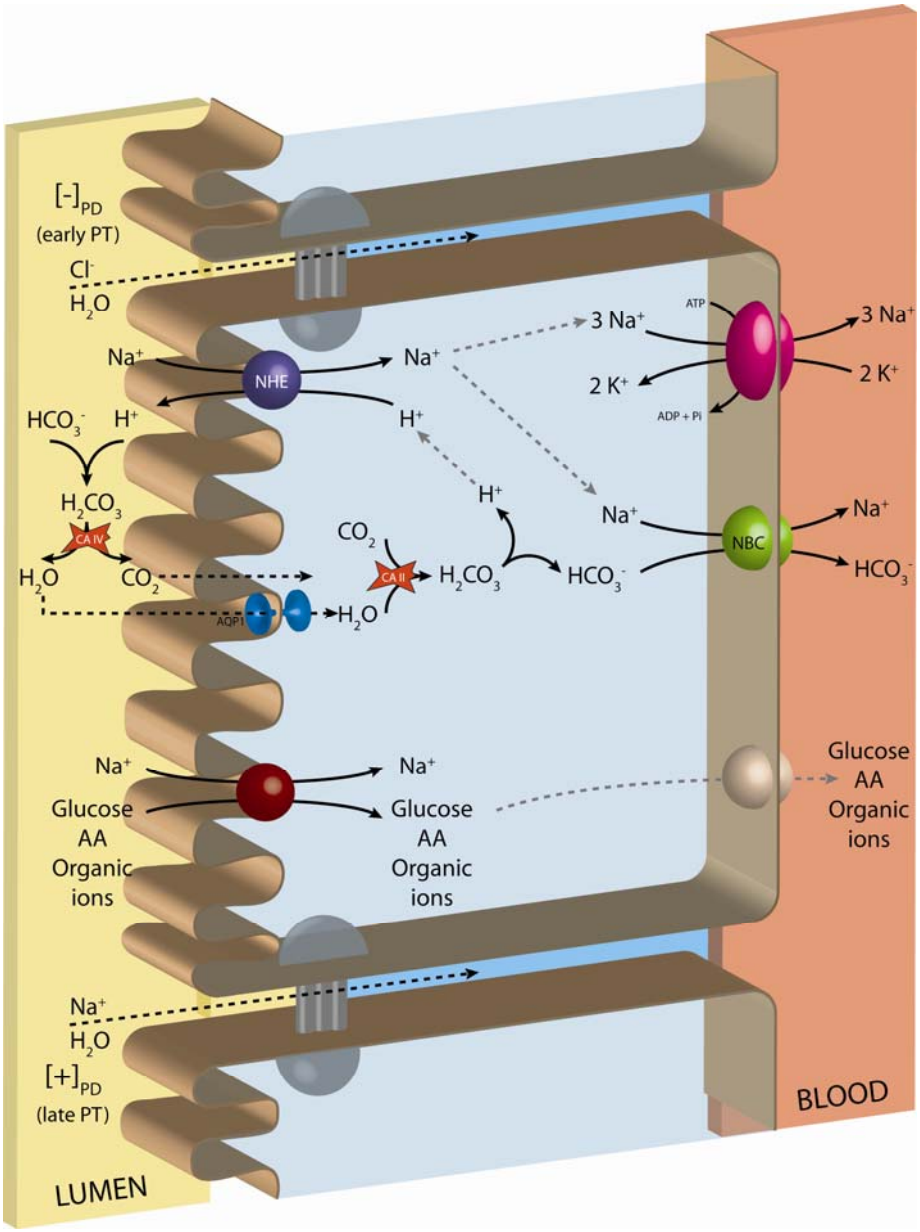

Figure 1-2. Na^+ transport mechanisms of the proximal tubule. In the proximal tubule (PT) apical Na^+ transport occurs by Na^+/ H^+ exchangers (NHE) and by symport with various molecules. Intracellular Na^+ is pumped into the interstitium by basolateral Na^+/K^+-ATPase and Na^+/HCO_3^- cotransporters (NBC). Luminal H^+ and HCO_3^- spontaneously form H_2CO_3, which carbonic anhydrase (CA) type IV converts to CO_2 and H_2O molecules that move back into the cell by diffusion or via aquaporin channels (AQP), respectively. Intracellular CA II catalyzes the reverse reaction to facilitate apical H^+ recycling and net HCO_3^- reabsorption. The early PT has a lumen negative potential difference ($[-]_{PD}$) that drives Cl^- and H_2O paracellular diffusion. Cl^- is reabsorbed via apical exchange for HCO_3^- (not shown). Anion removal in the early PT eventually generates a $[+]_{PD}$ in the late PT to drive paracellular Na^+ and H_2O diffusion.

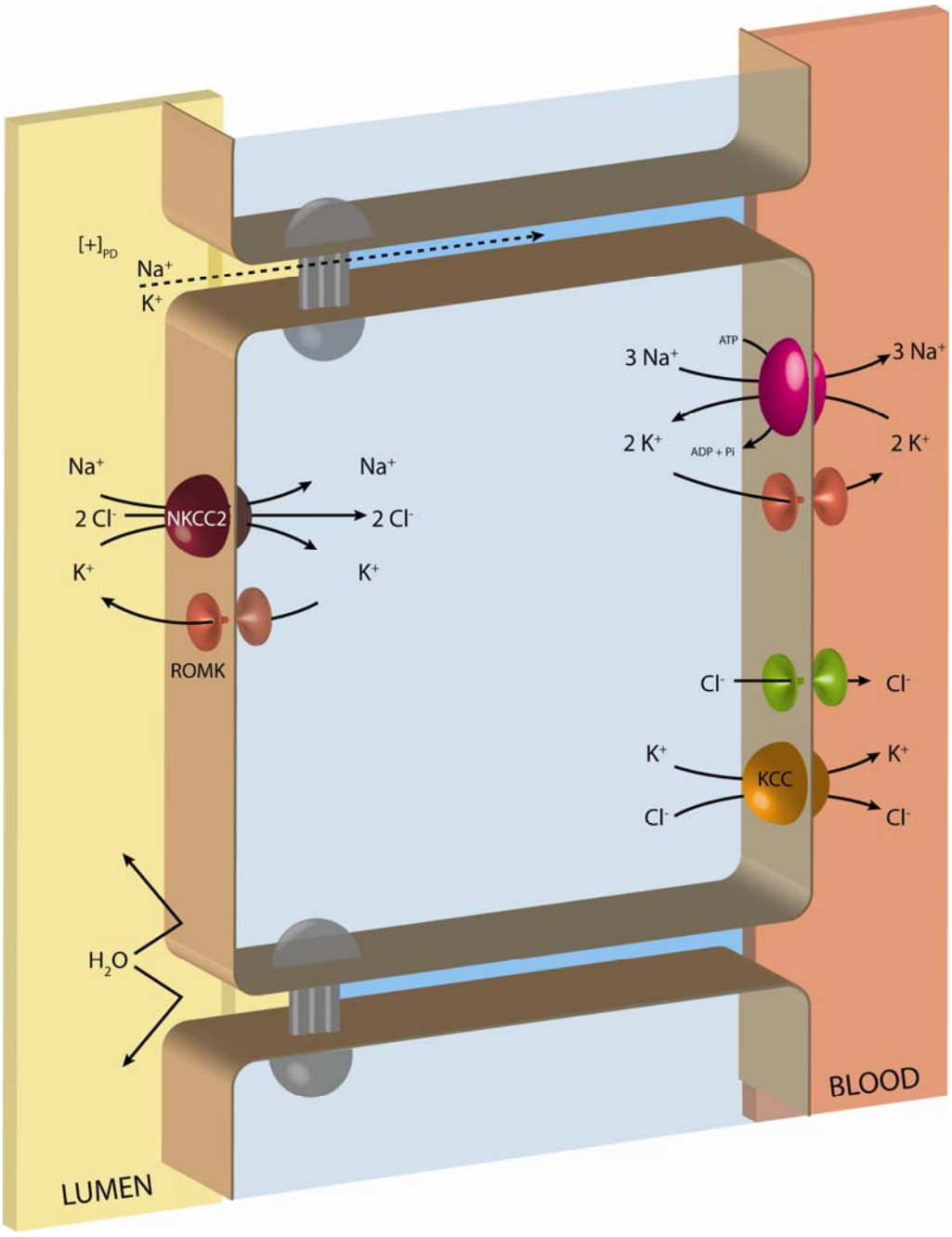

Figure 1-3. Na^+ transport mechanisms of the thick ascending limb of Henle. The majority of Na^+ reabsorption in this region of the tubule occurs via the apical $Na^+/K^+/2Cl^-$ cotransporter (NKCC2). Basolateral export mechanisms include the ubiquitous Na^+/K^+-ATPase pump, Cl^- channels, and the K^+/Cl^- cotransporter (KCC). K^+ recycling via the renal outer medullary K^+ channel (ROMK) is essential for NKCC2-dependent NaCl reabsorption. K^+ recycling also helps to generate a lumen positive potential difference ($[+]_{PD}$) that drives paracellular diffusion of Na^+ and K^+. This region of the tubule is also particularly impermeable to H_2O, which causes the tubular fluid to become progressively hypoosmotic as NKCC2 facilitates net NaCl reabsorption.

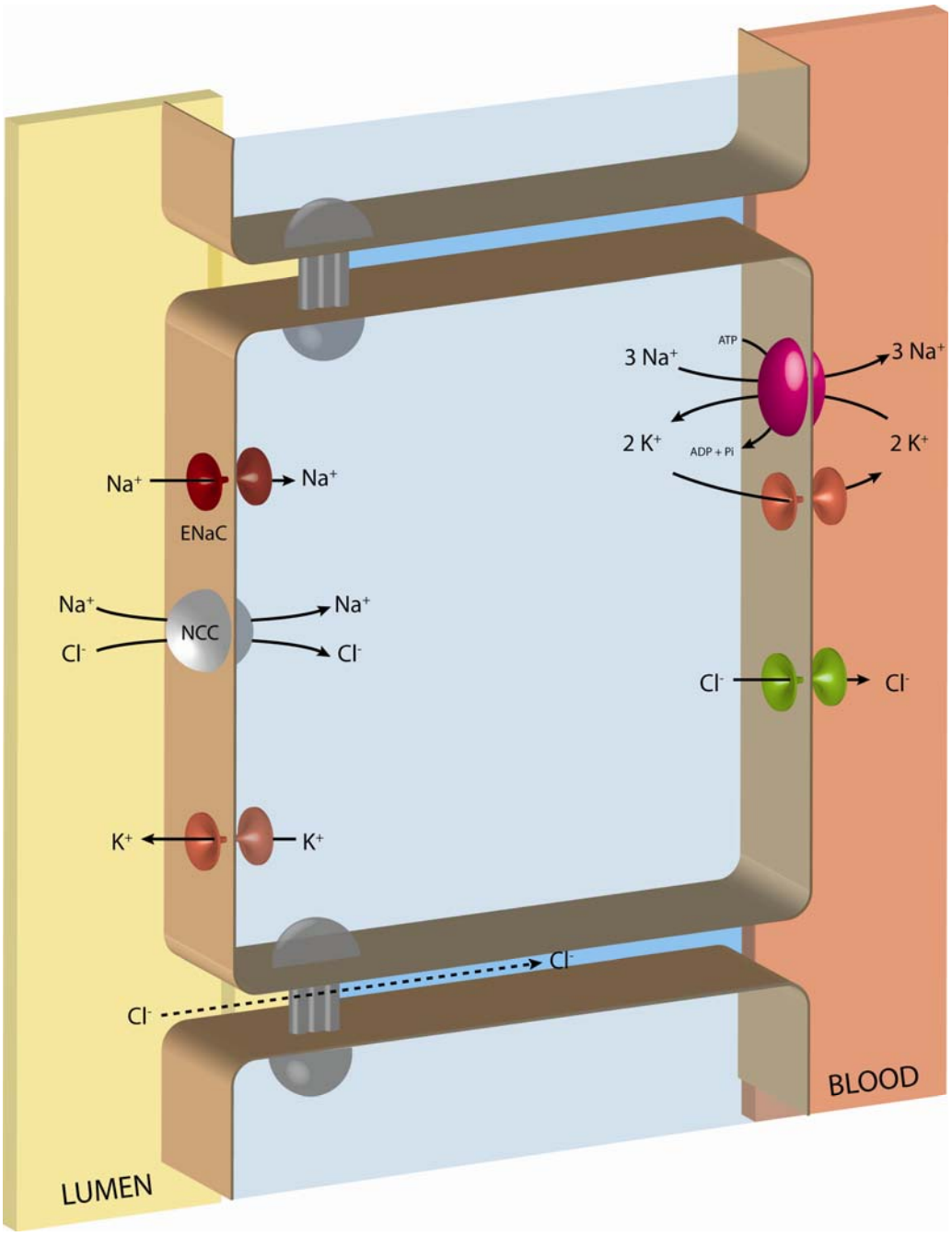

Figure 1-4. Na^+ transport mechanisms of the distal convoluted tubule. The Na^+/Cl^- cotransporter (NCC) is responsible for the majority of apical Na^+ entry, however the apical epithelial Na^+ channel (ENaC) is also present in this region of the tubule. Basolateral export mechanisms include the ubiquitous Na^+/K^+ ATPase pump and both K^+ and Cl^- channels. Intracellular K^+ can also be secreted into the lumen via apical K^+ channels. In addition, the removal of Na^+ from the lumen also drives paracellular Cl^- diffusion.

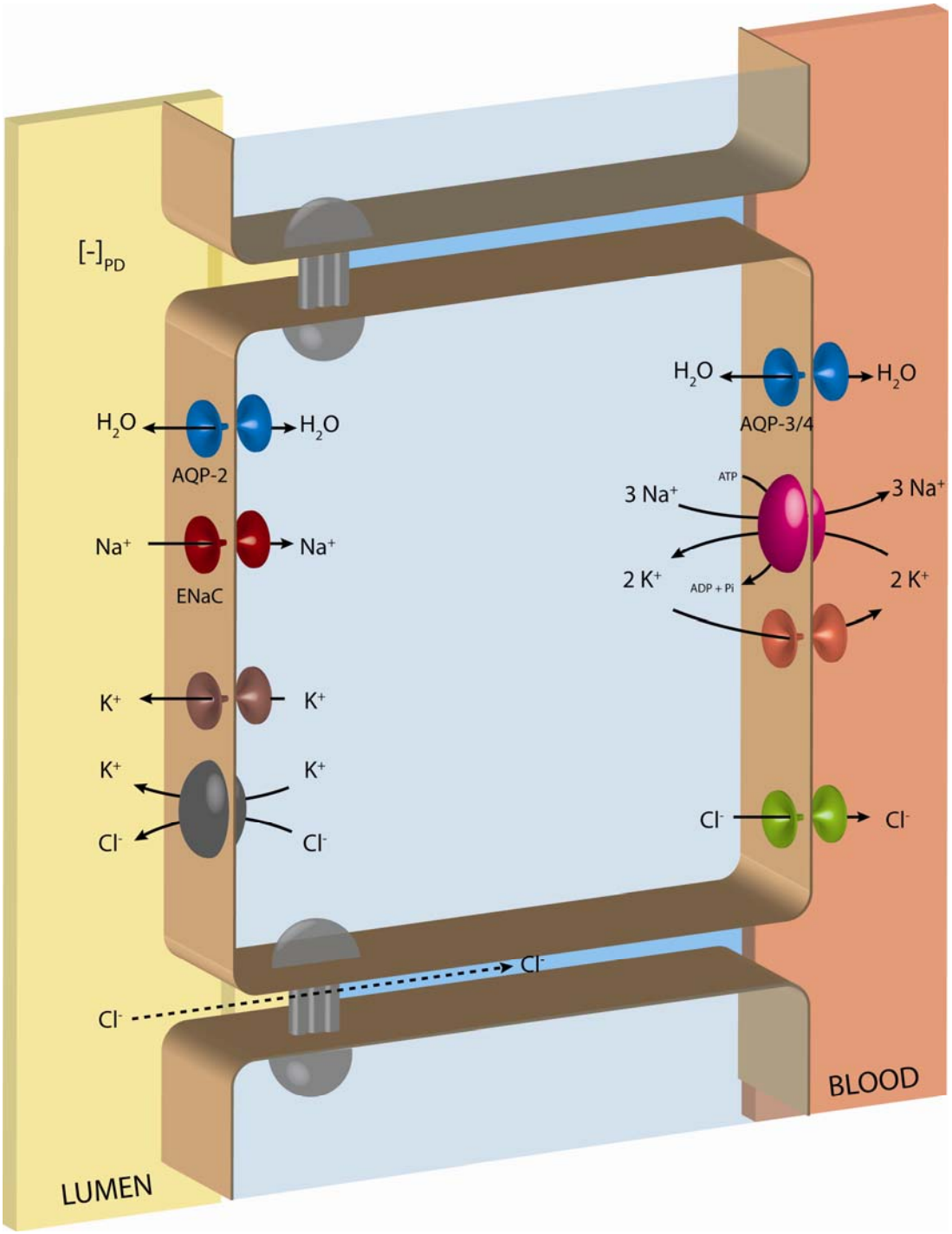

Figure 1-5. Na^+ transport mechanisms of the collecting duct. Na^+ reabsorption occurs in principal cells of the collecting duct and is facilitated by the apical ENaC and the basolateral Na^+/K^+ ATPase pump. Classically, the removal of Na^+ from the lumen causes a net negative potential difference that serves to drive paracellular Cl^- reabsorption. In addition, Na^+ reabsorption is closely coupled to K^+ secretion that occurs via K^+ channels and an apical K^+/Cl^- cotransport mechanism. Functional evidence has also demonstrated the existence of an apical H^+/K^+-ATPase (not pictured).

Figure 1-6. Overview of aldosterone action. (Left panel): In the absence of aldosterone, MR is located in the cytosol bound by chaperone heat shock proteins such as HSP90. Consequently, apical ENaC proteins are continuously targeted for internalization and degradation by a Nedd4-2 ubiquitin ligase. (Right panel) In the presence of aldosterone, the hormone enters a principal cell of the collecting duct and binds to MR, resulting in receptor nuclear translocation and dimerization. In the nucleus, aldosterone-bound MRs direct the transcription of target genes including genes involved in transepithelial Na^+ transport such as *sgk1*, *atp1a1*, and *scnn1a*. Aldosterone increases both ENaC and Na^+/K^+-ATPase proteins, and Sgk1-mediated phosphorylation and inhibition of Nedd4-2. Ultimately, these actions lead to an increase in transepithelial Na^+ transport.

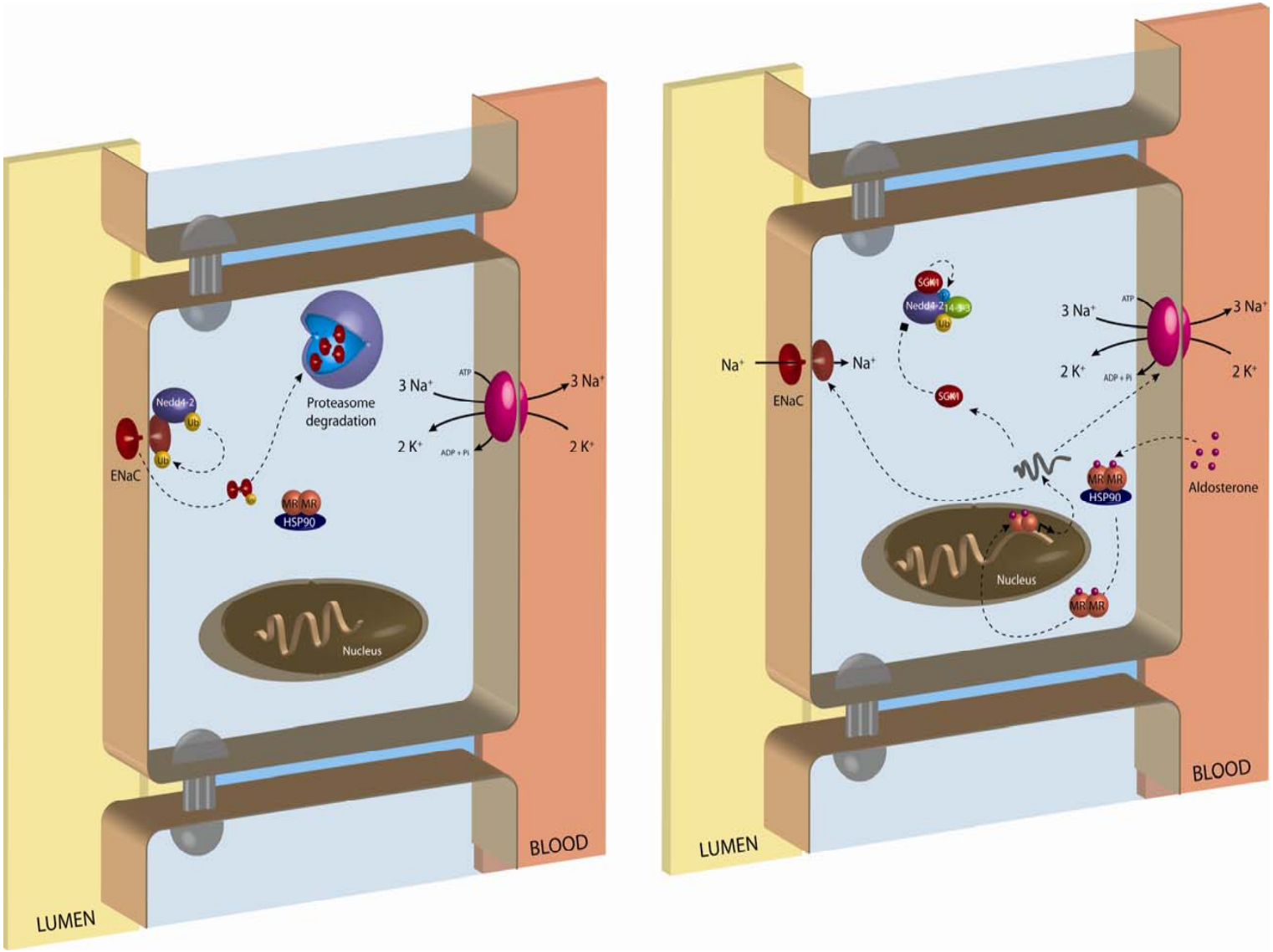
LUMEN
BLOOD
ENaC
Nedd4-2
Ub
Proteasome degradation
3 Na+
2 K+
ATP
ADP + Pi
MR MR
HSP90
Nucleus
Na+
SGK1
Aldosterone

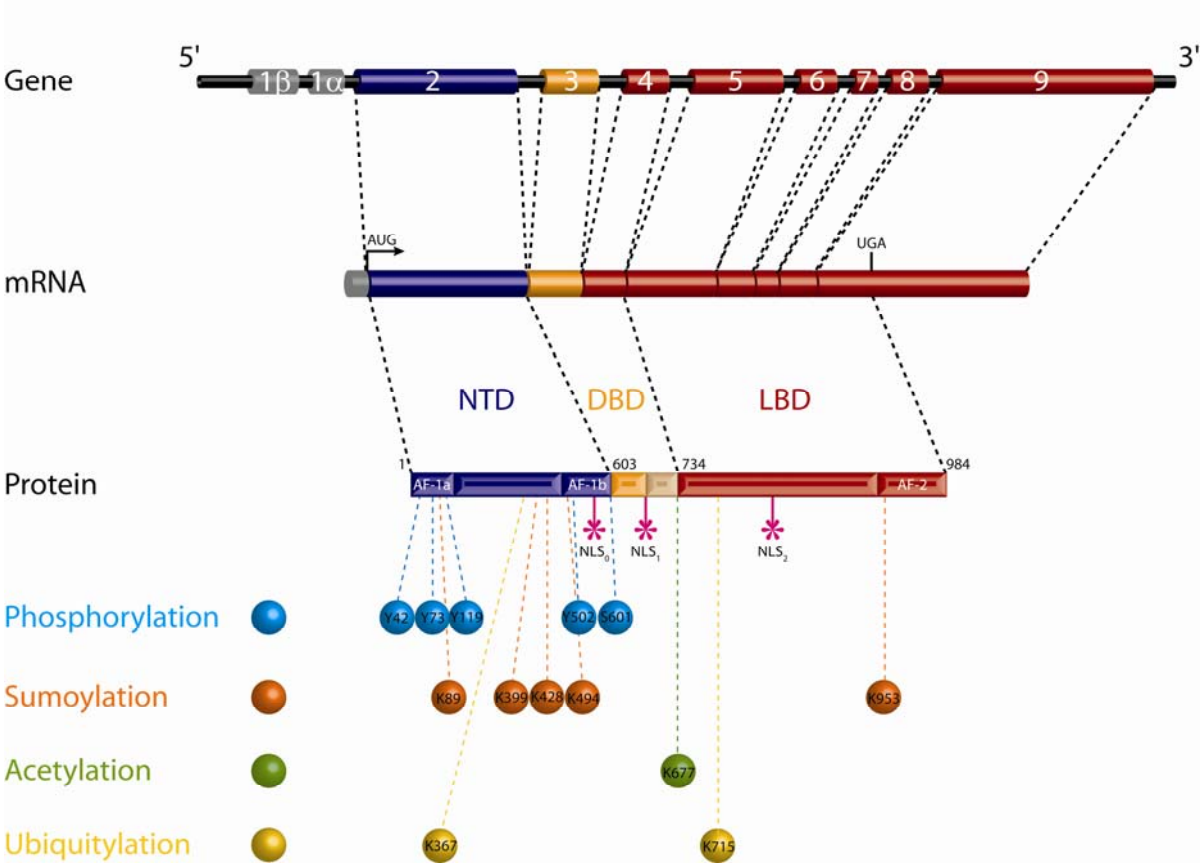

Figure 1-7. Overview of the mineralocorticoid receptor. The genomic organization of MR is shown on top indicating the two alternative exons 1 in gray, followed by the remaining exons 2 through 9. Exon 2 codes for the N-terminal domain (NTD), and exons 3 and 4 encode for the DNA binding domain (DBD) and hinge region. The ligand binding domain (LBD) is encoded for by exons 5-9. Known modifications to MR are indicated. Three nuclear localization signals are also indicated (NLS_0, NLS_1, NLS_2)

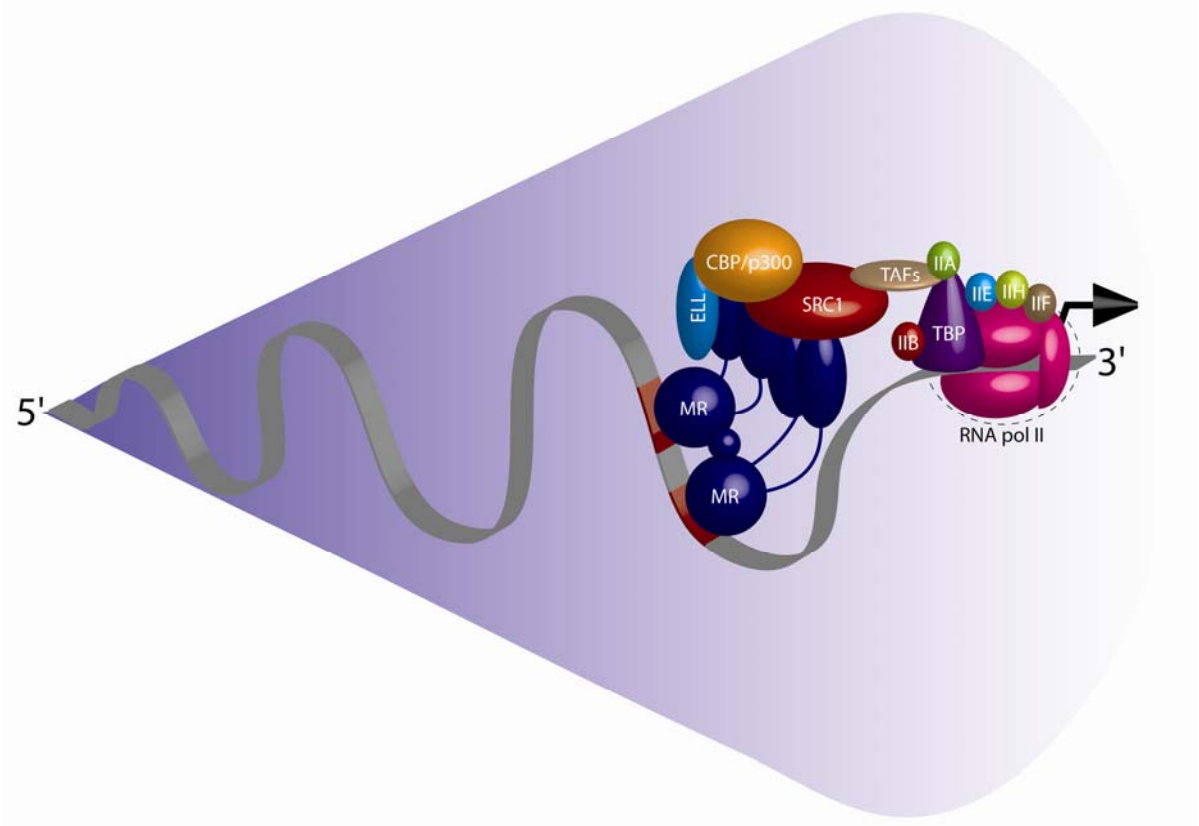

Figure 1-8. Overview of MR-directed gene transcription. MR binds directly to HREs in the DNA of target genes and typically binds in the preferred dimeric conformation. MR then recruits numerous coactivators including SRC-1, CBP/p300, and ELL. The RNA polymerase II (RNA pol II) transcription complex is also recruited. Figure based on data from (Pascual-Le Tallec and Lombès, 2005).

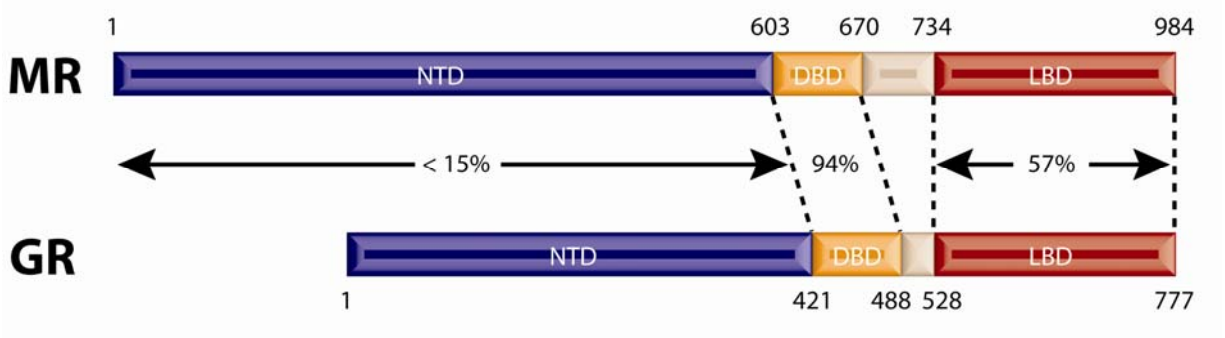

Figure 1-9. Comparison of MR and GR structural domains. The percent homology between MR and GR is indicated for each major domain. Blue corresponds to the N-terminal domain NTD), yellow corresponds to the DNA binding domain (DBD), beige corresponds to the hinge region and red corresponds to the ligand binding domain (LBD). Numbers correspond to the first amino acid residue in each domain, as well as the terminal amino acid residue in each receptor. Figure modeled on data from (Arriza et al., 1987).

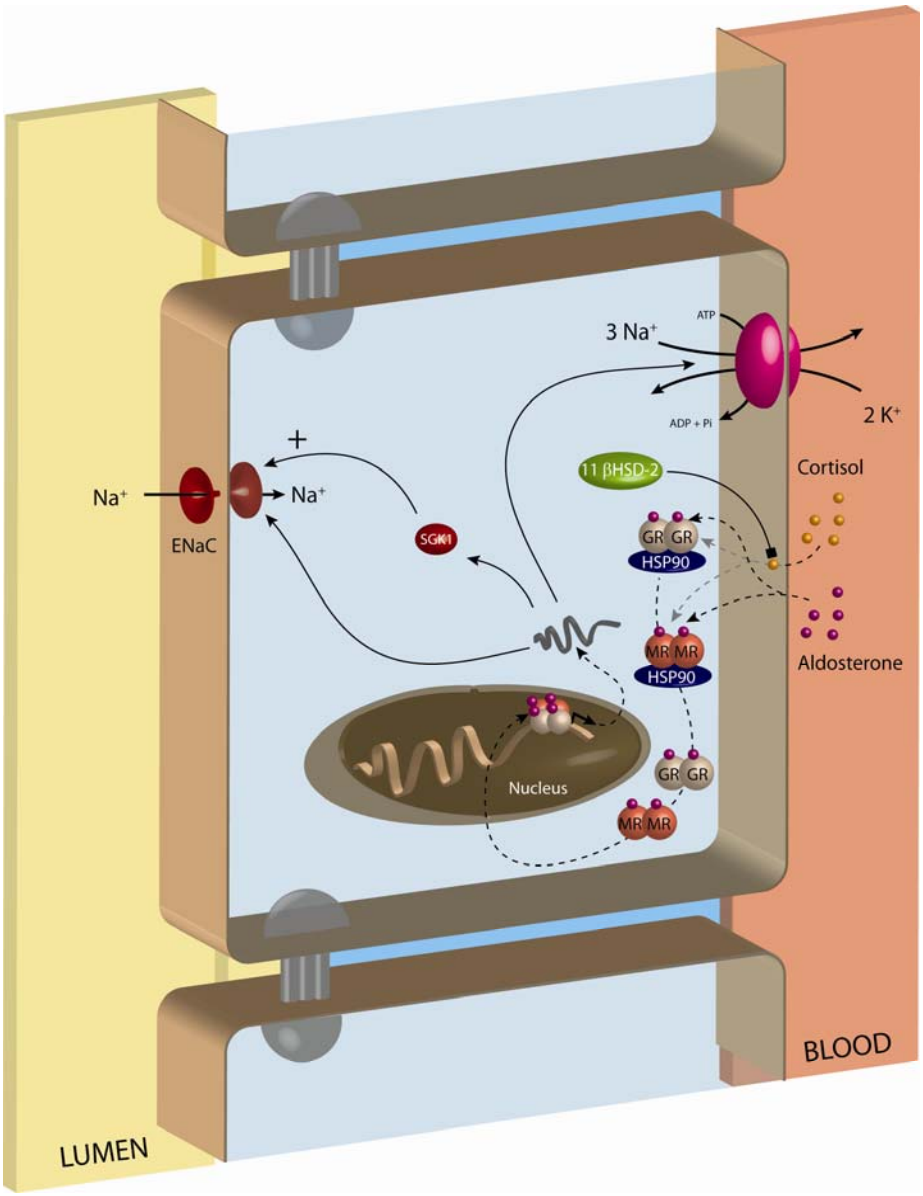

Figure 1-10. Potential role of GR in collecting duct cells. Collecting duct cells express 11βHSD-2 that inactivates the endogenous glucocorticoid, cortisol, and prevents cortisol-dependent activation of MR and GR and downstream stimulation of Na^+ transport mechanisms (gray arrows). However, aldosterone also has an affinity for GR and may activate both MR and GR to mediate aldosterone-dependent action and downstream Na^+ transport mechanisms.

Figure 1-11. Three-dimensional structure of a dimeric GR DNA binding domain complex interacting with a classical hormone response element. GR typically binds to HREs in a dimeric conformation. Nucleotides that make direct contacts with the hormone receptor are shown in red. Structural data obtained from Protein Data Bank 1R4R (Luisi et al., 2003).

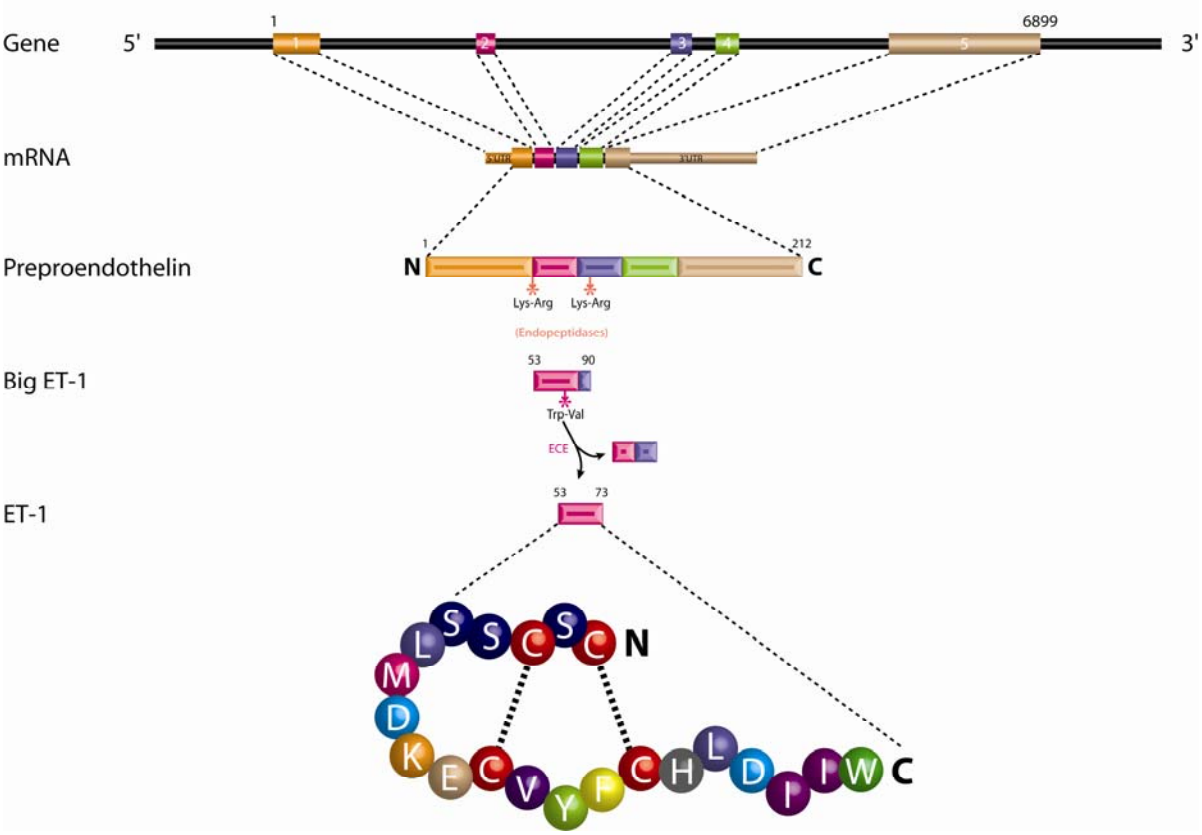

Figure 1-12. Overview of endothelin-1 gene and protein. The *edn1* gene contains 5 exons that code for mRNA. The protein product of *edn1* is a 212 amino acid prepropeptide. Endopepsidases cleave lysine (lys)- arginine (arg) residues to form the biologically inactive Big ET-1. The final cleavage step is mediated by endothelin converting enzymes (ECE) which cleaves at the trytophan (trp)-valine (val) residues to form the biologically active 21 amino acid peptide, ET-1. The secondary structure of ET-1 is shown on the bottom, indicating the disulfide bridges that form between cystine (C) residues.

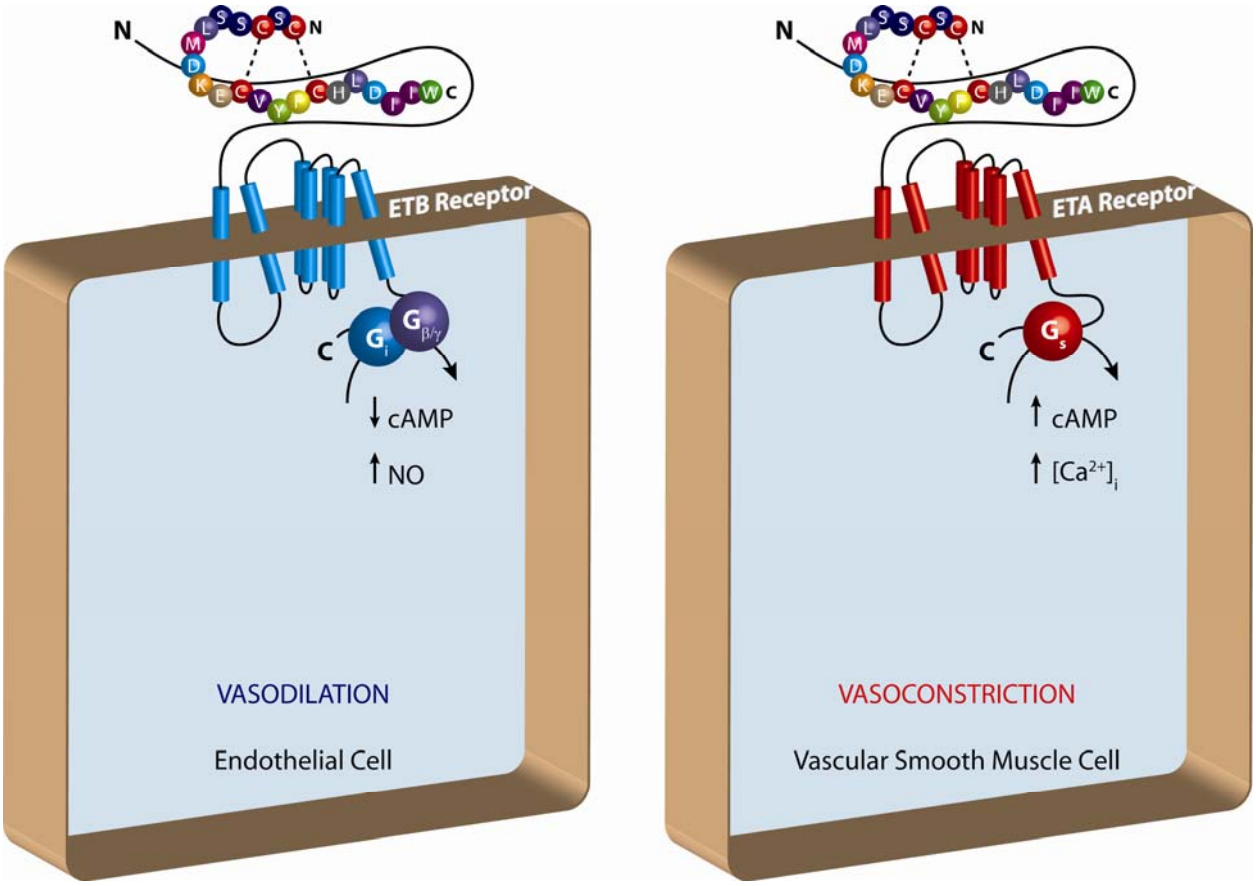

Figure 1-13. Overview of ET_A and ET_B receptor actions. In general, ET_B receptors (blue) are located on vascular endothelial cells are linked to vasodilatory signal transduction pathways that ultimately lead to an increase in nitric oxide synthase (NOS) and nitric oxide (NO). In contrast, ET_A receptors (red) are typically located on vascular smooth muscle cells and are linked to vasoconstriction through an increase in cAMP and intracellular Ca^+ concentrations.

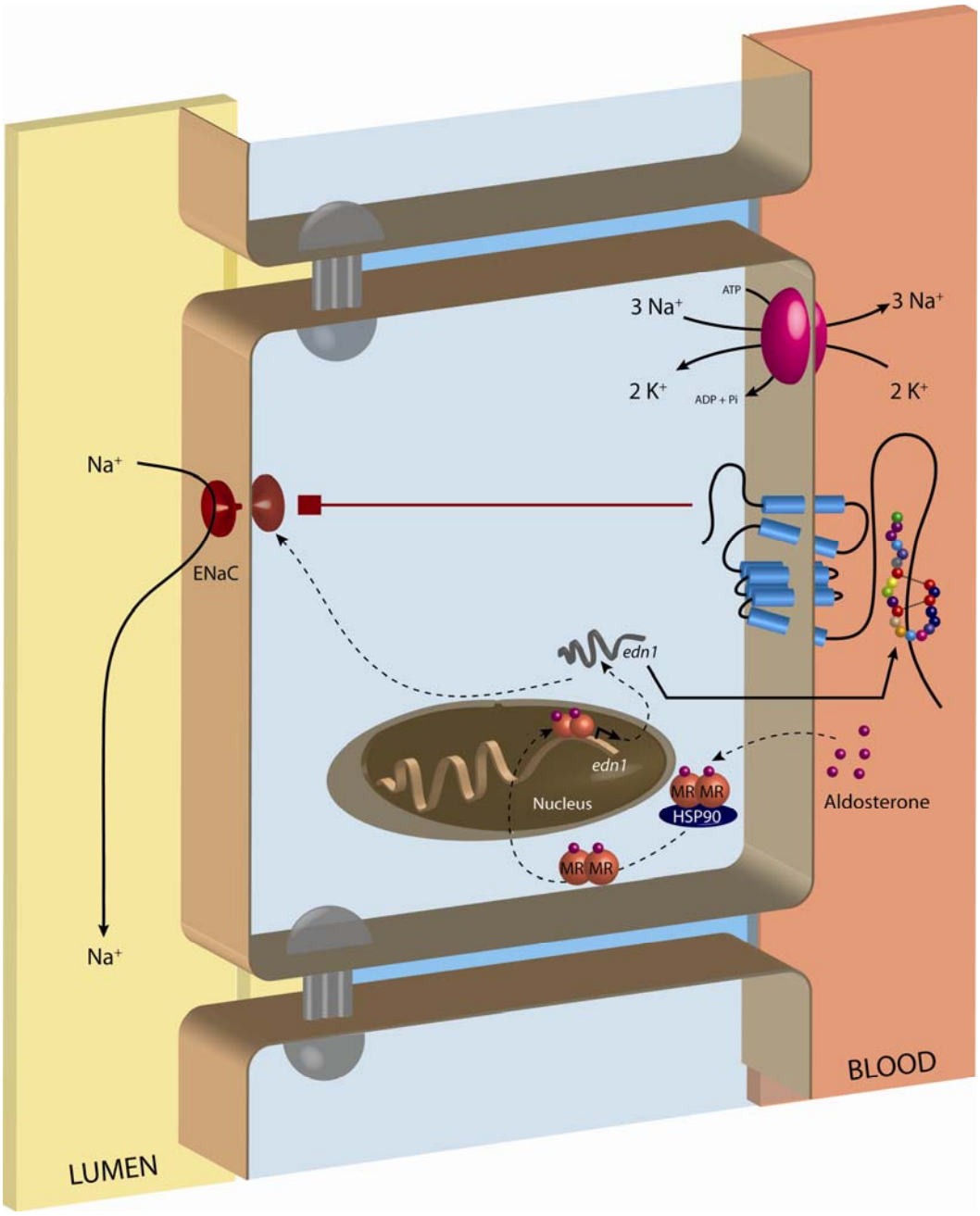

Figure 1-14. Hypothetical model of aldosterone-induced ET-1 action in the renal collecting duct. Aldosterone binds to MR in the cytosol and caused nuclear translocation, dimerization and activation of the *edn1* gene. *Edn1* is then translated into preproET-1 and processed to the active 21 amino acid peptide ET-1. ET-1 binds to basolateral ET_B receptors and via signal transduction pathway blocks ENaC activity.

CHAPTER 2
ALDOSTERONE STIMULATES ET-1 PEPTIDE IN THE RAT KIDNEY

Introduction

The *edn1* gene was previously identified as a novel aldosterone target gene in IMCD cells *in vitro* (Gumz et al., 2003). An interaction between aldosterone and ET-1 may have important implications for the regulation of Na^+ transport by ENaC, the major pathway for regulated Na^+ reabsorption in the distal nephron and collecting duct. In the kidney, aldosterone action results in an increase in *scnn1a* (αENaC) transcription and an increase in ENaC activity (Figure 1-6) that ultimately results in an increase in extracellular fluid volume and blood pressure (Masilamani et al., 1999; Mick et al., 2001). The importance of aldosterone in Na^+ and fluid homeostasis is underscored by the fact that defects in aldosterone or a component of the aldosterone-signaling pathway have been implicated in the pathogenesis of both monogenic and essential hypertension (Lang et al., 2005; Martinez-Aguayo and Fardella, 2009; Pravenec and Petretto, 2008).

In contrast to the action of aldosterone, the renal ET-1 system has direct inhibitory actions on Na^+ transport in the collecting duct. Several investigators have reported that ET-1 signals through ET_B receptors to rapidly reduce the open probability of ENaC in collecting duct cells *in vitro* and *in vivo* (Bugaj et al., 2008; Gallego and Ling, 1996; Gilmore et al., 2001). Published evidence further suggests that ET-1 may be responsible for the tonic inhibition of ENaC (Bugaj et al., 2008). Consistent with this concept is the observation that collecting duct cell specific *edn1* knockout mice exhibit salt sensitive hypertension, which appeared to be a consequence of excessive ENaC-dependent activity (Ahn et al., 2004). Studies have also shown that renal ET-1 stimulates natriuretic and diuretic compounds in the kidney including ET_B receptor-mediated release of nitric oxide (Stricklett et al., 2006) and cGMP (Edwards et al., 1992). Furthermore,

urinary ET-1 positively correlates with Na^+ intake in healthy humans (Modesti et al., 1998), but negatively correlates in patients with salt-sensitive hypertension (Hoffman et al., 1994). These data suggest that renal ET-1 mediates normal natriuretic responses in human, and that a reduction of renal ET-1 may lead to inappropriate Na^+ retention and hypertension. Despite these observations, a clear role for ET-1 in human hypertension remains to be elucidated (Dhaun et al., 2008). Given that the inhibitory actions of ET-1 on ENaC directly oppose the action of aldosterone, a functional interaction between aldosterone and ET-1 may represent an important negative feedback loop on aldosterone dependent Na^+ reabsorption in the collecting duct.

In order to test this hypothesis it was first important to determine if aldosterone stimulated *edn1* mRNA or ET-1 peptide in the kidney *in vivo*. Several attempts to quantify aldosterone-dependent *edn1* gene expression were unsuccessful. However, the characterization of basal *edn1* mRNA levels was accomplished. These studies revealed both regional heterogeneity and age-dependent effects on the expression of *edn1* as well as other genes involved in ET-1 or aldosterone signaling in the kidney. Finally, data reported here demonstrated for the first time that administration of aldosterone stimulated an increase in the concentration of the ET-1 peptide in renal inner medulla *in vivo*.

Materials and Methods

Animals

Male wild-type C57Bl/6J mice (Jackson Labs) and male Sprague Dawley rats (Harlan) were housed at the University of Florida Animal Care Services rodent facilities. Standard rodent chow (0.29% Na^+, 1.04% K^+; Teklab 8604) and tap water were provided ad libitum. All procedures adhered to the Animal Care Services guidelines and were approved by the University of Florida Institutional Animal Care and Use Committee.

Subcutaneous Osmotic Minipump Implantation

The implantation was performed with full sterile surgical technique under isoflurane anesthesia. A mid-scapular incision was made for the insertion of a hemostat, and the subcutaneous tissue was separated to create a pocket for the pump (Alzet Model 2001, Durect Corp., Cupertino, CA). Pre-primed pumps were loaded to deliver aldosterone (1.2 mg/kg body weight/24 h) or vehicle (polyethylene glycol 300). Pumps were weighed before and after filling to ensure proper dosing. Each pump was inserted into the pocket, delivery portal first and the incision was closed with wound clips.

Chronic Vascular Catheters and Plasma Aldosterone Determination

Adult rats were implanted with chronic indwelling vascular catheters according to the method of Qiu et al. (Qiu et al., 1995). Catheters were hand-fashioned using pulled tygon tubing and gas sterilized prior to implantation. Rats were anesthetized with inhaled isoflurane and given buprenorphine (0.05 mg/kg) as an analgesic. The surgical sites were shaved, cleaned with a 1:1 betadyne-ethanol mixture and isolated with sterile drapes. Ophthalmic ointment was applied to both eyes and body temperature was maintained with a circulating heating pad. Catheters were inserted into the left femoral artery and vein and held in place with non-absorbable 3.0 silk sutures. Blunt ended scissors were used to gently separate the skin from the fascia and a trocar was inserted to guide the catheters to the back of the neck where they were exteriorized. Exterior wounds were closed wound clips. Catheters were primed with 1:1 dextrose: heparin (1000 units) solution and monitored every day for integrity. After 4 days of recovery animals were given either an intraperitoneal (ip) or intravenous (iv) injection of vehicle (20 µl/kg ethanol) or aldosterone (1 mg/kg body weight). In all cases the final injection volume was 1 ml/kg body weight. A baseline blood sample (150 µl) was drawn just prior to hormone injection. Blood samples (150 µl) were also taken at 15, 30, 60, 90, 120, and 180 minutes (min) following the

injection. Each sample was immediately spun at 1000x *g* at 4 °C. Plasma was aliquoted, snap frozen in liquid nitrogen and stored at -80 °C until use. After each blood draw, red blood cells were reconstituted with 150 µl 13.4% sterile Ficoll and returned to the animal to prevent hemorrhage. Plasma samples were thawed on ice and aldosterone concentrations were determined using a acetylcholinesterase-conjugate based competitive enzyme immunoassay (EIA) (Cayman Chemical).

Intraperitoneal Aldosterone Administration

Rats were given aldosterone (1 mg/kg, ip) or vehicle (20 µl/kg ethanol, ip). After 1 - 24 h rats were anesthetized with inhaled isoflurane and kidneys were flushed by an *in vivo* aortic perfusion of ice-cold phosphate buffered saline (PBS) (pH 7.4) with the vena cava vented. Kidneys were removed and dissected into cortex, outer medulla, and inner medulla. Tissues were immediately snap frozen in liquid nitrogen and stored at -80 °C until use.

Measurement of Tissue ET-1

ET-1 was extracted from renal tissues using a protocol originally described by Yorikane et al. (Yorikane et al., 1993). Briefly, samples were homogenized in 1 molar (M) acetic acid containing 10 µg/ml pepstatin A protease inhibitor. Samples were incubated at 100 ºC for 10 min, chilled on ice, and centrifuged at 20,000x *g* at 4 ºC for 30 min. The supernatant containing the soluble protein fraction was removed and analyzed for ET-1 peptide levels by chemiluminescent enzyme linked immunosorbant assay (ELISA) (QuantiGlo®, R&D Systems). Immunoreactive ET-1 peptide was normalized to total protein content as determined by Bradford protein assay (Bio-Rad).

Quantification of mRNA Expression in Tissues.

Frozen tissue was thawed directly in TRIzol® (Invitrogen) and immediately homogenized for RNA extraction according to the manufacturer's instructions with the exception

that RNA-ethanol pellets were precipitated overnight at – 80 °C. RNA pellets were dissolved in RNase-free H_2O and stored at -80 ºC until analysis. RNA concentration was determined by spectrophotometric absorbance at 260 nm and RNA integrity was analyzed by visualizing 18S ribosomal RNA on an agarose gel. RNA (2 μg) was treated with DNase (Ambion) to remove genomic contamination and first-strand complementary DNA (cDNA) was synthesized with oligo dT, random hexamers and SuperScript™ III reverse transcriptase (Invitrogen). Resulting cDNAs (32 μg) were used as templates in duplicate quantitative real-time polymerase chain reactions (QPCR) (Applied Biosystems). Cycle threshold (C_T) values were normalized against β-actin (*actb*) and relative quantification was performed using the $\Delta\Delta C_T$ method (Livak and Schmittgen, 2001). All QPCR experiments were performed with TaqMan® primer/probe sets that have guaranteed 100% PCR efficiency over six logarithms of template DNA (Applied Biosystems, 2006). TaqMan® primer/probes for rat genes are indicated in Table 2-1 and TaqMan® primer/probe sets for mouse are indicated in Table 5-1.

Results

Axial Heterogeneity in ET-1 Pathway Gene Expression in the Rat Kidney

In order to better understand the role of ET-1 and its potential interaction with aldosterone in the kidney, initial studies were conducted to characterize the relative expression of ET-1 signaling genes as well as classical aldosterone response genes in the three major regions of the kidney; the cortex, outer medulla and inner medulla. Gene expression analyses were conducted on control kidneys isolated from adult rats that were vehicle treated for 1 h prior to tissue harvest. Levels of mRNA were determined by QPCR, normalized to *actb* (β-actin) and expressed as the fold change relative to cortical mRNA levels (Figure 2-1). The expression of *edn1* and the ET_B receptor (*etbr*) exhibited an increase in mRNA abundance along the cortico-medullary axis with the highest level of both mRNAs localized to the inner medulla (Figure 2-1). Similarly, the

expression of two established aldosterone response genes, *sgk1* and *per1*, were highest in inner medullary extracts. Only a minor increase in the expression of the endothelin converting enzyme-1 gene (*ece1*) was detected in the outer medulla.

To evaluate the potential heterogeneity in the expression of the α, β and γ subunits of ENaC, the different regions of the adult kidney were also evaluated for *scnn1a*, *scnn1b*, and *scnn1g* expression. The expression of each ENaC subunit gene was detected in the cortex, outer medulla and inner medulla (Figure 2-2), and this consistent with published reports (Frindt et al., 2007). The *scnn1b* and *scnn1g* genes exhibited a decrease in expression along the cortico-medullary axis. However, the highest level of *scnn1a* expression was unexpectedly in the outer medulla, not the cortex (Figure 2-2).

Age-Dependent Gene Expression

To identify the specific structures in the kidney responsible for the observed regional heterogeneity in gene expression, a series of experiments on individual microdissected nephron segments were proposed. However, the microdissection of individual nephrons from adult rats was not possible due to naturally occurring renal fibrosis. Accordingly, the approach was modified for use with younger rats (30 days old) and the optimized procedure can be found in Appendix A. Since the modified technique required the use of younger animals and *edn1* expression levels have been documented to change with age (Pedersen et al., 2007), it was first important to determine if there were age dependent effects on *edn1* expression in the kidney.

Experiments were conducted to evaluate the relative gene expression in cortical, outer medullary and inner medullary extracts from young rats (30 days old). In contrast to adult rats, *edn1* mRNA levels were highest in the outer medulla (Figure 2-3). The region pattern of *etbr, ece1* and *sgk1* mRNA expression was similar between the age groups. However, levels of *sgk1*

mRNA in the inner medulla were a remarkable 65.1 ± 1.5 fold higher compared to the cortex (Figure 2-3).

Gene expression profiles were also directly compared between young and adult rats (Figure 2-4). While the *etbr* gene was expressed at moderately 2.2 ± 0.1 fold higher level in the cortex of young animals, the most prominent differences in gene expression were observed in the outer and inner medulla. The *edn1*, *etbr*, *ece1* and *sgk1* mRNA levels were notably higher in outer medullary extracts from young animals compared to outer medullary extracts from adult rats (Figure 2-4). *Edn1* and *etbr* mRNA expression levels were 3.5 ± 0.1 and 3.2 ± 0.3 fold higher in young rat outer medullas, respectively. However, the largest difference in gene expression between the age groups was observed for *sgk1* in inner medullary homogenates, which was 15.5 ± 0.4 fold higher in young animals (Figure 2-4). These data indicated that basal gene expression profiles were different between young rats and adult rats.

Validation of Aldosterone Delivery Method

A primary goal of the animal experiments presented in this chapter was to determine if aldosterone and ET-1 interacted *in vivo*. The original report identifying *edn1* as an aldosterone target gene was conducted after 1 h of hormone stimulation *in vitro* (Gumz et al., 2003). Therefore, it seemed reasonable that *edn1* would be stimulated after an aldosterone treatment *in vivo*. In order to investigate the effect of an acute aldosterone treatment in rats, the hormone needed to be delivered either intravenous (iv) or intraperitoneal (ip). Therefore, preliminary experiments were conducted to evaluate the difference in aldosterone absorption or clearance rate following an iv or ip dosing (Figure 2-5). Adult rats were implanted with femoral catheters to allow for repeated blood sampling and animals were given an iv or ip injection of aldosterone (1 mg/kg) or vehicle (20 µl ethanol/kg). Plasma aldosterone concentrations were virtually the

same following either injection method (Figure 2-5). This data indicated that either delivery route was acceptable for studying acute aldosterone responses.

Aldosterone Dependent ET-1 Peptide Levels in the Kidney

Since the potential interaction between aldosterone and ET-1 *in vivo* has implications for renal Na^+ transport and blood pressure, initial experiments were conducted to determine both the basal and aldosterone dependent concentration of ET-1 in the rat kidney. Consistent with published reports, adult animals had basal levels of ET-1 that were approximately 50 times greater in the inner medulla compared to cortex or outer medulla (Table 2-2) (Kitamura et al., 1989). Since the original report identifying *edn1* as a novel aldosterone target gene was conducted at 1 h (Gumz et al., 2003), initial aldosterone experiments in rats were conducted at 2 h to allow time for translation and enzymatic processing to the biologically active ET-1 peptide. A 2 h aldosterone treatment resulted in a near doubling of ET-1 peptide concentrations in the inner medulla, but had no significant effect on the cortex or outer medulla (Figure 2-6).

To determine if ET-1 was stimulated at another time point, studies were conducted to evaluate inner medullary ET-1 peptide levels 1, 6 and 24 h after aldosterone treatment. However, inner medullary ET-1 peptide levels were increased only after 2 h of aldosterone treatment (Figure 2-7). Since plasma aldosterone levels indicated a supraphysiological spike following an ip dose of the hormone (Figure 2-5), studies were conducted to determine if a constant lower dose of aldosterone had an effect on renal ET-1. Rats were implanted with subcutaneous osmotic minipumps to deliver 50 μg/kg/h (1.2 mg/day) of aldosterone or vehicle (polyethylene glycol 300). After 24 h, inner medullary ET-1 levels were not statistically different in aldosterone treated animals (1.00 ± 0.15 fold change relative to vehicle, n=4).

Since inner medullary gene expression profiles were different between the age groups (Figure 2-4), similar experiments were conducted to analyze the effect of aldosterone on inner

medullary ET-1 peptide levels in young rats. The basal concentration of ET-1 in the inner medulla of young rats was similar to adults (Table 2-4). However, aldosterone treatment had no effect on inner medullary ET-1 peptide levels in young rats after 2 or 6 h of hormone treatment (Figure 2-8). Taken together, these data suggest that the renal ET-1 system if differentially regulated with age.

Aldosterone Dependent Gene Expression in the Rat Kidney

Studies conducted on adult rats indicated that ET-1 peptide levels were increased 2 h after a bolus injection of aldosterone. An increase in ET-1 peptide at this time point is consistent with an acute transcriptional response. Therefore, experiments were conducted to evaluate gene expression on adult rats treated with vehicle or aldosterone (1 mg/kg, ip) for 1 h. As shown in Figure 2-9, there was no detectable change in *edn1* mRNA in the cortex, outer medulla or inner medulla. However, moderate increases were observed for *sgk1* in each region and *scnn1a* in the cortex and inner medulla (Figure 2-9). The circadian rhythm genes *per1* and *per2* appeared to be stimulated in the inner medulla, but the change was not significant due to high standard error. There were no significant changes in the mRNA levels of βENaC or γENaC (*scnn1b* or *scnn1g*), the ET receptor genes (*etar* or *etbr*) or *ece1*. Similarly, no changes were observed in the expression of neuronal NOS (nNOS, *nos1*), endothelial NOS (eNOS, *nos3*), or the sirtuin 1 gene (*sirt1*).

Gene expression in the kidney was also analyzed after a 2 h aldosterone injection (Figure 2-10), 6 h aldosterone injection (Figure 2-11) and a 24 h aldosterone injection (Figure 2-12). After 2 h of aldosterone treatment, *sgk1* mRNA remained increased in the outer medulla, but had returned to level that not was significantly different from vehicle control levels in the cortex and inner medulla (Figure 2-10). An aldosterone-dependent second increase in *sgk1* mRNA was detected in the inner medulla after 6 h of aldosterone treatment (Figure 2-11). However, *sgk1*

mRNA levels in other regions or after 24 h were not significantly different in aldosterone treated animals. The expression of *scnn1a* was moderately increased in outer and inner medullary homogenates after 6 h, but not 24 h of aldosterone treatment (Figure 2-11 versus Figure 2-12). The most prominent of change in gene expression was observed for *per1* at 6 h, which demonstrated an approximate 3-fold increase in each region of the kidney.

The observation that *sgk1* and *scnn1a* mRNAs were not increased at higher levels at any of the time points tested was unexpected and suggested that the experimental approach was not adequate for studying an aldosterone response. Commonly, investigators will use adrenalectomized animals in order to observe aldosterone-dependent responses *in vivo* (Brennan and Fuller, 2006; Muller et al., 2003). Therefore, similar experiments were conducted on adrenalectomized rats (Harlan) treated with vehicle or aldosterone (1 mg/kg, ip) for 1 h. Adrenalectomy dramatically sensitized the kidney to aldosterone as indicated by greater than 5 fold changes in *sgk1* and *per1* expression in the cortex and outer medulla and greater than 2 fold changes in each gene in the inner medulla (Figure 2-13). Unfortunately, there was no detectable change in *edn1* mRNA in any region.

The absence of aldosterone-dependent *edn1* expression in adrenalectomized rats was particularly unexpected given that a recent report from Wong et al. showed a moderate, but significant increase in *edn1* mRNA in whole kidney homogenates from adrenalectomized rats injected with 0.5 mg/kg aldosterone (Wong et al., 2007). Only minor differences existed between the study in Figure 2-13 and the Wong study. Indeed, Wong and colleagues reported quantifying renal *edn1* mRNA by SyBr Green PCR. Therefore, *edn1* and *sgk1* primers homolgous to the sequences reported by Wong et al. were ordered (Table 2-3). These primers were used in a SyBr Green QPCR experiment to re-analyze the relative gene expression in the

adrenalectomized animals. *Sgk1* mRNA levels were roughly 2.5 fold higher in aldosterone treated adrenalectomized rats. However, *edn1* mRNA levels were actually reduced (0.62 ± 0.1 fold change relative to vehicle).

The inability to detect an increase in *edn1* mRNA using the same experimental parameters reported by Wong et al. indicated that selective RNA degradation may have interfered with the quantification of *edn1*. Indeed, *edn1* mRNA is known to be extremely unstable with a half-life of 15 minutes (Inoue et al., 1989). Consequently, a pilot experiment was conducted using a modified tissue preparation technique (personal communication with Dr. Donald Kohan, University of Utah, Salt Lake City, Utah). In these experiments, wild type adrenal-intact rats were given a 1 h injection of vehicle or aldosterone (1 mg/kg, ip). Kidneys were immediately removed, two coronal slices were made to allow faster freezing and the samples were snap frozen. Frozen tissues were thawed directly in ice cold TRIzol® (Invitrogen) and cortex, outer medulla and inner medulla regions were dissected. *Sgk1* mRNA levels were increased in the cortex and outer medulla (2.8 ± 0.1 and 2.7 ± 0.1 fold change, respectively, n = 3). However, there was no change in *edn1* expression in the cortex or outer medulla (1.1 ± 0.2 and 0.9 ± 0.1 fold change, respectively, n = 3). Furthermore, there was no change in *edn1*, *sgk1* or *etbr* expression observed in inner medullary homogenates (Figure 2-14).

A final experiment was conducted to determine if species-specific differences influenced the aldosterone-dependent expression of *edn1* in the kidney. Wild-type C57 Bl/6J mice, the background strain for the collecting duct cell specific *edn1* knockout mice, were given a bolus injection of vehicle or aldosterone (1 mg/kg, ip) and analyzed for gene expression after 1 h. Kidneys were removed, dissected and immediately processed for *edn1* or *sgk1* mRNA by QPCR. Cortical and outer medullary *sgk1* mRNA levels were 1.6 ± 0.3 fold and 2.0 ± 0.1 fold higher in

aldosterone treated animals, respectively. However, aldosterone had no effect on *edn1* mRNA levels in the cortex or outer medulla. Similarly, no changes in *edn1* or *sgk1* mRNA levels were observed in the inner medulla of aldosterone treated mice (Figure 2-15).

Discussion

Experiments presented in this chapter demonstrated for the first time that aldosterone-stimulated an increase in ET-1 peptide levels in the rat kidney *in vivo* and that the increase in renal ET-1 was exclusive to the inner medulla. Furthermore, basal mRNA expression of *edn1* and *sgk1* and basal ET-1 peptide levels were highest in the renal inner medulla in both young and adult rats. However, a direct comparison between the age groups revealed age-specific expression levels for *edn1*, *etbr* and *sgk1* in the kidney.

The failure of aldosterone to stimulate an increase in *edn1* mRNA was unexpected since aldosterone-dependent *edn1* expression has now been documented by several groups (Gumz et al., 2003; Stow et al., 2009; Wolf et al., 2006; Wong et al., 2007). In fact, Wong et al. reported a 50% increase in *edn1* mRNA after 1 h of aldosterone treatment in adrenalectomized Sprague Dawley rats. An attempt was made to reproduce the experimental conditions by Wong and colleagues. However, an increase in *edn1* mRNA was not detected in our hands. A possible explanation for this discrepancy is that *edn1* mRNA is known to be highly unstable with a half-life of only 15 min (Inoue et al., 1989). Most likely, the *edn1* mRNA signal was lost during sample preparation. In fact, this rationale is supported by the fact that experiments in Chapter 4 demonstrate that aldosterone stimulates *edn1* mRNA in acutely isolated rat IMCDs *ex vivo* (Stow et al., 2009).

The aldosterone-dependent increase in ET-1 peptide concentration in the renal medulla *in vivo* strongly supported the concept that aldosterone functionally interacted with ET-1 in the kidney. Moreover an analysis of the renal inner medulla gene expression profile revealed that all

of the necessary molecular machinery was present for aldosterone-induced ET-1 to mediate the proposed negative feedback loop on aldosterone. First, all three ENaC subunits (*scnn1a*, *scnn1b* and *scnn1g*) were expressed. Furthermore, the highest increase in aldosterone-dependent *scnn1a* expression was observed in the inner medulla of adrenal-intact, adult animals after 6 h of hormone stimulation. The expression of *sgk1* mRNA was markedly higher in the inner medulla compared to either the cortex or the outer medulla. This observation was consistent with published reports (Shigaev et al., 2000). Basal levels of *edn1* and *etbr* expression were also highest in the inner medulla. Again, these observations were consistent with the reported abundance of ET-1 and ET_B receptor protein levels in the kidney (Chen et al., 1993; Kitamura et al., 1989; Kohan, 1991; Pupilli et al., 1994). Finally, *per1* expression levels were also highest in the inner medulla (1.8 ± 0.3 fold higher relative to cortex). While the inner medullary *per1* expression data from this dissertation were recently published (Gumz et al., 2009a), the observed cortico-medullary heterogeneity in *per1* has not been previously reported.

Taken together, the renal inner medulla co-expressed ENaC and its modulators, *sgk1* and *per1*. This supported the concept that ENaC-dependent Na^+ transport occurred in the inner medulla and that the process could be regulated, at least in part, by Sgk1 and Per1 action. The inner medulla also expressed high levels of *edn1* and *etbr*, which suggested that an ET-1-ET_B receptor pathway was present in this region. Although an increase in aldosterone-dependent *edn1* mRNA was not detected for expected technical reasons, aldosterone did result in an increase in the biologically active ET-1 peptide in rat inner medullas *in vivo*. Therefore, it seemed reasonable that ET-1 would act through inner medullary ET_B receptors, resulting in ENaC inhibition and a decrease in aldosterone-dependent Na^+ transport.

Table 2-1. TaqMan® assays sets for QPCR on rat

Gene	Gene Product	Assay ID
edn1	ET-1	Rn00561129_m1
sgk1	Sgk1	Rn00570285_m1
scnn1a	αENaC	Rn00580652_m1
scnn1b	βENaC	Rn00561892_m1
scnn1g	γENaC	Rn00566891_m1
per1	Per1	Rn01325256_m1
per2	Per2	Rn0058158177_m1
ece1	ECE-1	Rn00585943_m1
etar	ET_A Receptor	Rn00561137_m1
etbr	ET_B Receptor	Rn00561129_m1
sirt1	Sirt1	Rn01428096_m1
nos1	NOS1 (nNOS)	Rn00583793_m1
nos3	NOS3 (eNOS)	Rn02132634_s1
actb	β-actin	4352931E
gapdh	Gapdh	4352338E

Table 2-2. Renal ET-1 peptide concentrations in adult rats

Kidney Region	ET-1 (pg/mg protein)
cortex	9.8 ± 0.8
outer medulla	12.0 ± 2.4
inner medulla	543.8 ± 112.2

Table 2-3. Primer sequences for rat SyBr Green QPCR

Gene	Primer Sequence
edn1	Forward: 5'- CTCTGCTGTTTGTGGCTTTC-3'
	Reverse: 5'- CCTCTGCCAGTCTGAACAAG-3'
sgk1	Forward: 5'- TAGCAATCCTCATCGCTTTC-3'
	Reverse: 5'- GAGTTGTTGGCAAGCAAGCTT-3'
actb	Forward: 5'- CACCCTGTGCTGCTCACC-3'
	Reverse: 5'- TCCATCACAATGCCAGTGG-3'

Table 2-4. Renal ET-1 peptide concentrations in young rats

Kidney Region	ET-1 (pg/mg protein)
cortex	8.0 ± 0.9
outer medulla	13.2 ± 1.9
inner medulla	407.2 ± 34.8

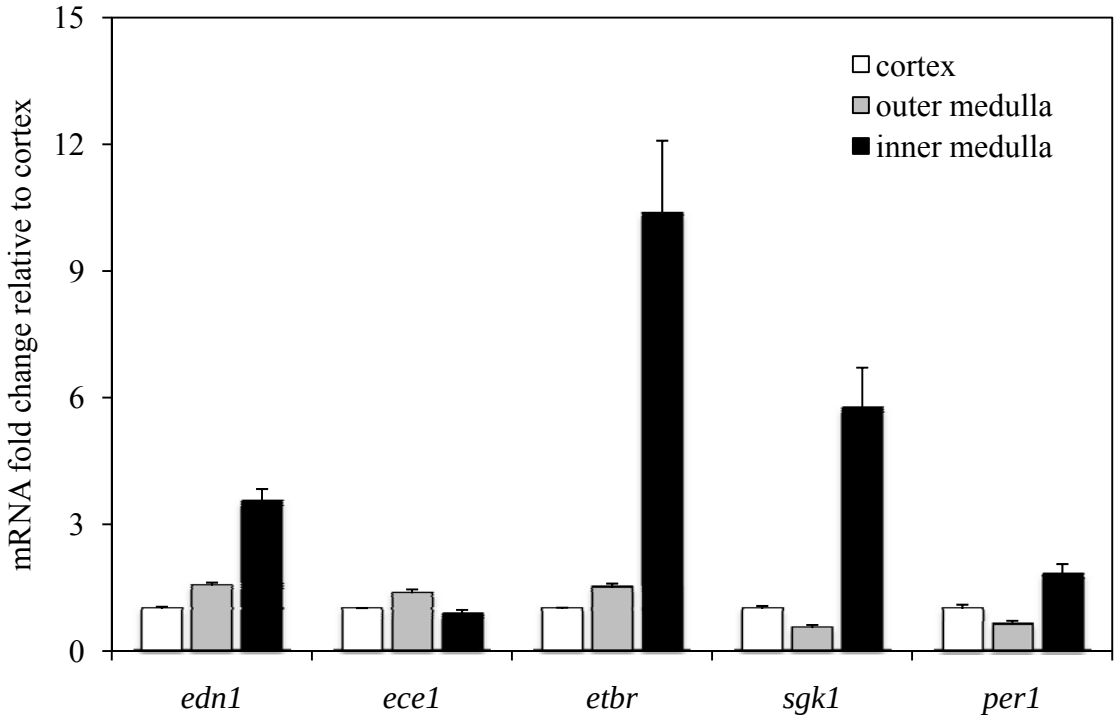

Figure 2-1. Relative mRNA expression of genes involved in ET-1 or aldosterone signaling in adult rat kidneys. Kidneys were isolated from 1 h vehicle (ethanol) treated adult rats, dissected into cortex, outer medulla and inner medulla and homogenized in TRIzol® (Invitrogen) for total RNA extraction. The cDNA was prepared and analyzed for the expression of each gene indicated by QPCR for the cortex (open bars), outer medulla (gray bars) and inner medulla (closed bars). Values were normalized to *actb* (β-actin) and are expressed as the mean fold change relative to cortex ± SE. (n=6)

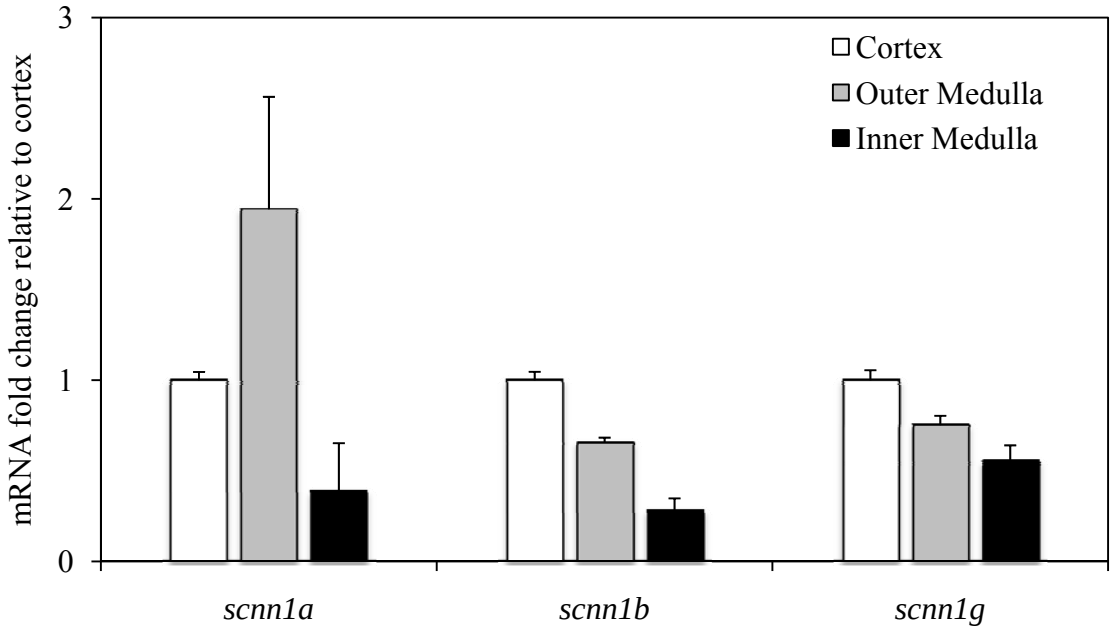

Figure 2-2. Relative mRNA expression of ENaC subunit genes in adult rat kidneys. Kidneys were isolated from vehicle treated controls rats, sectioned into cortex (open bars), outer medulla (gray bars) and inner medulla (closed bars) and homogenized for total RNA and QPCR analysis as described above. Values for *scnn1a*, *scnn1b* and *scnn1g* were normalized to *actb* and are expressed as the mean fold change relative to cortex ± SE. (n=6)

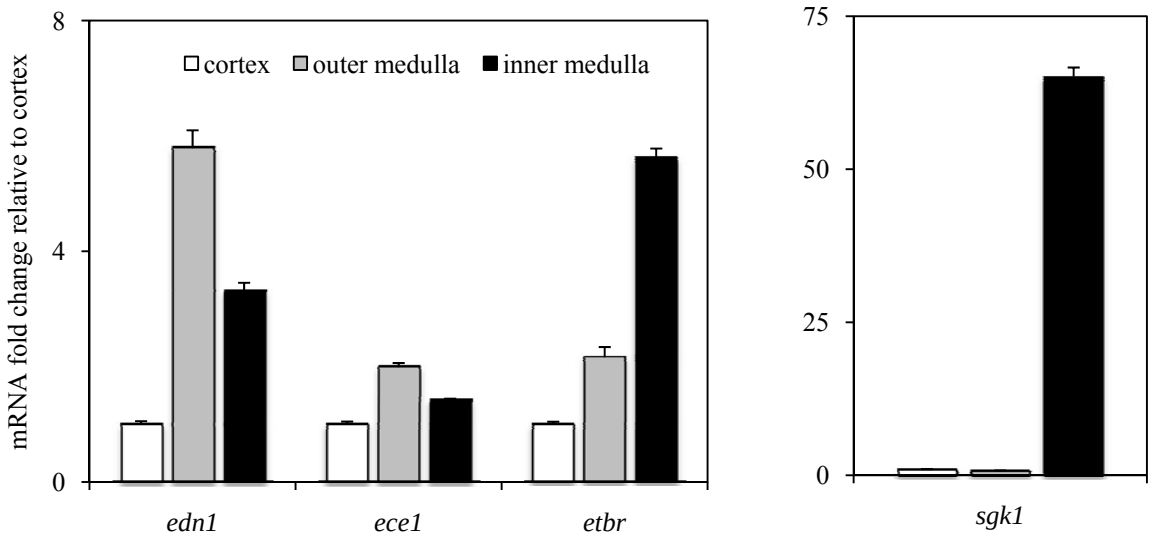

Figure 2-3. Relative mRNA expression genes involved in ET-1 or aldosterone signaling in young rats. Kidneys were harvested from young rats (30 days old) from a 1 h vehicle treated control group. Kidneys were sectioned and RNA was prepared as described above for QPCR analysis of cortex (open bars), outer medulla (gray bars) and inner medulla (closed bars). Values for *edn1*, *ece1*, *etbr* and *sgk1* were normalized to *actb* and are expressed as the mean fold change relative to cortex ± SE. ($n \geq 4$)

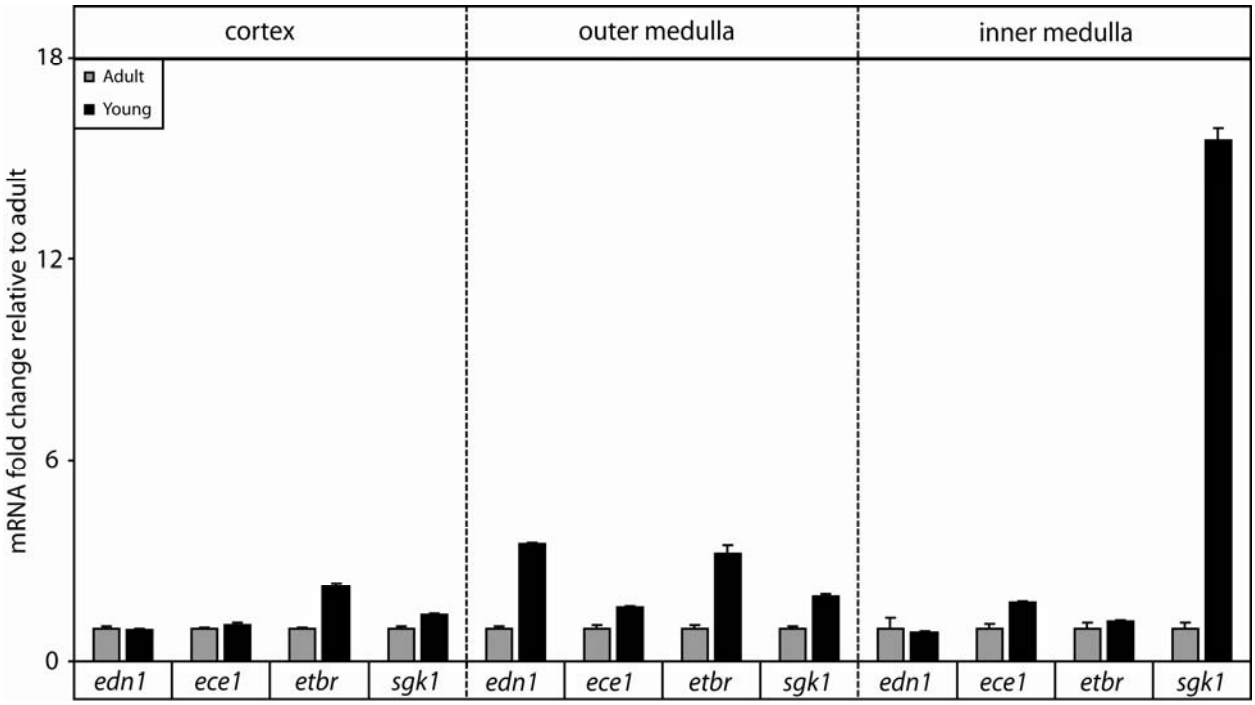

Figure 2-4. Effect of age on gene expression profiles in the rat kidney. Young and adult rat kidney samples were evaluated for the mRNA expression of *edn1*, *ece1*, *etbr* and *sgk1* genes by QPCR. Values were normalized to *actb*. Gene expression values for young animals were compared to adult values in the same region of the kidney. Values are expressed as mean fold change relative to adult ± SE. ($n \geq 4$)

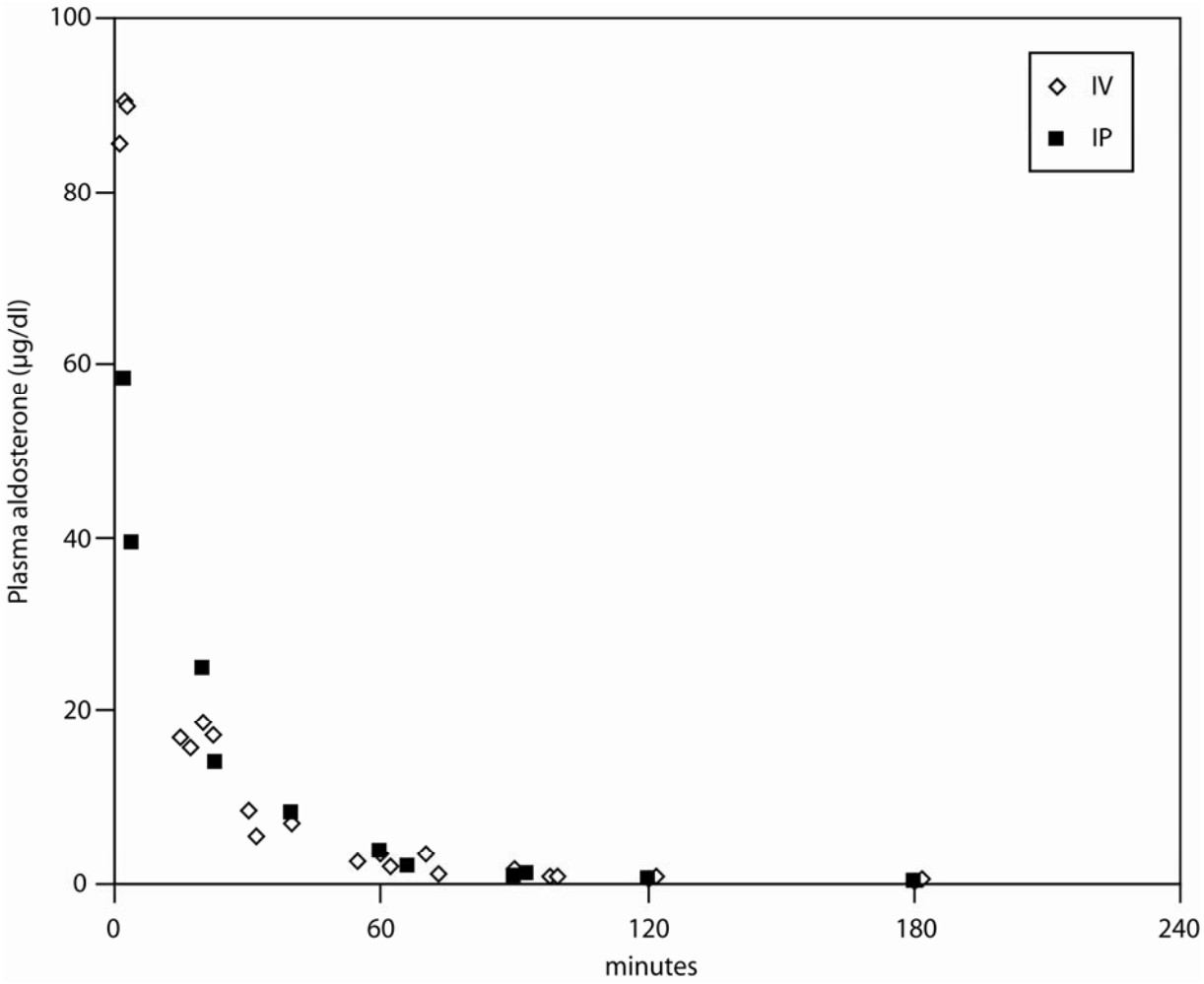

Figure 2-5. Validation of aldosterone delivery method in adult rats. Conscious chronically catheterized rats were given an intravenous (iv, open bars) or intraperitoneal (ip, closed bars) injection of aldosterone (1 mg/kg) and blood samples (150 µl) were collected at the time indicated for plasma aldosterone concentration determination by enzymatic immunoassay (Cayman Chemical). Plasma aldosterone values are expressed as µg/deciliter (dl). Time 0 indicates time of injection. (n=4)

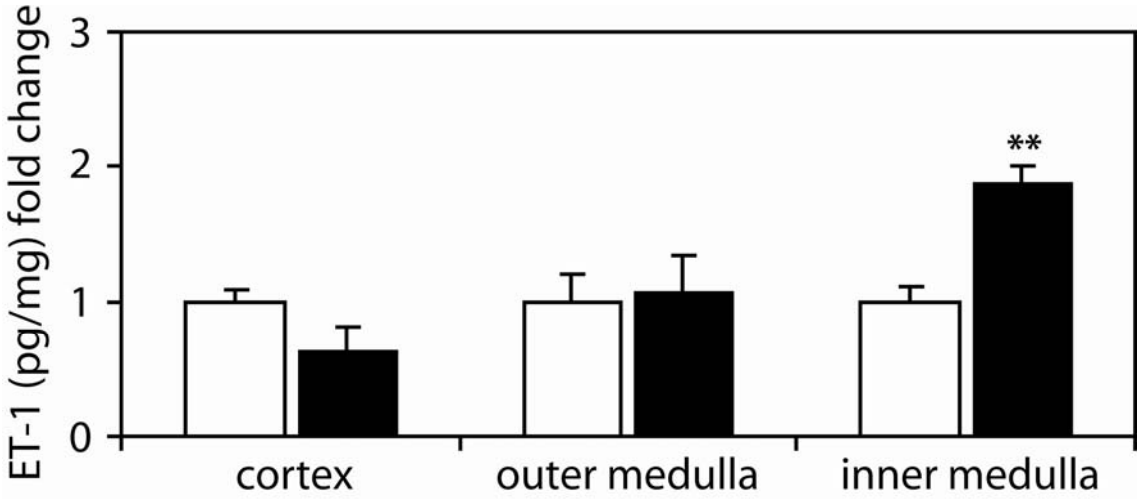

Figure 2-6. Effect of aldosterone on renal ET-1 peptide concentrations in adult rats. Rats were given an injection of vehicle (20 µl/kg ethanol, ip) (open bars) or aldosterone (1 mg/kg, ip) (closed bars). After 2 h rats were anesthetized with isoflurane and the kidneys were flushed via an *in vivo* aortic perfusion of ice-cold PBS (pH 7.4) with the vena cava vented. Kidneys were removed and dissected into cortex, outer medulla and inner medulla before being frozen in liquid nitrogen. Samples were thawed and protein was extracted in 1 M acetic acid plus 10 µg/ml pepstatin A. Renal ET-1 content was determined by ELISA (R&D Systems). Values were normalized to total protein and are expressed as mean fold change relative to vehicle ± SE ($^{**}p<0.005$, $n \geq 6$).

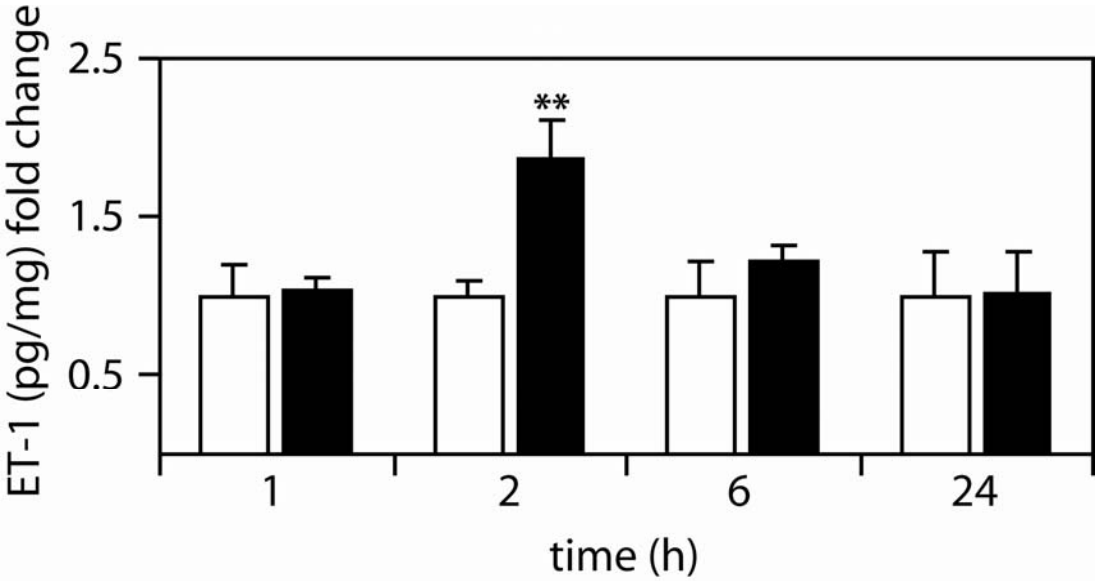

Figure 2-7. Effect of time on aldosterone-dependent ET-1 peptide levels in the rat inner medulla. Adult rats were given an injection (ip) of vehicle (open bars) or 1 mg/kg aldosterone (closed bars). Animals were sacrificed at the time indicated and kidneys were prepared as described in Figure 2-6. Inner medullary ET-1 content was assayed by ELISA (R&D Systems). Values were normalized to total protein and are expressed as mean fold change relative to vehicle ± SE ($^{**}p<0.005$, $n \geq 5$).

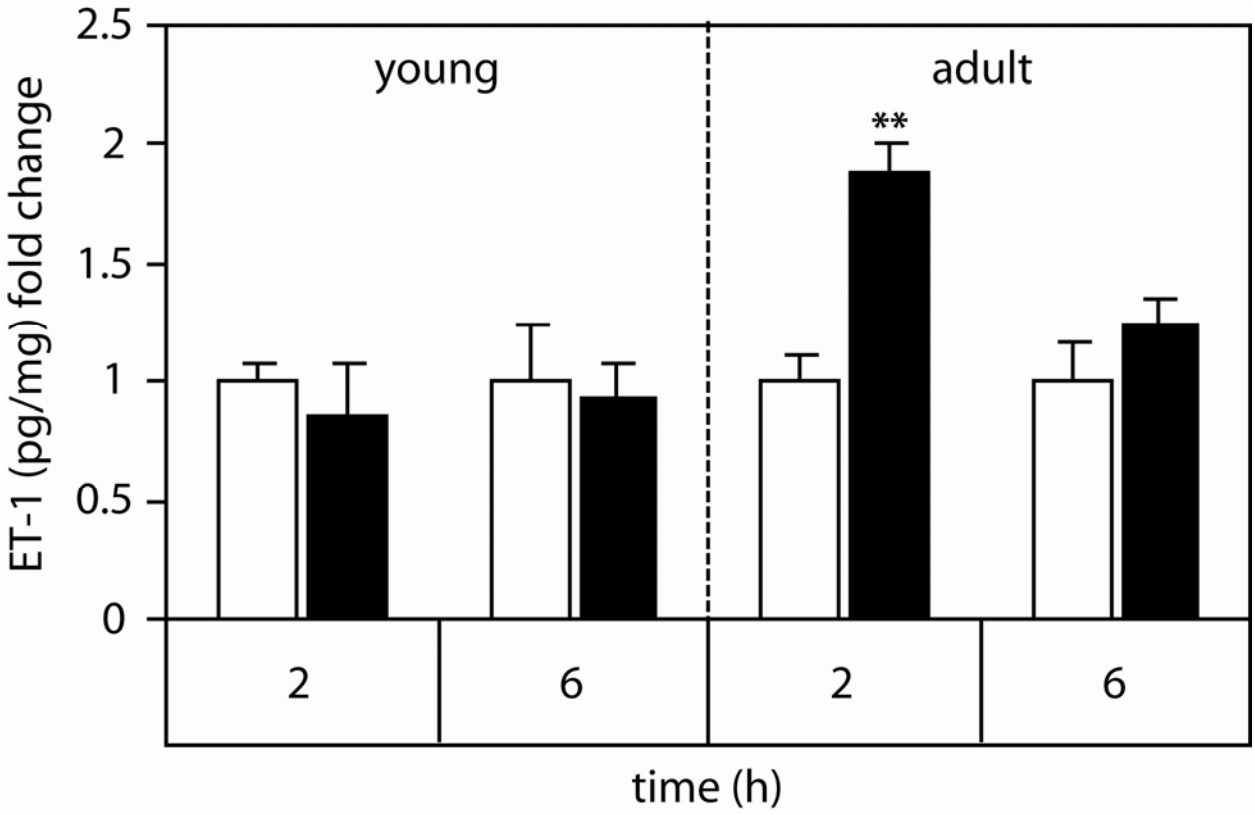

Figure 2-8. Effect of age on aldosterone-dependent ET-1 peptide levels in the inner medulla. Young rats (30 days old) were given an injection of vehicle (0.2% ethanol) (open bars) or aldosterone (1 mg/kg, ip) (closed bars). After 2 or 6 h kidneys were harvested as described above and inner medullary ET-1 content was assayed by ELISA and total protein concentrations were determined by Bradford assay. Values were normalized to total protein and are expressed as mean fold change relative to vehicle ± SE ($^{**}p<0.005$, $n \geq 5$).

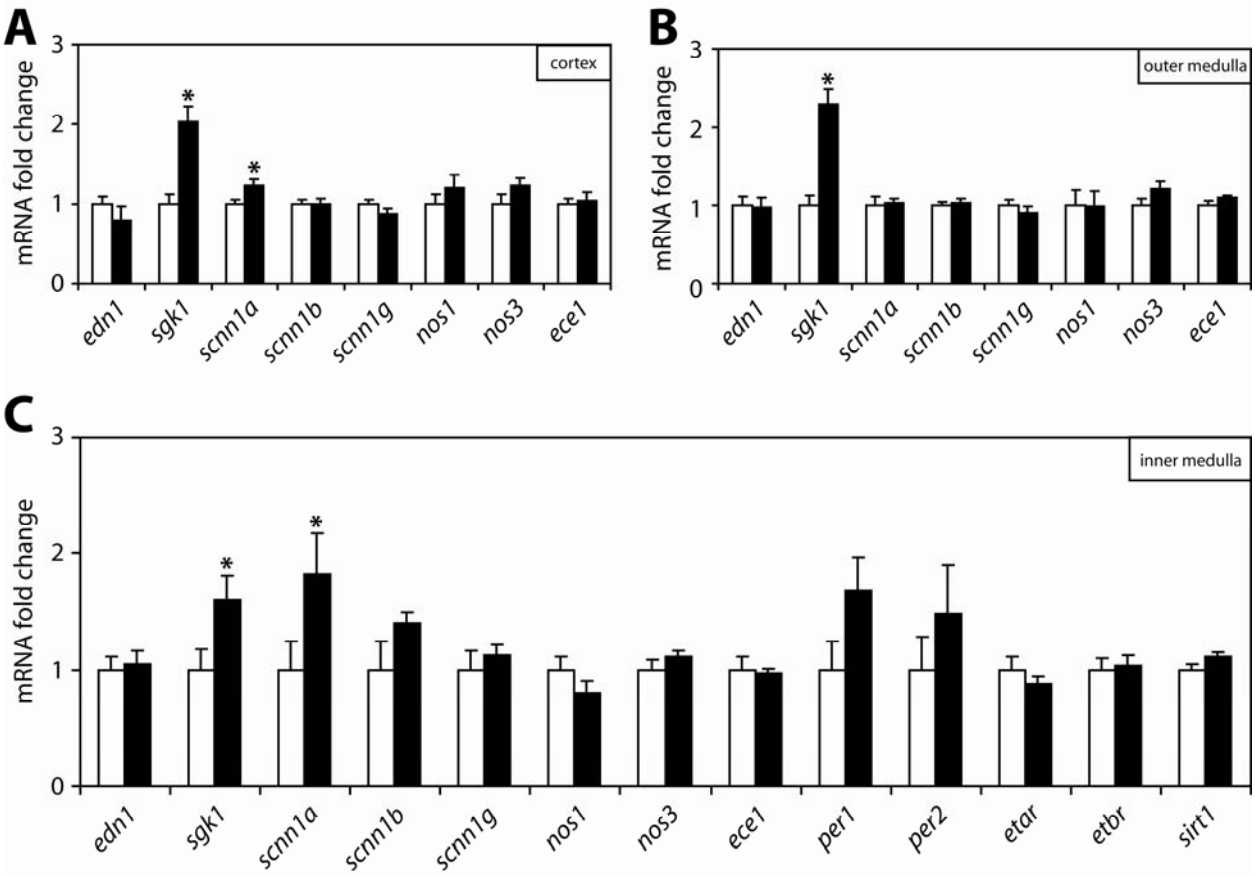

Figure 2-9. Effect of 1 h aldosterone treatment on gene expression in the adult rat kidney. Male Sprague Dawley rats were given a 1 h injection (ip) of vehicle (open bars) or aldosterone (closed bars). Rats were anesthetized with isoflurane and the aorta was cannulated for an *in vivo* aortic perfusion of PBS (pH 7.4) with the vena cava vented to flush the kidneys. Kidneys were removed and dissected into cortex, outer and inner medulla and snap frozen in liquid nitrogen. Frozen tissues were thawed and RNA was extracted for gene expression analysis using QPCR. Values were normalized against *actb* and are expressed at the mean fold change relative to vehicle ± SE. ($^{*}p < 0.05$, $n \geq 6$)

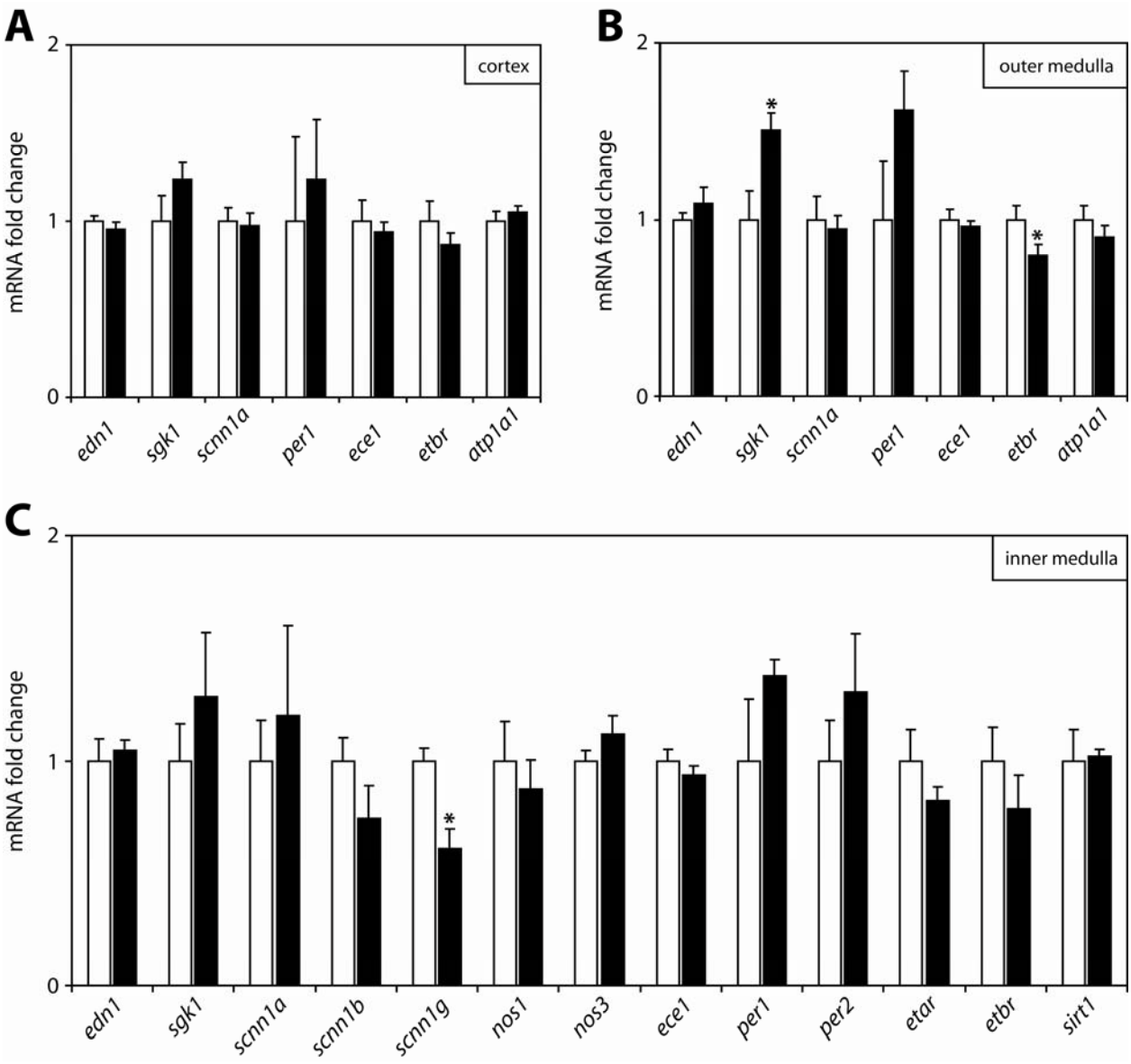

Figure 2-10. Effect of 2 h aldosterone treatment on gene expression in the adult rat kidney. Rats were given a 2 h injection (ip) of vehicle (open bars) or aldosterone (closed bars). Rats were anesthetized and the kidneys were flushed by an *in vivo* aortic perfusion of PBS (pH 7.4) with the vena cava vented. Kidneys were removed and dissected into cortex, outer and inner medulla and snap frozen in liquid nitrogen. Frozen tissues were thawed and RNA was extracted for gene expression analysis using QPCR. Values were normalized against *actb* and are expressed at the mean fold change relative to vehicle ± SE. ($^{*}p < 0.05$, $n \geq 6$)

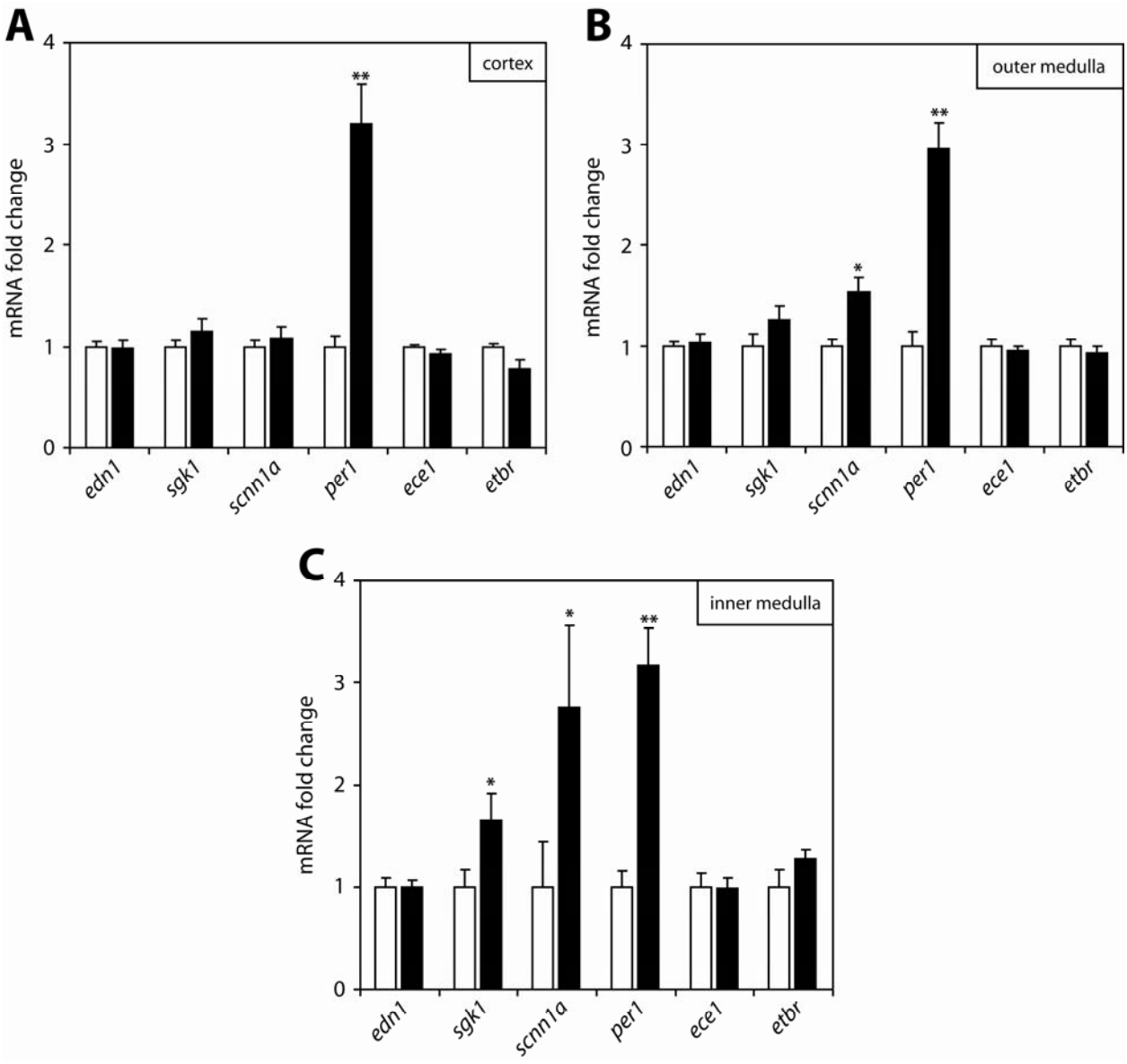

Figure 2-11. Effect of 6 h aldosterone treatment on gene expression in the adult rat kidney. Rats were given a 6 h injection (ip) of vehicle (open bars) or aldosterone (closed bars). Rats were anesthetized and kidneys were flushed by an *in vivo* aortic perfusion of PBS (pH 7.4) with the vena cava vented. Kidneys were removed and dissected into cortex, outer and inner medulla and snap frozen in liquid nitrogen. Frozen tissues were thawed and RNA was extracted for gene expression analysis using QPCR. Values were normalized against *actb* and are expressed at the mean fold change relative to vehicle ± SE. ($n \geq 6$)

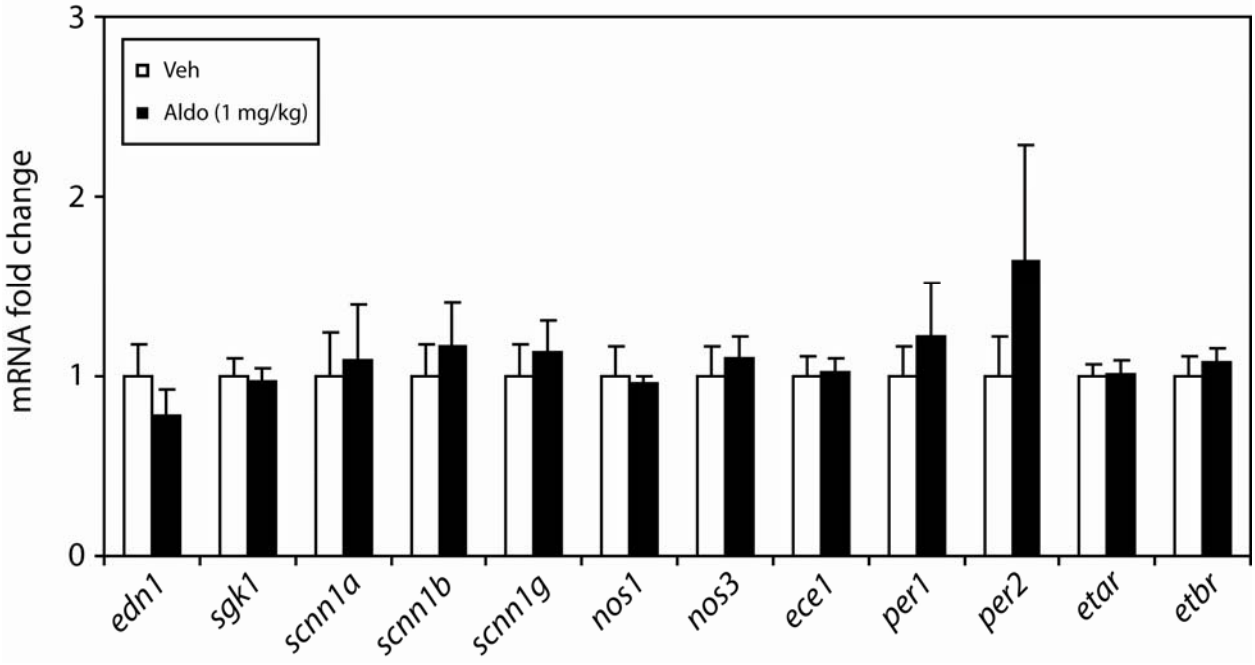

Figure 2-12. Effect of 24 h aldosterone treatment on gene expression in the adult rat kidney. Rats were given a 24 h injection of vehicle (open bars) or aldosterone (closed bars). Rats were anesthetized and the aorta was cannulated for an *in vivo* aortic perfusion of PBS (pH 7.4) with the vena cava vented to flush the kidneys. Kidneys were removed and dissected into cortex, outer and inner medulla and snap frozen in liquid nitrogen. Frozen tissues were thawed and RNA was extracted for gene expression analysis using QPCR. Values were normalized against *actb* and are expressed at the mean fold change relative to vehicle ± SE. ($^{*}p < 0.05$, $n \geq 6$)

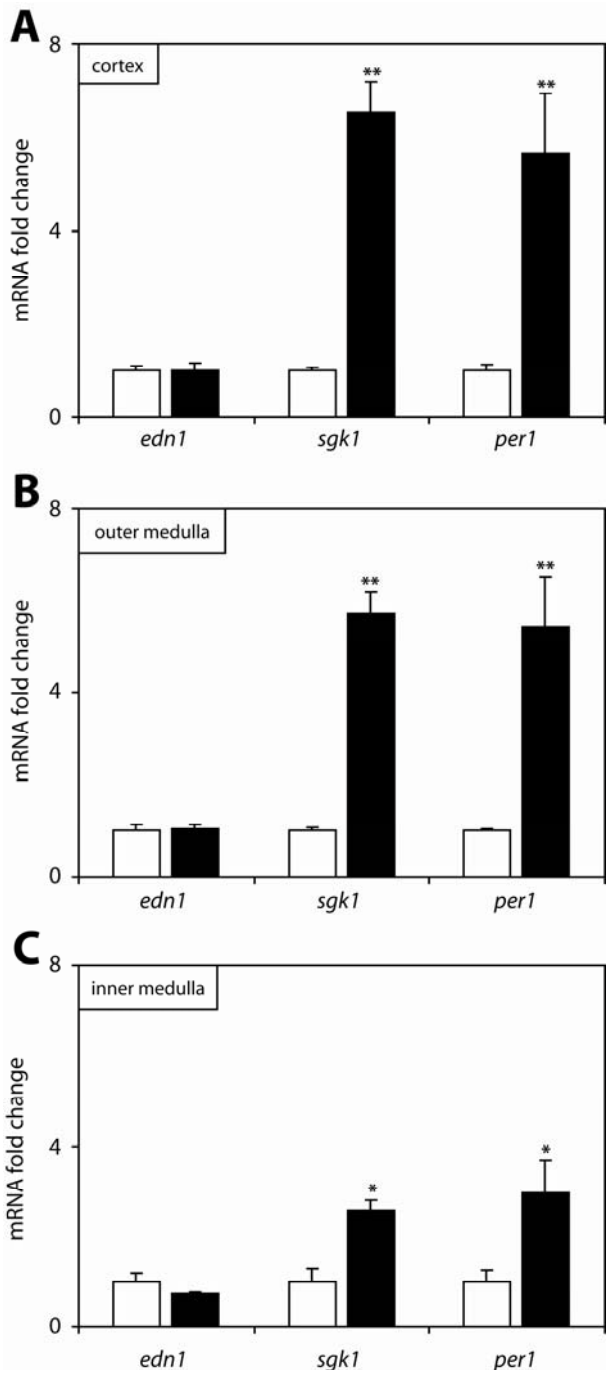

Figure 2-13. Effect of 1 h aldosterone treatment on gene expression in adrenalectomized rats. Bilaterally adrenalectomized rats were purchased from Harlan and maintained on 0.9% saline. Rats were given vehicle (open bars) or aldosterone (closed bars) for 1 h. Kidneys were prepared as described above and RNA extracted for gene expression analysis by QPCR. Values were normalized against *actb* and are expressed at the mean fold change relative to vehicle ± SE. (n = 5)

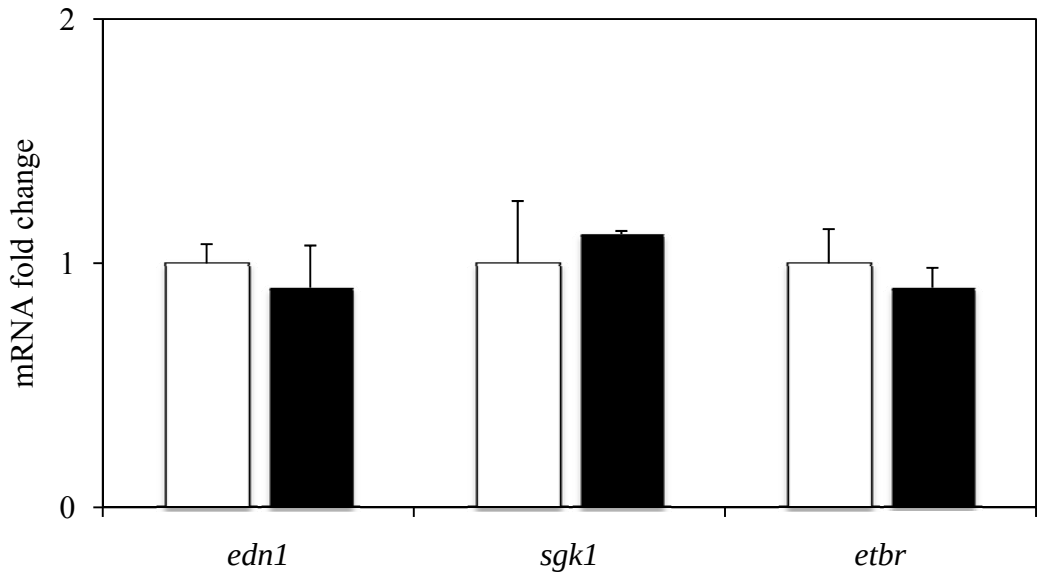

Figure 2-14. Effect of an alternative dissection method on aldosterone-dependent gene expression in adult rats. Rats were given an injection of vehicle (open bars) or aldosterone (closed bars). After 1 h rats were anesthetized and kidneys were removed. Two coronal slices were quickly made and the tissues were immediately snap frozen without further dissection. Frozen kidneys were thawed and inner medullas were dissected in TRIzol® (Invitrogen) at 4 °C. Isolated RNA was converted to cDNA and analyzed for *edn1*, *sgk1*, or *etbr* mRNA expression by QPCR. Values were normalized to *actb* and are expressed at the mean fold change relative to vehicle ± SE. (n=3)

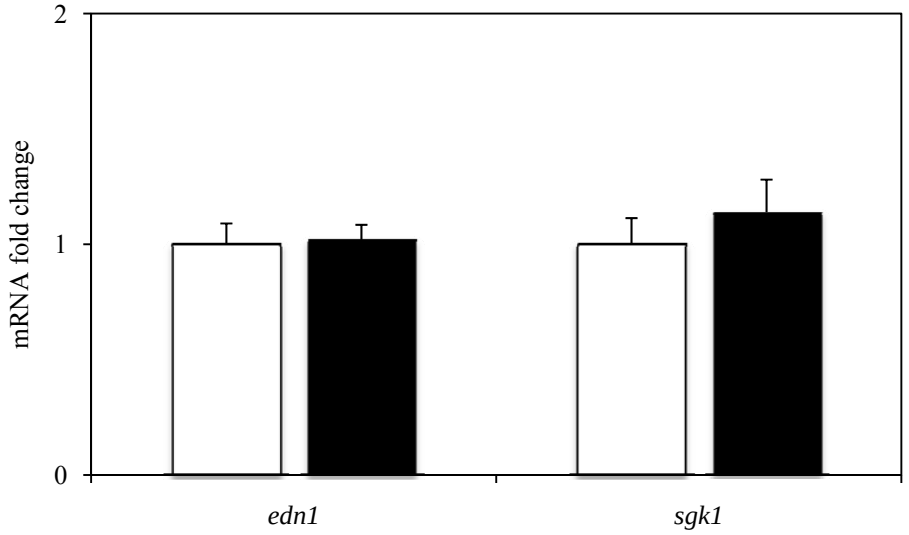

Figure 2-15. Aldosterone-dependent gene expression in wild-type C57 Bl/6J mice. Mice were given an injection of vehicle (open bars) or aldosterone (closed bars) for 1 h. The mice were anesthetized and kidneys were immediately removed and inner medullas were dissected and flash frozen in liquid nitrogen. Frozen tissues were thawed and RNA was extracted for gene expression analysis using QPCR. Values were normalized to *actb* and are expressed as the mean fold change relative to vehicle ± SE. (n=3)

CHAPTER 3
ENDOTHELIN-1 PROMOTER ACTIVITY IN LUCIFERASE REPORTER ASSAYS

Introduction

In 1961 spironolactone was patented by G.D. Searle & Co as the first pharmacological antagonist of MR (Cella and Tweit, 1961). In the years that followed MR blockade was quickly established as a cornerstone of antihypertensive therapy; however, researchers had only begun to appreciate the transcriptional mechanism of action (Horisberger and Rossier, 1992; Rossier, 1978). More than two decades passed between the time spironolactone was introduced to the market and the first aldosterone-regulated gene was identified. While the discoveries of aldosterone target genes involved in vectorial Na^+ transport such as *scnn1a* (αENaC) and *atp1a1* (Na^+/K^+ ATPase α1) provided insight into the molecular action of aldosterone, relatively few transcripts have been validated beyond these canonical response genes.

One problem in identifying new aldosterone target genes is the fact that most HREs deviate from the classical response element: 5'-GGTACAnnnTGTTCT-3' (Beato, 1989). In fact, this element was initially identified as the glucocorticoid response element that bound a GR-GR homodimer (Luisi et al., 1991). While it is known that both MR and GR bind this target sequence, it is not known if both receptors bind to non-canonical response elements or if these unique sequences somehow confer selective responses. Indeed, the ability of "degenerate" response elements to recruit hormone receptors and mediate transcription is an active area of investigation (Meijsing et al., 2009). Since it is not possible to identify aldosterone response genes by sequence analysis alone, several investigators have used gene microarray technology to identify new target genes. This approach led to the discovery of several genes including *gilz* (Soundararajan et al., 2005), *usp2-45* (Fakitsas et al., 2007), and the circadian rhythm gene *per1* (Gumz et al., 2003; Gumz et al., 2009a); all of these genes have been linked to stimulatory

effects on ENaC. Microarray analysis also identified *edn1* as an aldosterone-induced transcript (Gumz et al., 2003). The stimulation of *edn1* was of particular interest given that the ET-1 peptide is known to block Na^+ reabsorption by ENaC in aldosterone-target cells of the renal collecting duct (Bugaj et al., 2008). A mechanism for turning off MR-directed transcription or downstream MR signaling has not been identified. Thus, the *edn1* gene is an attractive candidate for mediating a negative feedback loop on aldosterone-driven Na^+ transport in the collecting duct.

Since aldosterone is known to act at the level of gene expression, we hypothesized that the *edn1* gene was under transcriptional regulation by MR. A useful technique to study the transcriptional regulation of a particular gene is an *in vitro* reporter assay. For this approach, a plasmid containing the promoter of interest is fused to a reporter gene and transfected into an appropriate cell line (Alam and Cook, 1990). A common reporter gene is the *Photinus pyralis* (firefly) luciferase (*luc*) gene because the gene is not found in mammalian cells and the enzyme requires no post-translational processing for activity and can be easily detected using a luminometer (de Wet et al., 1985; Wood et al., 1984). The enzyme luciferase catalyzes the bioluminescent oxidation of luciferin resulting in photon emission. Luciferase reporter assays have been successfully used to demonstrate the calcium-dependent repression of the *edn1* promoter (Strait et al., 2007). In addition, reporter assays have also been successfully used to study the hormonal regulation of several genes including *scnn1a* (Chow et al., 1999; Mick et al., 2001; Sayegh et al., 1999), *atp1a1* (Kolla et al., 1999), and phenylethanolamine N-methyltransferase (*pnmt*) (Ross et al., 1990).

In this chapter, the transcriptionally active region of the *edn1* promoter and 5'-UTR was cloned into the plasmid pEdn1 that contained a luciferase reporter gene. Sequence analysis

revealed several putative HREs in the promoter. The reporter gene driven by the *edn1* promoter demonstrated cell-line dependent expression levels in two collecting duct cell models. However, the pEdn1 reporter gene demonstrated excessive transcriptional activity that was not sensitive to hormone treatment. These studies indicated that an important transcriptional repressive mechanism was missing from the reporter assay conditions and the observations were critical for the development of experiments in later chapters.

Materials and Methods

Reagents

Stocks of aldosterone (Fluka), dexamethasone, spironolactone and RU486 (Sigma) were prepared at 1 mg/ml in 100% ethanol and stored at -20 °C until use. FuGENE 6 (Roche) and Lipofectamine 2000 (Invitrogen) transfection reagents were stored at 4 °C until use. KpnI, BglII, XbaI and XhoI restriction enzymes were purchased from Promega and stored at -20 °C.

Plasmids

The pGL3-Basic and pGL3-Pro vectors each contained a firefly luciferase gene and were purchased from Promega. The pGL3-Basic plasmid was promoterless and the pGL3-Pro plasmid contained a constitutively active SV40 promoter. The pRL-TK vector contained a *Renilla* luciferase gene driven by the herpes simplex virus thymidine kinase (HSV-TK) promoter and was also obtained from Promega. The pEdn1 construct was a kind gift of Dr. Brian Cain and contained 1990 bp of the murine *edn1* promoter and 5'-untranslated region (UTR) inserted upstream of the firefly luciferase gene. The pEdn1 construct was made in the following manner: The RP23-438J18 commercial bacterial artificial clone was purchased and PCR primers were designed to amplify a 1990 bp segment containing 1714 bp of the *edn1* promoter and 276 bp of the *edn1* 5'-UTR. The PCR product was ligated into the TOPO cloning vector (Invitrogen) and the nucleotide sequence determined by the University of Florida core facility. The sequence was

identical to that documented in GenBank. The *edn1* promoter fragment was excised from the cloning vector and transferred to the firefly luciferase reporter gene vector pGL3-Basic using KpnI and XhoI restriction enzymes. The resulting reporter vector was termed pEdn1. The pEdn1Δ1 plasmid was also a gift of Dr. Brian Cain. This deletion construct was made by digesting pEdn1 with BglII restriction enzyme to remove 194 bp from the *edn1* 5'-UTR and re-ligating the vector. Each of the above plasmids contained an ampicillin resistance gene for selection. Vectors were transformed into DH5α cells and grown overnight on Luria-Bertani (LB) agar plates containing 200 μg/ml ampicillin. A single colony was used to inoculate LB broth and propagate the plasmid. Plasmid DNA was prepared using the Maxiprep kit from Qiagen. Amplification of the appropriate plasmid was validated by restriction enzyme digestion (Figure 3-1) and concentrations were determined by ultraviolet absorption at 260 nm.

Cell Culture and Transient Transfection

The mpkCCD$_{c14}$ cells were a kind gift of Dr. Alain Vandewalle (Duong Van Huyen et al., 1998) and mIMCD-3 cells were purchased from American Type Culture Collection. Both cell lines were maintained in DMEM/F12 plus 10% FBS and 50 μg/ml gentamicin. It is important to note that most of the experimental conditions for transfection, cell culture, and hormone treatments were varied in an attempt to optimize the *in vitro* reporter system (Table 3-1). However, unless otherwise stated the general protocol was as follows: cells were seeded at 1 x 10^5 cells/ml into 12-well Transwell dishes (Corning) 24 h prior to transfection. One of the experimental firefly luciferase vectors (0.18 μg) was transiently cotransfected along with a fixed quantity of the transfection control pRL-TK vector (0.02 μg) into cells using FuGENE 6 (0.6 μl). At the time of transfection the media was changed to DMEM/F12 plus 10% charcoal-dextran stripped FBS (Invitrogen). After 24 h of transfection the cells were confluent and treated with

vehicle (ethanol), hormone (aldosterone or dexamethasone), or antagonists (spironolactone or RU486) for 1-48 hours (See Table 3-3).

Luciferase Reporter Assay

The Dual-Luciferase® Reporter Assay System was purchased from Promega. This assay measured the activities of two different luciferases, the firefly luciferase and the *Renilla* luciferase. The bioluminescent reaction catalyzed by the *Renilla* luciferase requires a different substrate, coelentrerate-luciferin. Therefore, its quantitation was used to normalize for transfection efficiency and cell viability. At the time of each luciferase assay, cells were treated with passive lysis buffer (Promega) and frozen at -80 °C for at least 1 h to ensure complete lysis. Cell lysates were thawed and gently transferred to a microcentrifuge tube. A pipette tip was used to gently scrape cells that remained attached to the bottom of the well to ensure complete sample transfer. Lysates were cleared by brief centrifugation and assayed according to the manufacturers instructions (Promega) using a SIRIUS Luminometer V2.2 set for a 2 second delay and a 10 second read time. Firefly values were normalized to Renilla values and are expressed as relative light units (RLUs) ± SE.

Results

Sequence Analysis of the *edn1* Promoter

Most aldosterone response genes have HREs located within 1000 bp upstream from the transcriptional start site (Derfoul et al., 1998; Kolla et al., 1999; Sayegh et al., 1999). Furthermore, the known regulatory elements in the *edn1* promoter are located in this proximal region (Figure 3-2). Therefore, 1990 bp of the *edn1* promoter and 5'-UTR were analyzed for potential MR binding sites using the Transcription Element Search Software (TESS) available online at http://www.cbil.upenn.edu/tess (Schug, 2003). Although the *edn1* promoter did not contain any elements that were 100% homologous to either the consensus 5'-

GGTACAnnnTGTTCT-3' (Beato, 1989), several putative HRE half-sites were identified (Table 3-1, Figure 3-2). Of note, visual inspection of the region surrounding the HRE1 half-site (5'-TGGTGGA-3') revealed that the sequence was directly repeated eight nucleotides downstream. These two adjacent half-sites likely form a complete HRE. Similarly, HRE2 (nucleotides -690 to -671) was identified by visual inspection. This element contained two half-sites separated by eight nucleotides and arranged as an inverted palindrome, which is the preferred orientation for hormone receptor binding (Luisi et al., 1991). Furthermore, the upstream half-site in HRE2 (5'-TGTACC -3') was homologous to the reverse complement of the consensus GR binding site. Of note, HRE2 (nucleotides -690 to -671) is immediately adjacent to a region identified by TESS analysis ($HRE2_{TESS}$) that may also contribute to the functionality of HRE2.

The *edn1* promoter was also analyzed using the online program EMBOSS (European Molecular Biology Open Software Suite) for its composition of cytosines (C) and guanines (G). Mammalian gene promoters typically have methylation-resistant regions containing a higher than expected percentage of adjacent Cs and Gs forming a "CpG island." EMBOSS was set to identify regions containing a C + G content of greater than 50% and a CpG frequency (observed/ expected) to 0.6. Four potential CpG islands were identified (Table 3-2). The location of CpG1 was consistent with a known CpG island that extends further into the *edn1* 5'-UTR (Vallender and Lahn, 2006). In addition, HRE2 and HRE1 were sandwiched in between two CpG islands supporting the hypothesis that these HREs are functional promoter elements.

Characterization of the pEdn1 and Control Luciferase Vectors

The 1990 bp region of the *edn1* promoter was cloned into the pGL3 reporter vector immediately upstream of the firefly luciferase gene (Figure 3-1A). The resulting vector containing the *edn1* promoter was termed pEdn1 and was 6871 bp in length. The pEdn1 vector was transformed into DH5α bacterial cells and propagated plasmid DNA was validated by

restriction enzyme digestion. The bottom panel on Figure 3-1A shows a representative agarose gel indicating the irregular migration pattern of the uncut circular plasmid. In addition, the gel shows that linearization of pEdn1 with either KpnI or XhoI resulted in a single migratory band that corresponded to the correct molecular weight (Figure 3-1A). Double digestion of pEdn1 with KpnI and XhoI yielded two bands corresponding to a 4787 bp fragment containing the luciferase gene and a 2084 bp fragment containing the *edn1* promoter region (Figure 3-1A, bottom panel).

The negative control pGL3-Basic and positive control pGL3-Pro vectors were also transformed into DH5α bacterial cells for vector amplification. Purified plasmids were validated by restriction enzyme digestion (Figure 3-1B-C). Both uncut plasmids exhibited irregular migration patterns, whereas KpnI digestions linearized each vector and resulted in the expected migration patterns for both pGL3-Basic (4818 bp) and pGL3-Pro (5010 bp) (Figure 3-1B-C). Double digestion of pGL3-Basic with KpnI and XbaI resulted in two bands of the expected size: 3081 bp and 1737 bp (Figure 3-1B). Similarly, double digestion of the pGL3-Pro with KpnI and XbaI resulted in two bands of the expected size: 3081 bp and 1929 bp (Figure 3-1C).

The *edn1* Promoter Construct is Transcriptionally Active in Collecting Duct Cells *In Vitro*

To determine if the cloned region of the *edn1* promoter was transcriptionally active, the pEdn1 plasmid was transiently transfected into mIMCD-3 cells for 24 h. In these pilot experiments, luciferase activity was more than 30 times greater in pEdn1 transfected cells than in pGL3-Basic transfected cells (Figure 3-3). Surprisingly, the *edn1* promoter was so strong that cells transfected with pEdn1 demonstrated luciferase activity that was approximately 4 times higher than cells transfected with the positive control pGL3-Pro (Figure 3-3). This observation was unexpected since pGL3-Pro contains a strong, constitutively active SV40 promoter that is known to generate high luciferase activity in mIMCD-3 cells (Bai et al., 2001; Zhang et al.,

2006). Taken together, these observations demonstrated that the region of the *edn1* gene cloned into pEdn1 contained a strong, transcriptionally active promoter. Furthermore, a deletion of 194 bp of the *edn1* 5'-UTR using the Bgl II restriction enzyme (pEdn1Δ1) had no significant effect on the level of reporter gene expression (Figure 3-3).

Since the pEdn1 plasmid contained a transcriptionally active *edn1* promoter and aldosterone is known to stimulate endogenous *edn1* mRNA levels in collecting duct cells (Stow et al., 2009) (Chapter 4), we hypothesized that aldosterone treatment would result in increased luciferase activity in pEdn1 transfected cells. Luciferase vectors were transfected into mIMCD-3 as well as mpkCCD$_{c14}$ cells, another aldosterone-responsive collecting duct cell line. After 24 h of transfection in the presence of 10% charcoal-stripped FBS cells were treated with 1 μM aldosterone or vehicle (ethanol) for 1 h. Unexpectedly, aldosterone treatment did not result in a further increase in luciferase activity in either cell line transfected with pEdn1 (Figure 3-4). However, the basal luciferase activity was notably higher in mIMCD-3 cells compared to mpkCCD$_{c14}$ cells (Figure 3-4). This observation is consistent with the expression levels of the endogenous *edn1* gene in each cell line (Stow et al., 2009) (Chapter 4).

Optimization of *In Vitro* Luciferase Assay

The observation that the pEdn1 luciferase gene was not responsive to aldosterone indicated that experimental parameters might not have been appropriate to reproduce aldosterone action. Several possibilities could explain why the initial reporter assays failed were addressed in the following experiments and are summarized in Table 3-3. First, aldosterone-dependent *edn1* expression is known to be biphasic (Gumz et al., 2003) and it was possible that the initial experiments were conducted at an inappropriate time point. To address this concern a 24 h time-course experiment was conducted on mIMCD-3 cells transfected with pEdn1, pEdn1Δ1, pGL3-Basic or pGL3-Pro in the presence or absence of 1 μM aldosterone (Figure 3-5). As expected,

transfection of the positive control pGL3-Pro resulted luciferase activity that was an average of 6.4 ± 0.2 fold higher than pGL3-Basic luciferase activity throughout the course of the experiment. Furthermore, pEdn1 transfection resulted in luciferase activity that was an average of 2.6 ± 0.1 fold higher than pGL3-Pro and an average of 15.9 ± 0.2 fold higher than pGL3-Basic throughout the 24 h time course. However, 1 μM aldosterone did not induce a further increase in luciferase activity in cells transfected with pEdn1 or pEdn1Δ1 at any time point (Figure 3-5). These data are consistent with observations made in Figure 3-3 and rule out a time-point issue.

Another potential pitfall of the original experimental design was that the endogenous *edn1* promoter may have been regulated by GR, not MR. I recently validated the original report by Gumz et al. showing that aldosterone-dependent mRNA expression of *edn1* was sensitive to MR antagonism as well as GR antagonism (Stow et al., 2009) (Chapter 6). Therefore, it was possible that *edn1* was controlled by GR and pEdn1 would be responsive to glucocorticoid hormones. To test this possibility, a time-course experiment was conducted in parallel to the one described above on mIMCD-3 cells. In this case, cells were treated with 1 μM dexamethasone or 1 μM dexamethasone plus 1 μM aldosterone. These treatments were also unable to stimulate a further increase in pEdn1 or pEdn1Δ1 luciferase activity (Figure 3-5).

The experiments conducted up until this point were all conducted with 1 μM aldosterone, which is the same concentration used in the original report identifying *edn1* as an aldosterone response gene (Gumz et al., 2003). Since aldosterone failed to stimulate an increase in reporter gene activity, it did not seem plausible that the assay failed due to supra-physiological hormone concentrations. However, a high hormone concentration is a common concern for *in vitro* experiments. Therefore, aldosterone and dexamethasone were tested at concentrations of 1 nM and 1 μM on pEdn1 transfected mIMCD-3 cells. Transfection of the positive control pGL3-Pro

and pEdn1 vectors resulted in higher luciferase activity compared to the negative control pGL3-Basic. However, there was no significant change in pEdn1 reporter gene activity in the presence 1 nM or 1 μM aldosterone or dexamethasone treatments for either 3 or 9 h (Figure 3-6).

Since we observed high basal activity of the pEdn1 luciferase gene and it was possible that our control assay reagents had residual steroid hormones at levels high enough to induce transcription of aldosterone response genes. Since serum would be the source of steroid contaminants, experiments were conducted in the presence of reduced serum or serum-free media preparations. However, the modifications made to the media (See Table 3-3) had no effect on aldosterone responsiveness of the pEdn1 reporter gene. To verify these results, 1 μM or the MR or GR antagonist spironolactone and RU486, respectively were added before or after transfection (Table 3-3). Again, the pEdn1 reporter gene consistently showed no response to hormones in the presence or absence of the hormone receptor antagonist. In conclusion, the transiently transfected pEdn1 plasmid cannot reproduce aldosterone-dependent gene expression in an *in vitro* reporter assay.

Discussion

The experiments presented in this chapter demonstrated that the 1990 bp region of the *edn1* gene cloned into pEdn1 plasmid contained a strong, transcriptionally active promoter *in vitro*. Sequence analysis of the *edn1* promoter region indicated five putative HREs; two of which were complete elements containing two half-sites. The pEdn1 reporter gene demonstrated higher basal expression in mIMCD-3 cells compared to mpkCCD$_{c14}$ cells, which is consistent with the endogenous *edn1* expression in each cell line (Stow et al., 2009) (Chapter 4). However, the pEdn1 reporter gene activity was so high that it surprisingly exceeded the reporter activity from the positive control pGL3-Pro plasmid that contained an SV40 promoter. The pEdn1 reporter

gene was also unexpectedly insensitive to aldosterone or dexamethasone and was not affected by hormone receptor blockade.

Aldosterone studies were conducted on both mIMCD-3 and mpkCCD$_{c14}$ cells transfected with pEdn1. The reporter gene did not respond to aldosterone treatment in either cell line, which is in contrast to the reported hormone responsiveness of the endogenous *edn1* gene in both cell lines (Stow et al., 2009). However, the difference in the overall levels of luciferase activity between mIMCD-3 and mpkCCD$_{c14}$ cells lines was consistent with the difference between the endogenous *edn1* gene expression in the respective portions of the collecting duct. Therefore, the differences in pEdn1 activity between mIMCD-3 and mpkCCD$_{c14}$ cells was most likely due to differences in available transcriptional machinery in each cell line.

The observed inability of aldosterone to stimulate a further increase in pEdn1 reporter gene activity was unexpected. Indeed, the original microarray study that identified *edn1* gene as an early aldosterone response gene was conducted in mIMCD-3 cells, the same cell line used in these studies (Gumz et al., 2003). The reported studies were conducted using 1 μM aldosterone; a concentration that was also tested in these studies. Furthermore, this original report also validated aldosterone stimulation of *edn1* using real-time QPCR and Northern blot analysis using comparable conditions. Moreover, I will report aldosterone regulation of the endogenous *edn1* gene in IMCD cells *ex vivo* and in both mIMCD-3 and mpkCCD$_{c14}$ cells in the following chapter (Stow et al., 2009) (Chapter 4). All of these data support the concept that the *edn1* promoter is under direct regulation by aldosterone and hormone receptors.

Differences in hormone-dependent reporter gene activity and the endogenous gene have been observed for other genes such as *pnmt* (Ross et al., 1990). Several possibilities may account for the discrepancy between the aldosterone-responsiveness of the pEdn1 reporter gene and the

endogenous *edn1* gene. First, the aldosterone responsive element may reside outside of the 1990 bp cloned into pEdn1. However, most aldosterone responsive HREs are located within 1000 bp of the transcriptional start site (Kolla et al., 1999; Mick et al., 2001). Furthermore, the pEdn1 reporter gene was transcriptionally active indicating that a functional promoter was cloned into the vector. In fact, the excessive promoter activity could be explained if the assay conditions lacked an important inhibitory transcription mechanism. For example, the *edn1* gene may be controlled by a negative enhancer element that resides outside of the 1990 bp region cloned into the reporter vector.

Another explanation for excessive pEdn1 reporter gene activity and a notable disadvantage of *in vitro* reporter assays is that the DNA in the promoter construct does not reflect the endogenous gene environment in the context of eukaryotic chromatin. Transiently transfected plasmids will not assemble histones as the endogenous gene. The association of histones and the packaging of eukaryotic DNA into chromatin results in transcriptional repression since the DNA is no longer accessible to transcription factors (Struhl, 1999). The lack of properly associated histones with pEdn1 could leave the *edn1* promoter freely accessible to transcription factors in the nucleus. This concept is supported by the differences in reporter gene activity observed in mIMCD-3 and mpkCCD$_{c14}$ cells. Furthermore, steroid receptors play a role in chromatin remodeling (Truss et al., 1995) and MR is known to associate with several chromatin remodeling complexes (Pascual-Le Tallec and Lombès, 2005). One way to circumvent this issue is to create a stably transfected cell line such that pEdn1 would integrate into the genome and associate with histones. However, this approach may also have technical issues depending on where pEdn1 inserts into the genome. Vector integration often occurs in areas of transcriptionally active euchromatin and pEdn1 may still exhibit excessive reporter gene activity. Therefore, the better

experiment is to test the aldosterone responsiveness of the endogenous *edn1* gene in the context of the native chromatin. This will be explored in Chapter 4.

Table 3-1. Putative HREs in the murine *edn1* promoter

HRE	Sequence	Position	Identification Method
HRE0	5'- AGAACTG-3'	-15 to -9	TESS
HRE1	5'- TGGTGGAaggggtggTGGTGGA -3'	-572 to -551	TESS: -572 to -566 half-site Visual inspection: -557 to -551 half-site
$HRE2_{TESS}$	5'- TGTTGTTGTT -3'	-670 to -661	TESS
HRE2	5'- TGTACCtgacaaaaCCACAT -3'	-690 to -671	Visual inspection
HRE3	5'- TGTGCCT -3'	-1255 to -1249	TESS
HRE4	5'- TGTTGTT -3'	-1351 to -1345	TESS
HRE5	5'- AGTTGTT -3'	-1641 to -1635	TESS

Table 3-2. Potential CpG islands in the murine *edn1* promoter

CpG Island	Position	Detection Method
CpG1	-49 to +145	EMBOSS
CpG2	-215 to -132	EMBOSS
CpG3	-769 to -719	EMBOSS
CpG4	-903 to -852	EMBOSS

Table 3-3. Experimental parameters tested in luciferase assays.

Parameter Affected	Potential Pitfall	Experimental Modification
Time point	Aldosterone response is biphasic	24 h time course conducted
Hormone treatment conditions	Inappropriate aldosterone dose	1 nM and 1 μM aldosterone tested
	edn1 regulated by GR	1 nM and 1 μM dexamethasone tested
	edn1 regulated by MR, but not GR	1 μM aldosterone + 2 μM RU486 (GR antagonist)
	edn1 regulated by GR, but not MR	1 μM dexamethasone + 2 μM spironolactone (MR antagonist)
	edn1 regulated by both MR and GR	1 μM Dexamethasone + 1 μM aldosterone tested
Cell culture medium	Cell culture reagents have contaminating hormones causing pEdn1 reporter gene activity	10% charcoal-dextran stripped FBS 0.2% charcoal-dextran stripped FBS 0% FBS Opti-MEM (Gibco), a serum free transfection medium Serum free plus 5 μg/ml transferrin, 50 μg/ml gentamycin, 5 nM triiodothyronine, 50 nM hydrocortisone, 5 μg/ml insulin, 10 nM sodium selenite, and 1% (w/v) bovine serum albumin (BSA) (hydrocortisone and BSA removed after 6 h transfection) 1-2 μM spironolactone (MR antagonist) added before or after transfection 1-2 μM RU486 (GR antagonist) added before or after transfection
Transfection conditions	Inadequate transfection	FuGene6 (6-24 h) Lipofectamine 2000 (24 h)

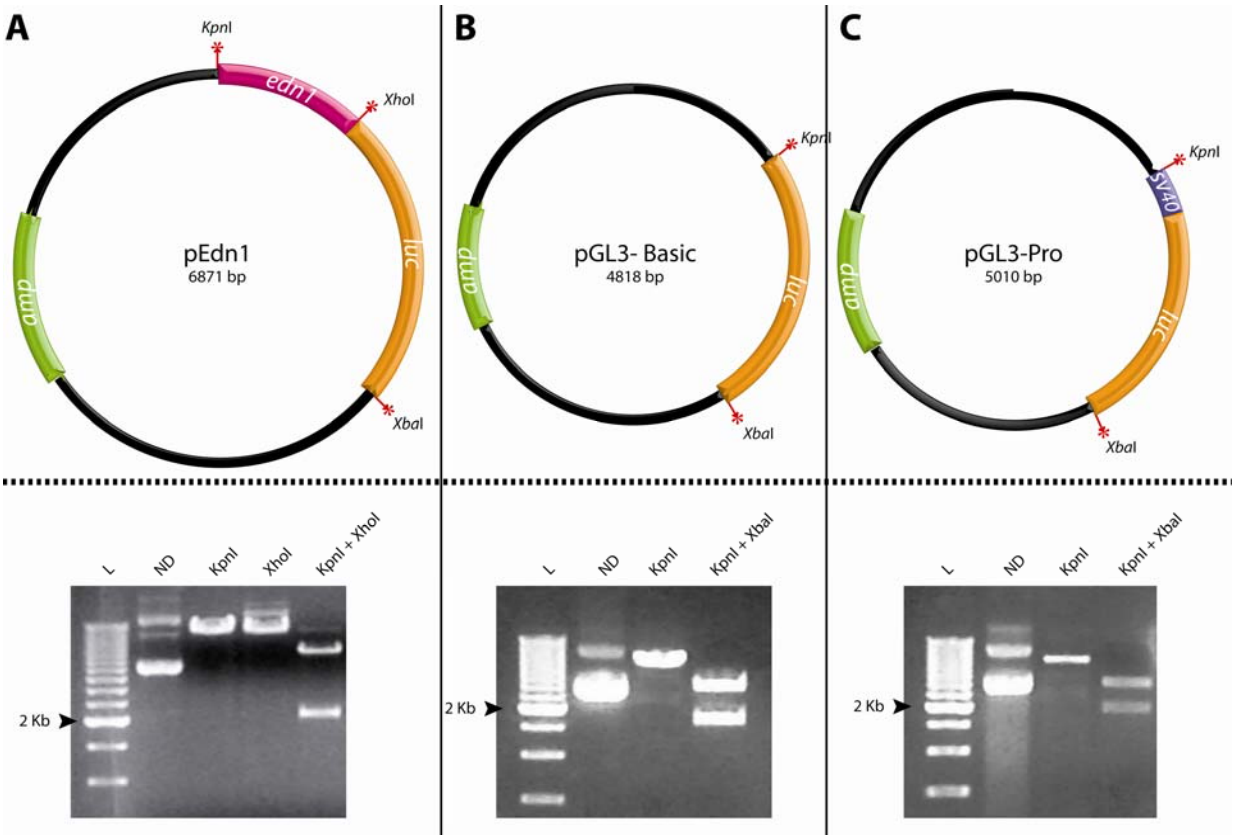

Figure 3-1. Map of luciferase vectors. A) The pEdn1 vector contained 1990 bp fragment of the *edn1* promoter. A representative agarose gel is shown below the vector map. Lanes correspond to pEdn1 that was not digested (ND), linearized with Kpn1 or XhoI individually, or double digested with Kpn1 and Xho1. The latter double digestion resulted in the excision of the *edn1* promoter insert. B) Vector map of the negative control pGL3-Basic plasmid that lacks a functional promoter. A representative agarose gel is indicated below the map showing both the digestion with Kpn1 and the double digestion with Kpn1 and Xba1. C) Vector map of the positive control pGL3-Pro vector contains an SV40 promoter. Digestion with Kpn1 linearized the vector and codigestion with Kpn1 and Xba1. (L, ladder)

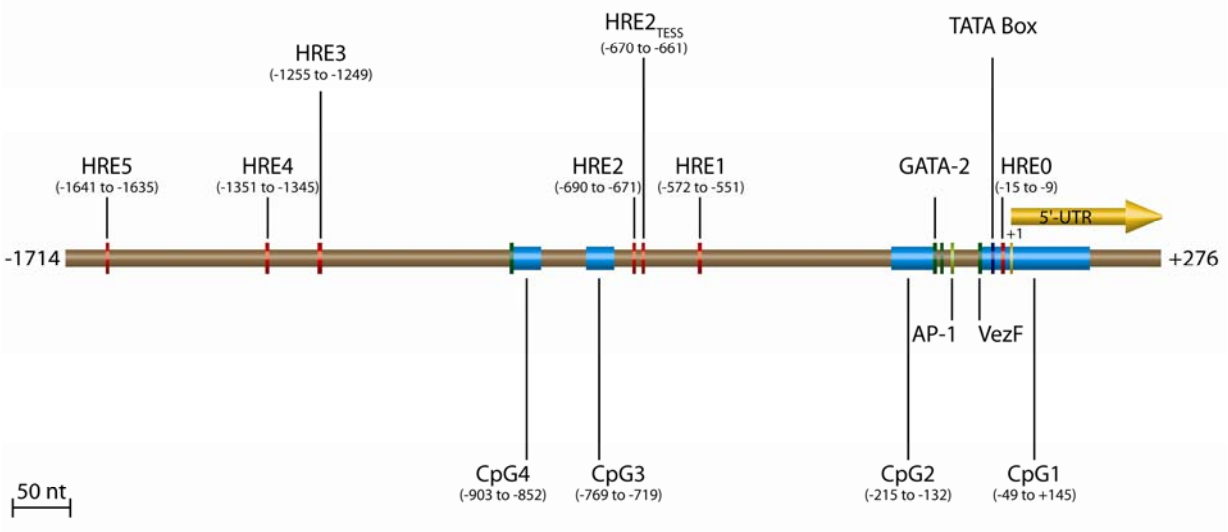

Figure 3-2. Putative HREs in the murine *edn1* promoter. The 1990 bp fragment of the *edn1* promoter and 5'UTR is shown above. The transcriptional start site, as determined by primer extension and S1 nuclease analysis (Inoue et al., 1989), is indicated as +1 and the 5'UTR is shown in yellow. Known promoter elements are also indicated including the TATA box (Inoue et al., 1989; Sakurai et al., 1991), AP-1 (Lee et al., 1991a), GATA-2 (Lee et al., 1991b; Yamashita et al., 2001), and vascular endothelial zinc finger (VezF) (Aitsebaomo et al., 2001) binding sites. Possible CpG islands were identified by EMBOSS analysis and are shown in blue. Putative HREs were identified by TESS analysis and visual inspection and are shown in red.

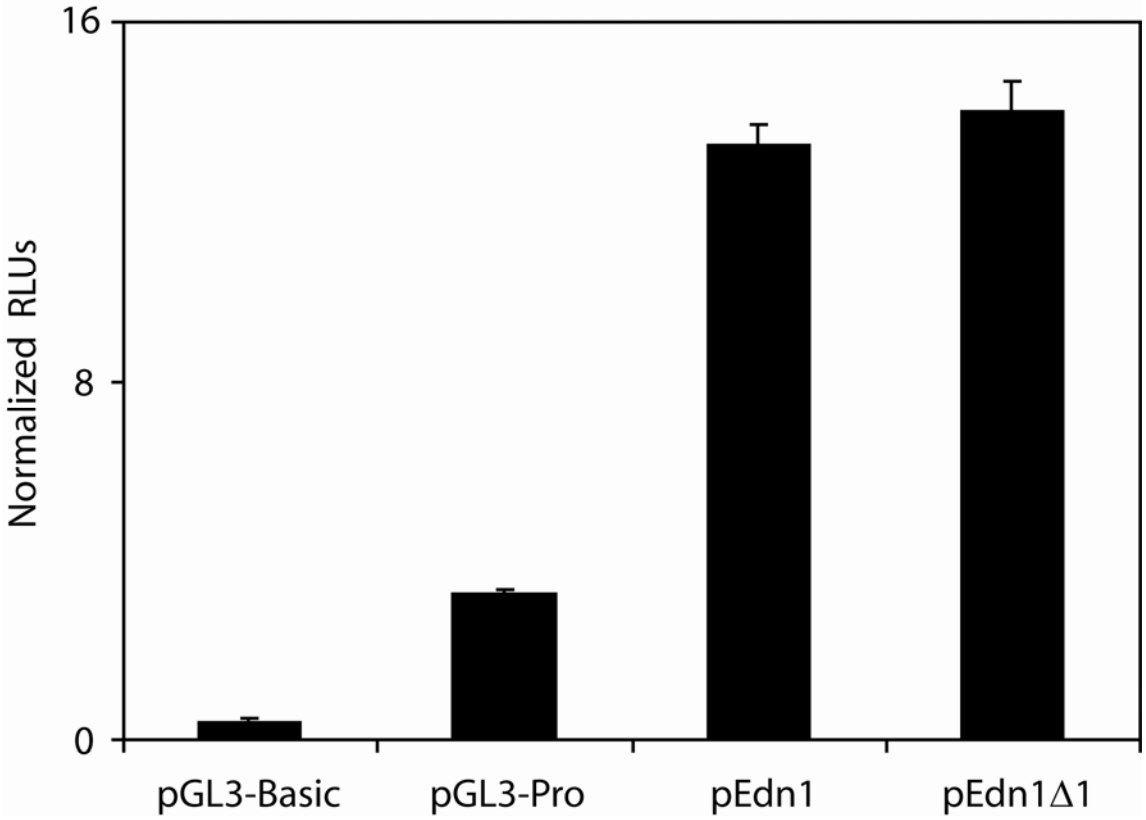

Figure 3-3. The *edn1* promoter is transcriptionally active. Comparison of luciferase activity in mIMCD-3 cells transiently transfected for 24 h with pGL3-Basic, pGL3-Pro, pEdn1, or pEdn1Δ1. Luciferase activity is normalized to *Renilla* (pRL-TK) and expressed as relative light units (RLUs) ± SE. ($n \geq 3$).

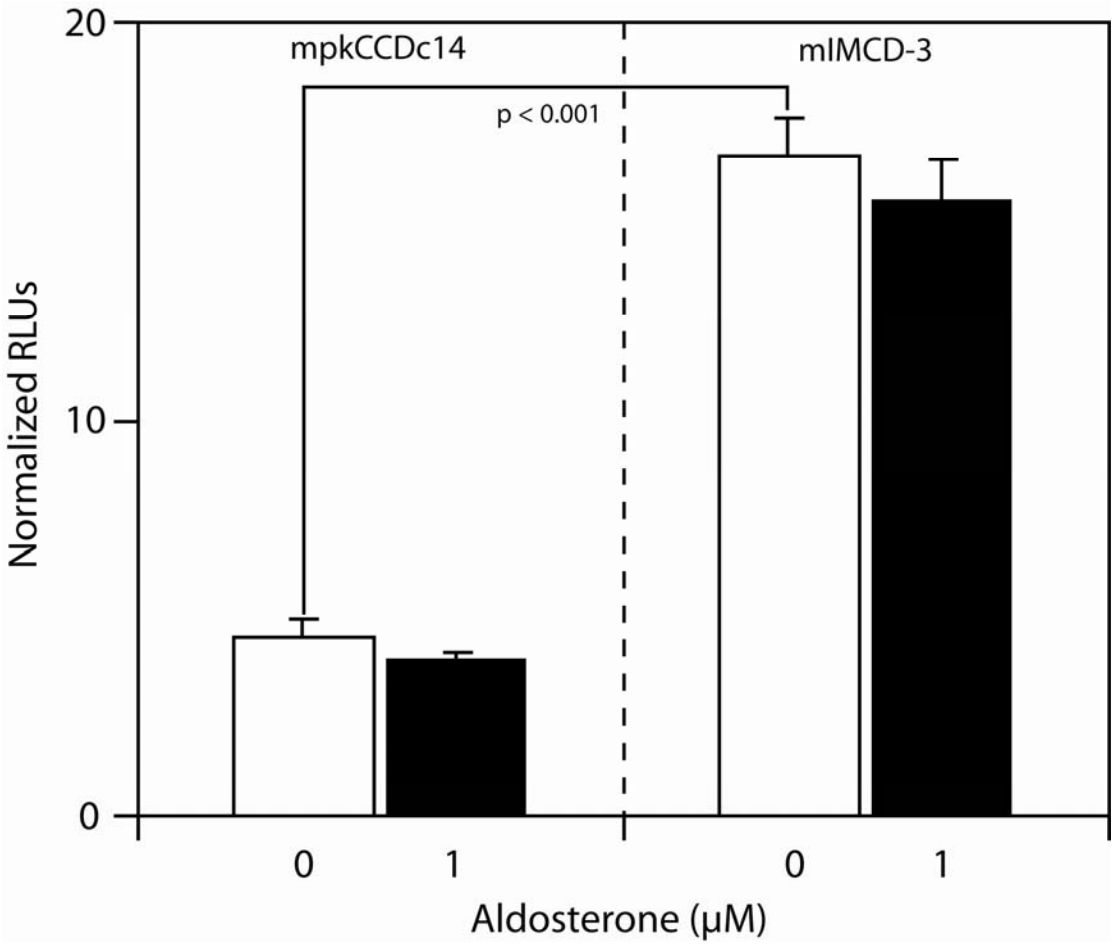

Figure 3-4. Comparison of pEdn1 activity in mpkCCD$_{c14}$ and mIMCD-3 cells. Cells were transiently transfected with pEdn1 for 24 h prior to treatment with vehicle (open bars) or 1 μM aldosterone (closed bars) for 1 h. Following hormone treatment cells were harvested for analysis of luciferase activity. Values were normalized for control *Renilla* luciferase activity and expressed as relative light units (RLUs) ± SE. ($n \geq 3$)

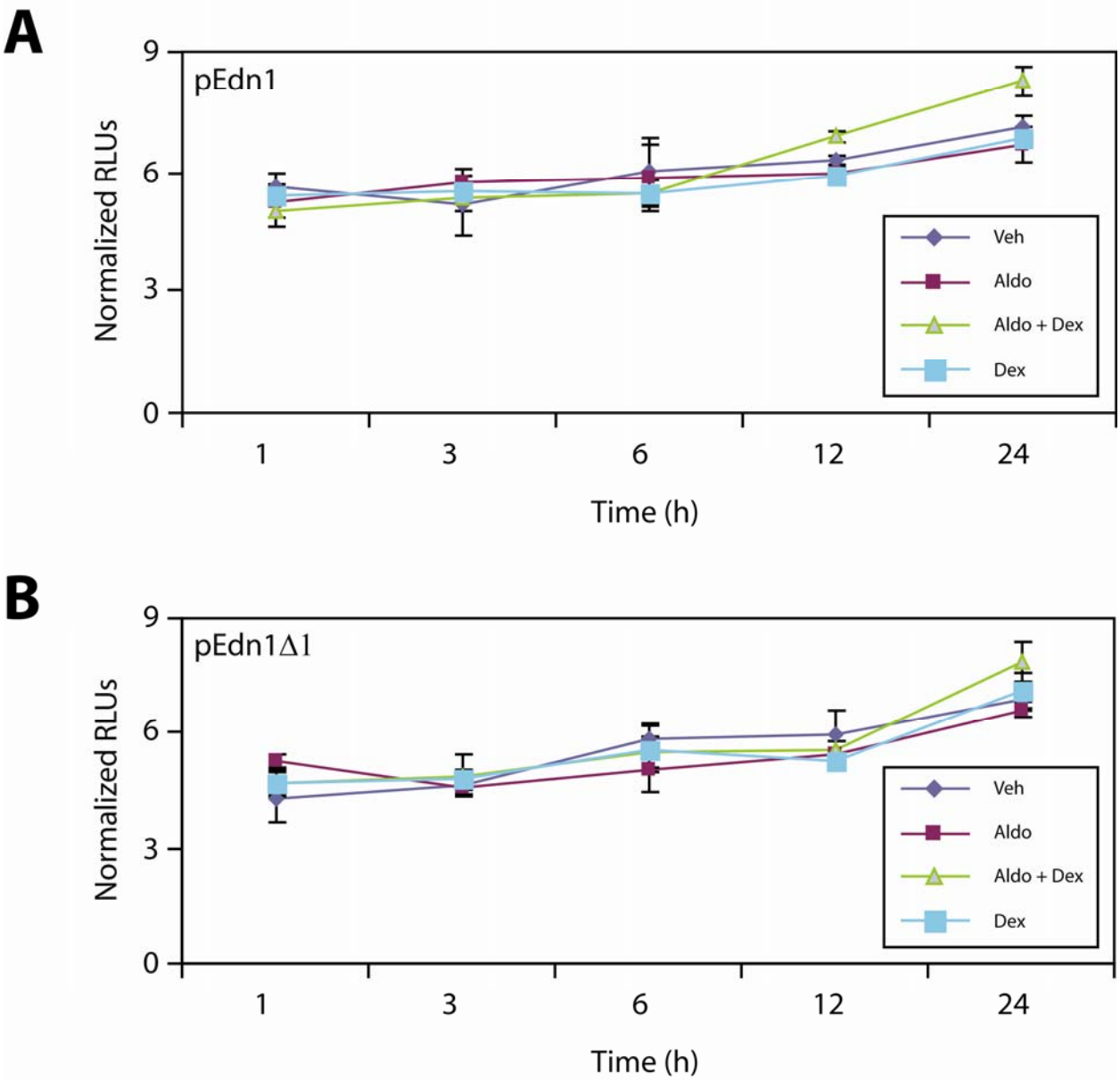

Figure 3-5. Time course of luciferase activity in hormone treated mIMCD-3 cells. The mIMCD-3 cells were transfected for 24 h with either A) pEdn1 or B) pEdn1Δ1 in the presence of 10% charcoal-dextran stripped FBS. Cells where then treated with vehicle (veh), 1 μM aldosterone (aldo), 1 μM aldo plus 1 μM dexamethasone (dex), or 1 μM dex alone for 1 - 24 h. Luciferase activity was normalized to *Renilla* and expressed as relative light units (RLUs). ($n \geq 2$)

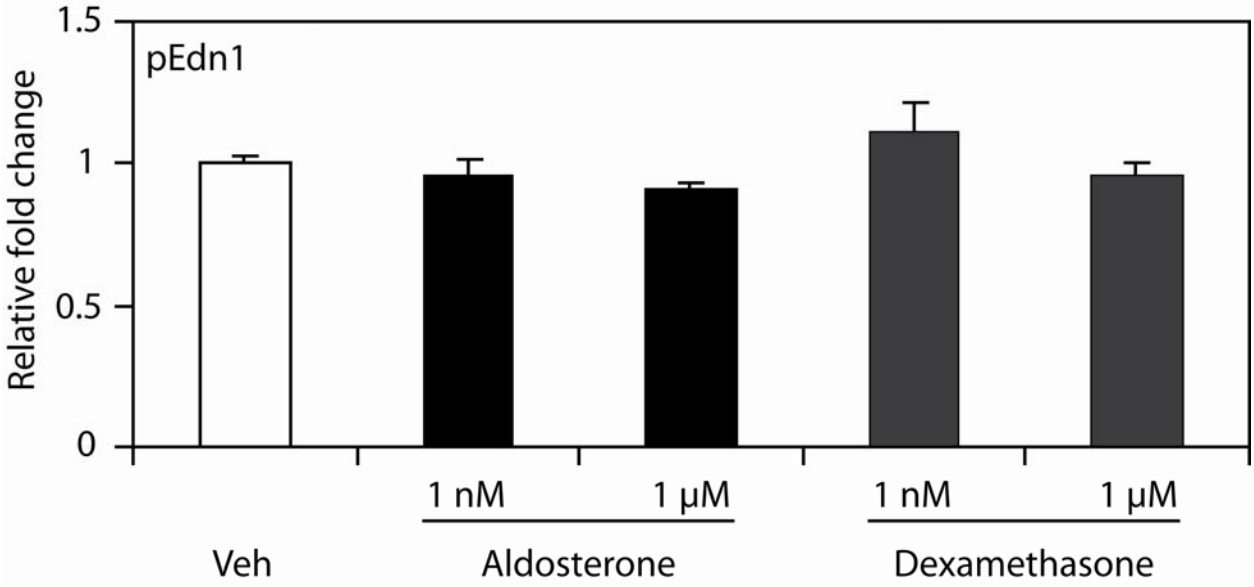

Figure 3-6. Effect of low and high dose aldosterone or dexamethasone on pEdn1 reporter gene activity. The pEdn1 plasmid was transiently transfected in mIMCD-3 cells for 24 h in the presence of 10% charcoal-dextran stripped FBS. Cells were then treated with vehicle (veh, open bars), 1 nM or 1 µM aldosterone (aldo, closed bars) or 1 nM or 1 µM dexamethasone (dex, gray bars) for 3 h. Luciferase activity was normalized to Renilla to control for transfection and cell viability. Values are expressed as relative fold change compared to vehicle ± SE. (n=3). Experiments were also conducted at 9 h and similar results were obtained.

CHAPTER 4
ALDOSTERONE MODULATES STERIOD RECEPTOR BINDING TO THE ENDOTHELIN-1 GENE (*EDN1*)

Introduction

The steroid hormone aldosterone is critical for Na^+ homeostasis and blood pressure control. Aldosterone works by modulating the fine regulation of Na^+ reabsorption in the distal nephron and collecting duct of the kidney. Classical aldosterone action is mediated through the mineralocorticoid receptor (MR), a member of the nuclear receptor family of proteins that function as ligand-dependent transcription factors (Arriza et al., 1987). MR acts on cells of the distal nephron and collecting duct to stimulate transcription of genes involved in transepithelial Na^+ transport including *scnn1a* (αENaC), *atp1a1* (Na^+/K^+-ATPase α1), and *sgk1* (Rogerson and Fuller, 2000). The increase in expression of genes involved in Na^+ transport results in net Na^+ reabsorption followed by in increase in extracellular fluid volume and a consequent increase in blood pressure. Indeed, MR antagonists such as spironolactone and eplerenone are used clinically as diuretic and anti-hypertensive agents (McManus et al., 2008; Struthers et al., 2008).

The mechanism of MR action is consistent with a classical steroid receptor mechanism (Beato and Klug, 2000). Prior to activation MR resides in the cytosol. Ligand binding induces a conformational change that releases chaperone proteins and reveals a nuclear localization signal. Nuclear MR binds directly to DNA at hormone response elements (HREs) in target genes to modulate their transcription. A typical HRE for MR consists of two receptor binding half-sites with the consensus sequence: 5'-TGTTCT-3' arranged as an inverted palindrome (Arriza et al., 1987; Geserick et al., 2005). These HREs facilitate binding of steroid receptors in a dimeric conformation. Once bound to a gene promoter MR serves as a molecular platform for the recruitment of transcription factors such as the steroid receptor coactivator-1 (SRC-1) and RNA polymerase II (Hellal-Levy et al., 2000; Li et al., 2005; Pascual-Le Tallec and Lombès, 2005).

MR is highly homologous to the glucocorticoid receptor (GR) and can bind glucocorticoids with equal affinity to aldosterone (Arriza et al., 1987). However, inappropriate glucocorticoid activation of MR can lead to severe hypertension (Frey et al., 2004; Ulick et al., 1979). Aldosterone responsive cells are protected from glucocorticoids by the activity of 11β-hydroxysteroid dehydrogenase type 2 (11β-HSD2), an enzyme that converts glucocorticoids into 11-ketosteroids that have very little affinity for MR or other steroid receptors (Funder et al., 1988; Rebuffat et al., 2004). Alternatively, GR can bind mineralocorticoids (K_D = 14-60 nM) (Arriza et al., 1987) and may contribute to aldosterone action. MR and GR share 94% homology in their DNA binding domains and have conserved amino acids at each residue shown to make direct contacts with DNA (Arriza et al., 1987; Luisi et al., 1991). Indeed, MR and GR are known to bind to the same HRE in several genes (Derfoul et al., 1998; Itani et al., 2002; Kolla et al., 1999; Mick et al., 2001; Webster et al., 1993).

Previously, we identified endothelin-1 (*edn1*) as a novel aldosterone response gene in inner medullary collecting duct (mIMCD-3) cells (Gumz et al., 2003). Similarly, this interaction has been documented in whole kidney extracts from rat (Wong et al., 2007). The gene product of *edn1* is a 212 amino acid prepropeptide that is enzymatically processed to form the biologically active 21 amino acid peptide, ET-1. ET-1 plays a complex role in cardiovascular and renal physiology. Several reports have demonstrated aldosterone induction of *edn1* in vascular smooth muscle and cardiac tissue (Doi et al., 2008; Wolf et al., 2004). In these cell types, systemic ET-1 is largely vasoconstrictive and profibrotic. In fact, both ET-1 and aldosterone have been implicated in cardiac and renal fibrosis, glomerular damage and proteinuric disease (Barton, 2008; Barton and Yanagisawa, 2008; Funder and Mihailidou, 2009). In the kidney, ET-1 has effects on renal hemodynamics (Baylis, 1999; Inscho et al., 2005), Na^+ and water homeostasis

(Kohan, 2009), and acid-base balance (Khanna et al., 2005). These same processes are also influenced by aldosterone. However, renal ET-1 is a well-documented natriuretic peptide that directly blocks Na^+ transport in the collecting duct (Ahn et al., 2004; Kizer et al., 1995; Kohan, 2006; Nakano et al., 2008; Schneider et al., 2008). The physiological importance of collecting duct ET-1 is emphasized by the fact that collecting duct cell-specific *edn1* knockout mice exhibit salt sensitive hypertension (Ahn et al., 2004). Thus, in the renal collecting duct, the actions of aldosterone and ET-1 on Na^+ transport directly oppose each other.

The goal of the present report was to characterize aldosterone regulation of *edn1* in the renal collecting duct. Indeed, studies presented here demonstrate aldosterone-stimulated *edn1* in cortical, outer medullary, and IMCD cells *in vitro*, and *edn1* and ET-1 peptide in the rat kidney *in vivo*. Putative HREs in the *edn1* promoter were identified. These elements were evaluated for the recruitment of hormone receptors and the assembly of an aldosterone-dependent transcription complex.

Materials and Methods

Chemicals

Aldosterone, spironolactone and RU486 (Sigma) were prepared in 100% ethanol at 1 mg/ml stock concentrations and stored at -20 °C. Collagenase type I (MP Biomedicals), hyaluronidase type IV (Sigma), and DNase I (Sigma) were prepared fresh on the day of the experiment.

Animals

Male Sprague Dawley rats (300-350 g) were obtained from Harlan and housed at the University of Florida Animal Care Services rodent facilities. Standard rat chow and tap water were provided ad libitum. All procedures adhered to the Animal Care Services guidelines and were approved by the University of Florida Institutional Animal Use and Care Committee.

Acutely Isolated Rat IMCD Cells

Rats were euthanized by sodium pentobarbital (50 mg/kg body weight) and cervical dislocation. Kidneys were immediately removed and the inner medulla was carefully dissected for acute IMCD isolation according to Stricklett et al. (Stricklett et al., 2006). In brief, minced tissue was incubated at 37 °C in a digestion solution containing collagenase type I (3 mg/ml), hyaluronidase type IV (2 mg/ml) and DNase I (0.1 mg/ml). Digested IMCDs were collected by centrifugation through a sucrose buffer. Isolated IMCDs were resuspended in DMEM/F-12 and equilibrated in a 5% CO_2 incubator at 37 °C for 20 min. Inner medullas from the left and right kidney of each rat were processed in tandem, but separately, to allow for a paired analysis between vehicle (0.04% ethanol) and 1 μM aldosterone treatments. Thus, each rat served as its own internal control. After 1 h cells were immediately pelleted by gentle centrifugation at 4 °C and resuspended in TRIzol® Reagent (Invitrogen) for RNA isolation as described below.

Aldosterone Administration in Rat and ET-1 Peptide Measurement

Rats were given an intraperitoneal (ip) injection (1 ml/kg body weight) of aldosterone (1 mg/kg) or vehicle (2% ethanol in saline). After 2 h rats were anesthetized with inhaled isoflurane and kidneys were flushed by an aortic perfusion of ice-cold PBS with the vena cava vented. Kidneys were removed and dissected into cortex, outer medulla, and inner medulla. Tissues were immediately snap frozen in liquid nitrogen and stored at -80 °C until use. ET-1 was extracted from renal tissues using a protocol originally described by Yorikane et al. (Yorikane et al., 1993). Immunoreactive ET-1 peptide was detected by chemiluminescent ELISA (R&D Systems) and normalized to total protein content as determined by standard protein assays (Bio-Rad).

Cell Culture and Aldosterone Treatments

All cells were maintained in DMEM/F12 plus 10% FBS and 50 μg/ml gentamicin. The mpkCCD$_{c14}$ cells were a kind gift of Dr. Alain Vandewalle (Bens et al., 1999), OMCD-1 cells were a kind gift of Dr. Thomas DuBose from Wake Forest Medical School (Guntupalli et al., 1997), mIMCD-K2 cells were a gift of Dr. Bruce Stanton from Dartmouth Medical School (Kizer et al., 1995) and mIMCD-3 cells were purchased from American Type Culture Collection. For all hormone experiments cells were grown 24 h past confluency and changed to DMEM/F12 plus 10% charcoal-dextran stripped FBS (Invitrogen Corp.). After 24 h, cells were treated with vehicle (ethanol) or aldosterone (0.01 to 1 μM) for 1 h.

Steady-State mRNA Determination

Hormone studies were conducted as described above on growth-arrested confluent monolayers grown in 6-well Costar Transwell plates (Corning). The final concentration of ethanol in all treatments was 0.1%. Total RNA (2 μg) was isolated from cells using TRIzol® Reagent (Invitrogen), treated with DNase I (Ambion) to eliminate genomic DNA, and reverse transcribed using oligo dT, random hexamers and Superscript™ III reverse transcriptase (Invitrogen). No reverse transcriptase served as a negative control. Resulting cDNAs (32 ng) were used as templates in duplicate QPCR reactions (Applied Biosystems). Cycle threshold (C_T) values were normalized against β-actin (*actb*) and relative quantification was performed using the $\Delta\Delta C_T$ method (Livak and Schmittgen, 2001). All QPCR was performed with TaqMan® primer/probe sets that have guaranteed 100% PCR efficiency over six logarithms of template (Applied Biosystems, 2006). Primer/probes for rat *edn1*, *sgk1*, and *actb* are indicated in Table 2-1 and primer/probe sets for mouse are indicated in Table 5-1.

Heterogeneous Nuclear RNA (hnRNA) Assay

As described by Lipson and Baserga (Lipson and Baserga, 1989), levels of unspliced *edn1* hnRNA were detected using primers designed to amplify a region between exon 4 and intron 4 (forward: 5'-GAAGTGTATCTATCAGCAGCTGG-3'; reverse: 5'-AGACCATGACGACTCTATTACTGG-3'). QPCR reactions were set up with 32 ng cDNA, 200 nM of each primer and SyBr Green mastermix (Bio-Rad). Expression of hnRNA was normalized to glyceraldehyde-3-phosphate dehydrogenase (*gapdh*) mRNA (forward primer: 5'-GAAGCCCATCACCATCTTCC-3'; reverse primer: 5'-TGATGATCCTTTTGGCTCC-3'). *Edn1* hnRNA and gapdh primers were validated for QPCR over 4 orders of magnitude of input cDNA for similar PCR efficiency (data not shown). Melting curves (55-95 °C) and agarose gel electrophoresis were used to verify product size.

Nuclear Translocation and Western Blots

Hormone experiments were conducted in mIMCD-3 cells as described above except that cells were grown in 150 mm dishes (Corning). Cells were treated with vehicle (0.15% ethanol), aldosterone, antagonist or aldosterone plus antagonist. Antagonists, spironolactone and RU486, were supplied at the final concentration of 10 μM in each experiment. In some cases, cells were pretreated with antagonists 1 h prior to aldosterone treatment. Cytoplasmic and nuclear extracts were obtained using the NE-PER® Reagents (Pierce Biotechnology). Protein concentrations were determined using the Bradford assay and 90 μg were separated on a 7.5% sodium dodecyl sulfate polyacrylamide gel (Bio-Rad). Proteins were transferred to PVDF overnight and visualized by Ponseau S. Membranes were blocked with 2% Rodeo blocker plus 0.05% saddle soap (United States Biochemical Corp.) in Tris buffered saline (TBS). The monoclonal MR antibody was a kind gift of Drs. Elise and Celso Gomez-Sanchez (Gomez-Sanchez et al., 2006). Detailed information on all primary and secondary antibodies used is listed in Supplemental

Table 1. Blots were washed with blocking solution and developed with Rodeo Western Detection Reagents (United States Biochemical Corp.). Densitometric analysis was performed with Quantity One® software (Bio-Rad).

For each nuclear translocation experiment blots were stripped using 2% sodium dodecyl sulfate plus 10% β-mercaptoethanol for 30 min at 70 °C. Blots were redeveloped to ensure completely antibody stripping, washed and reprobed using another primary antibody.

Hormone Receptor siRNA Knockdown

MR-siRNA (J-061269-09 NR3C2), GR-siRNA (J-045970-10 NR3C1) and control non-targeting siRNA against luciferase (#2 D-001210-02-05) were purchased from Dharmacon (Lafayette, CO, USA). Cells were seeded at a density of 75,000 cells per cm^2 on 6-well Transwell plates (Corning) and transfected for 24 h with 66 nM siRNA in 1.5 µl of DharmaFect 4. At the time of transfection cells were switched to phenol-red free DMEM/F12 plus 10 % charcoal dextran stripped FBS. After 24 h the cells were treated with 1 µM aldosterone or vehicle for 1 h. RNA was extracted and processed as described above for QPCR.

Chromatin Immunoprecipitation (ChIP) Assays

ChIP assays were performed as previously described (Leach et al., 2003). Briefly, cells were fixed with 1% formaldehyde and quenched with glycine. Nuclei were isolated and DNA was sonicated to approximately 500 bp. Fragment length was verified by gel electrophoresis. Specific antibodies (Table 4-1) were used to immunoprecipitate DNA-protein complexes on BSA-blocked protein-A sepharose beads. Crosslinks were reversed and DNA fractions were analyzed for bound *edn1* by PCR. Primers: forward 5'-TCTGATCGGCGATACTAGGG-3' and reverse 5'-CGCTCTTGAATCCCAGCTAC-3', amplify a 235 bp region containing putative HREs (Figure 4-7). Standard PCR products were visualized with SyBr Green on a 5% TBE gel. Alternatively, bound *edn1* was quantified by QPCR using SyBr Green mastermix (Bio-Rad).

Values were normalized to total input DNA and are expressed as fold change relative to control. Primers were validated for quantification by analyzing PCR efficiency over a serial dilution of input DNA. Melting curves confirmed specific PCR products and melting temperatures.

Coimmunoprecipitation

Cytosolic and nuclear extracts (175 μg) obtained from vehicle and aldosterone treated mIMCD-3 cells were diluted to a final volume of 250 μl in PBS with fresh protease inhibitors (Roche). Diluted samples were pre-cleared with 30 μl BSA-blocked protein-A sepharose beads and 0.4 μg of normal mouse IgG (Santa Cruz) for 30 min at room temperature with end-over-end rotation. Following gentle centrifugation supernatants (240 μl) were collected and subjected to immunoprecipitation with anti-MR or anti-GR (Table 4-1) and 40 μl blocked protein-A sepharose beads for 1 h. Beads were pelleted and washed three times with ice-cold PBS plus protease inhibitors. Wash supernatants were removed with flat-head gel-loading tips (USA Scientific) after each wash. Washed samples were resuspended in 40 μl of 2x lithium dodecyl sulfate sample buffer (Invitrogen Corp) plus 10% β mercaptoethanol, boiled for 5 min, and subjected to Western blotting as described above.

DNA-Affinity Purification Analysis

Cytosolic and nuclear extracts obtained from mIMCD-3 cells as described above were subjected to DNA-affinity purification analysis (DAPA) as recently described (Deng et al., 2003). Double stranded DNA probes were biotinylated on each 5' end (Sigma Genosys) and were homologous to HRE1: 5'-AGACTTGGTGGAAGGGGTGGTGGTGGAAAAGT or HRE2: 5'- GGATGTACCTGACAAAACCACATTGTTGTTGTTATC in the *edn1* promoter (Figure 3-6). Probes were immobilized on 50 μl of streptavidin coated agarose beads and incubated with 175 μg of cellular extract in the presence of freshly prepared protease inhibitors (Roche) for 1 h at room temperature with end-over-end rotation. Beads were pelleted. Supernatants were

removed and used for input controls by Western blotting for actin. Pelleted beads were washed four times with ice-cold PBS plus protease inhibitors. After the final wash, all liquid was aspirated from the beads with flat-headed gel loading tips and 50 µl of 2x lithium dodecyl sulfate sample buffer (Invitrogen Corp) plus β-mercaptoethanol. Samples were boiled for 5 min, chilled on ice, and loaded onto a 7.5% Tris-HCl sodium dodecyl sulfate polyacrylamide Ready Gel (Bio-Rad) for electrophoresis. Purified proteins were identified by Western analysis as described above except that blots were washed with TBS plus 0.05% saddle soap without blocking reagent. Equal loading was controlled for by Bradford assay, input control Westerns against actin, and reprobing DAPA blots with actin.

Statistics

Data are presented as the mean ± standard error (SE). Unless otherwise stated all experiments were performed in duplicate at least three independent times. Statistical significance was calculated using the two-tailed Student's *t* test and $p < 0.05$ was considered significant.

Results

Aldosterone Stimulates ET-1 in Rat Inner Medulla

Renal collecting duct cells are a target cell type for aldosterone action in the body. Indeed, our original report showed stimulation of *edn1* mRNA by aldosterone occurred in mIMCD-3 cells (Gumz et al., 2003). This interaction has also been documented in whole kidney extracts from rat (Wong et al., 2007). To determine if collecting duct cells were also the target cell type in the animal, aldosterone studies were conducted on acutely isolated rat IMCD cells *ex vivo*. Following a brief equilibration, IMCD cells isolated from a single rat were separated for a paired analysis between vehicle and 1 µM aldosterone treatments. After 1 h, aldosterone led to a 41 ± 6% increase in *edn1* mRNA expression compared to control (Figure 4-1A). The observed

stimulation in *edn1* exceeded the 28 ± 5% increase in the mRNA of the well-established aldosterone response gene *sgk1* (Flores et al., 2005; Vallon and Lang, 2005).

Animal studies were extended to investigate the level of ET-1 peptide in rat kidney. Earlier work had demonstrated that basal ET-1 levels were highest in the inner medulla (Table 2-2). Aldosterone injection (1 mg/kg body weight, ip) resulted in an approximate 2-fold increase in inner medullary ET-1 levels compared to control (Figure 4-2B). The observation that aldosterone stimulated ET-1 in inner medulla *in vivo*, combined with the known role of ET-1 in modulating renal Na^+ transport (Bugaj et al., 2008; Gilmore et al., 2001), supports the hypothesis that ET-1 is a regulator of aldosterone action in the kidney.

Aldosterone Stimulates Dose-Dependent Transcription of *edn1* in Collecting Duct Cells

To determine if the stimulation of *edn1* by aldosterone was specific to IMCD cells or was a more generalized collecting duct cell response the effect of aldosterone was evaluated in three renal cell lines thought to be representative of cortical, outer medullary and IMCD cells. These cell lines were $mpkCCD_{c14}$ (Bens et al., 1999), OMCD-1 (Guntupalli et al., 1997) and mIMCD-3 (Gumz et al., 2003; Rauchman et al., 1993) cells, respectively. Aldosterone (1 μM) led to an approximate 3-fold increase in *edn1* mRNA at 1 h in each cell line (Figure 4-2A). Aldosterone also stimulated a 2.5 ± 0.4 fold increase in *edn1* mRNA in mIMCD-K2 cells, an independently derived IMCD cell model (Kizer et al., 1995) (Figure 4-3). Taken together, this evidence indicates that aldosterone induction of *edn1* mRNA occurs in multiple collecting duct cells *in vitro*, and is likely to occur along the length of the collecting duct *in vivo*.

To more fully characterize aldosterone induction of *edn1*, aldosterone dose-response studies were conducted in mIMCD-3 cells. This cell line was selected because the inner medulla is an important site for ET-1 action *in vivo* and because this cell line has been validated as a model for aldosterone action (Boesen et al., 2008; Gumz et al., 2003; Kitamura et al., 1989;

Vassileva et al., 2003). *Edn1* mRNA exhibited a dose-dependent increase in the presence of aldosterone that was significant at concentrations as low as 0.1 μM (Figure 4-2B). Importantly, mRNA induction of *edn1* paralleled that of *sgk1* (Figure 4-2B), which ensured that hormone concentrations were appropriate to reproduce an aldosterone response *in vitro*. In addition, aldosterone treatment resulted in an increase in functional ET-1 peptide release from mIMCD-3 cells (Figure 4-4), which further validates this cell line as a model of aldosterone action on ET-1.

In general, aldosterone action is mediated at the level of transcription (Bhargava et al., 2004). To test the hypothesis that the increase in *edn1* mRNA in response to aldosterone also occurred at the level of transcription, the concentration of *edn1* heterogeneous nuclear RNA (hnRNA) was determined. Levels of hnRNA can generally be used to measure transcriptional activity of a specific gene because pre-splicing hnRNA molecules are not subject to factors affecting overall mRNA stability (Palii et al., 2006). Consistent with levels of steady state mRNA (Figure 4-2B), aldosterone stimulated a dose-dependent increase in *edn1* hnRNA (Figure 4-2C). Given the transcriptional mechanism of aldosterone, the increase in *edn1* hnRNA supports the hypothesis that the induction of *edn1* occurs by transcription.

Aldosterone Action on *edn1* Involves Both MR and GR.

Activation of MR is central to the mechanism by which aldosterone modulates transcription of target genes. However, aldosterone-regulated gene transcription may also be mediated through GR. Therefore, several approaches were used to investigate the contribution of each receptor in mediating aldosterone action. First, a Western blotting approach was adopted to follow nuclear translocation of MR (Figure 4-5A, top panel) or GR (Figure 4-5A, middle panel) in response to aldosterone treatment. Aldosterone (1 μM) resulted in comparable 10.9 ± 0.2 and 11.9 ± 0.8 fold increases in the abundance of nuclear MR and GR, respectively (Figure 4-5A-C). Furthermore, nuclear translocation of MR and GR was dose-dependent and occurred at

concentrations of aldosterone as low as 0.01 μM. Of note, this concentration of hormone failed to stimulate a detectable increase in *edn1* or *sgk1* mRNA (Figure 4-2B versus Figure 4-5B). These observations provide strong evidence that aldosterone action is mediated through both MR and GR in mIMCD-3 cells.

To determine if each receptor was directly involved in *edn1* transcription receptor blockade experiments were performed on mIMCD-3 cells. Consistent with previously reported data (Gumz et al., 2003), inhibition of MR or GR with spironolactone or RU486 respectively, completely blocked aldosterone induction of *edn1* mRNA (Figure 4-6A). To corroborate these findings, siRNA gene silencing was used to specifically knockdown MR or GR expression. Independent transfections of MR-siRNA or GR-siRNA resulted in nearly 90% knockdown of their relevant receptor mRNAs in mIMCD-3 cells (Gumz et al., 2009a). In the presence of aldosterone, transfection of MR-siRNA or GR-siRNA inhibited the induction of *edn1* mRNA by 35 ± 8% and 40 ± 4%, respectively (Figure 4-6B). Cotransfection of MR-siRNA and GR-siRNA together resulted in a 54 ± 4% reduction in *edn1* mRNA. However, the effect of cotransfection was not significantly additive compared to either siRNA transfected alone (Figure 4-6B). The additive trend by siRNA knockdown most likely reflects the different mechanism of receptor inhibition given that pharmacological blockade of either receptor alone completely prevented the induction of *edn1*. Nevertheless, the observation that targeted inhibition of GR blocked aldosterone-induced *edn1* demonstrates that MR was not able to compensate for the loss of GR. Thus, these data indicate that both MR and GR are functionally required for the aldosterone-mediated induction of *edn1*.

Aldosterone Modulates Hormone Receptor Binding to the *edn1* Promoter

The observation that both MR and GR were involved in aldosterone mediated *edn1* transcription suggested that the *edn1* promoter contained functional HREs. Luciferase studies

from Chapter 3 indicated that the proximal 1990 bp region of the murine *edn1* promoter and 5'-untranlated region contained a transcriptionally active promoter. Furthermore, sequence analysis revealed several putative HRE half-sites including two complete elements designated HRE1 and HRE2 (Figure 4-7A). In contrast to a classical element that contains receptor binding half-sites separated by three nucleotides, the identified HREs each have half-sites separated by eight nucleotides. Furthermore, each of the identified HREs are different from one another in that the downstream HRE1 consists of two directly repeated half-sites, while the upstream HRE2 has half-sites arranged as an imperfect inverted palindrome (Figure 4-7A).

Chromatin immunoprecipitation (ChIP) assays were performed on vehicle or 1 μM aldosterone treated mIMCD-3 cells in order to determine if MR or GR interacted directly with the *edn1* promoter. PCR primers were designed to flank both HREs (Figure 4-7A). After 1 h, aldosterone treatment resulted in a 5.4 ± 0.3 fold increase in MR and a 6.8 ± 1.2 fold increase in GR bound to the *edn1* promoter (Figure 4-7B). Furthermore, the aldosterone-dependent association of MR and GR was accompanied by a 2.6 ± 0.4 fold increase in the transcriptional coactivator SRC-1 associated with the *edn1* promoter. Regional histone H3 lysine 4 residues were dimethylated after treatment with aldosterone. This particular histone modification is widely associated with transcriptionally active promoters (Liang et al., 2004). Taken together, these data are consistent with the concept that the *edn1* promoter is more active in the presence of aldosterone.

The association of MR and GR in the same region of the *edn1* promoter suggested that the receptors bound directly to one or both of the identified HREs. Accordingly, higher resolution DAPA experiments were employed to map the aldosterone-dependent recruitment of MR and GR to either HRE1 or HRE2. DAPA allows one to use a small region of double stranded DNA,

in this case HRE1 or HRE2 of the *edn1* promoter, as bait in an affinity purification protocol to pull down the protein complex bound to the DNA (Deng et al., 2003). Aldosterone induced dose-dependent association of MR and GR with HRE2 (Figure 4-8A). Both receptors were also recruited to HRE1 in the presence of 1 μM aldosterone (Figure 4-8B). However, the relative abundance of either receptor recruited to HRE1 was approximately 10% of the total abundance of MR or GR bound to HRE2. Furthermore, receptors could not be consistently detected at lower concentrations of hormone suggesting that the upstream HRE2 is the primary response element governing *edn1* induction by aldosterone.

The observation that both MR and GR interacted with the same HRE suggested that both receptors might also be in the same transcription complex in the nucleus. Indeed, coimmunoprecipitation experiments performed on mIMCD-3 cells revealed that MR and GR were present in the same protein complex in the nucleus of aldosterone, but not vehicle treated cells (Figure 4-9A). The interaction of MR and GR in the nucleus was dose-dependent and occurred at concentrations of aldosterone as low as 0.01 μM. Coimmunoprecipitation experiments were also conducted on cytosolic extracts from vehicle and 1 μM aldosterone treated mIMCD-3 cells (Figure 4-9B, top panels). Both MR and GR were detected in the same protein complex in the presence or absence of aldosterone in the cytosol. Conversely, neither MR nor GR were precipitated from cytosolic extracts by DAPA using either HRE as bait (Figure 4-9B, middle panels). Together these data indicate that MR and GR are in the same protein complex in the cytosol prior to hormone activation. However, the association of either MR or GR with DNA is exclusive to aldosterone-activated receptors localized in the nucleus.

In order to test whether aldosterone-activated MR and GR could recruit RNA polymerase II to the *edn1* promoter, ChIP and DAPA experiments were performed. ChIP analysis revealed

that RNA polymerase II was present on the *edn1* promoter in aldosterone treated cells at levels 2.5 ± 0.5 fold higher than control (Figure 4-10A). Likewise, DAPA experiments showed dose-dependent recruitment of RNA polymerase II to HRE2 (Figure 4-10B). In summary, aldosterone stimulates *edn1* in collecting duct cells by a mechanism involving the assembly of a transcription complex at HRE2 in the *edn1* promoter that contains MR, GR, SRC-1, and RNA polymerase II.

Discussion

In this report the regulation of *edn1* by aldosterone was characterized in renal collecting duct cells. Aldosterone stimulated *edn1* in rat IMCD cells *ex vivo*, as well as four independent collecting duct cell models *in vitro*. We report the first direct evidence of aldosterone induction of ET-1 peptide in rat inner medulla *in vivo*. Coimmunoprecipitation experiments showed that MR and GR were present in the same protein complex in the cytosol prior to hormone activation. Nuclear translocation, pharmacological inhibition, siRNA silencing, ChIP and DAPA experiments all demonstrated that both MR and GR were involved in mediating aldosterone action on the *edn1* gene. Receptors bound directly to the *edn1* promoter to facilitate the assembly of a transcription complex that included the transcription coactivator SRC-1 and RNA polymerase II.

Supporting the hypothesis that ET-1 modulates aldosterone action in the kidney was the observation that aldosterone induction of *edn1* mRNA occurred in collecting duct cells, the target cell type for aldosterone action. Furthermore, induction of ET-1 peptide was detected in the renal inner medulla of rats given a 2 h injection of aldosterone. Inner medullary ET-1 is well-characterized natriuretic peptide that stimulates compounds such as nitric oxide and cyclic GMP (Edwards et al., 1992; Pollock, 2000). Similarly, ET-1 potently inhibits Na^+ transport through the ENaC channel in collecting duct cells (Bugaj et al., 2008; Gallego and Ling, 1996). Consequently, aldosterone induction of *edn1* may represent an important negative feedback loop

on aldosterone-stimulated Na^+ reabsorption in the collecting duct. Indeed, the renal ET-1 pathway is differentially regulated in animals with mineralocorticoid-induced hypertension (Hsieh et al., 2000; Matsumura et al., 2000a, b; Montezano et al., 2005). However, direct support for this concept comes from studies conducted on collecting duct cell-specific *edn1* knockout mice. These mice exhibit severe salt-sensitive hypertension that is effectively remediated by either ENaC or MR antagonists (Ahn et al., 2004; Ge et al., 2008).

Given the known functions of aldosterone and ET-1 in collecting duct cells, studies were conducted to more fully characterize aldosterone regulation of *edn1* in mIMCD-3 cells. Aldosterone treatment resulted in dose-dependent increases in *edn1* and *sgk1* mRNA and *edn1* hnRNA. This increase in hnRNA is consistent with the classical transcriptional mechanism of aldosterone.

Two HREs were mapped in the *edn1* promoter that each contained receptor binding half-sites separated by eight nucleotides in different orientations. Variations in spacer regions have been reported for several aldosterone response genes (Mick et al., 2001; Ou et al., 2001) and may influence cooperative binding of multiple hormone receptors (Ou et al., 2001). Indeed, both MR and GR interacted at the same HRE in the *edn1* promoter. Half-site orientation is also known to affect receptor binding as well as transcriptional activation (Geserick et al., 2005). Although GR can bind to directly repeated half-sites with low affinity (Aumais et al., 1996), structural studies revealed that GR preferentially binds to palindromic DNA sequences as a dimer in a "head-to-head" conformation (Luisi et al., 1991). Consistent with these reports, both MR and GR demonstrated a stronger affinity for HRE2 in comparison to HRE1. Moreover, only HRE2 could recruit RNA polymerase II. Similarly, the aldosterone response gene *scnn1a* also contains two

HREs in different orientations. Only the inverted HRE was capable of stimulating transcription (Sayegh et al., 1999).

Interestingly, inhibition of hormone receptors with spironolactone and RU486 resulted in hormone receptor nuclear translocation and *edn1* promoter binding (Figure 4-11). However, these antagonists are known to inhibit hormone receptors by altering receptor conformation and disrupting coactivator recruitment (Rogerson et al., 2003). Indeed, proper transcriptional coactivation by MR and GR requires the recruitment of SRC-1 (He et al., 2002; Li et al., 2005). ChIP analysis revealed that SRC-1 was recruited to the *edn1* promoter in the presence of aldosterone.

Multiple molecular studies in this report show that MR and GR were actively recruited to the *edn1* gene to mediate aldosterone action. Both hormone receptors have documented roles in regulating aldosterone response genes including *scnn1a* (Mick et al., 2001; Sayegh et al., 1999), *sgk1* (Chen et al., 1999; Itani et al., 2002), and *atp1a1* (Kolla et al., 1999; Whorwood et al., 1994). Both receptors have also been reported to mediate aldosterone stimulated Na^+ transport in the renal collecting duct (Bens et al., 1999; Gaeggeler et al., 2005). However, the role of GR in aldosterone action is actively debated due to the concept that GR would not active in aldosterone responsive cells that express 11β-HSD2 (Funder and Mihailidou, 2009; Funder et al., 1988; Gaeggeler et al., 2005; Odermatt and Atanasov, 2009). Indeed, 11β-HSD2 is an important enzyme that functions to inactive endogenous glucocorticoids and prevent glucocorticoid-mediated Na^+ retention by the collecting duct. However, 11β-HSD2 metabolites also lack an affinity for GR leaving GR expressed in collecting duct cells readily available for activation by another high affinity ligand such as aldosterone. Our studies show that MR and GR were present in the same protein complex. Several methods have demonstrated heterodimerization between

MR and GR (Liu et al., 1995; Savory et al., 2001) including Fluorescence Resonance Energy Transfer (Nishi et al., 2004). Moreover, these heterodimers exhibited distinct transcriptional properties (Liu et al., 1995). Indeed, aldosterone action mediated by two hormone receptors with different transcriptional properties would certainly provide a collecting duct cell with a higher degree of adaptability in the regulation of Na^+ transport.

Table 4-1 Antibodies and applications

Antibody	Source/Epitope	Application	Preparation	Supplier
anti-MR	monoclonal mouse anti-rat (aa 1-18)	Western/DAPA ChIP/ CoIP	1:100 10 µl/ IP	Kind gift of Drs. Elise and Celso Gomez-Sanchez
anti-GR	rabbit-anti-mouse (N-terminus)	Western/DAPA ChIP/ CoIP	1:5000 2.5 µl /IP	Santa Cruz (sc-1004x)
anti-SRC-1	monoclonal mouse anti-human (aa 477-947)	ChIP	1.5 µl /IP	Upstate (05-522)
anti-RNA pol II	monoclonal mouse anti-human (C-terminus)	Western/DAPA ChIP	1:1000 1 µl /IP	Upstate (05-623)
anti-H3	rabbit anti-human (C-terminus)	ChIP	2.5 µl /IP	Upstate (07-690)
anti-mK4-H3	rabbit anti-human (aa 1-8)	ChIP	5 µl /IP	Upstate (07-030)
anti-actin	goat-anti-human	Western/DAPA/CoIP	1:500	Santa Cruz (sc-1616)
secondary antibodies	anti-mouse HRP	Western	1:5000	USB (Rodeo Western Kit)
	anti-rabbit HRP	Western	1:5000	USB (Rodeo Western Kit)
	anti-goat HRP	Western	1:10000	Santa Cruz (sc-2768)

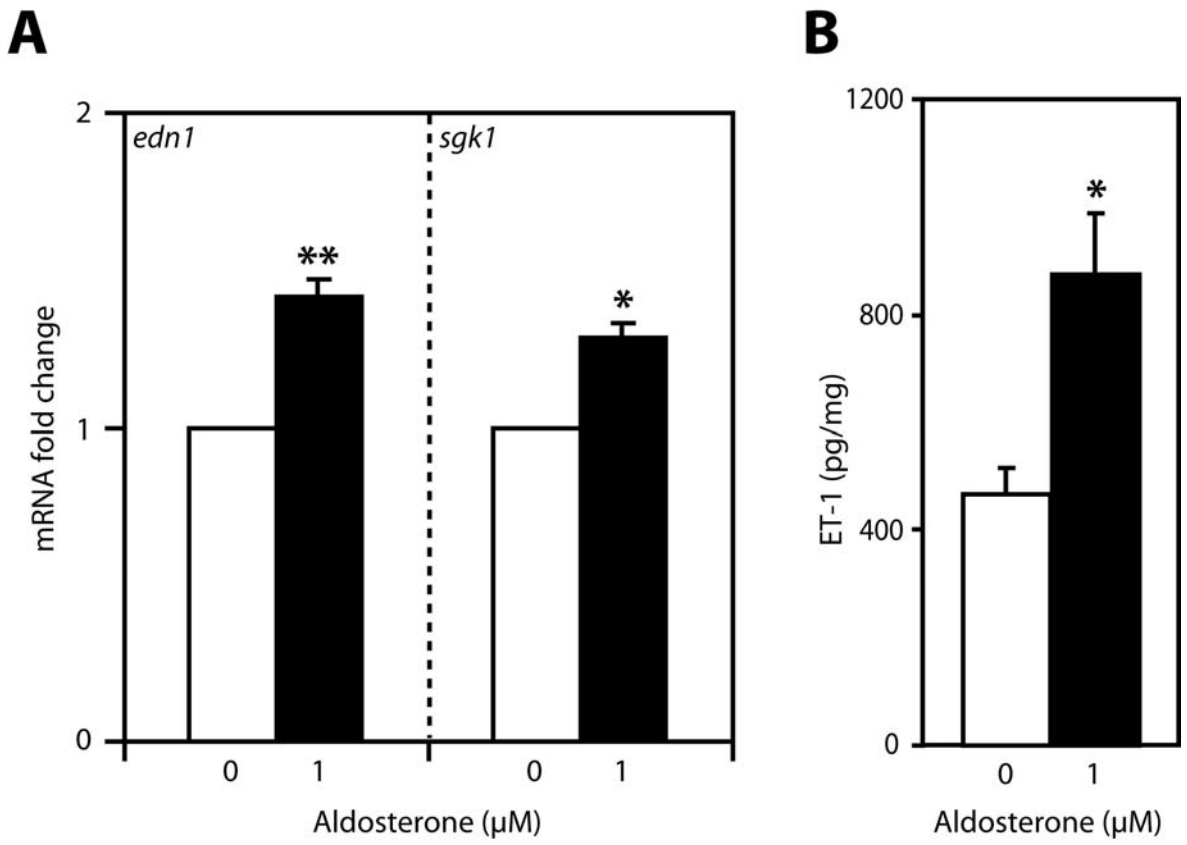

Figure 4-1. Aldosterone stimulation of inner medullary ET-1 expression in rat. A) IMCD cells were acutely isolated from rat and treated with vehicle (open bars) or 1 μM aldosterone (closed bars) for 1 h ex vivo. Levels of *edn1* and sgk1 mRNA were determined by QPCR, normalized to β-actin and expressed as fold change relative to vehicle ± SE. (n=4, *$p<0.05$, **$p<0.005$) B) Inner medullary ET-1 peptide levels were measured in kidneys isolated from rats injected with aldosterone (1 mg kg-1 body weight, ip) or vehicle for 2 h. Inner medullary ET-1 peptide levels were determined by ELISA and normalized to total protein content. Values are expressed as ET-1 (pg/mg protein) ± SE. ($n \geq 8$ per group, *$p<0.05$).

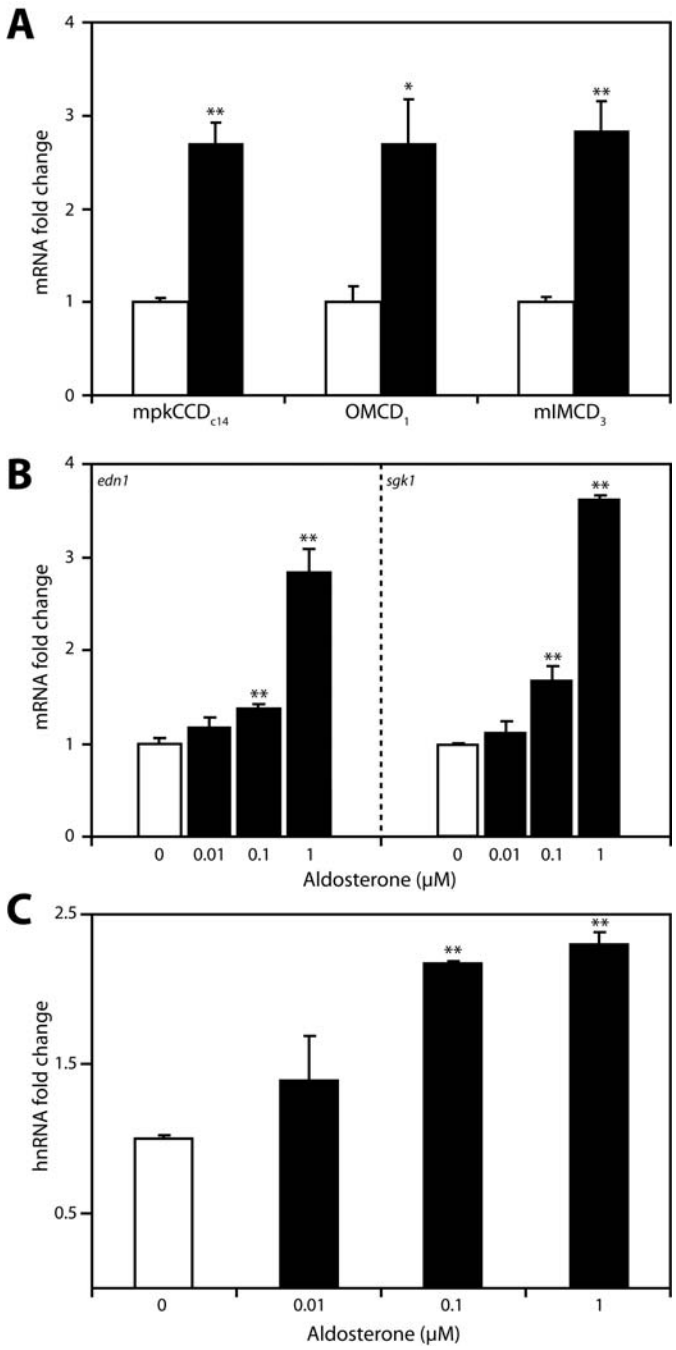

Figure 4-2. Aldosterone stimulation of *edn1* mRNA and hnRNA in collecting duct cells. A) Confluent monolayers of mpkCCD$_{c14}$, OMCD$_1$, or mIMCD-3 cells were treated with vehicle (open bars) or 1 μM aldosterone (closed bars) for 1 h. Steady state *edn1* mRNA was measured by QPCR, normalized to β-actin and expressed as mRNA fold change relative to vehicle ± SE. B) Steady state mRNA of *edn1* or sgk1 was quantified as above from mIMCD-3 cells treated with vehicle or aldosterone (0.01, 0.1, or 1 μM) for 1 h. C) Levels of *edn1* hnRNA were determined by SyBr Green QPCR, normalized to *gapdh* and expressed as hnRNA fold change relative to vehicle ± SE. ($n \geq 3$, $^{*}p<0.05$, $^{**}p<0.005$)

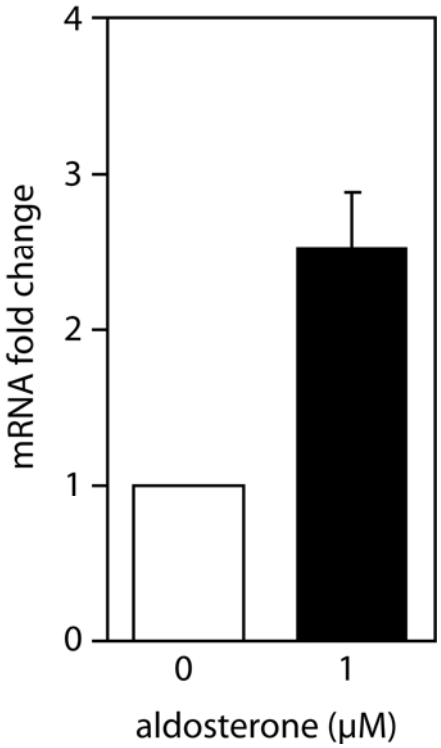

Figure 4-3. Aldosterone stimulation of *edn1* mRNA in mIMCD-K2 cells. Confluent monolayers of mIMCD-K2 cells were treated with vehicle (open bars) or 1 μM aldosterone (closed bars) for 1 h. Total RNA was extract, converted to cDNA and steady state *edn1* mRNA was measured by QPCR. Values were normalized to *gapdh* and are expressed as mean fold change relative to vehicle ± SE. (n=2)

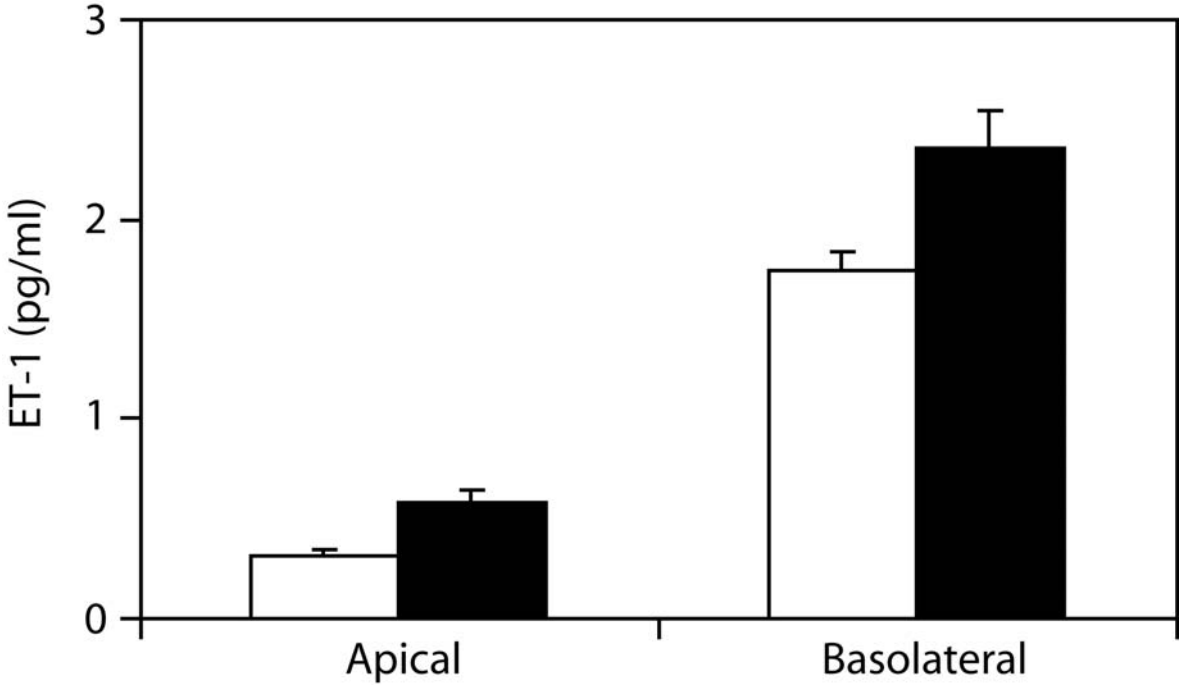

Figure 4-4. Aldosterone stimulation of ET-1 peptide release from mIMCD-3 cells. Confluent monolayers of mIMCD-3 cells were grown on permeable supports and treated with vehicle (open bars) or 1 μM aldosterone (closed bars) for 1 h. Media was collected from the top (apical) and bottom (basolateral) wells, and soluble ET-1 peptide was measured by ELISA. (n=3)

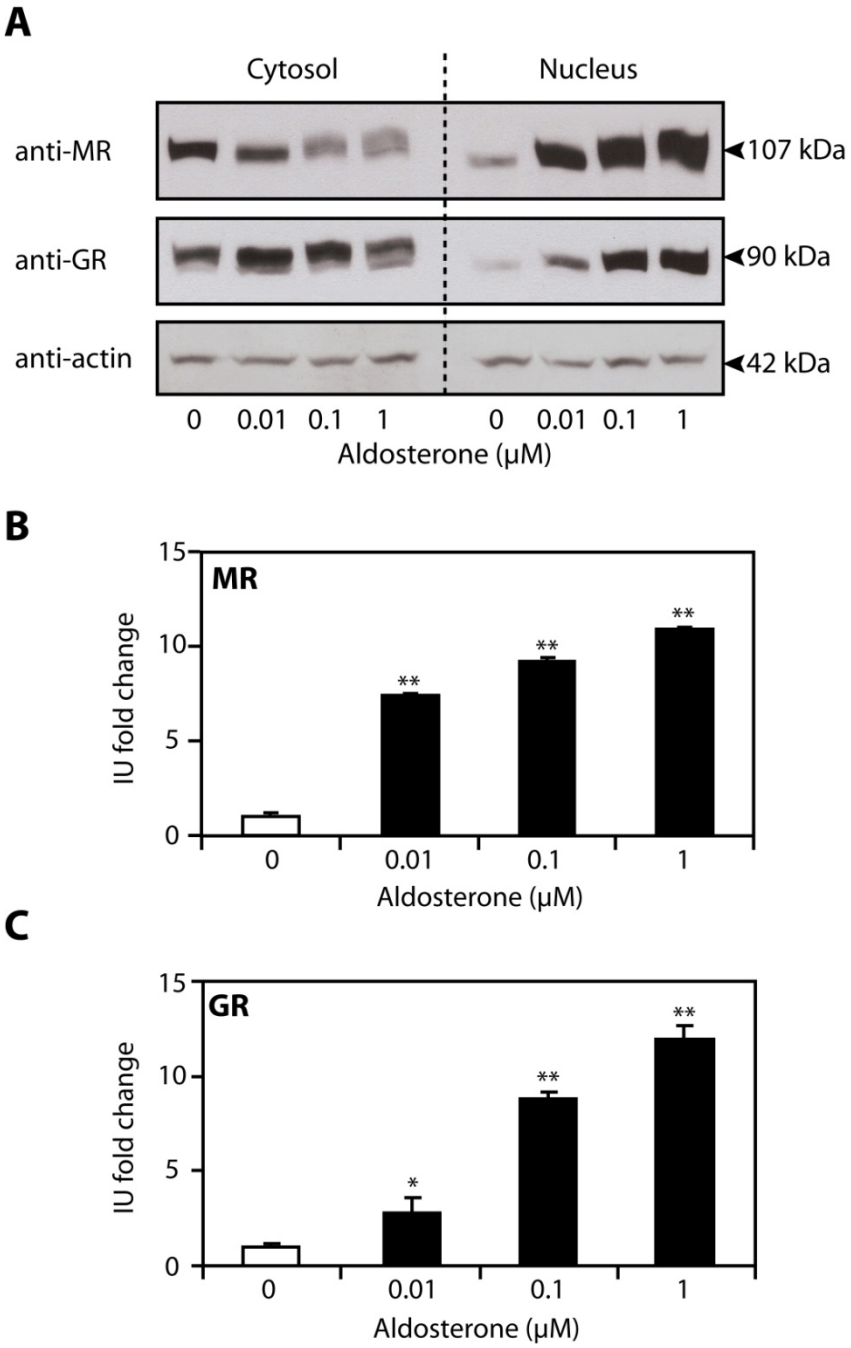

Figure 4-5. Aldosterone action in mIMCD-3 cells is mediated through MR and GR. A) Receptor nuclear translocation was followed by western blot for MR (top panel) and GR (middle panel) on cytosolic and nuclear extracts obtained from mIMCD-3 cells treated with vehicle or aldosterone (0.01, 0.1, or 1 μM) for 1 h. Blots were stripped and reprobed for actin (lower panel) to verify equal loading. B,C) Densitometry was used to quantify the relative abundance of MR (B) and GR (C) in the nucleus. Values are expressed as the fold change in intensity units (IU) relative to vehicle control ± SE. ($n \geq 3$, *$p<0.05$, **$p<0.005$)

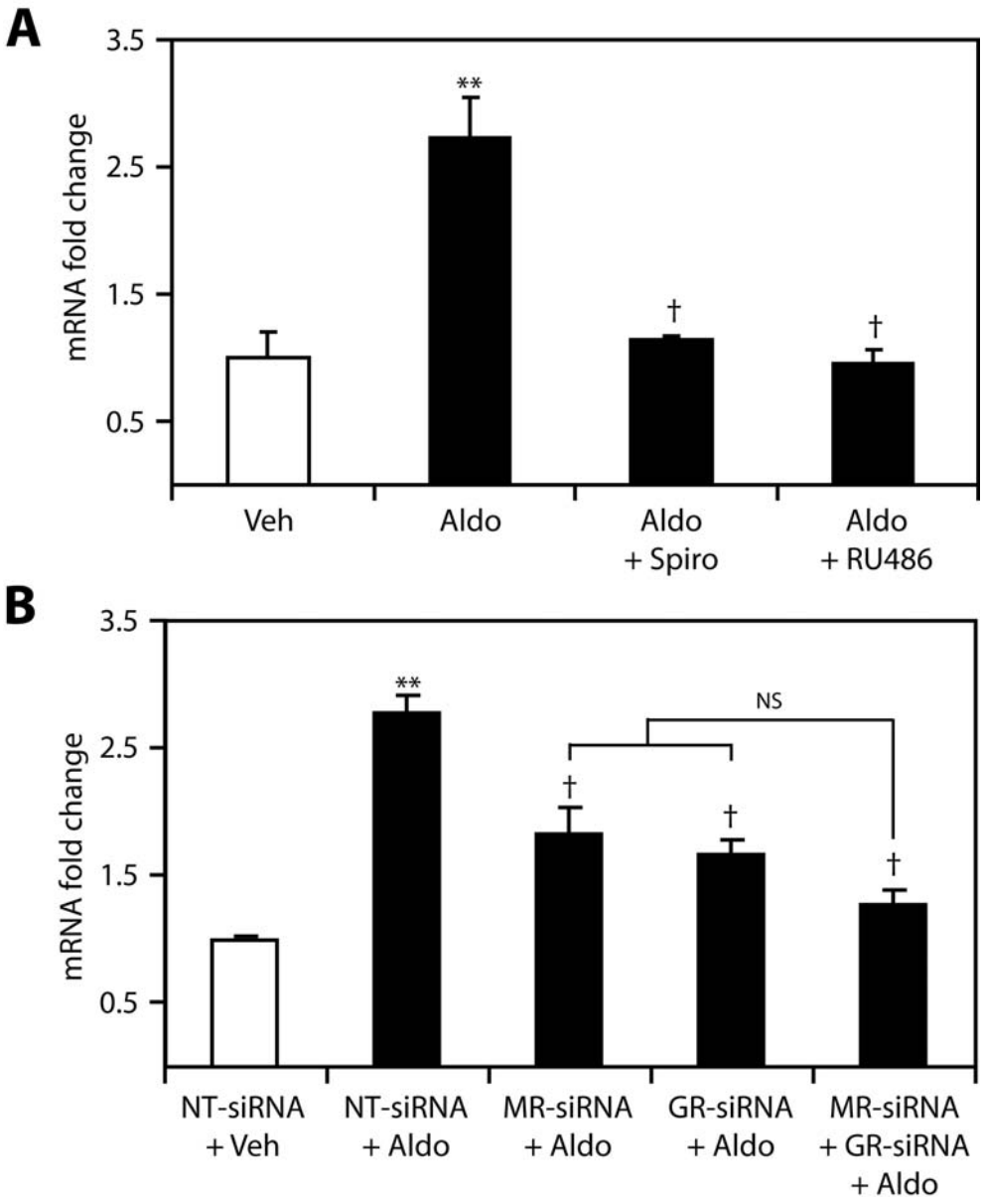

Figure 4-6. Blockade of MR or GR inhibits aldosterone induction of *edn1* mRNA. A) The effect of pharmacological inhibition of MR or GR on aldosterone-stimulated *edn1* mRNA was evaluated in mIMCD-3 cells treated with vehicle (veh, open bars), 1 μM aldosterone (aldo, closed bars), or 1 μM aldosterone in the presence of 10 μM spironolactone (spiro) or 10 μM RU486 for 1 h. *Edn1* mRNA levels were determined by QPCR. Values are expressed as mean fold change relative to vehicle ± SE. ($n \geq 3$, $^{**}p<0.005$ vs. vehicle; $^{t}p<0.005$ vs. aldosterone) B) The effect of siRNA silencing of MR or GR on aldosterone-stimulated *edn1* mRNA was evaluated. Cells were transfected with control non-target (NT)-siRNA, MR-siRNA or GR-siRNA 24 h prior to being treated with vehicle or 1 μM aldosterone for 1 h. Changes in mRNA were measured by QPCR as above. Values are expressed as mean fold change relative to vehicle treated cells transfected with NT-siRNA ± SE. ($n=3$, $^{**}p<0.005$ vs. NT-siRNA plus vehicle, $^{t}p<0.05$ vs. NT-siRNA + aldosterone, NS=not significant)

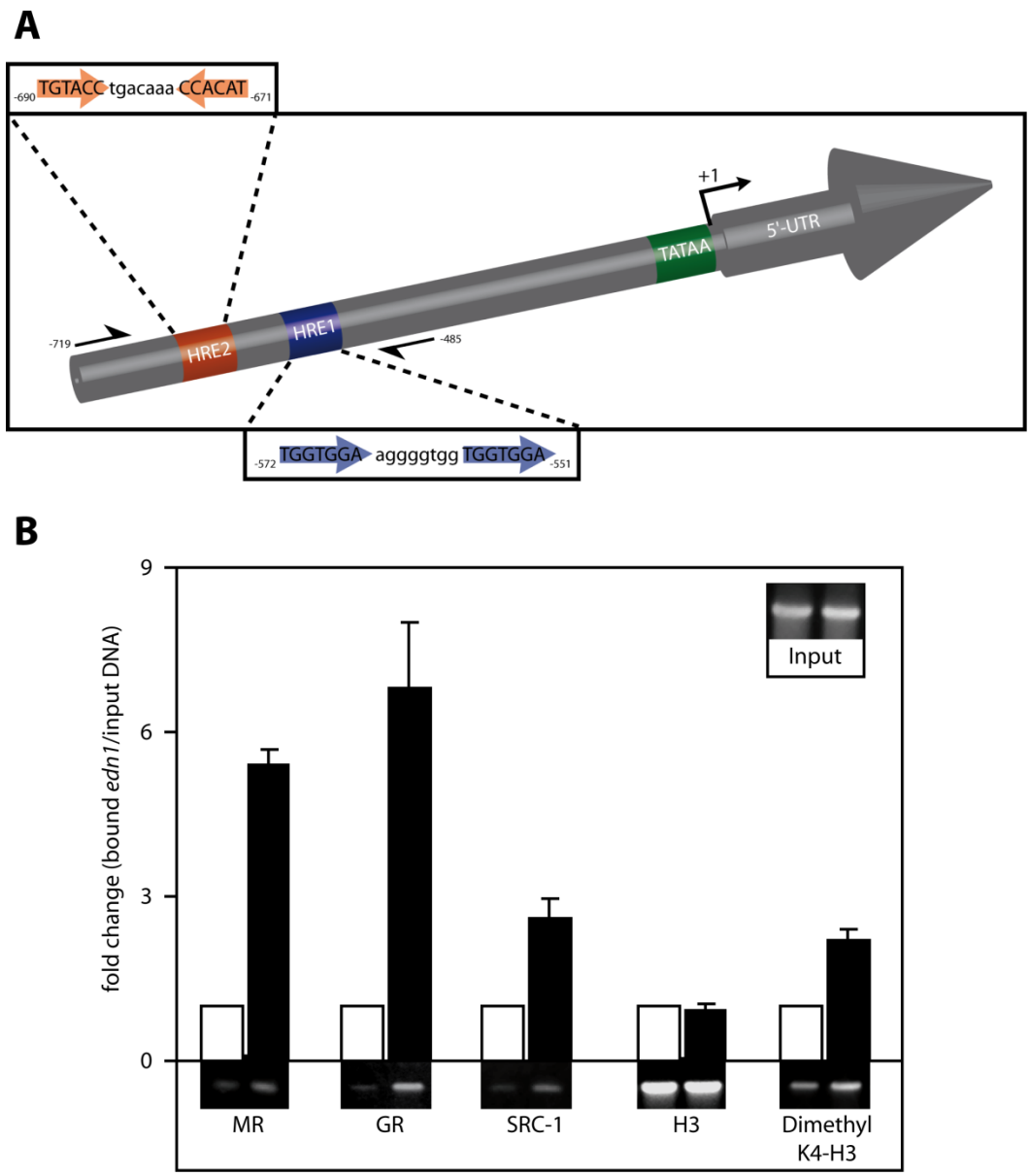

Figure 4-7. Aldosterone recruits steroid receptors to a region of the murine *edn1* promoter containing two putative HREs. A) Diagram of the *edn1* promoter indicating the position of the identified HREs relative to the transcriptional start site (+1) (not to scale). HRE sequences are magnified and receptor binding half-sites are shown in capital letters. Half-site orientation is indicated with arrows. Primers used in ChIP assays flank both HREs and are indicated with half arrows. B) ChIP assays were used to detect protein binding to the *edn1* promoter in vehicle (open bars) or 1 μM aldosterone (closed bars) treated mIMCD-3 cells. Antibodies used for immunoprecipitation are indicated below. Bound *edn1* DNA was quantified by SyBr Green QPCR. Values were normalized to total input DNA and expressed as mean fold change relative to vehicle ± SE. Additionally, standard PCR products were run on a 5 % TBE gel and imaged with SyBr green dye. Representative gels are displayed below their corresponding QPCR values. (n≥3)

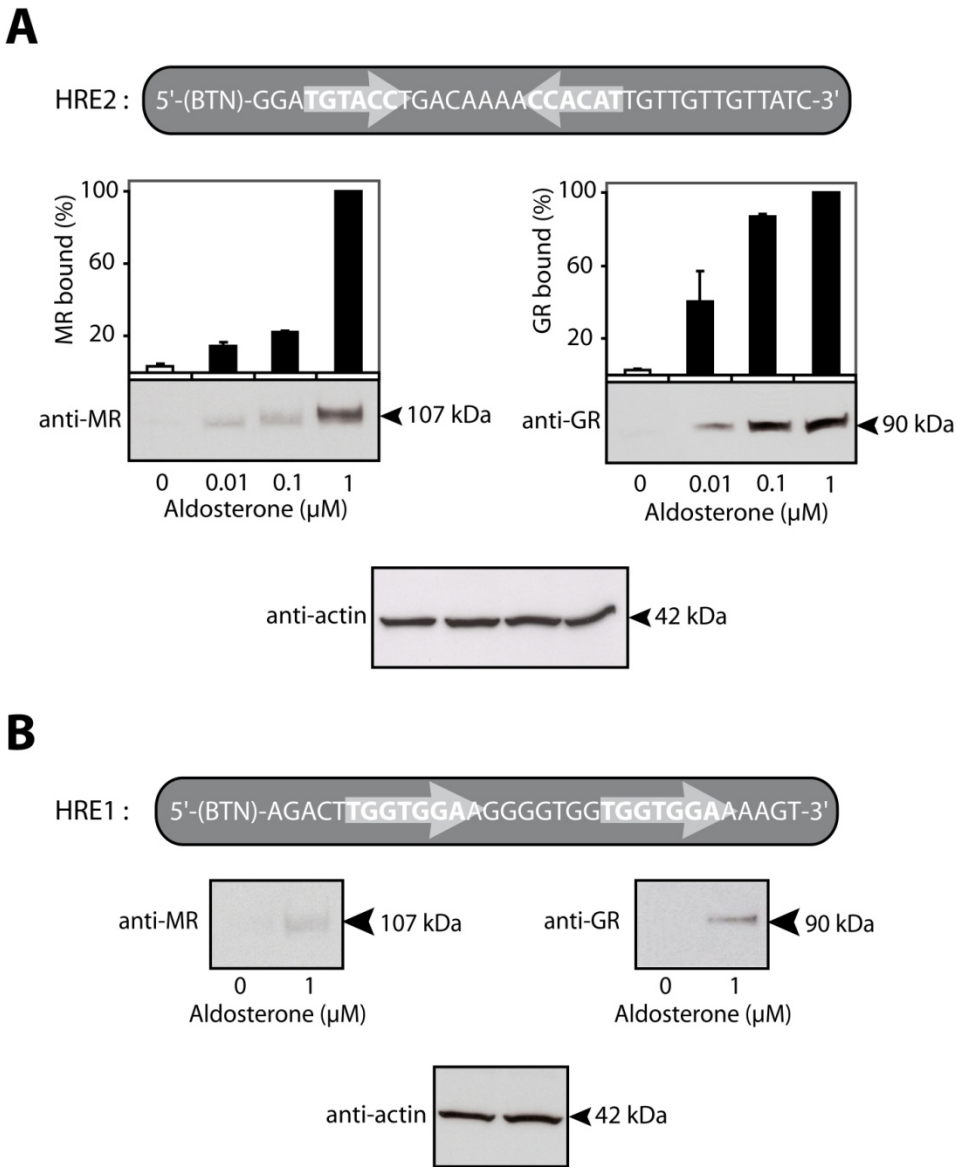

Figure 4-8. Steroid receptors bind directly to HRE1 and HRE2 in the *edn1* promoter. DAPA experiments were performed on nuclear extracts from vehicle and aldosterone treated mIMCD-3 cells in order to map receptor binding to either HRE with higher resolution. A) Representative immunoblots following DAPA experiments using HRE2 as bait are shown for MR (left panel) and GR (right panel). Immunoblots were quantified by densitometry. Values were normalized by setting total intensity units calculated for MR (or GR) in the presence of 1 μM aldosterone to 100%. Equal loading was verified by immunoblot against actin (bottom panel). (n≥3). It is also important to note that the DAPA probe (shown on top of panel A) contains a region of DNA immediately adjacent to HRE2 that may also contribute to hormone receptor binding (See Chapter 3). B) Representative immunoblots are shown for MR (left panel), GR (right panel), and actin (lower panel) from DAPA experiments using HRE1 as bait. Densitometry was not performed because MR and GR were not consistently detected at concentrations of aldosterone lower than 1 μM. (n≥3)

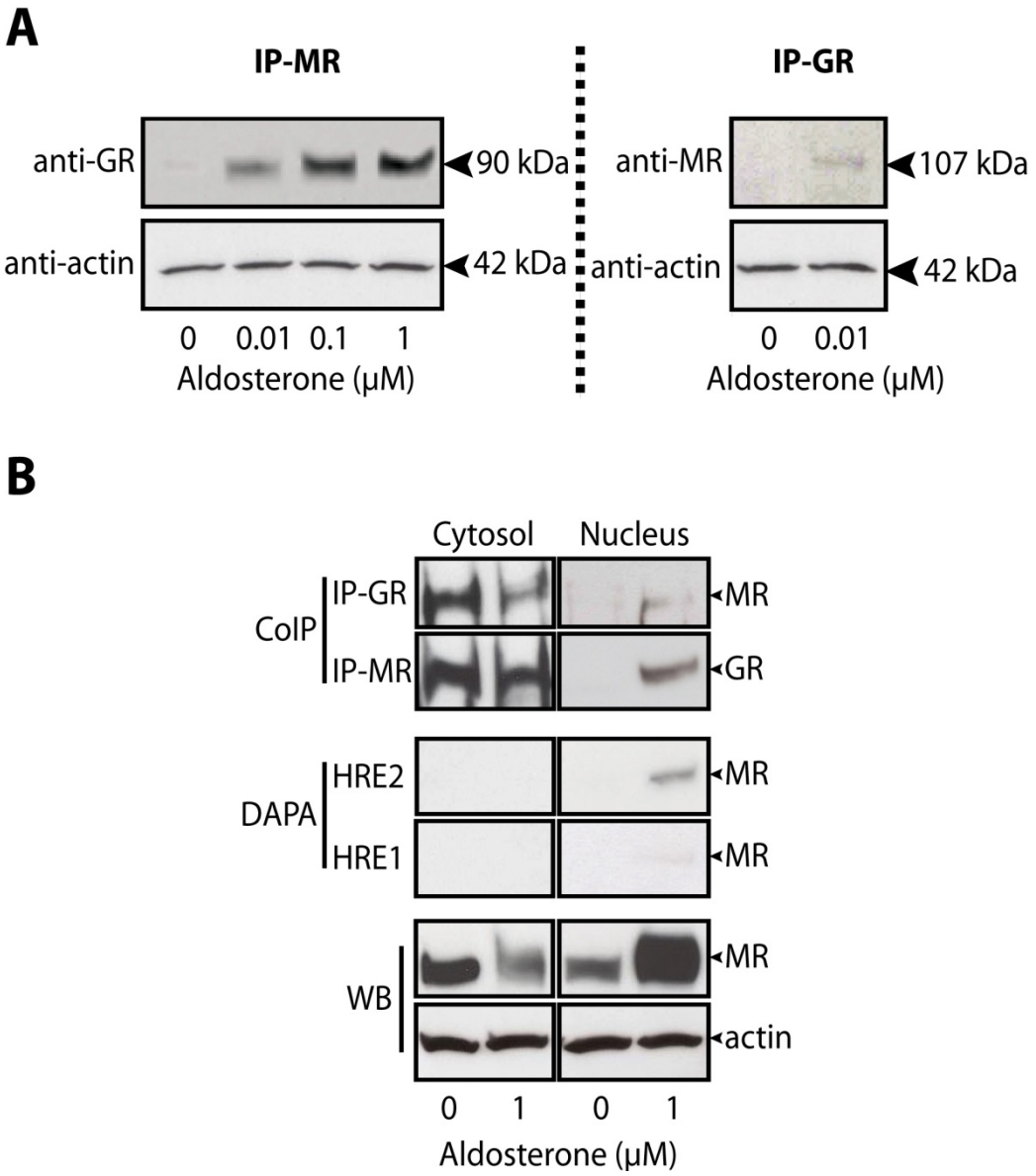

Figure 4-9. Aldosterone-dependent association of MR and GR by coimmunoprecipitation. A) Nuclear extracts from mIMCD-3 treated with vehicle, aldosterone, aldosterone plus 10 μM spironolactone (S), or 10 μM spironolactone alone were subjected to immunoprecipitation (IP) with anti-MR and subsequently immunoblotted for GR. As a control, nuclear extracts from vehicle and 1 μM aldosterone treated cells were subjected to the reverse immunoprecipitation by anti-GR followed by immunoblot against anti-MR. ($n \geq 3$) B) The ability of MR and GR interact with one another and with DNA was evaluated in cytosolic and nuclear extracts from mIMCD-3 cells. Coimmunoprecipitation (coIP) experiments were conducted as above using either anti-GR or anti-MR as bait. Similarly, cytosolic and nuclear extracts from vehicle or aldosterone treated cells were subjected to DAPA using either HRE2 or HRE1 as bait. Western blots against MR and actin are shown as controls.

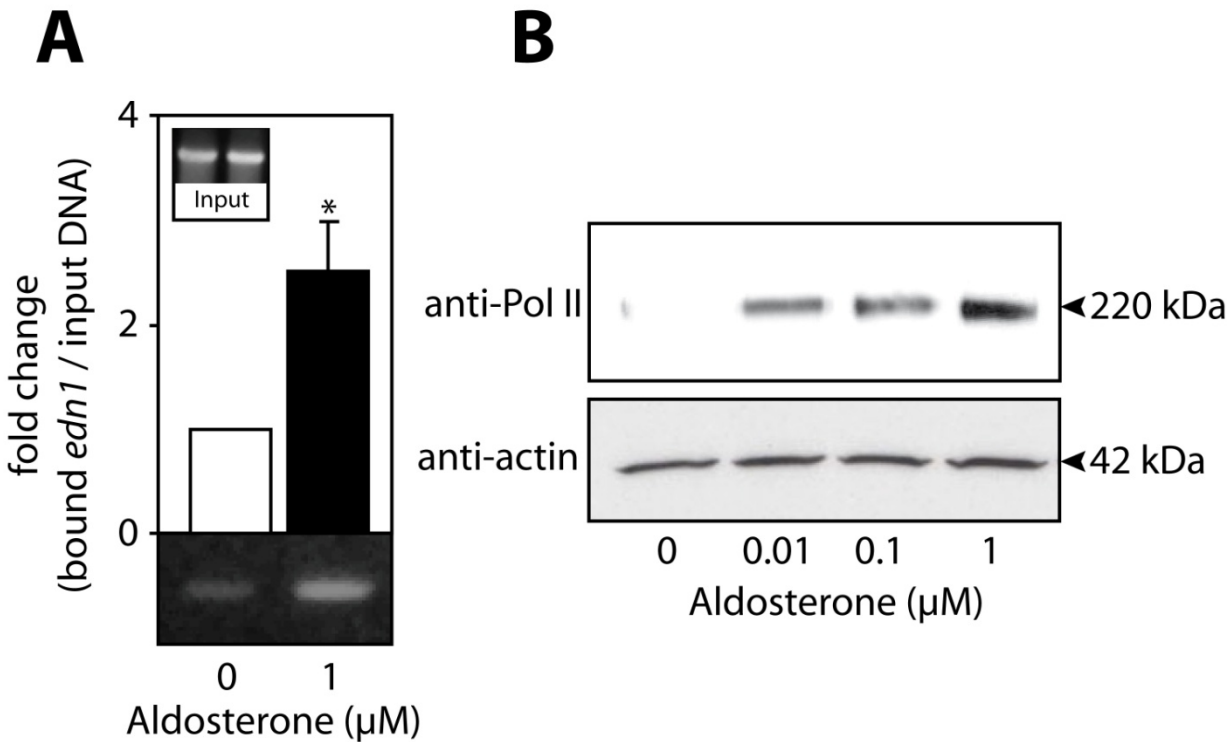

Figure 4-10. Aldosterone-dependent recruitment of RNA polymerase II to the *edn1* promoter. A) ChIP assays were used to detect RNA polymerase II (Pol II) binding to the *edn1* promoter in vehicle (open bars) or 1 μM aldosterone (closed bars) treated mIMCD-3 cells. Bound *edn1* DNA was quantified as above by SyBr Green QPCR or imaged by running standard PCR products on a 5% TBE gel. QPCR values are normalized to total input DNA and expressed as mean fold change relative to vehicle ± SE. (n≥3) B) Dose-dependent recruitment of RNA polymerase II to HRE2 was evaluated by DAPA on vehicle and aldosterone treated mIMCD-3 cells. Representative immunoblots for Pol II and actin loading controls are shown. (n=3)

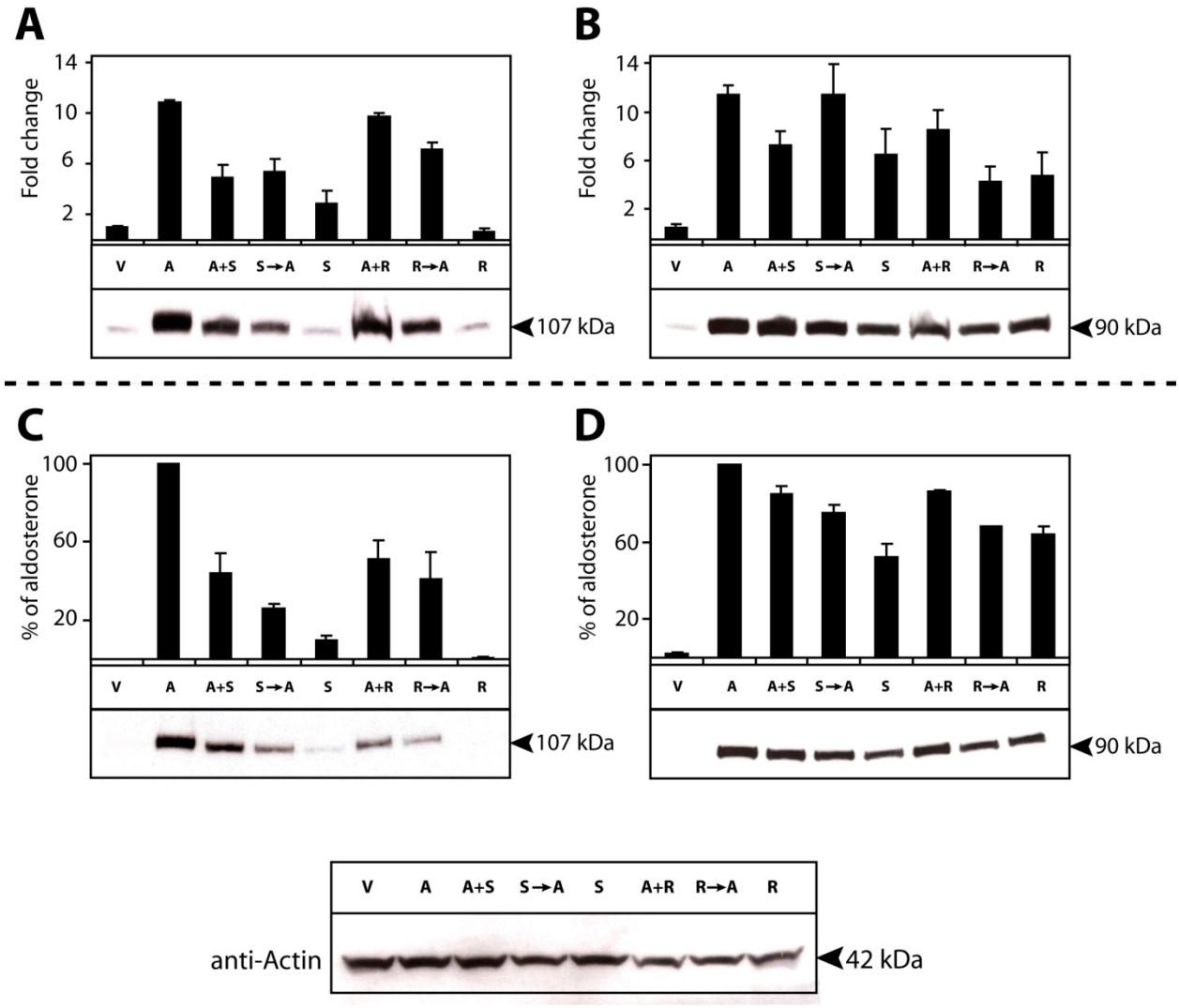

Figure 4-11. Spironolactone and RU486 induce nuclear translocation and binding of MR and GR to *edn1*. A,B) Nuclear translocation studies were performed on mIMCD-3 cells treated with vehicle (V), 1 μM aldosterone (A), 10 μM spironolactone (S), and/or 10 μM RU486 (R). Treatments are indicated above each lane. Aldosterone was added at the same time as antagonist in lane 3 (A+S) and lane 6 (A+R). Antagonists were added 1 h prior to aldosterone treatments in lane 4 (S®A) and lane 7 (R®A). Representative western blots are shown for MR (A) and GR (B) and densitometric values are indicated above each gel. (n≥3) C,D) DAPA experiments were performed on nuclear extracts obtained from mIMCD-3 cells treated as above to evaluated MR (C) and GR (D) binding to HRE2. Densitometric values are indicated above each blot. (n≥3) Actin loading control is shown at the bottom.

CHAPTER 5
DEXAMETHASONE STIMULATES ENDOTHELIN-1 GENE EXPRESSION IN COLLECTING DUCT CELLS IN VITRO

Introduction

The glucocorticoid receptor (GR) is ubiquitously expressed in the body and is responsible for modulating an extraordinarily wide range of physiological processes (Coutard et al., 1978; Kalinyak et al., 1987; Rashid and Lewis, 2005; Thompson, 1987; Turner et al., 2006). GR functions as a ligand-dependent transcription factor and is estimated to modulate 10% of the genes within the human genome (Galon et al., 2002; van der Laan et al., 2008). GR shares extensive structural homology and overlapping DNA targets with the mineralocorticoid receptor (MR) (Arriza et al., 1987). However, the expression and function of MR is more specific than GR. Most notably, MR is expressed in polarized epithelial cells involved in Na^+ transport including the mineralocorticoid-sensitive cells of the distal nephron and collecting duct of the kidney (Funder, 2005). In these cells, MR plays a vital role in the maintenance of Na^+ homeostasis and blood pressure control through the transcriptional regulation of genes involved in transepithelial Na^+ transport (Fuller, 2004; Odermatt and Atanasov, 2009; Viengchareun et al., 2007).

Renal collecting duct cells express both MR and GR *in vivo* (Todd-Turla et al., 1993). However, the function of GR in aldosterone-target cells is not well understood since these cells express 11β-hydroxysteroid dehydrogenase type II (11βHSD-2). This enzyme oxidizes endogenous glucocorticoids (cortisol in humans, corticosterone in rats) into 11-keto metabolites that are unable to activate MR or GR (Funder et al., 1988; Grossmann et al., 2004b). The absence of functional 11βHSD-2 in renal collecting duct cells can have detrimental effects. Indeed, glucocorticoids can bind to MR with similar affinity to aldosterone ($K_D \approx 0.5$ nM) (Arriza et al., 1987) and result in inappropriate salt retention and hypertension (Frey et al., 2004;

Ulick et al., 1979). However, under normal conditions endogenous glucocorticoids are inactivated, so the purpose of its cognate receptor, GR, is not well defined in renal collecting duct cells (Odermatt and Atanasov, 2009).

Aldosterone is known to bind GR with an affinity that is similar to cortisol ($K_D \approx 10$ nM) (Arriza et al., 1987; Hellal-Levy et al., 1999). Therefore, it is possible that GR functions in concert with MR to mediate aldosterone action. Consistent with this hypothesis is a recent study conducted on an inducible transgenic mouse line over expressing GR in the collecting duct (Nguyen Dinh Cat et al., 2009). In this study, mice exhibited an increase in *scnn1a* (αENaC) in the collecting duct and a decrease in urinary aldosterone levels, indicating a transient GR-dependent change in Na^+ balance *in vivo*. Furthermore, published data from Chapter 4 showed that aldosterone stimulated the transcription of *edn1* in collecting duct cells by a mechanism involving both MR and GR (Stow et al., 2009). Indeed, both receptors bound directly to the same HREs in the *edn1* promoter (Figure 4-8); a phenomenon that has been observed for several other aldosterone target genes (Itani et al., 2002; Kolla et al., 1999; Mick et al., 2001; Ou et al., 2001). Likewise, aldosterone-dependent GR activation has been previously reported (Gaeggeler et al., 2005; Gauer et al., 2007; Gumz et al., 2003; Liu et al., 1995) and signaling by both MR and GR are able to stimulate Na^+ transport in collecting duct cells (Husted et al., 1990).

While there is mounting evidence suggesting that GR can contribute to aldosterone action in the kidney, it is not known whether GR acts in concert with MR or if GR can act independently. The goal of the present study was to determine if GR could independently stimulate *edn1* expression in mIMCD-3 and mpkCCD$_{c14}$ collecting duct cell lines. Since collecting duct cells metabolize endogenous glucocorticoids, selective GR action on *edn1* was evaluated with dexamethasone, a synthetic glucocorticoid that is not inactivated by 11βHSD-2 .

Importantly, dexamethasone is advantageous for studying selective GR activation because it exhibits a very high affinity for GR and essentially no affinity for MR (Rebuffat et al., 2004). Data presented in this chapter shows that selective activation of GR by dexamethasone stimulates *edn1* expression in renal collecting duct cells.

Materials and Methods

Cell Culture and Hormone Treatment

The mpkCCD$_{c14}$ cells were a kind gift of Dr. Alain Vandewalle (Rebuffat et al., 2004) and mIMCD-3 cells were purchased from American Type Culture Collection. All cells were maintained in DMEM/F12 plus 10% FBS and 50 μg/ml gentamicin and passaged every 48 h. For all hormone experiments cells were plated on 6-well Costar Transwell plates (Corning Inc.). Cells were grown 24 h past confluency and changed to DMEM/F12 plus 10% charcoal-dextran stripped FBS (Invitrogen Corp.) for another 24 h prior to hormone treatments. Aldosterone, dexamethasone, spironolactone and RU486 were purchased from Sigma-Aldrich, prepared in 100% ethanol at 1 mg/ml stocks and stored at -20 °C until use. Cells were treated with vehicle (0.1% ethanol), 1 μM dexamethasone or 1 μM aldosterone for 1 h. For inhibitor studies, cells were treated with agonist plus RU486 (10 μM) or spironolactone (10 μM).

Steady-State mRNA Determination

Hormone studies were conducted as described above on growth-arrested confluent cell monolayers grown in 6-well Costar Transwell plates. Total RNA (2 μg) was isolated from cells using TRIzol® Reagent (Invitrogen), treated with DNase I (Ambion) to eliminate genomic DNA, and reverse transcribed using oligo dT, random hexamers and Superscript™ III (Invitrogen). No reverse transcriptase served as a negative control in the cDNA reaction. Resulting cDNAs (32 ng) were used as templates in duplicate QPCR reactions run on an Applied Biosystems QPCR machine. No template cDNA was used a negative control in QPCR experiments. Cycle

threshold (C_T) values were normalized against β-actin (*actb*) and relative quantification was performed using the $\Delta\Delta C_T$ method (Livak and Schmittgen, 2001). TaqMan® (Applied Biosystems) primer/probe sets for used are indicated in Table 5-1. Applied Biosystems guarantees that all TaqMan® primer/probe sets are target specific and were run with standardized QPCR conditions using the $\Delta\Delta C_T$ method. Importantly, Applied Biosystems guarantees that TaqMan® products have 100% PCR efficiency over six logarithms of template (Applied Biosystems, 2006).

Hormone Receptor siRNA Knockdown

MR-siRNA (J-061269-09 NR3C2), GR-siRNA (J-045970-10 NR3C1) and control non-targeting siRNA against luciferase (#2 D-001210-02-05) were purchased from Dharmacon (Lafayette, CO, USA). Cells were seeded at a density of 75,000 cells per cm^2 on 6-well Transwell plates (Corning Incorporated) and transfected for 24 h with 2 μM siRNA in 6 μl of DharmaFect 4. At the time of transfection cells were switched to phenol-red free DMEM/F12 plus 10% charcoal dextran stripped FBS. After 24 h the cells were treated with 1 μM dexamethasone or vehicle for 1 h. RNA was extracted and processed as described above for QPCR.

Statistics

Unless otherwise stated, all experiments were performed in duplicate at least three independent times. Statistical significance was determined using a two-tailed Student's *t* test and $p < 0.05$ was considered significant.

Results

Relative Expression of Hormone Receptors in mIMCD-3 cells

Published data presented in Chapter 4 showed that aldosterone treatment resulted in comparable increases in MR and GR bound to HRE2 of the *edn1* promoter (Figure 4-8) (Stow et

al., 2009). Furthermore, blockade of either MR or GR resulted in a comparable reduction in aldosterone-dependent *edn1* gene expression (Figure 4-6) (Stow et al., 2009). Therefore, we hypothesized that mIMCD-3 cells expressed the MR and GR genes, *nr3c2* and *nr3c1*, respectively. Furthermore, it seemed reasonable that the mRNA levels for both receptors would be present at approximately equal levels. To test this hypothesis, MR and GR mRNA expression levels were evaluated in mIMCD-3 cells from control experiments. QPCR was run using Taqman® assay reagents that have validated PCR efficiencies of 100% for each primer/probe set (Applied Biosystems, 2006). As expected, mIMCD-3 cells expressed both MR and GR mRNA (Figure 5-1), which is consistent with expression patterns *in vivo* (Todd-Turla et al., 1993). However, the expression of GR was unexpectedly 13.2 ± 0.4 fold higher than the expression of MR. Of note, the higher level of GR expression is roughly equal to the difference in aldosterone's affinity for MR (~ 0.5 nM) versus GR (~10 nM) (Arriza et al., 1987). These data support the concept that aldosterone action on collecting duct cells is mediated through both GR and MR in mIMCD-3 cells.

Dexamethasone-Dependent Gene Expression in Collecting Duct Cells

To test the hypothesis that selective GR activation could stimulate *edn1* gene transcription, mIMCD-3 cells were treated with vehicle, 1 μM dexamethasone or 1 μM aldosterone for 1 h. As expected, aldosterone induced a 2.72 ± 0.35 fold increase in *edn1* mRNA levels (Figure 5-2). Dexamethasone also stimulated an increase in *edn1* mRNA levels that was equal to 4.00 ± 0.08 fold increase compared to vehicle control, a level significantly higher in magnitude compared to *edn1* levels in the presence of 1 μM aldosterone (Figure 5-2).

The pattern of robust gene expression induced by dexamethasone was also observed for other aldosterone-regulated genes. The level of *sgk1* mRNA was 8.15 ± 0.20 fold higher in the presence of dexamethasone compare to vehicle. Similarly levels of *per1* mRNA was 9.14 ± 0.47

fold higher in the presence of dexamethasone compared to vehicle. For both genes, the magnitude of mRNA induction was greater in the presence of 1 μM dexamethasone than in the presence of 1 μM aldosterone (Figure 5-2). Of note, both aldosterone and dexamethasone stimulated a modest increase in αENaC (*scnn1a*) expression at 1 h. This low level of stimulation at 1 h is consistent with the fact that aldosterone-dependent *scnn1a* expression takes 2 to 4 h to observe a significant increase (Mick et al., 2001).

A similar hormone study was conducted in mpkCCD$_{c14}$ cells to determine if dexamethasone stimulation of *edn1* occurred in another collecting duct cell line. Importantly, this cell line also expresses functional 11βHSD-2 and both MR and GR at relatively high abundances (Bens et al., 1999). Consistent with results from mIMCD-3 cells, 1 μM dexamethasone stimulated robust increases in *sgk1* and *per1* mRNAs at 1 h (Figure 5-3). Furthermore, *edn1* and *scnn1a* mRNAs also exhibited moderate increases. In some experiments cells were also treated with 1 μM aldosterone as a positive control. On a technical note, these pilot experiments were conducted at a separate time than other reported studies (Chapter 4) and mpkCCD$_{c14}$ cells did not appear as responsive. However, as observed in mIMCD-3 cells, the trend for higher gene expression in the presence of dexamethasone compared to equal molar aldosterone was observed (Figure 5-3).

Effect of Pharmacological Inhibition of Hormone Receptors on Dexamethasone-Induced Gene Expression

The effect of MR or GR antagonism on dexamethasone-stimulated *edn1*, *sgk1*, and *scnn1a* expression was evaluated by treatment with spironolactone or RU486, respectively. RU486 is a GR antagonist with little affinity for MR. Treatment of mIMCD-3 cells with RU486 completely blocked dexamethasone induction of *edn1* mRNA (Figure 5-4). Likewise, RU486 greatly reduced dexamethasone induction of *sgk1* mRNA, although mRNA levels did not

completely return to levels in control treated cells (Figure 5-4). In contrast, antagonism of MR with spironolactone had no effect on dexametheasone-mediated *sgk1* and appeared to have very little effect on *scnn1a* mRNA. Spironolactone also resulted in only a modest reduction in dexamethasone-mediated *edn1* expression (Figure 5-4). Of note, spironolactone has a moderate antagonistic effects on GR (Couette et al., 1992) and studies in Chapter 4 that showed spironolactone was able to induce GR nuclear translocation and binding to the *edn1* promoter (Stow et al., 2009). Taken together, these data suggested that most if not all of the dexamethasone-dependent *edn1* gene expression was mediated through GR.

Effect of siRNA Knockdown of Hormone Receptors on Dexamethasone-Regulated Gene Expression

Because pharmacological inhibitors have overlapping specificities, the effect of MR or GR siRNA knockdown was evaluated in mIMCD-3 cells. Independent transfection of either MR- or GR-siRNA resulted in approximately 90% knockdown of their relevant mRNA (Gumz et al., 2009a). In the presence of 1 μM dexamethasone, siRNA blockade of GR blunted *edn1* and *sgk1* mRNA levels by approximately 50% (Figure 5-5). Conversely, siRNA of blockade of MR had no effect on dexamethasone-induced *edn1* mRNA levels (Figure 5-5). Interestingly, dexamethasone-induced *sgk1* mRNA was actually higher in the presence of MR-siRNA (Figure 5-5). Cotransfection of MR and GR siRNAs together had no additive effect on *edn1* or *sgk1* compared to GR-siRNA alone. These data strongly support the concept that dexamethasone action was mediated exclusively through GR. Moreover, these data support the concept that spironolactone is a partial antagonist of GR-dependent *edn1* transcription since siRNA against MR had no effect on *edn1* transcription but spironolactone tended to decrease *edn1* mRNA levels. There was no significant effect on the minimal dexamethasone-dependent *scnn1a* gene expression observed at 1 h (Figure 5-5, right panel).

Taken together, dexamethasone-stimulated gene expression of *edn1*, *sgk1*, and *per1* in mIMCD-3 and mpkCCD$_{c14}$ cells was consistently more robust than aldosterone-stimulated gene expression using equal molar amounts of aldosterone or dexamethasone. Furthermore, dexamethasone-dependent gene expression was mediated exclusively though GR.

Discussion

The studies presented here demonstrated that dexamethasone stimulated *edn1* gene expression in mIMCD-3 and mpkCCD$_{c14}$ collecting duct cells. QPCR analysis determined that mIMCD-3 cells expressed GR mRNA in addition to MR mRNA, which is consistent with protein expression in mIMCD-3 cells (Chapter 4) (Stow et al., 2009), mpkCCD$_{c14}$ cells (Bens et al., 1999) and in collecting ducts *in vivo* (Todd-Turla et al., 1993). Pharmacological and siRNA knockdown studies confirmed that the action of dexamethasone on *edn1* mRNA was mediated exclusively though GR. Furthermore, dexamethasone-dependent GR activation resulted in the robust stimulation of other aldosterone target genes tested including *sgk1* and *per1*. The magnitude of dexamethasone-dependent gene transcription in both mIMCD-3 and mpkCCD$_{c14}$ cells was higher than aldosterone-dependent gene transcription under the experimental conditions tested. There was also a minimal increase observed in *scnn1a* in the presence of aldosterone or dexamethasone that did not appear to be affected by MR or GR blockade. Indeed, the earliest stimulation in *scnn1a* may be due to non-genomic actions of MR and/or GR cascade signaling (Boldyreff and Wehling, 2003).

Given that aldosterone acts through both MR and GR, whereas dexamethasone is thought to have exclusive affinity for GR, the observation that dexamethasone resulted in a more robust increase in *edn1* mRNA suggests that GR might be a stronger transcription factor than MR for the *edn1* gene. Consistent with this concept, dexamethasone activation of GR resulted in a robust increase in Na^+ transport in primary cultures of rat inner medullary collecting ducts that

exceeded the response achieved by aldosterone (Husted et al., 1990). The apparent difference in the magnitude of dexamethasone-induced *edn1* mRNA compared to aldosterone induction may be explained by differences in transcriptional machinery recruited to GR versus MR. For example, the elongation factor ELL (11, 19-lysine rich leukemia) activates MR, but strongly represses GR (Pascual-Le Tallec et al., 2005). Furthermore, it is possible that MR and GR form a functional heterodimers in the presence of aldosterone. Indeed, heterodimerization between MR and GR is known to occur (Nishi et al., 2004; Ou et al., 2001; Pascual-Le Tallec et al., 2005) and exhibit distinct transcriptional properties compared to either receptor acting alone (Ou et al., 2001; Trapp and Holsboer, 1996).

Alternatively, the difference in transcription activation may be explained by ligand-mediated conformational changes in GR. Aldosterone and glucocorticoids have similar chemical structures, however each ligand induces different conformational changes in the receptor (Hultman et al., 2005; Kitagawa et al., 2002; Trapp and Holsboer, 1996). For example, aldosterone induces a stronger interaction between the N-terminal domain and ligand binding domain compared to cortisol (Rogerson and Fuller, 2003). Aldosterone, but not hydrocortisone causes an exclusive interaction of MR with the RNA helicase A (Rogerson and Fuller, 2003). Moreover, cortisol and dexamethasone stimulate different changes in Na^+ transport in cortical collecting duct cells (Kitagawa et al., 2002) indicating that dexamethasone has unique transactivation properties for GR.

In the present chapter, I demonstrate that dexamethasone stimulates *edn1* mRNA transcription in two independent collecting duct cells *in vitro*. While collecting duct cells express 11βHSD-2 and are not typically activated by endogenous glucocorticoids, ET-1 and dexamethasone have documented interactions in other cells types. For example, glucocorticoids

decrease ET-1 binding to vascular smooth muscle cells from wildtype and spontaneously hypertensive rats (Nambi et al., 1992; Provencher et al., 1995). Dexamethasone-induced *edn1* mRNA may also be clinically relevant in Na^+ transporting epithelia. Dexamethasone is commonly used in the clinic as an anti-inflammatory and immunosuppressant agent. However, many undesirable side effects are known to occur including alterations in Na^+ transport epithelia in the eye resulting in hypertension and open-angle glaucoma. In fact, dexamethasone is known to induce ET-1 in the trabecular meshwork and increased levels of ET-1 have been directly linked to the etiology of open angle glaucoma (Zhang et al., 2003). Dexamethasone can also stimulate ENaC mediated Na^+ transport in collecting duct cells and may contribute to unwanted pharmacological actions such as hypertension and electrolyte disorders. However, dexamethasone activated *edn1* mRNA in collecting duct cells may mitigate ENaC-dependent Na^+ reabsorption since ET-1 is known to directly block ENaC activity (Bugaj et al., 2008; Gilmore et al., 2001). It is important to understand the action of dexamethasone in various cell types in order to develop alternative glucocorticoid drugs with fewer side effects.

Table 5-1. TaqMan® assays used for QPCR

Gene	Gene Product	Applied Biosystems Assay ID
edn1	ET-1	Mm00438656_m1
sgk1	Sgk1	Mm00441380_m1
nr3c1	GR	Mm00433832_m1
nr3c2	MR	Mm01241597_m1
scnn1a	αENaC	Mm00803386_m1
per1	Per 1	Mm00501813_m1
actb	β-actin	Mm00607939_s1

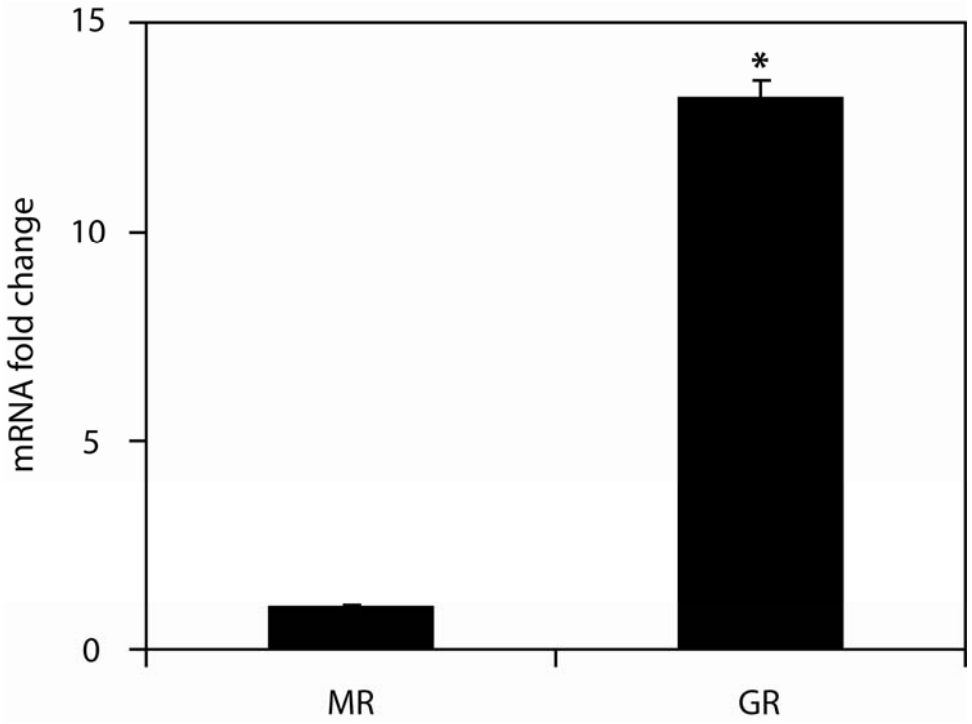

Figure 5-1. Relative mRNA expression of hormone receptors in mIMCD-3 cells. The levels of MR (*nr3c2*) and GR (*nr3c1*) gene expression were evaluated in mIMCD-3 control experiments. Confluent monolayers of mIMCD-3 cells were changed to 10% charcoal dextran stripped FBS for 24 h prior to a 1 h vehicle treatment. Total RNA was extracted and mRNA levels were determined by QPCR. GR values are expressed as mean fold difference ± SE compared to MR mRNA levels. ($^{*}p < 0.001$, n=3)

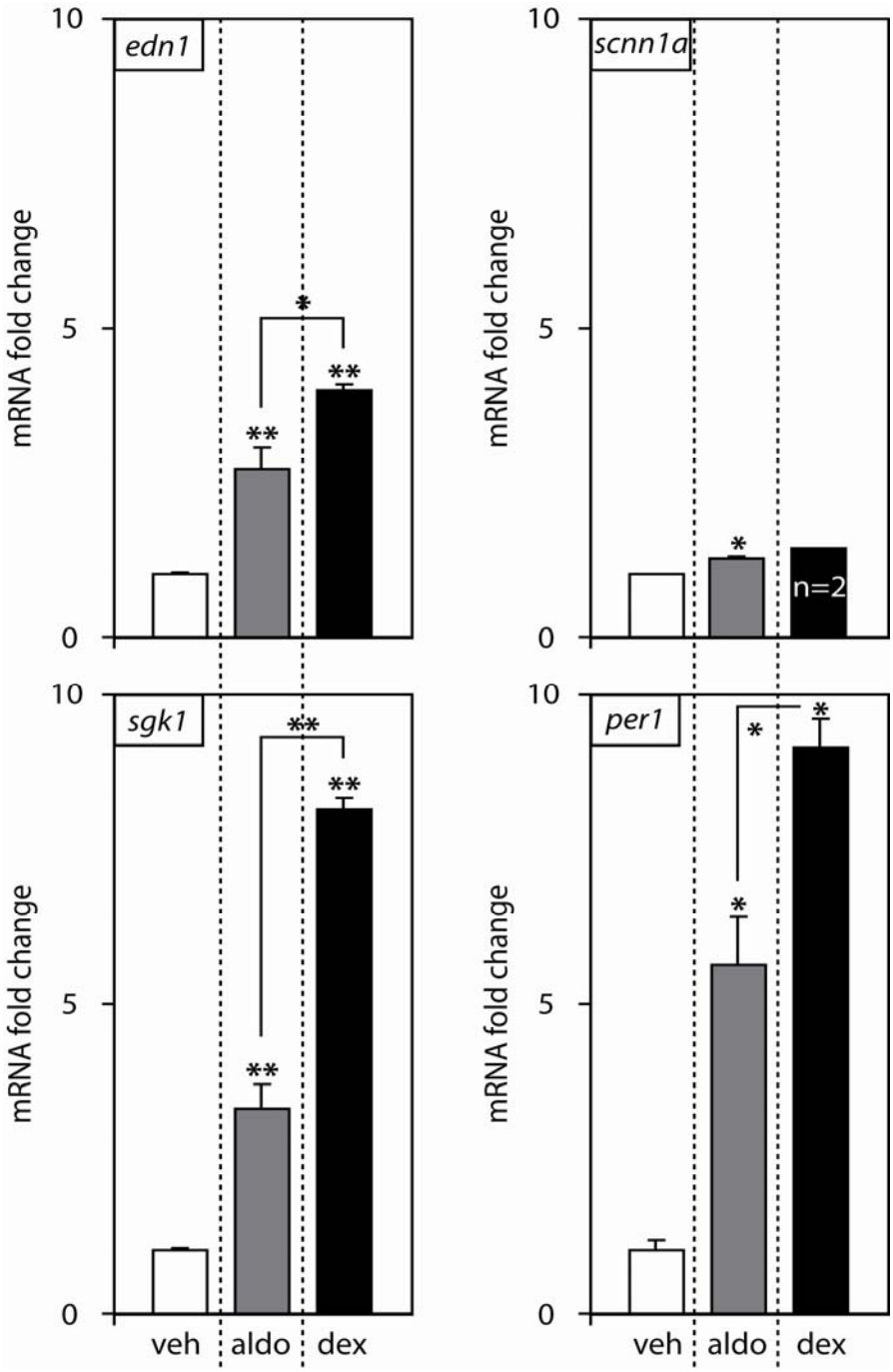

Figure 5-2. Dexamethasone-stimulated gene expression in mIMCD-3 cells. Confluent monolayers of mIMCD-3 cells were treated with vehicle (veh, open bars) or 1 μM dexamethasone (dex, closed bars) for 1 h. As a positive control, cells were also treated with 1 μM aldosterone (aldo, gray bars) for 1 h and data are shown as a reference. Steady state *edn1*, *sgk1*, *scnn1a*, and *per1* mRNA was measured by QPCR, normalized to *actb* (β-actin) and expressed as mRNA fold change relative to vehicle ± SE. ($^{*}p < 0.05$, $^{**}p < 0.001$ relative to vehicle; unless otherwise indicated $n \geq 3$)

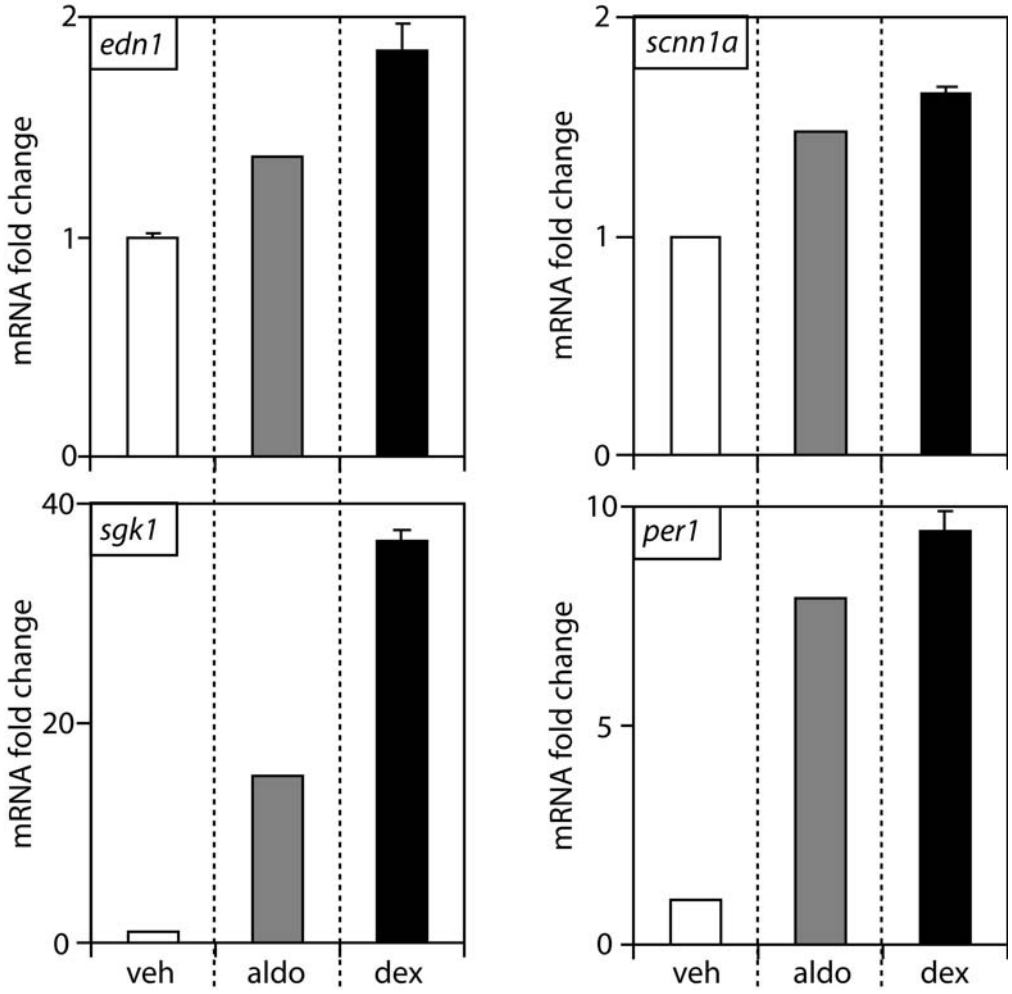

Figure 5-3. Dexamethasone-stimulated gene expression in mpkCCD$_{c14}$ cells. Confluent monolayers of mpkCCD$_{c14}$ cells were treated with vehicle (veh, open bars) or 1 μM dexamethasone (dex, closed bars) for 1 h. Cells treated with 1 μM aldosterone (aldo, gray bars) for 1 h are shown as a reference. Steady state *edn1*, *sgk1*, *scnn1a*, and *per1* mRNA was measured by QPCR, normalized to *actb* (β-actin) and expressed as mRNA fold change relative to vehicle ± SE. Of note, these experiments were conducted at a separate time compared to earlier studies on mpkCCD$_{c14}$ in Chapter 4. The overall *edn1* levels appeared to be lower in these experiments, therefore aldosterone was run as a control in the final dexamethosone experiment. (aldo: n=1, dex: n=3)

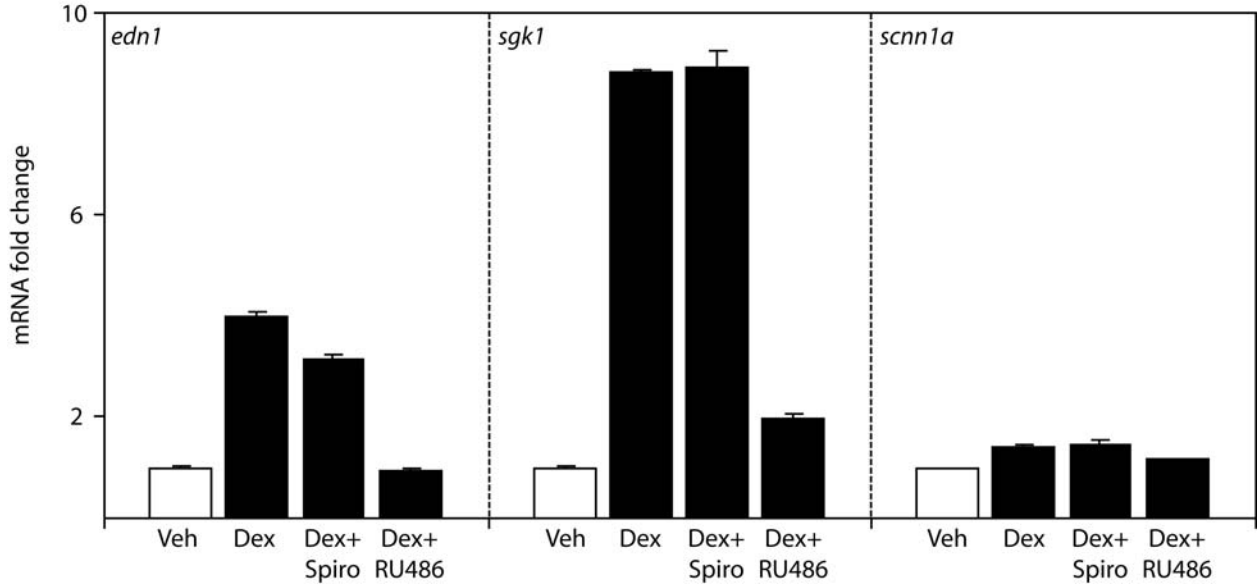

Figure 5-4. Effect of pharmacological blockade of MR and GR on dexamethasone-induced *edn1* gene expression in mIMCD-3 cells. The effect of pharmacological inhibition of MR or GR on dexamethasone-stimulated *edn1* mRNA was evaluated in mIMCD-3 cells treated with vehicle (veh, open bars), 1 μM dexamethasone (dex, closed bars), or 1 μM dexamethasone in the presence of 10 μM spironolactone (spiro) or 10 μM RU486 for 1 h. *Edn1*, *sgk1*, and *scnn1a* mRNA levels were determined by QPCR. Values are expressed as mean fold change relative to vehicle ± SE. ($n \geq 3$)

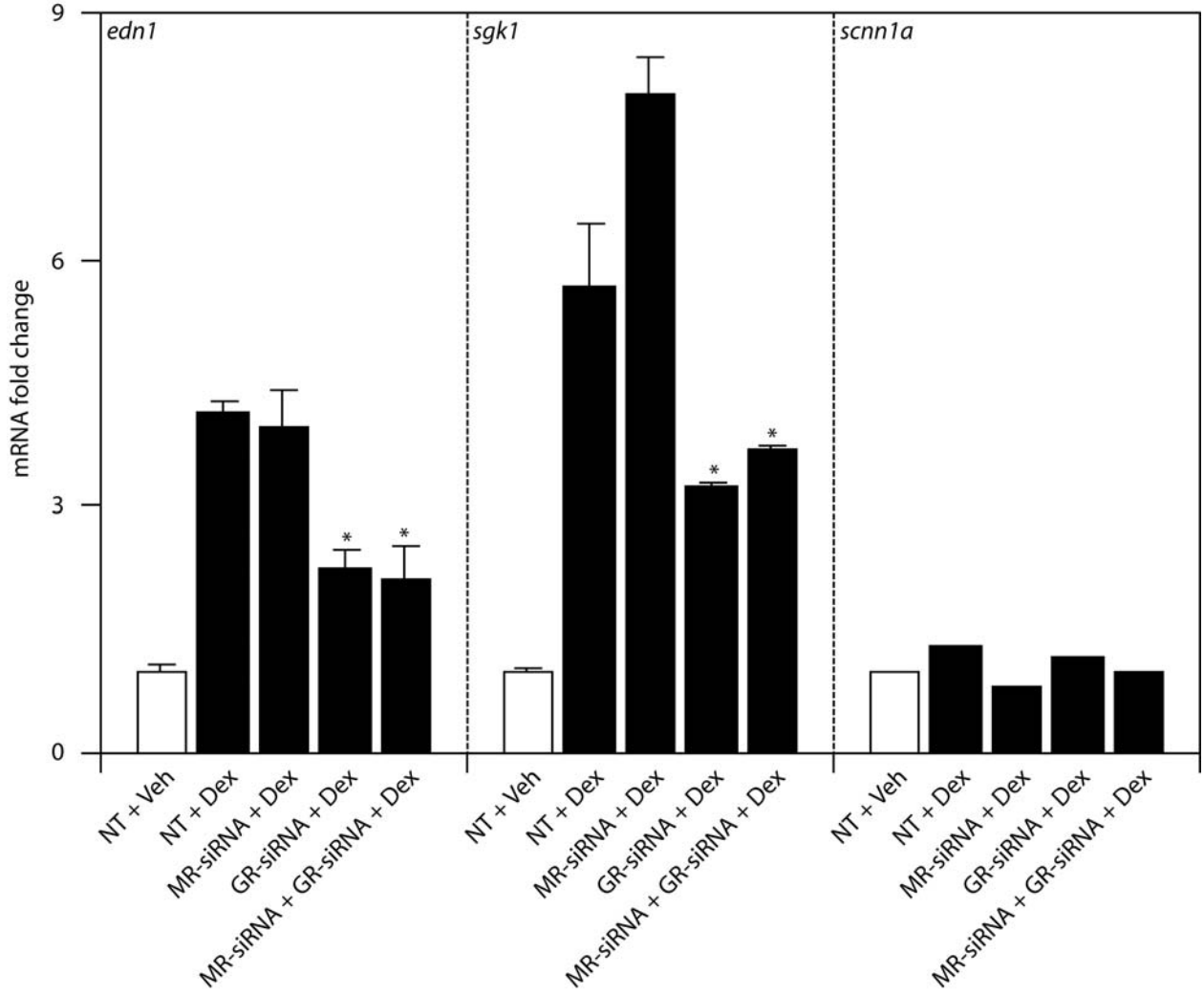

Figure 5-5. Effect of MR-siRNA or GR-siRNA on dexamethasone-induced gene expression in mIMCD-3 cells. Cells were transiently transfected with non-target (NT), MR- or GR-siRNA for 24 h prior to a 1 h dexamethasone (Dex) treatment. Changes in mRNA were measured by QPCR as above. Values are expressed as mean fold change relative to vehicle treated cells transfected with NT-siRNA ± SE. In the presence of NT-siRNA, dexamethasone resulted in a significant 4.13 ± 0.05 and a 5.66 ± 0.78 fold increase in *edn1* and *sgk1*, respectively. ($^{*}p<0.05$ vs. NT-siRNA + dexamethasone, n=3 except for *scnn1a* data that is representative of a single experiment)

CHAPTER 6
REDUCED *EDN1* EXPRESSION BY SIRNA ALTERS ALDOSTERONE TARGET GENES IN COLLECTING DUCT CELLS

Introduction

Greater than 90% of hypertensive patients are diagnosed with essential hypertension, for which there is currently no known cause despite a clear pattern of familial inheritance (Binder, 2007). In contrast to a disease resulting from a mutation in a single gene, essential hypertension is thought to be the result of multiple gene loci and their complex interaction with the environment (Deng, 2007). The essential hypertensive phenotype is acquired over time and is most likely caused by subtle genetic polymorphisms (Binder, 2007) or imbalances in gene expression (Doris and Fornage, 2005).

Many polymorphisms associated with clinical hypertension have been identified in aldosterone target genes, including *edn1* (Treiber et al., 2003), *sgk1* (Busjahn et al., 2002) and *scnn1a* (αENaC) (Iwai et al., 2002). Several of these polymorphisms are located in gene regulatory regions and were shown to alter the normal pattern of mRNA expression (Gonzalez et al., 2007; Iwai et al., 2002; Popowski et al., 2003). Abnormal patterns of aldosterone-dependent gene expression have also been observed in experimental models of hypertension (Aoi et al., 2006). Indeed, the concept that essential hypertension can originate from abnormal gene regulation is not new. The action of aldosterone, the primary hormone regulating systemic arterial blood pressure, is mediated at the level of gene transcription. A substantial amount of work has been done to elucidate novel aldosterone-regulated transcripts and normal patterns of aldosterone-dependent gene expression in collecting duct cells (Gumz et al., 2003; Soundararajan et al., 2005).

Experiments presented earlier in this dissertation have demonstrated that *edn1* was under direct transcriptional control by aldosterone in renal collecting duct cells (Chapter 4) (Stow et al.,

2009). In contrast to most aldosterone target genes that contribute to Na^+ reabsorption, aldosterone-dependent *edn1* expression is unique in that ET-1 is a potent inhibitor of Na^+ transport through ENaC in the collecting duct (Bugaj et al., 2008). Therefore, aldosterone-induced *edn1* likely mediates a negative feedback loop on aldosterone-dependent Na^+ transport. Consistent with this hypothesis is the observation that collecting duct cell specific *edn1* knockout mice, which exhibit severe salt-sensitive hypertension, did not adequately suppress their aldosterone levels during a dietary challenge (Ge et al., 2008). Moreover, renal *edn1* expression levels are reduced in experimental (Hughes et al., 1992; Vogel et al., 1999) and clinical hypertension (Hoffman et al., 1994; Zoccali et al., 1995). Indeed, if *edn1* mediates negative feedback on aldosterone action, the uncoupling of aldosterone and *edn1* might result in excessive Na^+ retention and hypertension.

Studies presented in this chapter were designed to evaluate the effect of aldosterone in collecting duct cells in the presence or absence of *edn1* knockdown. It was important that the experimental approach reduced *edn1* expression but not abolish it since the homozygous knockout of *edn1* is known to be lethal (Kurihara et al., 1994) so the complete loss of *edn1* is not relevant to human disease. Despite the fact that viable tissue-specific *edn1* knockout mice exist, an experimental approach that allowed for graded *edn1* knockdown would reflect more realistic changes that might occur in a particular cell. Therefore, an RNA interference technique using small interfering RNA (siRNA) was adopted to specifically knockdown *edn1* expression in collecting duct cells. In this approach a synthetic siRNA complementary to the mRNA of interest is introduced into the cell. Once inside the cell the siRNA harvests the endogenous cellular machinery called the RNA Induced Silencing Complex to bind to its complementary mRNA sequence and ultimately target the mRNA for degradation (Zamore, 2001).

The long-term goal of these studies was to develop an effective technique to block *edn1* mRNA in collecting duct cells in order to evaluate the role of aldosterone-induced *edn1* on ENaC-dependent Na^+ transport. Indeed, the overriding hypothesis was that *edn1* mediated a negative feedback loop on aldosterone and that the failure of aldosterone to induce *edn1* would result in excessive ENaC activity and consequent changes in the expression of aldosterone target genes involved in ENaC regulation. These studies demonstrated that the siRNA-dependent knockdown of *edn1* had a stimulatory effect on *sgk1* mRNA that was potentiated in the presence of aldosterone in mIMCD-3 cells. In contrast, *edn1* knockdown resulted in reduced *scnn1a* mRNA in the absence of aldosterone. This inhibitory effect of *edn1* knockdown could not be reversed in the presence of aldosterone in either mIMCD-3 or mpkCCD$_{c14}$ cells. These data indicate that *edn1* is required to maintain normal *scnn1a* expression levels and that a reduction in *edn1* renders the *scnn1a* gene unresponsive to aldosterone stimulation.

Materials and Methods

Cell Culture and Hormone Treatment

The mpkCCD$_{c14}$ cells were a kind gift of Dr. Alain Vandewalle (Rebuffat et al., 2004) and mIMCD-3 cells were purchased from American Type Culture Collection. All cells were maintained in DMEM/F12 plus 10% FBS and 50 μg/ml gentamicin and passaged every 48 h. For all hormone experiments cells were plated on 6-well Costar Transwell plates (Corning Inc.). Cells were grown 24 h past confluency and changed to DMEM/F12 plus 10% charcoal-dextran stripped FBS (Invitrogen Corp.) for another 24 h prior to hormone treatments. Aldosterone, dexamethasone, spironolactone and RU486 were purchased from Sigma-Aldrich, prepared in 100% ethanol at 1 mg/ml stocks and stored at -20 °C until use. Cells were treated with vehicle (0.1% ethanol), 1 μM dexamethasone or 1 μM aldosterone for 1 h. For inhibitor studies, cells were treated with agonist plus RU486 (10 μM) or spironolactone (10 μM).

edn1 siRNA Knockdown

The ON-TARGETplus® set of four *edn1* siRNAs (LQ-062546-01-0005) and control non-targeting siRNA against luciferase (siGENOME Non-Targeting siRNA #2, D-001210-02) were purchased from Dharmacon (Lafayette, CO, USA). In addition, a pilot experiment was also conducted to compare the NT-siRNA to another negative non-target control containing a scrambled sequence (siGENOME Non-Targeting siRNA #3, D-001210-03). Five nmoles of each siRNA were resuspended in 250 µl of PBS, aliquoted and stored at -80 °C until use. Cells were seeded at a density of 75,000 cells per cm^2 on 6-well Transwell plates (Corning Inc.) and transfected with 66.7 nM siRNA using 1.5 µl of DharmaFect 4. At the time of transfection cells were switched to phenol-red free DMEM/F12 plus 10% charcoal dextran stripped FBS. No-transfection and mock transfections served as negative controls for comparison. After 24 or 48 h of transfection cells were either harvested for RNA extraction. Alternatively, cells transfected for 24 h were subsequently treated with vehicle (ethanol) or 1 µM aldosterone for 1 to 6 h. The final concentration of ethanol in all treatments was 0.1%. Total RNA was extracted and processed as described below for QPCR.

Steady-State mRNA Determination

Hormone studies were conducted on growth-arrested confluent monolayers of mIMCD-3 or mpkCCD_{c14} cells as described above. Media was aspirated and cells were gently washed with PBS (pH 7.4) before 1 ml of TRIzol® (Invitrogen Corp.) was added directly to each well. Total RNA was extracted according to Invitrogen's instructions except that RNA-ethanol pellets were precipitated overnight at -80 °C. RNA concentration was determined by absorbance at A260 and a total of 2 µg was treated with DNase I (Ambion) to eliminate genomic DNA. Reverse transcription was conducted using oligo dT, random hexamers and Superscript™ III (Invitrogen Corp.). No reverse transcriptase served as a negative control. Resulting cDNAs (32 ng) were

used as templates in duplicate QPCR reactions (Applied Biosystems). Cycle threshold (C_T) values were normalized against *actb* (β-actin) and relative quantification was performed using the $\Delta\Delta C_T$ method (Livak and Schmittgen, 2001). Information for primer/probe sets for murine *edn1*, *sgk1*, *scnn1a*, *per1* and *actb* are shown in Table 5-1.

Statistics

Unless otherwise stated, all experiments were performed in duplicate at least three independent times. Statistical significance was determined using a two-tailed Student's *t* test and $p < 0.05$ was considered significant.

Results

Validation of siRNA Experimental Controls

Targeted gene silencing through siRNA has become a well-established technique to evaluate the specific function of a given gene. However, the introduction of siRNA into a cell can have non-specific effects and must be controlled for carefully. In general, off-target effects originate from three sources; the delivery method (Fedorov et al., 2005), siRNA-activation of the interferon response (Sledz et al., 2003), and non-specific siRNA-dependent effects (Snove and Holen, 2004). Preliminary experiments in mIMCD-3 cells were conducted to evaluate the effect of the liposomal transfection reagent DharmaFect® 4. Cells were either untreated or mock-transfected with 1.5 μl of DharmaFect® 4 for 24 h. Of note, this concentration of transfection reagent was shown to be effective for siRNA delivery to mIMCD-3 cells in Chapter 4 (Stow et al., 2009). Total RNA was isolated and converted to cDNA for analysis of gene expression by QPCR. There were no visible signs of cellular toxicity, and there were no significant changes in *actb* (β-actin) C_T values observed between untreated or mock transfected cells (Table 6-1). In comparison to untreated cells, mock-transfection caused a small increase in *sgk1* and *scnn1a* mRNAs and a small decrease in *per1* mRNA (Figure 6-1A). However, there was virtually no

effect of Dharmafect® 4 on *edn1* mRNA expression compared to untreated control cells (1.02 ± 0.04 fold) (Figure 6-1A).

Using mock-transfected cells as a negative control in siRNA experiments would easily control for the minor effect of lipofection. However, it was important to determine if there were any nonspecific effects attributed to the introduction of the siRNA itself, not just the delivery method. Since the advent of RNA interference technology, non-targeting siRNAs have become the gold standard for a negative control in siRNA experiments (Huppi et al., 2005). Two different non-targeting (NT)-siRNAs were purchased from Dharmacon and were evaluated for their use as negative controls in siRNA experiments. One of the non-targeting siRNAs contained a random RNA sequence with greater than four mismatches to any known murine or human gene transcript and is referred to as "NT-siRNA (scrambled)." The other siRNA was the same nonspecific control used in experiments from Chapters 4 and 5 and is referred to as "NT-siRNA" to be consistent with the terminology from earlier studies. The NT-siRNA sequence actually targets the firefly luciferase gene. However, it also contained greater than four mismatches to any known murine or human transcript. In order to determine if either NT-siRNA induced nonspecific effects on the baseline expression of *edn1* or other aldosterone target genes, mIMCD-3 cells were either mock-transfected or transfected with 66.7 nM of either NT-siRNA or NT-siRNA (scrambled) using 1.5 μl of DharmaFECT 4®.

Cells transfected with NT-siRNA demonstrated the least amount of nonspecific effects, which is consistent with earlier studies (Chapter 4) (Stow et al., 2009). The minor reduction in *edn1* mRNA (Figure 6-1B) was not a major concern considering that earlier studies validated that NT-siRNA had no effect on aldosterone-dependent *edn1* mRNA induction (Figure 4-6) (Stow et al., 2009). In contrast, delivery of the scrambled NT-siRNA caused large changes in the

expression of *edn1*, *sgk1*, and *scnn1a* (Figure 6-1B). Consequently, the scrambled NT-siRNA would not have been a useful negative control and was eliminated from further experiments. The NT-siRNA (against luciferase) was selected for use as a negative control in subsequent experiments.

Efficacy of Four Different siRNAs Targeting *edn1*

Four different siRNAs against murine *edn1* mRNA (siEdn1-09, -10, -11, -12) were designed by Dharmacon using a validated bioinformatics algorithm (Anderson et al., 2008). To determine the effectiveness of each siEdn1 on *edn1* knockdown, mIMCD-3 cells were transfected with NT-siRNA or one of the siEdn1 constructs using DharmaFect® 4. After 24 h, total RNA was prepared and *edn1* mRNA expression levels were determined by QPCR analysis. The most effective siRNA against *edn1* was siEdn1-09, which reduced *edn1* levels to approximately 50% of the expression levels compared to NT-siRNA control samples (Figure 6-2). Conversely, transfection of siEdn1-11 actually resulted in an increase in *edn1* mRNA levels and was consequently eliminated from further analysis (Figure 6-2). Furthermore, delivery of either siEdn1-10 or siEdn1-12 had no effect on *edn1* expression indicating that these siRNAs were ineffective under the condition tested (Figure 6-2). Doubling the amount of DharmaFect® 4 did not improve siEdn1-10 dependent silencing of *edn1* (1.08 ± 0.02 fold change relative to NT-siRNA, n=2). Similarly, increasing the siRNA transfection time to 48 h did not improve siEdn1-10 or siEdn1-12 mediated *edn1* knockdown (Figure 6-2). However, the longer incubation time resulted in a similar 50% reduction of *edn1* in the presence of siEdn1-09. Taken together, siEdn1-09 was effective at reducing *edn1* mRNA expression and was useful for studying both basal and aldosterone-dependent *edn1* expression between 24 and 48 h after siRNA delivery.

Effect of *edn1* Knockdown on Aldosterone Target Gene Expression

In order to determine if *edn1* knockdown had an effect on the basal expression of common aldosterone target genes, mIMCD-3 cells were transfected with NT-siRNA or siEdn1-09 for 24 h. As expected, siEdn1-09 reduced endogenous *edn1* mRNA levels to approximately 50% of NT-siRNA control cells (Figure 6-3). Transfection of siEdn1-09 had no significant effect on *per1* mRNA levels (Figure 6-3) or on the expression of sirtuin-1 (0.88 ± 0.2 fold change, n=3), a reported negative aldosterone response gene (Zhang et al., 2009). However, transfection of siEdn1-09 stimulated a 1.74 ± 0.24 fold increase in *sgk1* mRNA levels (Figure 6-3). Furthermore, siEdn1-09 transfected cells demonstrated a 0.26 ± 0.08 fold reduction in *scnn1a* mRNA levels ($p = 0.01$, $n = 4$). These data demonstrated that a 50% loss of *edn1* expression resulted in an abnormal mRNA expression pattern of classical aldosterone response genes involved in Na^+ transport.

Effect of *edn1* Knockdown on Aldosterone-Dependent Gene Expression in mIMCD-3 and mpkCCD$_{c14}$ cells

To test the effect of siEdn1-09 on aldosterone-dependent *edn1* expression, mIMCD-3 cells were transfected with NT-siRNA or siEdn1-09 in the presence of 10% charcoal dextran stripped FBS. After 24 h, cells were treated with vehicle or 1 μM aldosterone for 1 h. In the presence of NT-siRNA, aldosterone resulted in a 2.7 ± 0.14 fold change in *edn1* expression (Figure 6-4). This observation was entirely consistent with normal *edn1* expression levels reported in earlier experiments in Chapter 4 (Stow et al., 2009). However, in the presence of siEdn1-09, the level of aldosterone-induced *edn1* mRNA was not different from vehicle treated NT-siRNA control cells (Figure 6-4). This observation indicated that siEdn1-09 effectively blunted aldosterone-dependent *edn1* transcription in mIMCD-3 cells.

Transfection of the control NT-siRNA into mICMD-3 cells had no effect on the expected magnitude of aldosterone-induced gene expression for *sgk1*, *scnn1a*, or *per1* at 1 h (Figure 6-4). There was no effect of *edn1* knockdown on *per1* expression in the presence of aldosterone. However, *edn1* knockdown was associated with lower mRNA levels of the ET_A receptor gene (*etar*) suggesting that *edn1* knockdown may also affect the expression of genes involved in ET-1 signaling. The analysis of the ET_B receptor gene was not conducted because the mRNA levels were below the level of detection in mIMCD-3 cells.

The most apparent effect of *edn1* knockdown on aldosterone dependent transcription was on the *sgk1* gene. Transfection of siEdn1 resulted in a 4.2 ± 0.02 fold increase in *sgk1* mRNA in the presence of aldosterone compared to vehicle treated NT-siRNA transfected cells (Figure 6-4). Interestingly, the level of *sgk1* mRNA in control NT-siRNA transfected cells treated with aldosterone was only 2.9 ± 0.01 fold higher than vehicle. The aldosterone-dependent expression of *scnn1a* was also evaluated at 1 h. The expression of *scnn1a* was not different in NT-siRNA transfected cells treated with 1 μM aldosterone or vehicle. This observation is consistent with the fact that *scnn1a* generally requires several hours of aldosterone treatment to observe a significant increase in gene expression. In contrast, cells transfected with siEdn1-09 exhibited significantly lower *scnn1a* mRNA levels in the presence of aldosterone compared to vehicle treated NT-siRNA control cells (Figure 6-4). Taken together, these data indicated that *edn1* knockdown negatively affected *scnn1a* expression.

To determine if the effect of *edn1* knockdown to alter aldosterone-dependent gene expression occurred in another collecting duct cell model, similar siRNA experiments were conducted on vehicle or aldosterone treated mpkCCD_{c14} cells (Figure 6-5). A 1 h aldosterone treatment resulted in a 1.4 ± 0.1 fold increase in *edn1* mRNA expression in NT-siRNA control

cells. However, the levels of *edn1* mRNA were significantly reduced in aldosterone treated siEdn1-09 transfected cells compared to aldosterone treated NT-siRNA cells. In fact, the level of *edn1* expression in the presence of siEdn1-09 was 37 ± 5% lower compared to vehicle treated NT-siRNA transfected control cells. Consistent with results from mIMCD-3 cells, there was no effect of *edn1* knockdown on aldosterone-dependent *per1* expression. The levels of *sgk1* mRNA were increased in the presence of *edn1* knockdown, however the *sgk1* mRNA levels were lower compared to aldosterone treated NT-siRNA transfected cells which suggested that cell-line specific factors may also contribute to the consequent effect of *edn1* knockdown (Figure 6-5). However, the effect of *edn1* knockdown on *scnn1a* expression was consistent between the cells lines. Transfection of siEdn1-09 in aldosterone treated cells resulted in mRNA levels of *scnn1a* that were 40 ± 10% lower than vehicle treated NT-siRNA controls cells and 57 ± 10% lower than aldosterone treated NT-siRNA transfected cells (Figure 6-5).

Effect of *edn1* Knockdown on Aldosterone-Dependent *scnn1a* Expression at 6 Hours

In order to better test the effect of *edn1* knockdown on aldosterone-dependent *scnn1a* expression, siRNA experiments were conducted on mIMCD-3 cells treated with vehicle or 1 μM aldosterone for 6 h. Aldosterone-dependent increases in *scnn1a* mRNA levels were expected to be detected at this time point (May et al., 1997; Mick et al., 2001; Spindler et al., 1997). Indeed, NT-siRNA transfected cells treated with aldosterone demonstrated a 1.9 ± 0.3 fold increase in *scnn1a*. However, aldosterone treatment failed to induce *scnn1a* mRNA expression in cells transfected with siEdn1-09 (Figure 6-6). In contrast, transfection of siEdn1-09 had no effect on hormone-stimulated *sgk1* or *per1* expression (Figure 6-6). However, the level of *etar* expression remained blunted compared to either vehicle or aldosterone treated NT-siRNA control cells, indicating that the reduction in *etar* expression was independent of aldosterone action.

Since siEdn1-09 was demonstrated to affect the levels of *scnn1a* expression in the absence of aldosterone, it was possible that *scnn1a* mRNA increased in the presence of aldosterone, but that the levels of mRNA did not exceed those in NT-siRNA transfected vehicle treated cells. To clarify this issue, experiments were done on siEdn1-09 transfected cells treated with vehicle or 1μM aldosterone for 6 h (Figure 6-7). This experiment revealed that *edn1* knockdown blunted, but did not completely prevent the effect of aldosterone on *edn1* transcription. However, the reduced levels of *edn1* expression caused by siRNA knockdown completely prevented the induction of *scnn1a* by aldosterone. Taken together, these data suggested that the effect on *scnn1a* mRNA was the result of overall lower levels of *edn1* mRNA as opposed to the failure of aldosterone to induce *edn1*.

Discussion

Data presented in this chapter demonstrated that a 50% reduction in *edn1* mRNA expression was sufficient to alter the basal gene expression patterns for *scnn1a* and *sgk1* in collecting duct cells. In the absence of any hormonal stimuli, *edn1* knockdown resulted in increased levels of *sgk1* mRNA; whereas the levels of *scnn1a* mRNA were moderately and consistently decreased. In the presence of aldosterone, *edn1* knockdown was associated with decreased *scnn1a* mRNA levels in response to an acute aldosterone administration in both mIMCD-3 and mpkCCD$_{c14}$ cells. However, the most important finding was that after 6 h of aldosterone treatment *edn1* knockdown blocked the normal induction of *scnn1a* mRNA.

The overarching goal of the studies in this chapter was to develop an effective technique to study the role of *edn1* in aldosterone-dependent action in collecting duct cells. To do this, a siRNA approach was selected. While gene knockout technology has clear advantages in certain settings, the complete loss of both *edn1* alleles is not relevant to changes that might occur in normal cell since homozygous *edn1* knockout is perinatally lethal mice (Kurihara et al., 1994)

and has not been reported in humans. Moreover, complete genetic knockout animals typically activate compensatory mechanisms that may confound data interpretation. However, reduced quantities of urinary ET-1 levels, a marker of renal *edn1* expression, have been reported in the essential hypertensive patients (Hoffman et al., 1994; Zoccali et al., 1995). Therefore, the better experimental approach to investigate the role of aldosterone-induced *edn1* was a siRNA approach that would allow better control over the level of *edn1* knockdown.

It was important to validate the experimental parameters and negative controls in our siRNA experiment. Indeed, nonspecific effects from siRNA delivery can occur. A common source of off-target effects is the siRNA delivery method itself (Fedorov et al., 2005). However, the liposomal DharmaFect® 4 transfection reagent had no effect on *edn1* mRNA expression. Two NT-siRNAs were also evaluated for use as negative controls. Transfection of the scrambled NT-siRNA into mIMCD-3 cells resulted in substantial increases in *edn1* and *sgk1* and a decrease in *scnn1a* mRNA levels. The unexpected increase in *edn1* mRNA suggested that the scrambled NT-siRNA may have activated the interferon pathway since interferon γ is known to stimulate *edn1* (Woods et al., 1999). Indeed, activation of the interferon response is a common source of undesirable off-target effects of siRNA (Bridge et al., 2003). However, in contrast to the non-specific effects caused by the scrambled NT-siRNA, transfection of the NT-siRNA against luciferase had no significant effect on the genes studied and was therefore selected as a negative control.

The siEdn1-09 construct resulted in a 50% reduction in *edn1* mRNA levels under basal conditions. In contrast to a total gene knockout approach, this level of reduction in *edn1* mRNA expression is more relevant to changes that might occur in a collecting duct cell *in vivo*. Indeed, reduced but not absent levels of renal ET-1 have been documented in clinical hypertension

(Hoffman et al., 1994; Zoccali et al., 1995). The siEdn1-09 was effectively blunted aldosterone-induced *edn1* expression both mIMCD-3 and mpkCCD$_{c14}$ cells. *Edn1* knockdown had effects on *sgk1*, *scnn1a* and *etar* expression. However, the expression of *per1* was not affected by siEdn1-09 in the presence or absence of aldosterone in either mIMCD-3 or mpkCCD$_{c14}$ cells. This result indicated that *per1* expression was not directly affected by *edn1* expression. Both cells lines also exhibited decreased *etar* gene expression in the presence of aldosterone and *edn1* knockdown. The reduction in *etar* expression is likely a direct effect of *edn1* knockdown since ET-1 is known to mediate positive feedback on *etar* expression in other cell types (Landgraf and Jancar, 2008).

Edn1 knockdown resulted in higher *sgk1* mRNA expression levels in both control and aldosterone treated mIMCD-3 cells. However, *edn1* knockdown did not appear to affect aldosterone-induced *sgk1* mRNA in mpkCCD$_{c14}$ cells. This effect may be explained by innate differences between the cells lines since mIMCD-3 cells express higher levels of *sgk1* mRNA (5.6 ± 1.3 fold) compared to mpkCCD$_{c14}$ cells. However, a solid conclusion cannot be drawn for the effect of *edn1* knockdown on *sgk1* in mpkCCD$_{c14}$ cells because the level of *sgk1* mRNA was not determined in the absence of aldosterone. It was possible that *edn1* knockdown in the absence of hormone stimulated *sgk1* mRNA expression, as was seen in mIMCD-3 cells. Indeed, a more complete analysis of mpkCCD$_{c14}$ cells should be conducted in the future.

The effect of *edn1* knockdown was also tested on *scnn1a* mRNA expression. Experiments in both mIMCD-3 cells and mpkCCD$_{c14}$ cells treated with aldosterone for 1 h revealed that *edn1* knockdown resulted in reduced levels of *scnn1a* expression. Furthermore, experiments in mIMCD-3 cells in the absence of hormone also indicated that *edn1* knockdown resulted in a moderate decrease in basal *scnn1a* expression. These data showed that the loss of *edn1* expression directly or indirectly caused *scnn1a* levels to decrease. However, the most interesting

finding was that *scnn1a* failed to respond to aldosterone stimulation after 6 h treatment in cells transfected with siEdn1-09. Indeed, *scnn1a* should be markedly induced at this time point (Mick et al., 2001).

Substantial evidence exists that collecting duct derived ET-1 blocks the activity of ENaC (Bugaj et al., 2008; Gallego and Ling, 1996; Gilmore et al., 2001). Therefore, a decrease in local ET-1 levels caused by *edn1* knockdown might result in the consequent increase in ENaC activity. Excessive ENaC activity might result in a compensatory decrease in *scnn1a* mRNA. In fact, a compensatory decrease in *scnn1a* mRNA has been observed in several models of salt dependent hypertension. For example, increased ENaC activity was associated with a compensatory decrease in *scnna1* expression along the collecting duct in the Milan hypertensive rat model (Capasso et al., 2005). Similarly, a reduction in *scnn1a* was also observed in a model of prenatally programmed hypertension (Manning et al., 2002). In both cases, the reduction of *scnn1a* mRNA was moderate, which is comparable to the observations made in siEdn1-09 transfected cells.

The decrease in *scnn1a* may also explain the increase in *sgk1* mRNA if the response were secondary to the decrease in *scnn1a*. Alternatively, the change in *sgk1* mRNA levels could be explained by a primary effect of *edn1* knockdown. ET-1 signaling is directly involved in the transcriptional control of several other genes (Felx et al., 2006; Gerstung et al., 2007; Kao and Fong, 2008; Sutcliffe et al., 2009). The unifying observation between these studies is that ET-1-mediated transcription involves the activation of NF-κB. To date, the only known transcription factor to inhibit *sgk1* mRNA is also NF-κB (de Seigneux et al., 2008). Taken together, the loss of ET-1-dependent NF-κB signaling would result in the de-repression of *sgk1* transcription.

The data presented in this chapter demonstrate that *edn1* knockdown independently alters the normal expression pattern of *sgk1* and *scnn1a* in collecting duct cells. The decrease in *scnn1a* mRNA is likely a compensatory response due to over active ENaC activity, which would be consistent with observations in models of experimental hypertension. However, the observation that *edn1* knockdown completely prevented *scnn1a* mRNA induction by aldosterone at 6 hours suggests that the compensatory mechanism induced by the loss of *edn1* expression is able to alter normal aldosterone signaling. Furthermore, it is interesting to speculate that the increase in *sgk1* mRNA could be due to the loss of ET-1-dependent NF-κB signaling. This hypothesis is consistent with the role of ET-1-mediated negative feedback on aldosterone and is the first proposed mechanism for directly shutting off aldosterone-dependent transcription. Future studies should be conducted to explore the role of *edn1* knockdown on *sgk1*, *scnn1a* and ENaC-mediated Na^+ transport.

Table 6-1. C_T values for β-actin (*actb*) in mIMCD-3 control experiments.

Treatment Group	C_T Value
Untreated	17.6 ± 0.2
Mock-transfected	17.3 ± 0.1
NT-siRNA transfected	17.5 ± 0.1
NT-siRNA (scrambled) transfected	17.3 ± 0.1

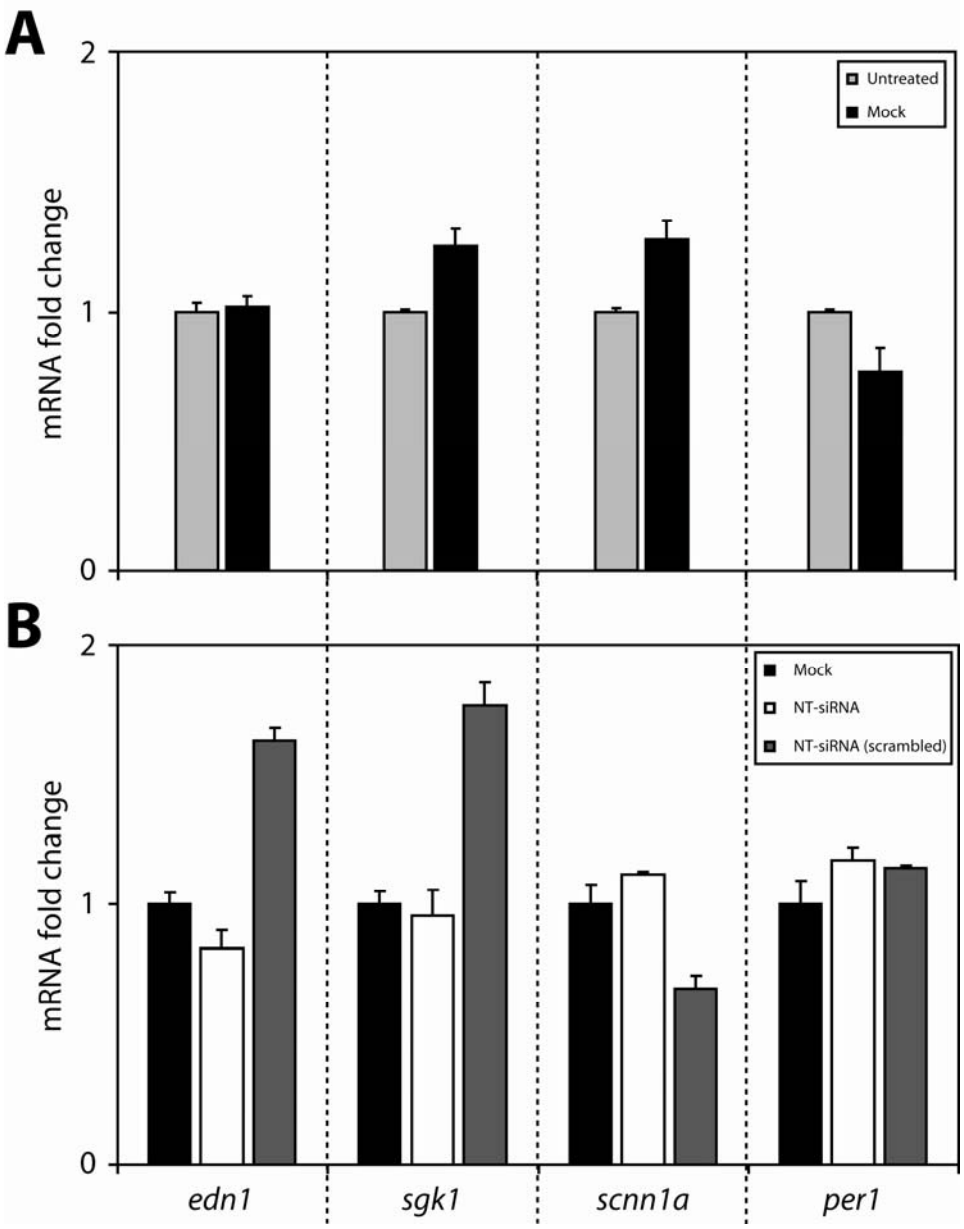

Figure 6-1. Effect of lipofection and NT-siRNA on aldosterone target gene expression in mIMCD-3 cells. A) Comparison of untreated and mock-transfected cells at 24 h. Mock-transfected cells were treated with 1.5 µl of the liposomal transfection reagent DharmaFect® 4. Total RNA was extracted, converted to cDNA and analyzed for *edn1*, *sgk1*, *scnn1a* or *per1* mRNA using QPCR. Values were normalized against *actb* (β-actin) and are expressed as mean fold change ± SE relative to untreated control cells. ($n \geq 3$) B) Cells were either mock-transfected or transfected with 66.7 nM of either a siRNA against luciferase (NT-siRNA) or an siRNA containing a scrambled sequence (NT-siRNA scrambled). After 24 h total RNA was extracted for QPCR analysis as above. Values are expressed as mean fold change ± SE relative to mock-transfected cells. ($n \geq 2$)

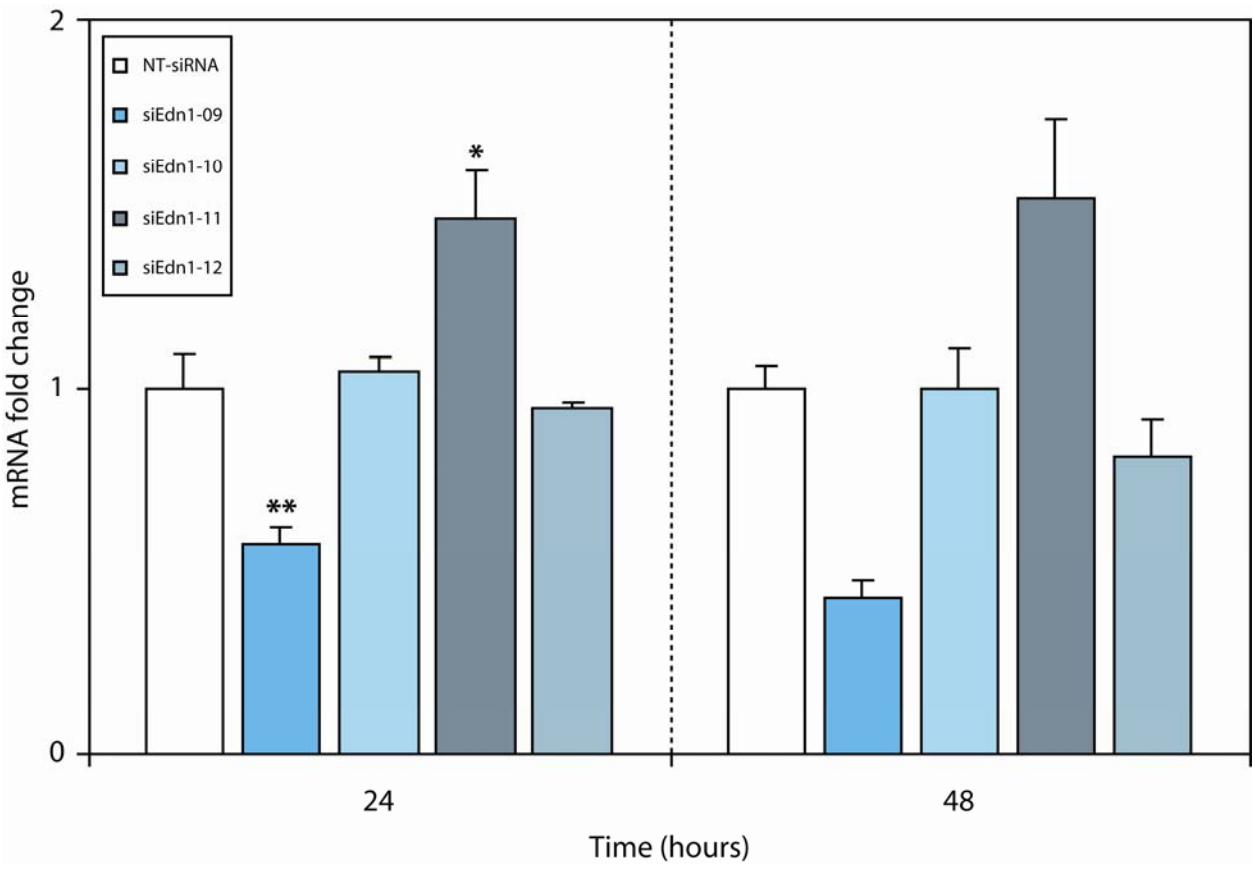

Figure 6-2. Efficacy of four different siRNAs against *edn1*. Murine IMCD-3 cells were transfected with 66.7 nM of NT-siRNA or one of the siRNAs against *edn1* (siEdn1-09, -10, -11, or -12) using 1.5 µl DharmaFect® for 24 or 48 h. Total RNA was extracted, converted to cDNA and analyzed for *edn1* mRNA expression using QPCR. Values were normalized to *actb* mRNA and are expressed as the mean fold change ± SE relative to NT-siRNA transfected cells. ($^{*}p < 0.05$, $^{**}p < 0.005$, data from 24 h represents $n \geq 3$; data from 48 h represents n=2)

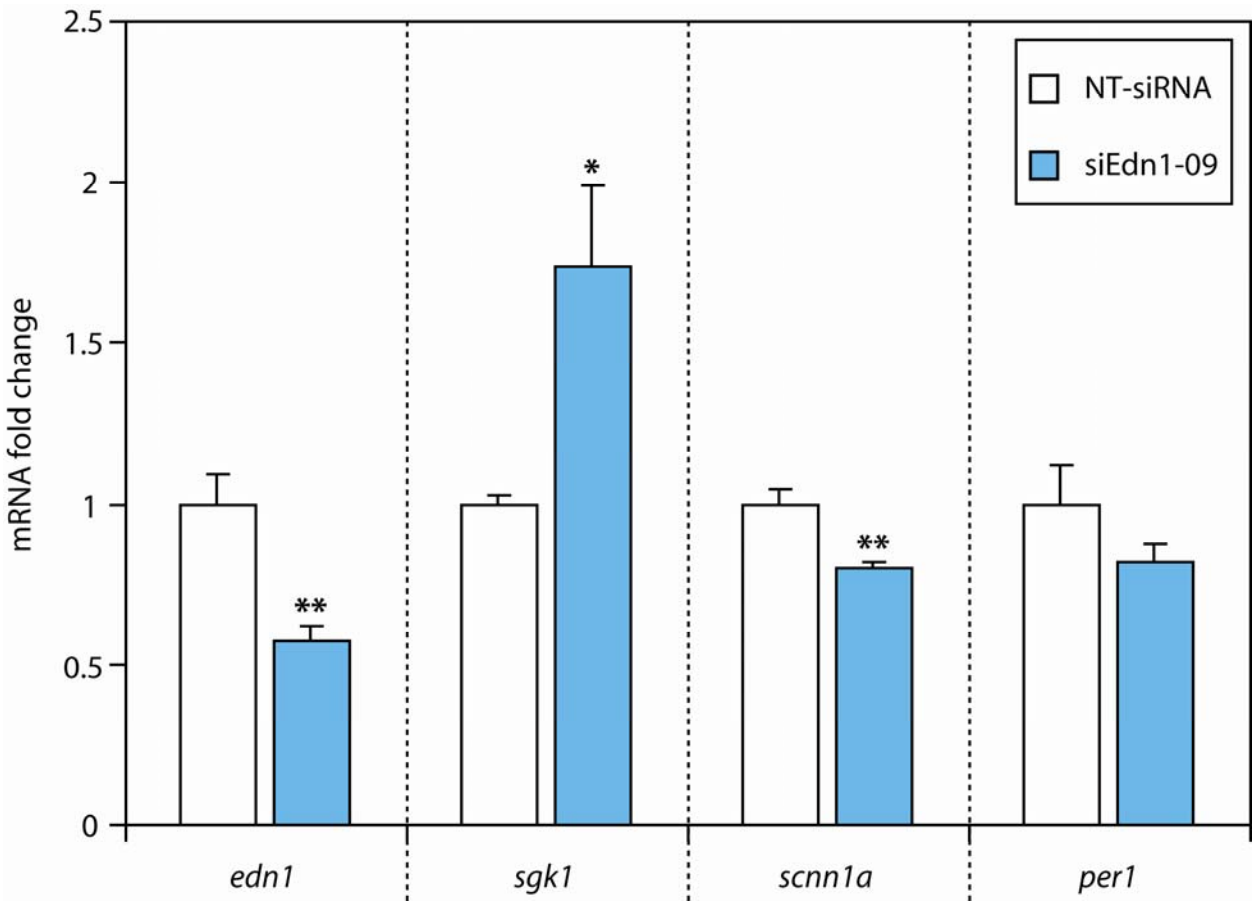

Figure 6-3. Effect of 24 h knockdown with siEdn1-09 on gene expression in mIMCD-3 cells. Cells were transiently transfected with siEdn1-09 for 24 h. Total RNA was extracted, converted to cDNA and analyzed for *edn1*, *sgk1*, *scnn1a* or *per1* mRNA by QPCR. Values were normalized to *actb* and are expressed as mean fold change ± SE relative to NT-siRNA transfected cells. ($^{*}p < 0.05$, $^{**}p < 0.005$, $n \geq 3$)

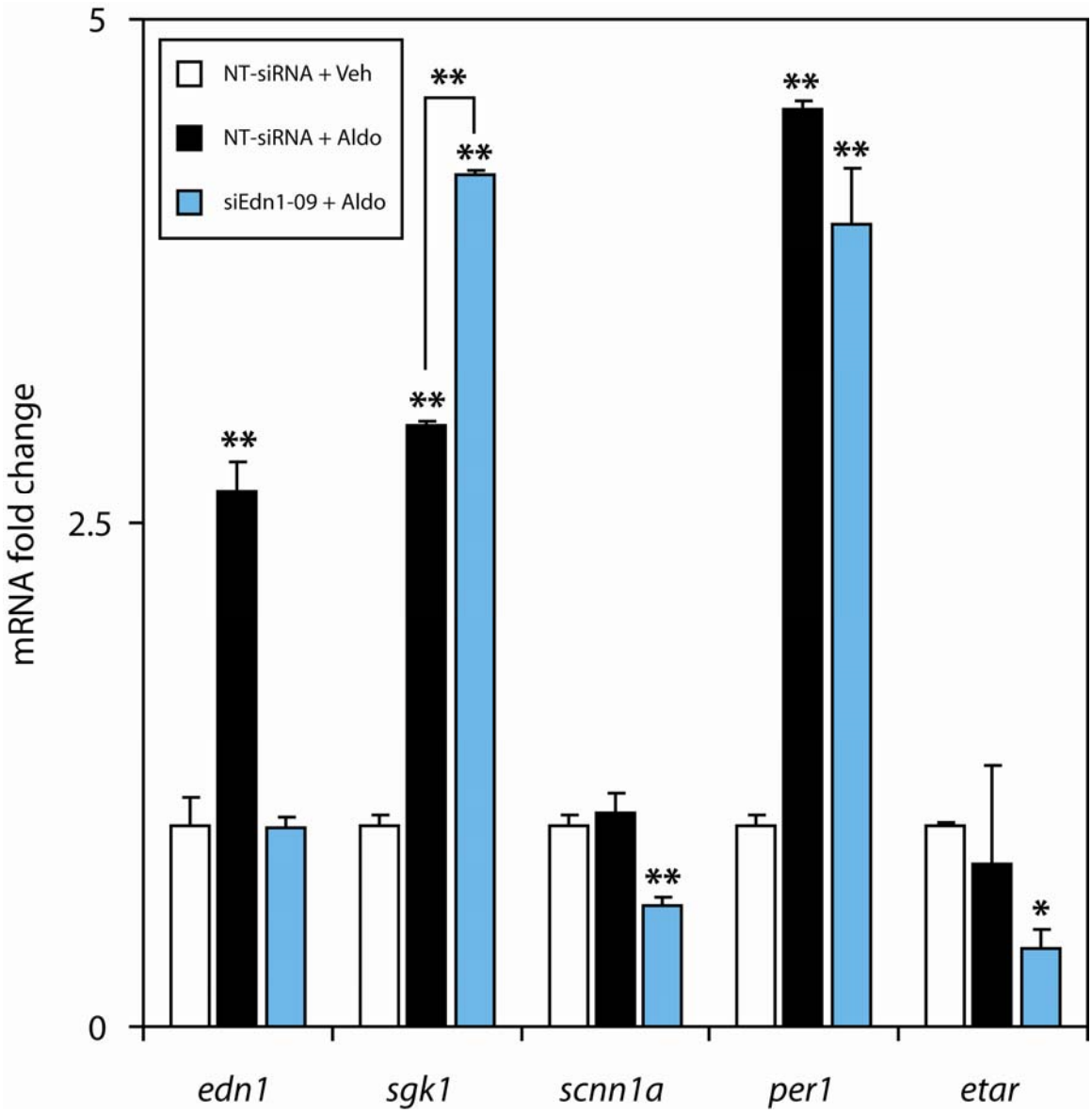

Figure 6-4. Effect of siEdn1-09 on aldosterone-induced gene expression in mIMCD-3 cells. Cells were transfected with 66.7 nM of NT-siRNA or siEdn1-09 for 24 h in the presence of 10% charcoal-dextran stripped FBS. Cells were then treated with vehicle (ethanol) or 1 μM aldosterone for 1 h. Total RNA was extracted, converted to cDNA and analyzed for *edn1*, *sgk1*, *scnn1a*, *per1* or *etar* mRNA expression using QPCR. Values were normalized against *actb* and are expressed as mean fold change ± SE relative to vehicle treated cells transfected with NT-siRNA. P values are relative to NT-siRNA + Veh unless otherwise indicated. ($^{*}p < 0.05$, $^{**}p < 0.005$, $n \geq 3$)

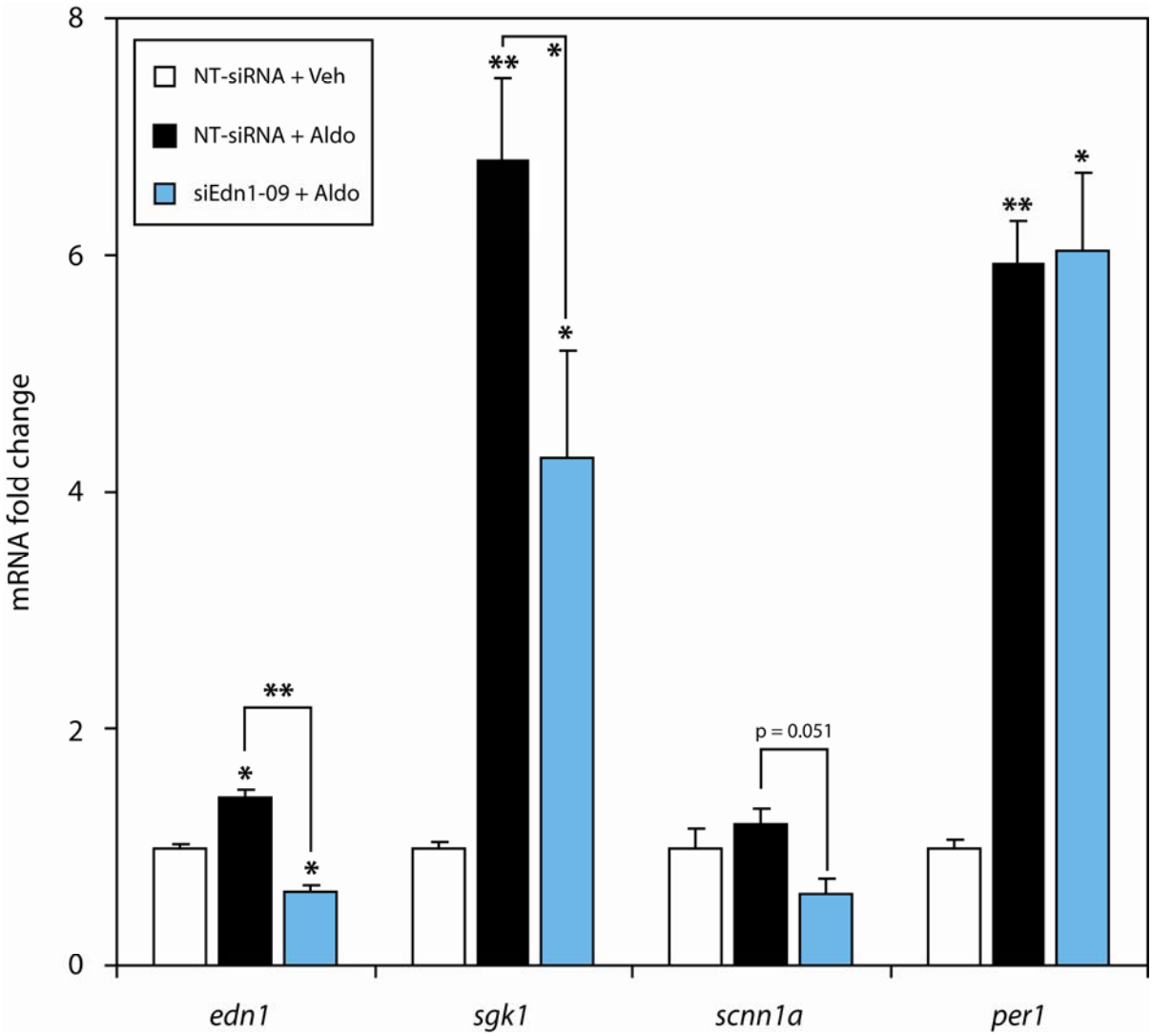

Figure 6-5. Effect of siEdn1-09 on aldosterone-mediated gene expression in mpkCCD$_{c14}$ cells. Cells were transfected with NT-siRNA or siEdn1-09 for 24 h prior to a 1 h vehicle (veh) or 1 μM aldosterone (aldo) treatment. Total RNA was extracted, converted to cDNA and analyzed for mRNA expression of the indicated genes by QPCR. Values for each gene were normalized to *actb* and are expressed as mean fold change ± SE relative to NT-siRNA + Veh. P values are relative to NT-siRNA + Veh unless otherwise indicated. ($^{*}p < 0.05$, $^{**}p < 0.005$, $n \geq 3$)

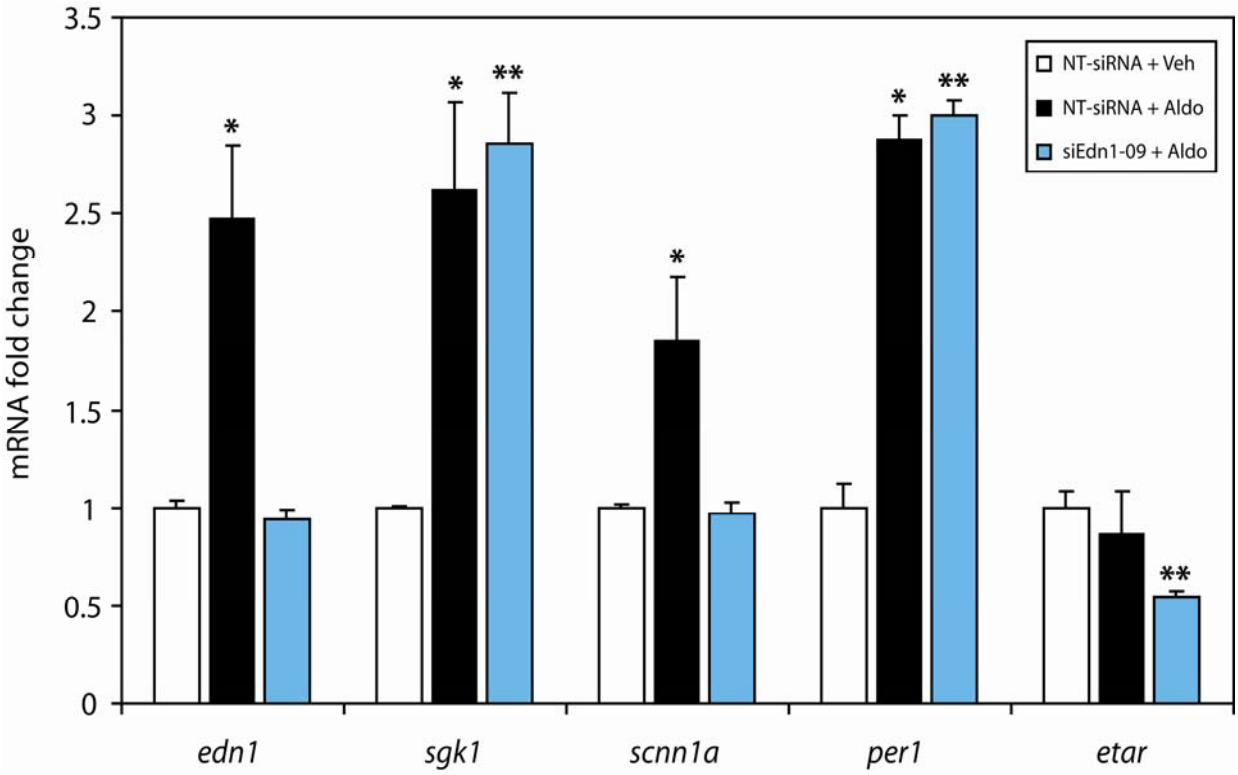

Figure 6-6. Effect of siEdn1-09 on aldosterone regulated gene expression at 6 h in mIMCD-3 cells. Cells were transfected with NT-siRNA or siEdn1-09 for 24 h prior to a 6 h vehicle (veh) or 1 μM aldosterone (aldo) treatment. Total RNA was extracted, converted to cDNA and analyzed for mRNA expression of the indicated genes by QPCR. Values for each gene indicated were normalized to *actb* and are expressed as mean fold change ± SE relative to NT-siRNA + Veh. P values are relative to NT-siRNA + Veh unless otherwise indicated. ($^{*}p < 0.05$, $^{**}p < 0.005$, $n \geq 3$)

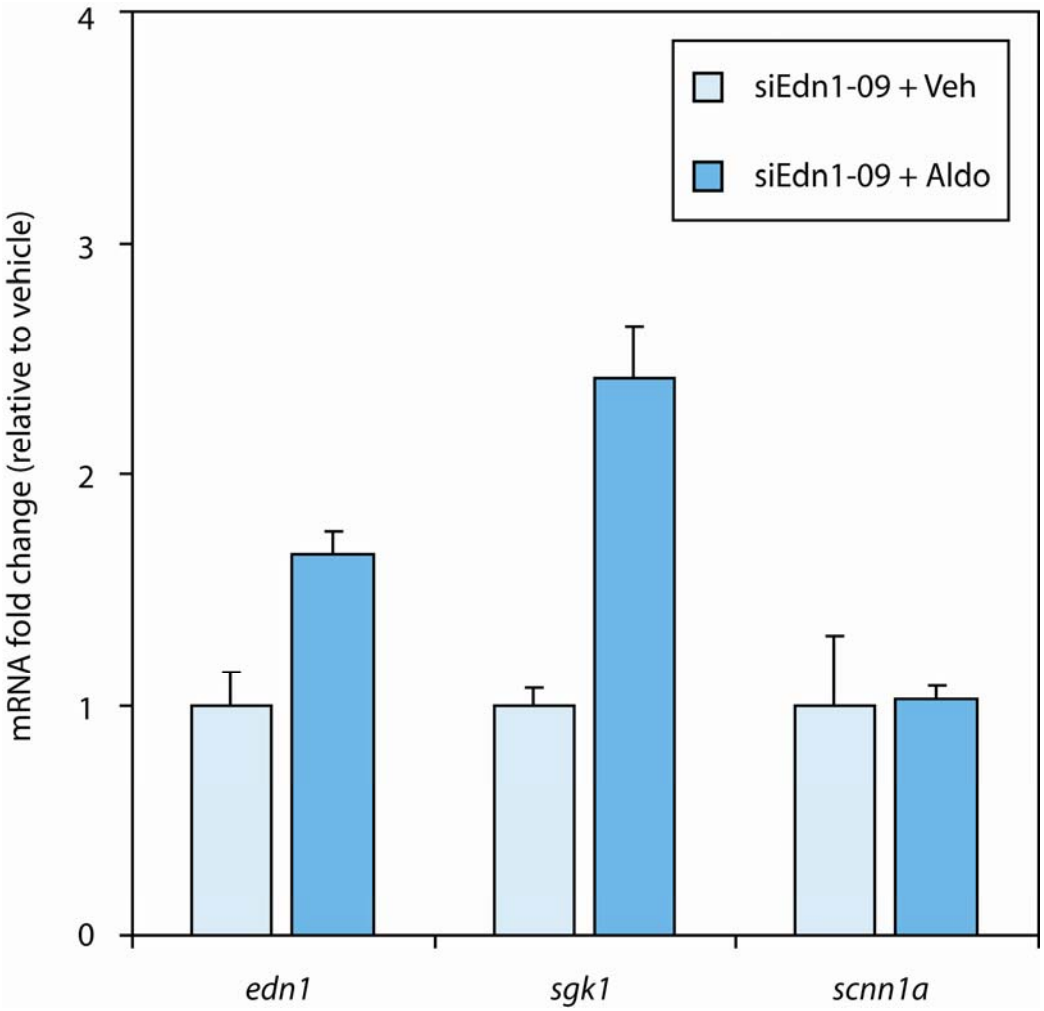

Figure 6-7. Effect of siEdn1-09 on aldosterone regulated gene expression at 6 h in mIMCD-3 cells. Cells were transfected with siEdn1-09 for 24 h prior to a 6 h vehicle (veh) or 1 μM aldosterone (aldo) treatment. Total RNA was extracted, converted to cDNA and analyzed for mRNA expression of the indicated genes by QPCR. Values for each gene indicated were normalized to *actb* and are expressed as mean fold change ± SE relative to NT-siRNA + Veh. (n = 3).

CHAPTER 7
CONCLUSIONS AND PERSPECTIVES

Summary of Results

The data presented in this dissertation have demonstrated for the first time that aldosterone stimulated an increase in ET-1 peptide levels in rat inner medulla *in vivo* and in increase of *edn1* mRNA in rat IMCD *ex vivo* (Stow et al., 2009). The aldosterone-dependent stimulation of *edn1* mRNA was confirmed in multiple renal collecting duct cells lines *in vitro*. A 1990 bp region of the *edn1* promoter demonstrated robust transcriptional activity in luciferase reporter assays. Sequence analysis revealed that this region contained several candidate HREs. Aldosterone action on *edn1* occurred at the level of transcription and involved the recruitment of both MR and GR to two HREs (HRE1 and HRE2) located in the *edn1* promoter. The activation of *edn1* in collecting duct cells could be recapitulated by the administration of dexamethasone, a synthetic glucocorticoid that demonstrates selective GR activation. Finally, siRNA knockdown of *edn1* in collecting duct cells caused a concomitant increase in *sgk1* and decrease in *scnn1a* expression levels in the absence of aldosterone. Surprisingly, *edn1* knockdown rendered the *scnn1a* gene unresponsive to a 1 or 6 h aldosterone treatment.

In contrast to most aldosterone target genes that contribute to Na^+ reabsorption, aldosterone-dependent *edn1* expression is unique in that ET-1 is a known inhibitor of Na^+ transport through ENaC in the collecting duct (Bugaj et al., 2008). Therefore, aldosterone-induced *edn1* likely mediates a negative feedback loop on aldosterone-dependent Na^+ transport.

Aldosterone-ET-1 Action in the Inner Medulla *in vivo*

Studies reported in Chapter 2 showed that aldosterone stimulated an increase inner medullary ET-1 peptide levels. The observed array of genes expressed in the inner medulla from control animals demonstrated that the necessary molecular machinery was present for a

functional ET-1-dependent feedback loop on aldosterone action. First, the inner medulla expressed important components for ENaC dependent Na^+ transport including *sgk1*, *per1* and the three ENaC subunits (*scnn1a*, *scnn1b* and *scnn1g*). The renal inner medulla also expressed the required components for ET-1 signaling including *edn1*, *ece1* and *etbr*. In fact, the inner medulla also contained the highest level of *etbr* gene expression in the kidney. Therefore, it seemed reasonable that an increase in inner medullary ET-1 levels, as was observed in the presence of aldosterone, would result in increased ET-1-ET_B receptor signaling in the inner medulla *in vivo*.

Aldosterone Action on *edn1* is Mediated Via GR and MR

Studies from Chapter 4 confirmed that the aldosterone-dependent stimulation of *edn1* involved both MR and GR recruitment to the *edn1* promoter. Similarly, both hormone receptors are known to regulate aldosterone response genes including *scnn1a* (Mick et al., 2001; Sayegh et al., 1999), *sgk1* (Chen et al., 1999; Itani et al., 2002), and *atp1a1* (Kolla et al., 1999; Whorwood et al., 1994). A role for MR and GR has also been implicated in aldosterone-dependent Na^+ transport in the renal collecting duct (Bens et al., 1999; Gaeggeler et al., 2005). Despite these observations, the role of GR in aldosterone action is actively debated due to the concept that GR would not be active in aldosterone responsive cells that express 11β-HSD2 (Funder and Mihailidou, 2009; Funder et al., 1988; Gaeggeler et al., 2005; Odermatt and Atanasov, 2009). Indeed, 11β-HSD2 is an important enzyme that functions to inactive endogenous glucocorticoids and prevent cortisol-mediated Na^+ retention by the collecting duct. However, 11β-HSD2 metabolites also lack an affinity for GR leaving GR expressed in collecting duct cells readily available for activation by another high affinity ligand such as aldosterone.

Studies from Chapter 4 further revealed that MR and GR were present in the same protein complex suggest that MR and GR may functionally interact with one another. Although the studies in Chapter 4 did not directly address whether MR and GR were forming heterodimers,

MR and GR heterodimers are known to exist (Liu et al., 1995; Savory et al., 2001). MR-GR heterodimers exhibited distinct transcriptional properties (Liu et al., 1995). Compared to aldosterone, dexamethsone stimulated greater increases in *edn1*, *sgk1* and *per1* mRNA expression (Chapter 5). Since dexamethsone does not have an affinity for MR these studies suggested that GR-GR homodimers (by dexamethasone stimulation) have distinct transcriptional properties compared to a mixed MR/GR activation (by aldosterone stimulation). Indeed, aldosterone action mediated by two hormone receptors with different transcriptional properties would certainly provide a collecting duct cell with a higher degree of adaptability in the regulation of Na^+ transport.

Analysis of *edn1* HREs

Two HREs were mapped in the *edn1* promoter that each demonstrated an ability to recruit MR and GR. These HREs were unique because they contained receptor binding half-sites separated by eight nucleotides. Variations in the spacer region exist in several aldosterone response genes including the human *atp1a1* gene (Mick et al., 2001) and may influence cooperative binding of multiple hormone receptors (Ou et al., 2001). For example, the aspartate aminotransferase gene has a HRE with an eight nucleotide spacer region (Garlatti et al., 1994). This unique element was more efficient in the cooperative binding of two hormone receptor dimers suggesting the formation of a unique tetrameric complex. Studies in Chapter 4 revealed that both MR and GR interacted at the same HRE in the *edn1* promoter. However, further studies need to be conducted to evaluate the stoichiometry of MR/GR binding to the *edn1* gene.

The identified HREs were also unique. HRE2 contained half-sites arranged as an inverted repeat, whereas HRE1 contained directly repeated half-sites. Half-site orientation is also known to affect receptor binding as well as transcriptional activation (Geserick et al., 2005). Although GR can bind to directly repeated half-sites with low affinity (Aumais et al., 1996), structural

studies revealed that GR preferentially binds to palindromic DNA sequences as a dimer in a "head-to-head" conformation (Luisi et al., 1991). Consistent with these reports, both MR and GR demonstrated a stronger affinity for HRE2 in comparison to HRE1. Moreover, only HRE2 could recruit RNA polymerase II. Similarly, the aldosterone response gene *scnn1a* also contains two HREs in different orientations. Only the inverted HRE was capable of stimulating transcription (Sayegh et al., 1999). Although GR can bind to directly repeated half-sites with lower affinity, these direct repeats are not thought to induce dimerization since inverting the orientation of the one half-site would also rotate the orientation of a GR monomer. Directly repeated half-sites may in fact represent a negative HRE (Aumais et al., 1996; Geserick et al., 2005). The neural seratonin (5-HT1A) gene contains a negative HRE that consists a direct repeat of 5'-TGTCCT-3' separated by 6 nucleotides. Interestingly, the affinity of this element was greater for MR/GR heterodimers than it was for MR or GR alone. This topology suggests that hormone receptors would bind to the DNA in a head-to-tail conformation. Interestingly, deletion of 3 nucleotides from the spacer region rotated the receptor dimer 180° and converted the negative HRE into a positive HRE that mediated glucocorticoid induced transcription. Thus, HRE1 represents a low affinity element that is only occupied at high concentrations of hormone. Although the functional activity of HRE1 remains to be elucidated, it is interesting to speculate on the evolutionary advantage of having negative response element to prevent excessive hormone activation.

Effect of *edn1* Knockdown on Aldosterone Target Gene Expression

Chapter 6 reports that siRNA knockdown of *edn1* resulted in an increase in *sgk1* mRNA expression. This observation could be explained if ET-1 mediated tonic inhibition of *sgk1* expression. ET-1 signaling has been linked to the transcriptional control of other genes and is known to involve the activation of NF-κB. Interestingly, the only known transcription factor that inhibits *sgk1* mRNA is NF-κB (de Seigneux et al., 2008). Knockdown of e*dn1* expression was

also associated with a decrease in *scnn1a* mRNA expression (Chapter 6). Given that ET-1 has been implicated in the tonic inhibition of ENaC (Bugaj et al., 2008), the reduction is *scnn1a* mRNA most likely reflected a compensatory response. Surprisingly, however, was that *edn1* knockdown was able to completely abrogate the expected increase in *scnn1a* mRNA after 1 or 6 h of hormone treatment.

Model of Aldosterone-Induced ET-1 Negative Feedback Loop

Based on the experiments presented in this dissertation a proposed model has been developed for the mechanism of aldosterone-induced ET-1. In this proposed model a physiological increase in plasma aldosterone activates both MR and GR in the collecting duct (Figure 7-1A). The aldosterone-bound MR/GR complex is transported into the nucleus where the receptors bind to HREs in the *edn1*, *sgk1*, *scnn1a* and *per1* promoter regions. The immediate response to aldosterone involves an increase in *edn1*, *sgk1* and *per1* mRNA. Translated Sgk1 then results in an increase in ENaC channel activity. However, the increase in *edn1* expression results in an increase ET-1 and the subsequent activation of ET_B receptors. ET_B receptor signal transduction results in rapid inhibition of ENaC open probability (Bugaj et al., 2008). The balance between Sgk1 activity and ET_B-mediated action is anticipated to determine the actual net Na^+ transport by ENaC.

In the second phase of aldosterone action (Figure 7-1B) ET_B-dependent activation of NF-κB results in a decrease in *sgk1* mRNA. The consequent decrease in Sgk1 results in ENaC ubiquitinylation and degradation. However, the increased Per1 product enters the nucleus where it binds to and upregulates *scnn1a* expression (Gumz et al., 2009a). Interestingly, Per1 has also been implicated in the inhibition of *edn1* (personal communication with Dr. Michelle Gumz, University of Florida). Therefore, Per1 also serves as a negative feedback signal for *edn1*. Finally, in this model Big-ET-1 is expected to shuttled to sub-membrane vesicles. As

aldosterone dependent Na^+ reabsorption restores normal Na^+ balance a consequent increase in tubular flow rate is expected to the distal nephron. Flow-dependent ET-1 mediated release then acts in a second wave of ET_B-dependent inhibition of ENaC. Taken together, this model provides the first potential negative feedback pathway on aldosterone dependent Na^+ transport and aldosterone-dependent transcription.

Perspectives and Future Directions

The goal of future studies should be designed with three major goals in mind. First, it is pertinent that future studies demonstrate the aldosterone-ET-1 axis has a functional role in Na^+ transport in the collecting duct cell. Second, studies should be designed to fully characterize the molecular mechanisms involved in the aldosterone-ET-1 axis. Finally, future studies should address the role of aldosterone-induced ET-1 in hypertension, as well as other human diseases. These studies should provide great insight into the role of aldosterone-induced ET-1 in the body.

A Functional Aldsosterone-ET-1 Axis

Immediate focus should be on determining whether or not aldosterone induced ET-1 has an effect on aldosterone-dependent Na^+ transport in renal collecting duct cells. The first studies should be conducted in mpkCCD_{c14} cells and mIMCD-3 cells *in vitro* since both of these cells lines are validated models for aldosterone action. A good experiment would be designed to apply the siRNA technique presented in Chapter 6 for use in combination with an Ussing chamber experiment to evaluate the role of ET-1 on ENaC-dependent transepithelial Na^+ voltage. Knockdown of *edn1* should result in an increase in ENaC activity in the presence or absence of aldosterone. This observation would also confirm that the decrease in *scnn1a* mRNA levels was a compensatory response due to increased ENaC activity. These functional studies should also be conducted over a 24-48 h time course in order to fully characterize the aldosterone-ET-1 mechanism. Furthermore, additional electrophysiological experiments, such as single-channel

patch clamp studies, should be conducted to confirm data collected using an Ussing chamber approach.

After initial studies have characterized the functional role of aldosterone-induced ET-1 in the collecting duct, experiments should then be designed to confirm the mechanism exists in an animal. An inducible, collecting duct cell specific *edn1* knockout mouse would allow investigators to study the specific role of *edn1* in response to aldosterone. Creating an inducible knockout would eliminate confounding compensatory responses during development. This mouse model would have a greater degree of clinical relevance to disease since aberrations, but not the complete loss of *edn1* has been documented in human disease.

It would also be highly advantageous to create a technique to allow of the identification of edn1 expression in vivo. Since the *edn1* mRNA is too liable for isolation from animal tissue extracts (Chapter 2), an alternative approach will be required. The best approach would involve the creation of another mouse model. The *edn1* promoter containing the functional HRE1 and HRE2 could be inserted upstream of a reporter gene such as luciferase or β-galatosidase. The reporter construct should then be delivered to a mouse embryo and inserted into the mouse genome to create a transgenic mouse model. Treating these mice with vehicle or aldosterone would allow researchers to identify cells that normally express *edn1*, as well as cells that modulate their *edn1* expression in response to aldosterone. This study would also determine if aldosterone-induced ET-1 is exclusive to the IMCD or occurs in CCD and OMCD, a question that has not been resolved *in vivo*. Moreover, this mouse model would be useful for identifying other regulatory signals that control *edn1* expression.

Molecular Machinery and Therapeutic Targets

Future experiments should also address the molecular mechanism for aldosterone induction of ET-1, as well as ET-1-mediated feedback on aldosterone action. The studies

presented in this dissertation have provided a great deal of insight into the mechanism of aldosterone action on *edn1*. Indeed, the studies presented in this dissertation have shown that aldosterone acts through both MR and GR to modulate *edn1* mRNA expression. However, it still remains to be confirmed that MR and GR form a functional heterodimer in collecting duct cells. Demonstration of a functional heterodimer in the kidney would change the clinical paradigm and most certainly provide new avenues for pharmacological drug design. An *in vivo* fluorescence resonance energy transfer experiment in collecting duct cells would directly address this issue. If, indeed, a MR-GR heterodimer is verified in collecting duct cells, it will be necessary to determine what set of genes this heteromeric complex regulates in collecting duct cells. It is possible that MR and GR homodimers and heterodimers regulate distinct sets of genes. Indeed, this hypothesis is consistent with observations in Chapters 4 and 5 that showed equimolar concentrations of aldosterone, which activated MR and GR, and dexamethasone, which activates only GR, demonstrated different magnitudes of mRNA induction. This added degree of transcriptional complexity would allow a particular cell to respond more specifically to a given physiological need. Moreover, expanding the cell's capacity to differentially regulate transcription would clearly be an evolutionary advantage. Gene microarray technology and candidate gene approaches should be used to evaluate differences in transcription in response homodimer or heterodimers.

Another important goal of future molecular studies should be to identify the key molecules and molecular mechanism involved in the aldosterone-ET-1 feedback loop (Figure 7-1). First, it is not known how PreproET-1 is processed to ET-1 in collecting duct cells. It is possible that signal transduction pathways regulate the secretion of Big-ET-1. Indeed, increased ET-1 secretion has been observed due to an increase in flow and shear stress (Kohan, 2009; Walshe et

al., 2005). The regulatory release of ET-1 in response to mechanical stimuli or other factors may explain why renal ET-1 is increased in both states of high (Fattal et al., 2004) and low (Klinger et al., 2008) NaCl intake in animals. Indeed, during states of low NaCl intake the body would release aldosterone in order to increase NaCl content by stimulating Na^+ transport in the distal nephron and collecting duct. Under these conditions, ET-1 is directly stimulated by aldosterone to mediate a negative feedback loop that either shuts down aldosterone signaling or simply prevents excessive Na^+ reabsorption. In contrast, a high NaCl intake stimulates ET-1 secretion via mechanical stimuli such as an increase in flow or shear stress. Under these conditions the increase in ET-1 likely facilitates natriuresis and prevents an increase in NaCl and blood pressure. Therefore, renal ET-1 can be stimulated to block Na^+ reabsorption during both high and low NaCl conditions. However, further mechanistic studies are needed to confirm this model of ET-1 action.

Other important molecular studies in the future should include evaluating the molecules involved in ET-1-ET_B receptor feedback. Current studies have demonstrated that nitric oxide, Src kinases and cGMP are involved in ET_B-dependent inhibition of ENaC activity (Bugaj et al., 2008; Gilmore et al., 2001). However, the full signal transduction cascade targeting ENaC activity has not been elucidated. Moreover, data in Chapter 6 suggests for the first time that an ET_B-dependent pathway blocking transcription of the aldosterone-target gene *sgk1* also exists. The potential role of NF-κB in mediating ET_B receptor-dependent inhibition of *sgk1* mRNA expression should be addressed. A combination of NF-κB antagonists and ET_B receptor antagonists should address this experimental question. Similarly, the molecules involved in ET_B receptor-mediated ENaC activity inhibition should be confirmed in order to identify new molecular targets for therapeutic intervention.

The Aldosterone-ET-1 Axis in Hypertension and Human Disease

The confirmation of a functional ET-1 mediated feedback loop on aldosterone action, and the identification of the molecular pathways involved have major implications for patients diagnosed with hypertension. Hypertension remains a major medical concern. In 2009, the American Heart Association reported that hypertension affected an astounding 73 million Americans, or one-third of our entire adult population. Hypertension is a leading risk factor for cardiovascular disease, stroke and all-cause mortality. Greater than 90% of hypertensive patients are diagnosed with essential hypertension (Binder, 2007). Essential hypertension is thought to be involve multiple gene loci (Deng, 2007) and is most likely caused by subtle genetic polymorphisms (Binder, 2007) or imbalances in gene expression that develop over time (Doris and Fornage, 2005).

Many polymorphisms associated with clinical hypertension have been identified in aldosterone target genes, including *edn1* (Treiber et al., 2003), *sgk1* (Busjahn et al., 2002) and *scnn1a* (αENaC) (Iwai et al., 2002). Several of these polymorphisms are located in gene regulatory regions and were shown to alter the normal pattern of mRNA expression (Gonzalez et al., 2007; Iwai et al., 2002; Popowski et al., 2003). Abnormal patterns of aldosterone-dependent gene expression have also been observed in experimental models of hypertension (Aoi et al., 2006). Indeed, if *edn1* mediates negative feedback on aldosterone action, the uncoupling of aldosterone and *edn1* might result in excessive Na^+ retention and hypertension. Molecular studies presented in this dissertation, combined with data collected in the proposed future experiments, could aid researchers in the development of more specific clinical interventions that treat the specific mechanism of essential hypertension in a given patient.

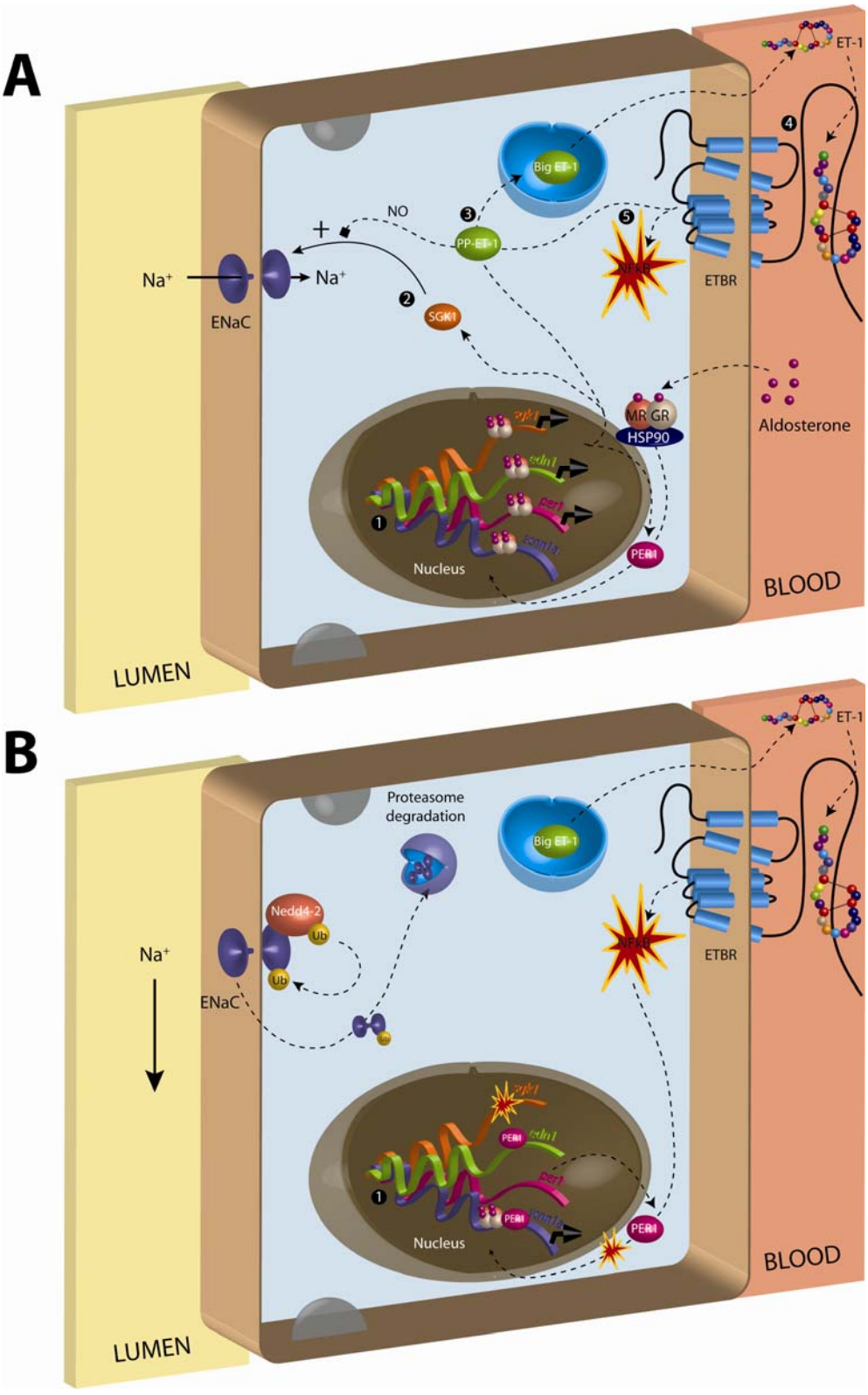

Figure 7-1 Proposed Model for ET-1 Mediated Negative Feedback on Aldosterone Action in the Kidney.

APPENDIX A
OPTIMIZED PROTOCOL FOR INDIVIDUAL NEPHRON DISSECTION IN RAT

Method

While microdissection of mouse nephron segments is a well-established procedure in our laboratory, the isolation of individual rat nephrons had not been previously performed. Due to naturally occurring interstitial fibrosis in the adult rat kidney, several technical parameters were modified. The following procedure allowed for isolation of >30 mm of cortical collecting ducts: Male Sprague Dawley rats (150 g; Harlan) were anesthetized with pentobarbital (100 mg/kg, ip) and kidneys were removed. Coronal slices were dissected into cortex, outer and inner medulla. Samples were torn with forceps and placed into 2 ml of collagenase digestion solution (CDS) that contained 1 mg/ml collagenase type II (Worthington Biochemical, Freehold, NJ), 5 mM glycine, 50 U/ml DNase I, 50 µg/ml soybean trypsin inhibitor, and 10 U/ml RNase inhibitor (Promega, Madison, WI) in 1:1 Dulbecco's Modified Eagle Medium/Ham's F-12 without HEPES (4-(2-hydroxyethyl)-1-piperazineethanesulfonic acid) or phenol red. Samples were agitated by hand and placed in a 5% CO_2 incubator. CDS was changed every 10 min and individual segments were present after approximately 35 min. Supernatant was transferred into glass tubes and tubules were sedimented on ice for 5 min. The CDS was removed and replaced with 1:1 Dulbecco's Modified Eagle Medium/Ham's F-12 plus 1% bovine serum albumin. Tubules were sorted for 1 h at 4 °C. Nephron and collecting duct segments were identified based on the sorting criteria below. Tubules were measured with a micrometer and transferred into 800 µl TRIzol® (Invitrogen) for conventional RNA extraction.

Table A-1. Identification criteria for microdissected nephron segments

Digestion	Nephron Segment	Identification Criteria
cortex	proximal convoluted tubule	white, reflective, convoluted, thicker than the distal convoluted tubule
	proximal straight tubule	reflective, smooth membrane, wide
	cortical thick ascending limb of Henle	thin, straight, wiry, uniform cell population
	distal convoluted tubule	white, reflective, convoluted, transition to connecting tubule
	connecting tubule	transition from distal convoluted tubule, not reflective, tall and uniform cells
	initial collecting tubule	branch points, not reflective, low and heterogeneous cell population
	cortical collecting duct	not reflective, gray, modeled membrane, sticky, and wider than initial collecting tubule
outer medulla	medullary thick ascending limb of Henle	straight, wiry, uniform cells, brighter and slightly thinner than outer medullary collecting duct
	outer medullary collecting duct	gray, modeled membrane, sticky
inner medulla	thin limbs (ascending and descending)	very thin, straight
	inner medullary collecting duct	very white, not reflective, sticky, flexible, and very wide

APPENDIX B
IMMUNOHISTOCHEMISTRY OF ETB RECEPTORS IN THE RAT KIDNEY

Method

Wild-type black swiss mice were anesthetized with isoflurane and kidneys were preserved by *in vivo* cardiac perfusion with PBS (pH 7.4) followed by periodate-lysine-2% paraformaldehyde fixative. Kidneys were removed, sectioned into 2 to 4 mm thick slices and immersed overnight at 4 ºC in the same fixative. Samples of kidney from each animal were embedded in polyester wax (polyethylene glycol 400 disterate, Polysciences, Warrington, PA). Sections (5 µm thick) were cut with a microtome and mounted on gelatin-coated glass slides.

Immunolocalization of the ET_B receptor was attempted with two different antibodies: a rabbit-anti-human antibody to the N-terminus (epitope: EERGFPPDRATPLLQ) (#91508, Assay Designs) and a rabbit-anti-rat antibody against residues 298-314 (CEMLFKKSGMQIALND) (Product #AER-002, Lot # AN-02, Alomone). A standard immunoperoxidase procedure was used (Vectastain Elite, Vector Laboratories, Burlingame, CA). Sections were dewaxed in a graded series of ethanol, rehydrated and rinsed in PBS. Sections were blocked for 15 min with 5% normal goat serum (Vector Laboratories) in PBS, and then incubated at 4 ºC overnight with one of the primary antibodies. Sections were washed in PBS and endogenous peroxidase activity was blocked by incubating the sections in 0.3% H_2O_2 for 30 min. The sections will be washed again in PBS and incubated for 30 min with biotinlyated goat anti-rabbit IgG secondary antibody (Vector Laboratories) diluted 1:200 in PBS and again washed in PBS. The sections were treated for 30 min with the avidin-biotin complex reagent, rinsed with PBS and then exposed to diaminobenzidine. The sections will then be dehydrated with xylene, mounted with Permount (Fisher, Fair Lawn, NJ) and observed by light microscopy. For controls in each of the

immunolocalization experiments, preimmune serum diluted at the same concentration as the primary antibody in PBS or PBS alone was substituted for the primary antibody.

Results

The antibodies each localized to different structures in the kidney, which confounded data interpretation.

LIST OF REFERENCES

Agus, Z.S., Gardner, L.B., Beck, L.H., and Goldberg, M. (1973). Effects of parathyroid hormone on renal tubular reabsorption of calcium, sodium, and phosphate. Am J Physiol *224*, 1143-1148.

Ahn, D., Ge, Y., Stricklett, P.K., Gill, P., Taylor, D., Hughes, A.K., Yanagisawa, M., Miller, L., Nelson, R.D., and Kohan, D.E. (2004). Collecting duct-specific knockout of endothelin-1 causes hypertension and sodium retention. J Clin Invest *114*, 504-511.

Aitsebaomo, J., Kingsley-Kallesen, M.L., Wu, Y., Quertermous, T., and Patterson, C. (2001). Vezf1/DB1 is an endothelial cell-specific transcription factor that regulates expression of the endothelin-1 promoter. J Biol Chem *276*, 39197-39205.

Alam, J., and Cook, J.L. (1990). Reporter genes: application to the study of mammalian gene transcription. Anal Biochem *188*, 245-254.

Anderson, E.M., Birmingham, A., Baskerville, S., Reynolds, A., Maksimova, E., Leake, D., Fedorov, Y., Karpilow, J., and Khvorova, A. (2008). Experimental validation of the importance of seed complement frequency to siRNA specificity. RNA *14*, 853-861.

Aoi, W., Niisato, N., Sawabe, Y., Miyazaki, H., and Marunaka, Y. (2006). Aldosterone-induced abnormal regulation of ENaC and SGK1 in Dahl salt-sensitive rat. Biochem Biophys Res Commun *341*, 376-381.

Applied Biosystems (2006). Amplification Efficiency of TaqMan Gene Expression Assays (Foster City, CA, Applied Biosystems).

Aquilla, E., Whelchel, A., Knot, H.J., Nelson, M., and Posada, J. (1996). Activation of multiple mitogen-activated protein kinase signal transduction pathways by the endothelin B receptor requires the cytoplasmic tail. J Biol Chem *271*, 31572-31579.

Arriza, J.L., Weinberger, C., Cerelli, G., Glaser, T.M., Handelin, B.L., Housman, D.E., and Evans, R.M. (1987). Cloning of human mineralocorticoid receptor complementary DNA: structural and functional kinship with the glucocorticoid receptor. Science *237*, 268-275.

Aumais, J.P., Lee, H.S., DeGannes, C., Horsford, J., and White, J.H. (1996). Function of directly repeated half-sites as response elements for steroid hormone receptors. J Biol Chem *271*, 12568-12577.

Bai, L., Collins, J.F., Xu, H., and Ghishan, F.K. (2001). Transcriptional regulation of rat Na(+)/H(+) exchanger isoform-2 (NHE-2) gene by Sp1 transcription factor. Am J Physiol Cell Physiol *280*, C1168-1175.

Battistini, B., Berthiaume, N., Kelland, N.F., Webb, D.J., and Kohan, D.E. (2006). Profile of past and current clinical trials involving endothelin receptor antagonists: the novel "-sentan" class of drug. Exp Biol Med (Maywood) *231*, 653-695.

Beato, M. (1989). Gene regulation by steroid hormones. Cell *56*, 335-344.

Beato, M., and Klug, J. (2000). Steroid hormone receptors: an update. Hum Reprod Update *6*, 225-236.

Bens, M., Vallet, V., Cluzeaud, F., Pascual-Letallec, L., Kahn, A., Rafestin-Oblin, M.E., Rossier, B.C., and Vandewalle, A. (1999). Corticosteroid-dependent sodium transport in a novel immortalized mouse collecting duct principal cell line. J Am Soc Nephrol *10*, 923-934.

Bhalla, V., and Hallows, K.R. (2008). Mechanisms of ENaC regulation and clinical implications. J Am Soc Nephrol *19*, 1845-1854.

Binder, A. (2007). A review of the genetics of essential hypertension. Curr Opin Cardiol *22*, 176-184.

Blair-West, J.R., Coghlan, J.P., Denton, D.A., Goding, J.R., and Wright, R.D. (1963). The effect of aldosterone, cortisol, and corticosterone upon the sodium and potassium content of sheep's parotid saliva. J Clin Invest *42*, 484-496.

Boldyreff, B., and Wehling, M. (2003). Rapid aldosterone actions: from the membrane to signaling cascades to gene transcription and physiological effects. J Steroid Biochem Mol Biol *85*, 375-381.

Brennan, F.E., and Fuller, P.J. (2006). Mammalian K-ras2 is a corticosteroid-induced gene in vivo. Endocrinology *147*, 2809-2816.

Brenner, B.M., and Rector, F.C. (2008). Brenner & Rector's the kidney, 8th edn (Philadelphia, Saunders Elsevier).

Bridge, A.J., Pebernard, S., Ducraux, A., Nicoulaz, A.L., and Iggo, R. (2003). Induction of an interferon response by RNAi vectors in mammalian cells. Nat Genet *34*, 263-264.

Bugaj, V., Pochynyuk, O., Mironova, E., Vandewalle, A., Medina, J.L., and Stockand, J.D. (2008). Regulation of the epithelial Na+ channel by endothelin-1 in rat collecting duct. Am J Physiol *295*, F1063-1070.

Burckhardt, G., Di Sole, F., and Helmle-Kolb, C. (2002). The Na+/H+ exchanger gene family. J Nephrol *15 Suppl 5*, S3-21.

Busjahn, A., Aydin, A., Uhlmann, R., Krasko, C., Bahring, S., Szelestei, T., Feng, Y., Dahm, S., Sharma, A.M., Luft, F.C., *et al.* (2002). Serum- and glucocorticoid-regulated kinase (SGK1) gene and blood pressure. Hypertension *40*, 256-260.

Cai, Z., Xin, J., Pollock, D.M., and Pollock, J.S. (2000). Shear stress-mediated NO production in inner medullary collecting duct cells. Am J Physiol *279*, F270-274.

Capasso, G., Rizzo, M., Evangelista, C., Ferrari, P., Geelen, G., Lang, F., and Bianchi, G. (2005). Altered expression of renal apical plasma membrane Na+ transporters in the early phase of genetic hypertension. Am J Physiol *288*, F1173-1182.

Cella, J., and Tweit, R. (1961). Alkanoylthio-17 alpha-carboxyethyl-17 beta-hydoxyandrosten-3-one lactones, U.S.P. Office, ed. (United States of America, G. D. Searle & Co).

Chambrey, R., Warnock, D.G., Podevin, R.A., Bruneval, P., Mandet, C., Belair, M.F., Bariety, J., and Paillard, M. (1998). Immunolocalization of the Na+/H+ exchanger isoform NHE2 in rat kidney. Am J Physiol *275*, F379-386.

Chen, M., Todd-Turla, K., Wang, W.H., Cao, X., Smart, A., Brosius, F.C., Killen, P.D., Keiser, J.A., Briggs, J.P., and Schnermann, J. (1993). Endothelin-1 mRNA in glomerular and epithelial cells of kidney. Am J Physiol *265*, F542-550.

Chen, S.Y., Bhargava, A., Mastroberardino, L., Meijer, O.C., Wang, J., Buse, P., Firestone, G.L., Verrey, F., and Pearce, D. (1999). Epithelial sodium channel regulated by aldosterone-induced protein sgk. Proc Natl Acad Sci USA *96*, 2514-2519.

Chou, S.Y., and Porush, J.G. (1995). Renal actions of endothelin-1 and endothelin-3: interactions with the prostaglandin system and nitric oxide. Am J Kidney Dis *26*, 116-123.

Chow, Y.H., Wang, Y., Plumb, J., O'Brodovich, H., and Hu, J. (1999). Hormonal regulation and genomic organization of the human amiloride-sensitive epithelial sodium channel alpha subunit gene. Pediatr Res *46*, 208-214.

Clapp, W.L., Madsen, K.M., Verlander, J.W., and Tisher, C.C. (1987). Intercalated cells of the rat inner medullary collecting duct. Kidney International *31*, 1080-1087.

Clavell, A.L., Stingo, A.J., Margulies, K.B., Brandt, R.R., and Burnett, J.C., Jr. (1995). Role of endothelin receptor subtypes in the in vivo regulation of renal function. Am J Physiol *268*, F455-460.

Corman, B., Pratz, J., and Poujeol, P. (1985). Changes in anatomy, glomerular filtration, and solute excretion in aging rat kidney. Am J Physiol *248*, R282-287.

Couette, B., Marsaud, V., Baulieu, E.E., Richard-Foy, H., and Rafestin-Oblin, M.E. (1992). Spironolactone, an aldosterone antagonist, acts as an antiglucocorticosteroid on the mouse mammary tumor virus promoter. Endocrinology *130*, 430-436.

Coutard, M., Osborne-Pellegrin, M.J., and Funder, J.W. (1978). Tissue distribution and specific binding of tritiated dexamethasone in vivo: autoradiographic and cell fractionation studies in the mouse. Endocrinology *103*, 1144-1152.

Cowley, A.W., Jr. (1997). Role of the renal medulla in volume and arterial pressure regulation. Am J Physiol *273*, R1-15.

Cupples, W.A. (2007). Interactions contributing to kidney blood flow autoregulation. Curr Opin Nephrol Hypertens *16*, 39-45.

D'Orleans-Juste, P., Labonte, J., Bkaily, G., Choufani, S., Plante, M., and Honore, J.C. (2002). Function of the endothelin(B) receptor in cardiovascular physiology and pathophysiology. Pharmacol Ther *95*, 221-238.

Davenport, A.P. (2002). International Union of Pharmacology. XXIX. Update on endothelin receptor nomenclature. Pharmacol Rev *54*, 219-226.

Davenport, A.P., O'Reilly, G., Molenaar, P., Maguire, J.J., Kuc, R.E., Sharkey, A., Bacon, C.R., and Ferro, A. (1993). Human endothelin receptors characterized using reverse transcriptase-polymerase chain reaction, in situ hybridization, and subtype-selective ligands BQ123 and BQ3020: evidence for expression of ETB receptors in human vascular smooth muscle. J Cardiovasc Pharmacol *22 Suppl 8*, S22-25.

de Seigneux, S., Leroy, V., Ghzili, H., Rousselot, M., Nielsen, S., Rossier, B.C., Martin, P.Y., and Féraille, E. (2008). NF-kappaB inhibits sodium transport via down-regulation of SGK1 in renal collecting duct principal cells. J Biol Chem *283*, 25671-25681.

de Wet, J.R., Wood, K.V., Helinski, D.R., and DeLuca, M. (1985). Cloning of firefly luciferase cDNA and the expression of active luciferase in Escherichia coli. Proc Natl Acad Sci U S A *82*, 7870-7873.

Debonneville, C., Flores, S.Y., Kamynina, E., Plant, P.J., Tauxe, C., Thomas, M.A., Munster, C., Chraibi, A., Pratt, J.H., Horisberger, J.D., *et al.* (2001). Phosphorylation of Nedd4-2 by Sgk1 regulates epithelial Na(+) channel cell surface expression. EMBO J *20*, 7052-7059.

Deng, A.Y. (2007). Genetic basis of polygenic hypertension. Hum Mol Genet *16 Spec No. 2*, R195-202.

Deng, W.G., Zhu, Y., Montero, A., and Wu, K.K. (2003). Quantitative analysis of binding of transcription factor complex to biotinylated DNA probe by a streptavidin-agarose pulldown assay. Anal Biochem *323*, 12-18.

Derfoul, A., Robertson, N.M., Lingrel, J.B., Hall, D.J., and Litwack, G. (1998). Regulation of the human Na/K-ATPase beta1 gene promoter by mineralocorticoid and glucocorticoid receptors. J Biol Chem *273*, 20702-20711.

Dhaun, N., Goddard, J., Kohan, D.E., Pollock, D.M., Schiffrin, E.L., and Webb, D.J. (2008). Role of endothelin-1 in clinical hypertension: 20 years on. Hypertension *52*, 452-459.

Doris, P.A., and Fornage, M. (2005). The transcribed genome and the heritable basis of essential hypertension. Cardiovasc Toxicol *5*, 95-108.

Dunn, T.B. (1949). Some observations on the normal and pathologic anatomy of the kidney of the mouse. J Natl Cancer Inst *9*, 285-301.

Dusilova-Sulkova, S. (2009). Vitamin D metabolism and vitamin D traditional and nontraditional, target organs: implications for kidney patients. J Ren Care *35 Suppl 1*, 39-44.

Eaton, D.C., and Pooler, J.P. (2004). Vander's renal physiology, 7th edn (New York, NY, Lange Medical Books/McGraw Hill, Medical Pub. Division).

Edwards, R.M., Pullen, M., and Nambi, P. (1992). Activation of endothelin ETB receptors increases glomerular cGMP via an L-arginine-dependent pathway. Am J Physiol *263*, F1020-1025.

Emoto, N., and Yanagisawa, M. (1995). Endothelin-converting enzyme-2 is a membrane-bound, phosphoramidon-sensitive metalloprotease with acidic pH optimum. J Biol Chem *270*, 15262-15268.

Estevez, R., Boettger, T., Stein, V., Birkenhager, R., Otto, E., Hildebrandt, F., and Jentsch, T.J. (2001). Barttin is a Cl- channel beta-subunit crucial for renal Cl- reabsorption and inner ear K+ secretion. Nature *414*, 558-561.

Fakitsas, P., Adam, G., Daidié, D., van Bemmelen, M.X., Fouladkou, F., Patrignani, A., Wagner, U., Warth, R., Camargo, S.M., Staub, O.*, et al.* (2007). Early aldosterone-induced gene product regulates the epithelial sodium channel by deubiquitylation. J Am Soc Nephrol *18*, 1084-1092.

Fattal, I., Abassi, Z., Ovcharenko, E., Shimada, K., Takahashi, M., Hoffman, A., and Winaver, J. (2004). Effect of dietary sodium intake on the expression of endothelin-converting enzyme in the renal medulla. Nephron Physiol *98*, p89-96.

Fedorov, Y., King, A., Anderson, E., Karpilow, J., Ilsley, D., Marshall, W., and Khvorova, A. (2005). Different delivery methods-different expression profiles. Nat Methods *2*, 241.

Felx, M., Guyot, M.C., Isler, M., Turcotte, R.E., Doyon, J., Khatib, A.M., Leclerc, S., Moreau, A., and Moldovan, F. (2006). Endothelin-1 (ET-1) promotes MMP-2 and MMP-9 induction involving the transcription factor NF-kappaB in human osteosarcoma. Clin Sci (Lond) *110*, 645-654.

Flores, S.Y., Loffing-Cueni, D., Kamynina, E., Daidié, D., Gerbex, C., Chabanel, S., Dudler, J., Loffing, J., and Staub, O. (2005). Aldosterone-induced serum and glucocorticoid-induced kinase 1 expression is accompanied by Nedd4-2 phosphorylation and increased Na+ transport in cortical collecting duct cells. J Am Soc Nephrol *16*, 2279-2287.

Frey, F.J., Odermatt, A., and Frey, B.M. (2004). Glucocorticoid-mediated mineralocorticoid receptor activation and hypertension. Curr Opin Nephrol Hypertens *13*, 451-458.

Frindt, G., Ergonul, Z., and Palmer, L.G. (2007). Na channel expression and activity in the medullary collecting duct of rat kidney. Am J Physiol *292*, F1190-1196.

Fuller, P.J. (2004). Aldosterone and DNA: the 50th anniversary. Trends Endocrinol Metab *15*, 143-146.

Funder, J.W. (2005). Mineralocorticoid receptors: distribution and activation. Heart failure reviews *10*, 15-22.

Funder, J.W., and Mihailidou, A.S. (2009). Aldosterone and mineralocorticoid receptors: Clinical studies and basic biology. Mol Cell Endocrinol *301*, 2-6.

Funder, J.W., Pearce, P.T., Smith, R., and Smith, A.I. (1988). Mineralocorticoid action: target tissue specificity is enzyme, not receptor, mediated. Science *242*, 583-585.

Gaeggeler, H.P., Gonzalez-Rodriguez, E., Jaeger, N.F., Loffing-Cueni, D., Norregaard, R., Loffing, J., Horisberger, J.D., and Rossier, B.C. (2005). Mineralocorticoid versus glucocorticoid receptor occupancy mediating aldosterone-stimulated sodium transport in a novel renal cell line. J Am Soc Nephrol *16*, 878-891.

Gallego, M.S., and Ling, B.N. (1996). Regulation of amiloride-sensitive Na+ channels by endothelin-1 in distal nephron cells. Am J Physiol *271*, F451-460.

Galon, J., Franchimont, D., Hiroi, N., Frey, G., Boettner, A., Ehrhart-Bornstein, M., O'Shea, J.J., Chrousos, G.P., and Bornstein, S.R. (2002). Gene profiling reveals unknown enhancing and suppressive actions of glucocorticoids on immune cells. FASEB J *16*, 61-71.

Gamba, G., Miyanoshita, A., Lombardi, M., Lytton, J., Lee, W.S., Hediger, M.A., and Hebert, S.C. (1994). Molecular cloning, primary structure, and characterization of two members of the mammalian electroneutral sodium-(potassium)-chloride cotransporter family expressed in kidney. J Biol Chem *269*, 17713-17722.

Ganong, W.F., Biglieri, E.G., and Mulrow, P.J. (1966). Mechanisms regulating adrenocortical secretion of aldosterone and glucocorticoids. Recent Prog Horm Res *22*, 381-430.

Gariepy, C.E., Ohuchi, T., Williams, S.C., Richardson, J.A., and Yanagisawa, M. (2000). Salt-sensitive hypertension in endothelin-B receptor-deficient rats. J Clin Invest *105*, 925-933.

Garlatti, M., Daheshia, M., Slater, E., Bouguet, J., Hanoune, J., Beato, M., and Barouki, R. (1994). A functional glucocorticoid-responsive unit composed of two overlapping inactive receptor-binding sites: evidence for formation of a receptor tetramer. Mol Cell Biol *14*, 8007-8017.

Gauer, S., Segitz, V., and Goppelt-Struebe, M. (2007). Aldosterone induces CTGF in mesangial cells by activation of the glucocorticoid receptor. Nephrol Dial Transplant *22*, 3154-3159.

Ge, Y., Bagnall, A., Stricklett, P.K., Strait, K., Webb, D.J., Kotelevtsev, Y., and Kohan, D.E. (2006). Collecting duct-specific knockout of the endothelin B receptor causes hypertension and sodium retention. Am J Physiol *291*, F1274-1280.

Ge, Y., Huang, Y., and Kohan, D.E. (2008). Role of the renin-angiotensin-aldosterone system in collecting duct-derived endothelin-1 regulation of blood pressure. Can J Physiol Pharmacol *86*, 329-336.

Ge, Y., Stricklett, P.K., Hughes, A.K., Yanagisawa, M., and Kohan, D.E. (2005). Collecting duct-specific knockout of the endothelin A receptor alters renal vasopressin responsiveness, but not sodium excretion or blood pressure. Am J Physiol *289*, F692-698.

Gerstung, M., Roth, T., Dienes, H.P., Licht, C., and Fries, J.W. (2007). Endothelin-1 induces NF-kappaB via two independent pathways in human renal tubular epithelial cells. Am J Nephrol *27*, 294-300.

Geserick, C., Meyer, H.A., and Haendler, B. (2005). The role of DNA response elements as allosteric modulators of steroid receptor function. Mol Cell Endocrinol *236*, 1-7.

Gilmore, E.S., Stutts, M.J., and Milgram, S.L. (2001). Src Family Kinases Mediate Epithelial Na+ Channel Inhibition by Endothelin. J Biol Chem *276*, 42610-42617.

Gonzalez, A.A., Carvajal, C.A., Riquelme, E., Krall, P.M., Munoz, C.R., Mosso, L.M., Kalergis, A.M., and Fardella, C.E. (2007). A polymorphic GT short tandem repeat affecting beta-ENaC mRNA expression is associated with low renin essential hypertension. Am J Hypertens *20*, 800-806.

Gottschalk, C.W., and Mylle, M. (1958). Evidence that the mammalian nephron functions as a countercurrent multiplier system. Science *128*, 594.

Grantcharova, E., Furkert, J., Reusch, H.P., Krell, H.W., Papsdorf, G., Beyermann, M., Schulein, R., Rosenthal, W., and Oksche, A. (2002). The extracellular N terminus of the endothelin B (ETB) receptor is cleaved by a metalloprotease in an agonist-dependent process. J Biol Chem *277*, 43933-43941.

Grantcharova, E., Reusch, H.P., Grossmann, S., Eichhorst, J., Krell, H.W., Beyermann, M., Rosenthal, W., and Oksche, A. (2006). N-terminal proteolysis of the endothelin B receptor abolishes its ability to induce EGF receptor transactivation and contractile protein expression in vascular smooth muscle cells. Arterioscler Thromb Vasc Biol *26*, 1288-1296.

Greger, R. (1985). Ion transport mechanisms in thick ascending limb of Henle's loop of mammalian nephron. Physiol Rev *65*, 760-797.

Grossmann, C., Freudinger, R., Mildenberger, S., Krug, A.W., and Gekle, M. (2004a). Evidence for epidermal growth factor receptor as negative-feedback control in aldosterone-induced Na+ reabsorption. Am J Physiol *286*, F1226-F1231.

Grossmann, C., Scholz, T., Rochel, M., Bumke-Vogt, C., Oelkers, W., Pfeiffer, A.F., Diederich, S., and Bahr, V. (2004b). Transactivation via the human glucocorticoid and mineralocorticoid receptor by therapeutically used steroids in CV-1 cells: a comparison of their glucocorticoid and mineralocorticoid properties. Eur J Endocrinol *151*, 397-406.

Grundy, H.M., Simpson, S.A., and Tait, J.F. (1952). Isolation of a highly active mineralocorticoid from beef adrenal extract. Nature *169*, 795-796.

Gumz, M.L., Popp, M.P., Wingo, C.S., and Cain, B.D. (2003). Early transcriptional effects of aldosterone in a mouse inner medullary collecting duct cell line. Am J Physiol *285*, F664-673.

Gumz, M.L., Stow, L.R., Lynch, I.J., Greenlee, M.M., Rudin, A., Cain, B.D., Weaver, D.R., and Wingo, C.S. (2009a). The circadian clock protein Period 1 regulates expression of the renal epithelial sodium channel in mice. J Clin Invest.

Gumz, M.L., Stow, L.R., Lynch, I.J., Greenlee, M.M., Rudin, A., Cain, B.D., Weaver, D.R., and Wingo, C.S. (2009b). The circadian clock protein Period 1 regulates expression of the renal epithelial sodium channel in mice. J Clin Invest *119*, 2423-2434.

Gumz, M.L., Stow, L.R., and Xia, S.L. (2009c). Epithelial Transport Physiology. In, G. Gerencser, ed. (Humana Press).

Guntupalli, J., Onuigbo, M., Wall, S., Alpern, R.J., and DuBose, T.D., Jr. (1997). Adaptation to low-K+ media increases H(+)-K(+)-ATPase but not H(+)-ATPase-mediated pHi recovery in OMCD1 cells. Am J Physiol *273*, C558-571.

Gutzwiller, J.P., Hruz, P., Huber, A.R., Hamel, C., Zehnder, C., Drewe, J., Gutmann, H., Stanga, Z., Vogel, D., and Beglinger, C. (2006). Glucagon-like peptide-1 is involved in sodium and water homeostasis in humans. Digestion *73*, 142-150.

Guyton, A.C. (1981). The relationship of cardiac output and arterial pressure control. Circulation *64*, 1079-1088.

Guyton, A.C. (1991). Blood pressure control--special role of the kidneys and body fluids. Science *252*, 1813-1816.

Guyton, A.C., Coleman, T.G., Cowley, A.V., Jr., Scheel, K.W., Manning, R.D., Jr., and Norman, R.A., Jr. (1972). Arterial pressure regulation. Overriding dominance of the kidneys in long-term regulation and in hypertension. Am J Med *52*, 584-594.

Haraldsson, B., and Jeansson, M. (2009). Glomerular filtration barrier. Curr Opin Nephrol Hypertens *18*, 331-335.

Haraldsson, B., Nystrom, J., and Deen, W.M. (2008). Properties of the glomerular barrier and mechanisms of proteinuria. Physiol Rev *88*, 451-487.

He, Y., Szapary, D., and Simons, S.S., Jr. (2002). Modulation of induction properties of glucocorticoid receptor-agonist and -antagonist complexes by coactivators involves binding to receptors but is independent of ability of coactivators to augment transactivation. J Biol Chem *277*, 49256-49266.

Hellal-Levy, C., Couette, B., Fagart, J., Souque, A., Gomez-Sanchez, C.E., and Rafestin-Oblin, M. (1999). Specific hydroxylations determine selective corticosteroid recognition by human glucocorticoid and mineralocorticoid receptors. FEBS Lett *464*, 9-13.

Herrera, M., and Garvin, J.L. (2004). Endothelin stimulates endothelial nitric oxide synthase expression in the thick ascending limb. Am J Physiol *287*, F231-235.

Herrera, M., and Garvin, J.L. (2005). A high-salt diet stimulates thick ascending limb eNOS expression by raising medullary osmolality and increasing release of endothelin-1. Am J Physiol *288*, F58-64.

Hickey, K.A., Rubanyi, G., Paul, R.J., and Highsmith, R.F. (1985). Characterization of a coronary vasoconstrictor produced by cultured endothelial cells. Am J Physiol *248*, C550-556.

Hoffman, A., Abassi, Z.A., Brodsky, S., Ramadan, R., and Winaver, J. (2000). Mechanisms of big endothelin-1-induced diuresis and natriuresis : role of ET(B) receptors. Hypertension *35*, 732-739.

Hoffman, A., Grossman, E., Goldstein, D.S., Gill, J.R., Jr., and Keiser, H.R. (1994). Urinary excretion rate of endothelin-1 in patients with essential hypertension and salt sensitivity. Kidney International *45*, 556-560.

Horisberger, J.D., and Rossier, B.C. (1992). Aldosterone regulation of gene transcription leading to control of ion transport. Hypertension *19*, 221-227.

Hsieh, T.J., Lin, S.R., Lee, Y.J., Shin, S.J., Lai, Y.H., Hsu, C.H., and Tsai, J.H. (2000). Increased renal medullary endothelin-1 synthesis in prehypertensive DOCA- and salt-treated rats. Am J Physiol *279*, F112-121.

Hughes, A.K., Cline, R.C., and Kohan, D.E. (1992). Alterations in renal endothelin-1 production in the spontaneously hypertensive rat. Hypertension *20*, 666-673.

Hultman, M.L., Krasnoperova, N.V., Li, S., Du, S., Xia, C., Dietz, J.D., Lala, D.S., Welsch, D.J., and Hu, X. (2005). The ligand-dependent interaction of mineralocorticoid receptor with coactivator and corepressor peptides suggests multiple activation mechanisms. Mol Endocrinol *19*, 1460-1473.

Huppi, K., Martin, S.E., and Caplen, N.J. (2005). Defining and assaying RNAi in mammalian cells. Mol Cell *17*, 1-10.

Husted, R.F., Laplace, J.R., and Stokes, J.B. (1990). Enhancement of electrogenic Na+ transport across rat inner medullary collecting duct by glucocorticoid and by mineralocorticoid hormones. J Clin Invest *86*, 498-506.

Inoue, A., Yanagisawa, M., Takuwa, Y., Mitsui, Y., Kobayashi, M., and Masaki, T. (1989). The human preproendothelin-1 gene. Complete nucleotide sequence and regulation of expression. J Biol Chem *264*, 14954-14959.

Inscho, E., Imig, J., Cook, A., and Pollock, D. (2005). ETA and ETB receptors differentially modulate afferent and efferent arteriolar responses to endothelin. Br J Pharmacol *146*, 1019-1026.

Itani, O.A., Liu, K.Z., Cornish, K.L., Campbell, J.R., and Thomas, C.P. (2002). Glucocorticoids stimulate human sgk1 gene expression by activation of a GRE in its 5'-flanking region. Am J Physiol Endocrinol Metab *283*, E971-979.

Ito, S. (1995). Nitric oxide in the kidney. Curr Opin Nephrol Hypertens *4*, 23-30.

Iwai, N., Baba, S., Mannami, T., Ogihara, T., and Ogata, J. (2002). Association of a sodium channel alpha subunit promoter variant with blood pressure. J Am Soc Nephrol *13*, 80-85.

Izzo, J.L., Sica, D.A., Black, H.R., and Council for High Blood Pressure Research (American Heart Association) (2008). Hypertension primer, 4th edn (Philadelphia, PA, Lippincott Williams & Wilkins).

Jacobson, L.O., Goldwasser, E., Fried, W., and Plzak, L.F. (1957). Studies on erythropoiesis. VII. The role of the kidney in the production of erythropoietin. Trans Assoc Am Physicians *70*, 305-317.

Jarad, G., and Miner, J.H. (2009). Update on the glomerular filtration barrier. Curr Opin Nephrol Hypertens *18*, 226-232.

Just, A., Olson, A.J., and Arendshorst, W.J. (2004). Dual constrictor and dilator actions of ET(B) receptors in the rat renal microcirculation: interactions with ET(A) receptors. Am J Physiol *286*, F660-668.

Kalinyak, J.E., Dorin, R.I., Hoffman, A.R., and Perlman, A.J. (1987). Tissue-specific regulation of glucocorticoid receptor mRNA by dexamethasone. J Biol Chem *262*, 10441-10444.

Kao, Y.S., and Fong, J.C. (2008). Endothelin-1 induces glut1 transcription through enhanced interaction between Sp1 and NF-kappaB transcription factors. Cell Signal *20*, 771-778.

Kearney, P.M., Whelton, M., Reynolds, K., Muntner, P., Whelton, P.K., and He, J. (2005). Global burden of hypertension: analysis of worldwide data. Lancet *365*, 217-223.

Khanna, A., Simoni, J., and Wesson, D.E. (2005). Endothelin-induced increased aldosterone activity mediates augmented distal nephron acidification as a result of dietary protein. J Am Soc Nephrol *16*, 1929-1935.

Kitagawa, H., Yanagisawa, J., Fuse, H., Ogawa, S., Yogiashi, Y., Okuno, A., Nagasawa, H., Nakajima, T., Matsumoto, T., and Kato, S. (2002). Ligand-selective potentiation of rat mineralocorticoid receptor activation function 1 by a CBP-containing histone acetyltransferase complex. Mol Cell Biol *22*, 3698-3706.

Kitamura, K., Tanaka, T., Kato, J., Eto, T., and Tanaka, K. (1989). Regional distribution of immunoreactive endothelin in porcine tissue: abundance in inner medulla of kidney. Biochem Biophys Res Commun *161*, 348-352.

Kitamura, K., Yukawa, T., Morita, S., Ichiki, Y., Eto, T., and Tanaka, K. (1990). Distribution and molecular form of immunoreactive big endothelin-1 in porcine tissue. Biochem Biophys Res Commun *170*, 497-503.

Kizer, N.L., Lewis, B., and Stanton, B.A. (1995). Electrogenic sodium absorption and chloride secretion by an inner medullary collecting duct cell line (mIMCD-K2). Am J Physiol *268*, F347-355.

Klinger, F., Grimm, R., Steinbach, A., Tanneberger, M., Kunert-Keil, C., Rettig, R., and Grisk, O. (2008). Low NaCl intake elevates renal medullary endothelin-1 and endothelin A (ETA) receptor mRNA but not the sensitivity of renal Na+ excretion to ETA receptor blockade in rats. Acta Physiol (Oxf) *192*, 429-442.

Koeppen, B.M., Biagi, B.A., and Giebisch, G.H. (1983). Intracellular microelectrode characterization of the rabbit cortical collecting duct. Am J Physiol *244*, F35-47.

Kohan, D.E. (1991). Endothelin synthesis by rabbit renal tubule cells. Am J Physiol *261*, F221-226.

Kohan, D.E. (1993). Autocrine role of endothelin in rat inner medullary collecting duct: inhibition of AVP-induced cAMP accumulation. J Cardiovasc Pharmacol *22 Suppl 8*, S174-179.

Kohan, D.E. (2006). The renal medullary endothelin system in control of sodium and water excretion and systemic blood pressure. Curr Opin Nephrol Hypertens *15*, 34-40.

Kohan, D.E. (2009). Biology of endothelin receptors in the collecting duct. Kidney international *76*, 481-486.

Kohan, D.E., and Fiedorek, F.T., Jr. (1991). Endothelin synthesis by rat inner medullary collecting duct cells. J Am Soc Nephrol *2*, 150-155.

Kohan, D.E., and Padilla, E. (1993). Osmolar regulation of endothelin-1 production by rat inner medullary collecting duct. J Clin Invest *91*, 1235-1240.

Kolla, V., Robertson, N.M., and Litwack, G. (1999). Identification of a mineralocorticoid/glucocorticoid response element in the human Na/K ATPase alpha1 gene promoter. Biochem Biophys Res Commun *266*, 5-14.

Kotelevtsev, Y., and Webb, D.J. (2001). Endothelin as a natriuretic hormone: the case for a paracrine action mediated by nitric oxide. Cardiovasc Res *51*, 481-488.

Kurihara, Y., Kurihara, H., Suzuki, H., Kodama, T., Maemura, K., Nagai, R., Oda, H., Kuwaki, T., Cao, W.H., Kamada, N., *et al.* (1994). Elevated blood pressure and craniofacial abnormalities in mice deficient in endothelin-1. Nature *368*, 703-710.

Landgraf, R.G., and Jancar, S. (2008). Endothelin A receptor antagonist modulates lymphocyte and eosinophil infiltration, hyperreactivity and mucus in murine asthma. Int Immunopharmacol *8*, 1748-1753.

Lang, F., Capasso, G., Schwab, M., and Waldegger, S. (2005). Renal tubular transport and the genetic basis of hypertensive disease. Clin Exp Nephrol *9*, 91-99.

Lee, M.E., Dhadly, M.S., Temizer, D.H., Clifford, J.A., Yoshizumi, M., and Quertermous, T. (1991a). Regulation of endothelin-1 gene expression by Fos and Jun. J Biol Chem *266*, 19034-19039.

Lee, M.E., Temizer, D.H., Clifford, J.A., and Quertermous, T. (1991b). Cloning of the GATA-binding protein that regulates endothelin-1 gene expression in endothelial cells. J Biol Chem *266*, 16188-16192.

Lehrke, I., Waldherr, R., Ritz, E., and Wagner, J. (2001). Renal endothelin-1 and endothelin receptor type B expression in glomerular diseases with proteinuria. J Am Soc Nephrol *12*, 2321-2329.

Lemke, C., and Muller, A. (1989). [Erythropoietin--a review]. Folia Haematol Int Mag Klin Morphol Blutforsch *116*, 715-721.

Li, Y., Suino, K., Daugherty, J., and Xu, H.E. (2005). Structural and biochemical mechanisms for the specificity of hormone binding and coactivator assembly by mineralocorticoid receptor. Mol Cell *19*, 367-380.

Liang, G., Lin, J.C., Wei, V., Yoo, C., Cheng, J.C., Nguyen, C.T., Weisenberger, D.J., Egger, G., Takai, D., Gonzales, F.A., *et al.* (2004). Distinct localization of histone H3 acetylation and H3-K4 methylation to the transcription start sites in the human genome. Proc Natl Acad Sci USA *101*, 7357-7362.

Liu, W., Wang, J., Sauter, N.K., and Pearce, D. (1995). Steroid receptor heterodimerization demonstrated in vitro and in vivo. Proc Natl Acad Sci USA *92*, 12480-12484.

Livak, K.J., and Schmittgen, T.D. (2001). Analysis of relative gene expression data using real-time quantitative PCR and the 2(-Delta Delta C(T)) Method. Methods *25*, 402-408.

Loffing, J., Pietri, L., Aregger, F., Bloch-Faure, M., Ziegler, U., Meneton, P., Rossier, B.C., and Kaissling, B. (2000). Differential subcellular localization of ENaC subunits in mouse kidney in response to high- and low-Na diets. Am J Physiol *279*, F252-258.

Lombes, M., Kenouch, S., Souque, A., Farman, N., and Rafestin-Oblin, M.E. (1994). The mineralocorticoid receptor discriminates aldosterone from glucocorticoids independently of the 11 beta-hydroxysteroid dehydrogenase. Endocrinology *135*, 834-840.

Luetscher, J.A., Boyers, D.G., Cuthbertson, J.G., and McMahon, D.F. (1973). A model of the human circulation. Regulation by autonomic nervous system and renin-angiotensin system, and influence of blood volume on cardiac output and blood pressure. Circ Res *32*, Suppl 1:84-98.

Luisi, B.F., Xu, W.X., Otwinowski, Z., Freedman, L.P., Yamamoto, K.R., and Sigler, P.B. (1991). Crystallographic analysis of the interaction of the glucocorticoid receptor with DNA. Nature *352*, 497-505.

Luisi, B.F., Xu, W.X., Otwinowski, Z., Freedman, L.P., Yamamoto, K.R., and Sigler, P.B. (2003). Crystallographic analysis of the interaction of the glucocorticoid receptor with DNA (Research Collaboratory for Structural Bioinformatics Protein Data Bank, www.pdb.org).

Madsen, K.M., Verlander, J.W., and Tisher, C.C. (1988). Relationship between structure and function in distal tubule and collecting duct. J Electron Microsc Tech *9*, 187-208.

Manning, J., Beutler, K., Knepper, M.A., and Vehaskari, V.M. (2002). Upregulation of renal BSC1 and TSC in prenatally programmed hypertension. Am J Physiol *283*, F202-206.

Marsenic, O. (2009). Glucose control by the kidney: an emerging target in diabetes. Am J Kidney Dis *53*, 875-883.

Martinez-Aguayo, A., and Fardella, C. (2009). Genetics of hypertensive syndrome. Horm Res *71*, 253-259.

Martinez-Rumayor, A., Richards, A.M., Burnett, J.C., and Januzzi, J.L., Jr. (2008). Biology of the natriuretic peptides. Am J Cardiol *101*, 3-8.

Masilamani, S., Kim, G.H., Mitchell, C., Wade, J.B., and Knepper, M.A. (1999). Aldosterone-mediated regulation of ENaC alpha, beta, and gamma subunit proteins in rat kidney. J Clin Invest *104*, R19-23.

May, A., Puoti, A., Gaeggeler, H.P., Horisberger, J.D., and Rossier, B.C. (1997). Early effect of aldosterone on the rate of synthesis of the epithelial sodium channel alpha subunit in A6 renal cells. J Am Soc Nephrol *8*, 1813-1822.

McCormick, J.A., Bhalla, V., Pao, A.C., and Pearce, D. (2005). SGK1: a rapid aldosterone-induced regulator of renal sodium reabsorption. Physiology (Bethesda, Md) *20*, 134-139.

Mehta, P.K., and Griendling, K.K. (2007). Angiotensin II cell signaling: physiological and pathological effects in the cardiovascular system. Am J Physiol Cell Physiol *292*, C82-97.

Meijsing, S.H., Pufall, M.A., So, A.Y., Bates, D.L., Chen, L., and Yamamoto, K.R. (2009). DNA binding site sequence directs glucocorticoid receptor structure and activity. Science *324*, 407-410.

Meneton, P., Loffing, J., and Warnock, D.G. (2004). Sodium and potassium handling by the aldosterone-sensitive distal nephron: the pivotal role of the distal and connecting tubule. Am J Physiol *287*, F593-601.

Michigami, T. (2007). Vitamin D metabolism and action. Clin Calcium *17*, 1493-1498.

Mick, V.E., Itani, O.A., Loftus, R.W., Husted, R.F., Schmidt, T.J., and Thomas, C.P. (2001). The alpha-subunit of the epithelial sodium channel is an aldosterone-induced transcript in mammalian collecting ducts, and this transcriptional response is mediated via distinct cis-elements in the 5'-flanking region of the gene. Mol Endocrinol *15*, 575-588.

Modesti, P.A., Cecioni, I., Migliorini, A., Naldoni, A., Costoli, A., Vanni, S., and Serneri, G.G. (1998). Increased renal endothelin formation is associated with sodium retention and increased free water clearance. Am J Physiol *275*, H1070-1077.

Molenaar, P., O'Reilly, G., Sharkey, A., Kuc, R.E., Harding, D.P., Plumpton, C., Gresham, G.A., and Davenport, A.P. (1993). Characterization and localization of endothelin receptor subtypes in the human atrioventricular conducting system and myocardium. Circ Res *72*, 526-538.

Muller, O.G., Parnova, R.G., Centeno, G., Rossier, B.C., Firsov, D., and Horisberger, J.D. (2003). Mineralocorticoid effects in the kidney: correlation between alphaENaC, GILZ, and Sgk-1 mRNA expression and urinary excretion of Na+ and K+. J Am Soc Nephrol *14*, 1107-1115.

Nambi, P., Pullen, M., Wu, H.L., Nuthulaganti, P., Elshourbagy, N., and Kumar, C. (1992). Dexamethasone down-regulates the expression of endothelin receptors in vascular smooth muscle cells. J Biol Chem *267*, 19555-19559.

Nguyen Dinh Cat, A., Ouvrard-Pascaud, A., Tronche, F., Clemessy, M., Gonzalez-Nunez, D., Farman, N., and Jaisser, F. (2009). Conditional transgenic mice for studying the role of the glucocorticoid receptor in the renal collecting duct. Endocrinol *150*, 2202-2210.

Nielsen, S., Frokiaer, J., Marples, D., Kwon, T.H., Agre, P., and Knepper, M.A. (2002). Aquaporins in the kidney: from molecules to medicine. Physiol Rev *82*, 205-244.

Nishi, M., Tanaka, M., Matsuda, K., Sunaguchi, M., and Kawata, M. (2004). Visualization of glucocorticoid receptor and mineralocorticoid receptor interactions in living cells with GFP-based fluorescence resonance energy transfer. J Neurosci *24*, 4918-4927.

Odermatt, A., and Atanasov, A.G. (2009). Mineralocorticoid receptors: Emerging complexity and functional diversity. Steroids *74*, 163-171.

Ohkita, M., Wang, Y., Nguyen, N.D., Tsai, Y.H., Williams, S.C., Wiseman, R.C., Killen, P.D., Li, S., Yanagisawa, M., and Gariepy, C.E. (2005). Extrarenal ETB plays a significant role in controlling cardiovascular responses to high dietary sodium in rats. Hypertension *45*, 940-946.

Oparil, S., Ehrlich, E.N., and Lindheimer, M.D. (1975). Effect of progesterone on renal sodium handling in man: relation to aldosterone excretion and plasma renin activity. Clin Sci Mol Med *49*, 139-147.

Ou, X.M., Storring, J.M., Kushwaha, N., and Albert, P.R. (2001). Heterodimerization of mineralocorticoid and glucocorticoid receptors at a novel negative response element of the 5-HT1A receptor gene. J Biol Chem *276*, 14299-14307.

Pascual-Le Tallec, L., and Lombès, M. (2005). The mineralocorticoid receptor: a journey exploring its diversity and specificity of action. Mol Endocrinol *19*, 2211-2221.

Pascual-Le Tallec, L., Simone, F., Viengchareun, S., Meduri, G., Thirman, M.J., and Lombès, M. (2005). The elongation factor ELL (eleven-nineteen lysine-rich leukemia) is a selective coregulator for steroid receptor functions. Mol Endocrinol *19*, 1158-1169.

Pedersen, L.G., Offenberg, H., Moesgaard, S.G., Thomsen, P.D., Pedersen, H.D., and Olsen, L.H. (2007). Transcription levels of endothelin-1 and endothelin receptors are associated with age and leaflet location in porcine mitral valves. J Vet Med A Physiol Pathol Clin Med *54*, 113-118.

Pollock, D.M., Allcock, G.H., Krishnan, A., Dayton, B.D., and Pollock, J.S. (2000). Upregulation of endothelin B receptors in kidneys of DOCA-salt hypertensive rats. Am J Physiol *278*, F279-286.

Pollock, J.S., and Pollock, D.M. (2008). Endothelin and NOS1/nitric oxide signaling and regulation of sodium homeostasis. Curr Opin Nephrol Hypertens *17*, 70-75.

Popowski, K., Sperker, B., Kroemer, H.K., John, U., Laule, M., Stangl, K., and Cascorbi, I. (2003). Functional significance of a hereditary adenine insertion variant in the 5'-UTR of the endothelin-1 gene. Pharmacogenetics *13*, 445-451.

Portik-Dobos, V., Harris, A.K., Song, W., Hutchinson, J., Johnson, M.H., Imig, J.D., Pollock, D.M., and Ergul, A. (2006). Endothelin antagonism prevents early EGFR transactivation but not increased matrix metalloproteinase activity in diabetes. Am J Physiol Regul Integr Comp Physiol *290*, R435-441.

Pravenec, M., and Petretto, E. (2008). Insight into the genetics of hypertension, a core component of the metabolic syndrome. Curr Opin Clin Nutr Metab Care *11*, 393-397.

Preuss, H.G. (1993). Basics of renal anatomy and physiology. Clin Lab Med *13*, 1-11.

Provencher, P.H., Saltis, J., and Funder, J.W. (1995). Glucocorticoids but not mineralocorticoids modulate endothelin-1 and angiotensin II binding in SHR vascular smooth muscle cells. J Steroid Biochem Mol Biol *52*, 219-225.

Pupilli, C., Brunori, M., Misciglia, N., Selli, C., Ianni, L., Yanagisawa, M., Mannelli, M., and Serio, M. (1994). Presence and distribution of endothelin-1 gene expression in human kidney. Am J Physiol *267*, F679-687.

Qiu, C., Samsell, L., and Baylis, C. (1995). Actions of endogenous endothelin on glomerular hemodynamics in the rat. Am J Physiol *269*, R469-473.

Rashid, S., and Lewis, G.F. (2005). The mechanisms of differential glucocorticoid and mineralocorticoid action in the brain and peripheral tissues. Clin Biochem *38*, 401-409.

Rebuffat, A.G., Tam, S., Nawrocki, A.R., Baker, M.E., Frey, B.M., Frey, F.J., and Odermatt, A. (2004). The 11-ketosteroid 11-ketodexamethasone is a glucocorticoid receptor agonist. Mol Cell Endocrinol *214*, 27-37.

Riepe, F.G. (2009). Clinical and molecular features of type 1 pseudohypoaldosteronism. Horm Res *72*, 1-9.

Rogerson, F.M., and Fuller, P.J. (2000). Mineralocorticoid action. Steroids *65*, 61-73.

Rogerson, F.M., and Fuller, P.J. (2003). Interdomain interactions in the mineralocorticoid receptor. Mol Cell Endocrinol *200*, 45-55.

Rogerson, F.M., Yao, Y.Z., Smith, B.J., Dimopoulos, N., and Fuller, P.J. (2003). Determinants of spironolactone binding specificity in the mineralocorticoid receptor. J Mol Endocrinol *31*, 573-582.

Romero, D.G., Plonczynski, M.W., Welsh, B.L., Gomez-Sanchez, C.E., Zhou, M.Y., and Gomez-Sanchez, E.P. (2007). Gene expression profile in rat adrenal zona glomerulosa cells stimulated with aldosterone secretagogues. Physiol Genomics *32*, 117-127.

Ross, M.E., Evinger, M.J., Hyman, S.E., Carroll, J.M., Mucke, L., Comb, M., Reis, D.J., Joh, T.H., and Goodman, H.M. (1990). Identification of a functional glucocorticoid response element in the phenylethanolamine N-methyltransferase promoter using fusion genes introduced into chromaffin cells in primary culture. J Neurosci *10*, 520-530.

Rossier, B.C. (1978). Role of RNA in the action of aldosterone on Na+ transport. J Membr Biol *40 Spec No*, 187-197.

Russell, F.D., Coppell, A.L., and Davenport, A.P. (1998). In vitro enzymatic processing of radiolabelled big ET-1 in human kidney. Biochem Pharmacol *55*, 697-701.

Saita, Y., Koizumi, T., Yazawa, H., Morita, T., Takenaka, T., and Honda, K. (1997). Endothelin receptors and their cellular signal transduction mechanism in human cultured prostatic smooth muscle cells. Br J Pharmacol *121*, 687-694.

Sakurai, T., Yanagisawa, M., Inoue, A., Ryan, U.S., Kimura, S., Mitsui, Y., Goto, K., and Masaki, T. (1991). cDNA cloning, sequence analysis and tissue distribution of rat preproendothelin-1 mRNA. Biochem Biophys Res Commun *175*, 44-47.

Salvetti, A., and Ghiadoni, L. (2006). Thiazide diuretics in the treatment of hypertension: an update. J Am Soc Nephrol *17*, S25-29.

Sands, J.M., and Layton, H.E. (2009). The physiology of urinary concentration: an update. Semin Nephrol *29*, 178-195.

Sansom, S.C., Weinman, E.J., and O'Neil, R.G. (1984). Microelectrode assessment of chloride-conductive properties of cortical collecting duct. Am J Physiol *247*, F291-302.

Savory, J.G., Préfontaine, G.G., Lamprecht, C., Liao, M., Walther, R.F., Lefebvre, Y.A., and Haché, R.J. (2001). Glucocorticoid receptor homodimers and glucocorticoid-mineralocorticoid receptor heterodimers form in the cytoplasm through alternative dimerization interfaces. Mol Cell Biol *21*, 781-793.

Sayegh, R., Auerbach, S.D., Li, X., Loftus, R.W., Husted, R.F., Stokes, J.B., and Thomas, C.P. (1999). Glucocorticoid induction of epithelial sodium channel expression in lung and renal epithelia occurs via trans-activation of a hormone response element in the 5'-flanking region of the human epithelial sodium channel alpha subunit gene. J Biol Chem *274*, 12431-12437.

Schnermann, J. (1998). Juxtaglomerular cell complex in the regulation of renal salt excretion. Am J Physiol *274*, R263-279.

Schug, J. (2003). Using TESS to Predict Transcription Factor Binding Sites in DNA Sequence. In Current Protocols in Bioinformatics, A.D. Baxevanis, ed.

Schulz, E., Ruschitzka, F., Lueders, S., Heydenbluth, R., Schrader, J., and Muller, G.A. (1995). Effects of endothelin on hemodynamics, prostaglandins, blood coagulation and renal function. Kidney international *47*, 795-801.

Serneri, G.G., Modesti, P.A., Cecioni, I., Biagini, D., Migliorini, A., Costoli, A., Colella, A., Naldoni, A., and Paoletti, P. (1995). Plasma endothelin and renal endothelin are two distinct systems involved in volume homeostasis. Am J Physiol *268*, H1829-1837.

Shankar, S.S., and Brater, D.C. (2003). Loop diuretics: from the Na-K-2Cl transporter to clinical use. Am J Physiol *284*, F11-21.

Shen, J.P., and Cotton, C.U. (2003). Epidermal growth factor inhibits amiloride-sensitive sodium absorption in renal collecting duct cells. Am J Physiol *284*, F57-64.

Shigaev, A., Asher, C., Latter, H., Garty, H., and Reuveny, E. (2000). Regulation of sgk by aldosterone and its effects on the epithelial Na(+) channel. Am J Physiol *278*, F613-619.

Simpson SA, T.J., Wettstein A, Neher R, von Euw J, Reichstein T (1953). Isolierung eines neuen kristallisierten Hormons aus Neben nieren mit besonders hoher Wiksamkeit auf den Mineral-stoffwechsel. Experientia, 333-335.

Sledz, C.A., Holko, M., de Veer, M.J., Silverman, R.H., and Williams, B.R. (2003). Activation of the interferon system by short-interfering RNAs. Nat Cell Biol *5*, 834-839.

Snove, O., Jr., and Holen, T. (2004). Many commonly used siRNAs risk off-target activity. Biochem Biophys Res Commun *319*, 256-263.

Soundararajan, R., Zhang, T.T., Wang, J., Vandewalle, A., and Pearce, D. (2005). A novel role for glucocorticoid-induced leucine zipper protein in epithelial sodium channel-mediated sodium transport. J Biol Chem *280*, 39970-39981.

Spat, A., and Hunyady, L. (2004). Control of aldosterone secretion: a model for convergence in cellular signaling pathways. Physiol Rev *84*, 489-539.

Spindler, B., Mastroberardino, L., Custer, M., and Verrey, F. (1997). Characterization of early aldosterone-induced RNAs identified in A6 kidney epithelia. Pflugers Arch *434*, 323-331.

Starling, E.H. (1899). The glomerular functions of the kidney. J Physiol *24*, 317-330.

Stokes, J.B. (1981). Potassium secretion by cortical collecting tubule: relation to sodium absorption, luminal sodium concentration, and transepithelial voltage. Am J Physiol *241*, F395-402.

Stow, L.R., Gumz, M.L., Lynch, I.J., Greenlee, M.M., Rudin, A., Cain, B.D., and Wingo, C.S. (2009). Aldosterone modulates steroid receptor binding to the endothelin-1 gene (Edn1). J Biol Chem.

Strait, K.A., Stricklett, P.K., Kohan, J.L., Miller, M.B., and Kohan, D.E. (2007). Calcium regulation of endothelin-1 synthesis in rat inner medullary collecting duct. Am J Physiol *293*, F601-606.

Stricklett, P.K., Hughes, A., and Kohan, D.E. (2006). Endothelin-1 stimulates NO production and inhibits cAMP accumulation in rat inner medullary collecting duct through independent pathways. Am J Physiol *290*, F1315-1319.

Stricklett, P.K., Nelson, R.D., and Kohan, D.E. (1999). The Cre/loxP system and gene targeting in the kidney. Am J Physiol *276*, F651-657.

Struhl, K. (1999). Fundamentally different logic of gene regulation in eukaryotes and prokaryotes. Cell *98*, 1-4.

Sutcliffe, A.M., Clarke, D.L., Bradbury, D.A., Corbett, L.M., Patel, J.A., and Knox, A.J. (2009). Transcriptional regulation of monocyte chemotactic protein-1 release by endothelin-1 in human airway smooth muscle cells involves NF-kappaB and AP-1. Br J Pharmacol *157*, 436-450.

Thompson, E.B. (1987). The structure of the human glucocorticoid receptor and its gene. J Steroid Biochem *27*, 105-108.

Thomson, S.C., and Blantz, R.C. (2008). Glomerulotubular balance, tubuloglomerular feedback, and salt homeostasis. J Am Soc Nephrol *19*, 2272-2275.

Todd-Turla, K.M., Schnermann, J., Fejes-Tóth, G., Naray-Fejes-Tóth, A., Smart, A., Killen, P.D., and Briggs, J.P. (1993). Distribution of mineralocorticoid and glucocorticoid receptor mRNA along the nephron. Am J Physiol *264*, F781-791.

Tomita, K., Nonoguchi, H., Terada, Y., and Marumo, F. (1993). Effects of ET-1 on water and chloride transport in cortical collecting ducts of the rat. Am J Physiol *264*, F690-696.

Tostes, R.C., David, F.L., Carvalho, M.H., Nigro, D., Scivoletto, R., and Fortes, Z.B. (2000). Gender differences in vascular reactivity to endothelin-1 in deoxycorticosterone-salt hypertensive rats. J Cardiovasc Pharmacol *36*, S99-101.

Trapp, T., and Holsboer, F. (1996). Heterodimerization between mineralocorticoid and glucocorticoid receptors increases the functional diversity of corticosteroid action. Trends Pharmacol Sci *17*, 145-149.

Treiber, F.A., Barbeau, P., Harshfield, G., Kang, H.S., Pollock, D.M., Pollock, J.S., and Snieder, H. (2003). Endothelin-1 gene Lys198Asn polymorphism and blood pressure reactivity. Hypertension *42*, 494-499.

Truss, M., Candau, R., Chavez, S., and Beato, M. (1995). Transcriptional control by steroid hormones: the role of chromatin. Ciba Found Symp *191*, 7-17; discussion 17-23.

Tsai, Y.H., Ohkita, M., and Gariepy, C.E. (2006). Chronic high-sodium diet increases aortic wall endothelin-1 expression in a blood pressure-independent fashion in rats. Exp Biol Med (Maywood) *231*, 813-817.

Turner, J.D., Schote, A.B., Macedo, J.A., Pelascini, L.P., and Muller, C.P. (2006). Tissue specific glucocorticoid receptor expression, a role for alternative first exon usage? Biochem Pharmacol *72*, 1529-1537.

Ulick, S., Levine, L.S., Gunczler, P., Zanconato, G., Ramirez, L.C., Rauh, W., Rosler, A., Bradlow, H.L., and New, M.I. (1979). A syndrome of apparent mineralocorticoid excess associated with defects in the peripheral metabolism of cortisol. J Clin Endocrinol Metab *49*, 757-764.

Unwin, R.J., and Capasso, G. (2006). Bartter's and Gitelman's syndromes: their relationship to the actions of loop and thiazide diuretics. Curr Opin Pharmacol *6*, 208-213.

Vallender, T.W., and Lahn, B.T. (2006). Localized methylation in the key regulator gene endothelin-1 is associated with cell type-specific transcriptional silencing. FEBS Lett *580*, 4560-4566.

Vallon, V. (2003). Tubuloglomerular feedback and the control of glomerular filtration rate. News Physiol Sci *18*, 169-174.

Vallon, V., and Lang, F. (2005). New insights into the role of serum- and glucocorticoid-inducible kinase SGK1 in the regulation of renal function and blood pressure. Curr Opin Nephrol Hypertens *14*, 59-66.

van der Laan, S., Sarabdjitsingh, R.A., Van Batenburg, M.F., Lachize, S.B., Li, H., Dijkmans, T.F., Vreugdenhil, E., de Kloet, E.R., and Meijer, O.C. (2008). Chromatin immunoprecipitation scanning identifies glucocorticoid receptor binding regions in the proximal promoter of a ubiquitously expressed glucocorticoid target gene in brain. J Neurochem *106*, 2515-2523.

Vassileva, I., Mountain, C., and Pollock, D.M. (2003). Functional role of ETB receptors in the renal medulla. Hypertension *41*, 1359-1363.

Viengchareun, S., Le Menuet, D., Martinerie, L., Munier, M., Pascual-Le Tallec, L., and Lombès, M. (2007). The mineralocorticoid receptor: insights into its molecular and (patho)physiological biology. Nucl Recept Signal *5*, e012.

Vogel, V., Backer, A., Heller, J., and Kramer, H.J. (1999). The renal endothelin system in the Prague hypertensive rat, a new model of spontaneous hypertension. Clin Sci (Lond) *97*, 91-98.

von Bohlen und Halbach, O., and Albrecht, D. (2006). The CNS renin-angiotensin system. Cell Tissue Res *326*, 599-616.

Walker, W.J., Elkins, J.T., Jr., and Wood, L.W. (1964). Effect of Potassium in Restoring Myocardial Response to a Subthreshold Cardiac Pacemaker. N Engl J Med *271*, 597-601.

Walshe, T.E., Ferguson, G., Connell, P., O'Brien, C., and Cahill, P.A. (2005). Pulsatile flow increases the expression of eNOS, ET-1, and prostacyclin in a novel in vitro coculture model of the retinal vasculature. Invest Ophthalmol Vis Sci *46*, 375-382.

Wang, W.H. (2006). Regulation of ROMK (Kir1.1) channels: new mechanisms and aspects. Am J Physiol *290*, F14-19.

Whorwood, C.B., Ricketts, M.L., and Stewart, P.M. (1994). Regulation of sodium-potassium adenosine triphosphate subunit gene expression by corticosteroids and 11 beta-hydroxysteroid dehydrogenase activity. Endocrinology *135*, 901-910.

Williams, L.R., and Leggett, R.W. (1989). Reference values for resting blood flow to organs of man. Clin Phys Physiol Meas *10*, 187-217.

Wingo, C.S. (1989a). Potassium secretion by the cortical collecting tubule: effect of C1 gradients and ouabain. Am J Physiol *256*, F306-313.

Wingo, C.S. (1989b). Reversible chloride-dependent potassium flux across the rabbit cortical collecting tubule. Am J Physiol *256*, F697-704.

Wolf, S.C., Schultze, M., Risler, T., Rieg, T., Lang, F., Schulze-Osthoff, K., and Brehm, B.R. (2006). Stimulation of serum- and glucocorticoid-regulated kinase-1 gene expression by endothelin-1. Biochem Pharmacol *71*, 1175-1183.

Wong, S., Brennan, F.E., Young, M.J., Fuller, P.J., and Cole, T.J. (2007). A direct effect of aldosterone on endothelin-1 gene expression in vivo. Endocrinology *148*, 1511-1517.

Wood, K.V., de Wet, J.R., Dewji, N., and DeLuca, M. (1984). Synthesis of active firefly luciferase by in vitro translation of RNA obtained from adult lanterns. Biochem Biophys Res Commun *124*, 592-596.

Woods, M., Mitchell, J.A., Wood, E.G., Barker, S., Walcot, N.R., Rees, G.M., and Warner, T.D. (1999). Endothelin-1 is induced by cytokines in human vascular smooth muscle cells: evidence for intracellular endothelin-converting enzyme. Mol Pharmacol *55*, 902-909.

Yamashita, K., Discher, D.J., Hu, J., Bishopric, N.H., and Webster, K.A. (2001). Molecular regulation of the endothelin-1 gene by hypoxia. Contributions of hypoxia-inducible factor-1, activator protein-1, GATA-2, AND p300/CBP. J Biol Chem *276*, 12645-12653.

Ye, Q., Chen, S., and Gardner, D.G. (2003). Endothelin Inhibits NPR-A and Stimulates eNOS Gene Expression in Rat IMCD Cells. Hypertension *41*, 675-681.

Yorikane, R., Sakai, S., Miyauchi, T., Sakurai, T., Sugishita, Y., and Goto, K. (1993). Increased production of endothelin-1 in the hypertrophied rat heart due to pressure overload. FEBS Lett *332*, 31-34.

Zamore, P.D. (2001). RNA interference: listening to the sound of silence. Nat Struct Biol *8*, 746-750.

Zeidel, M.L. (1993). Hormonal regulation of inner medullary collecting duct sodium transport. Am J Physiol *265*, F159-173.

Zeidel, M.L., Brady, H.R., Kone, B.C., Gullans, S.R., and Brenner, B.M. (1989). Endothelin, a peptide inhibitor of Na(+)-K(+)-ATPase in intact renaltubular epithelial cells. Am J Physiol *257*, C1101-1107.

Zhang, D., Li, S., Cruz, P., and Kone, B.C. (2009). Sirtuin 1 Functionally and Physically Interacts with Disruptor of Telomeric Silencing-1 to Regulate {alpha}-ENaC Transcription in Collecting Duct. J Biol Chem *284*, 20917-20926.

Zhang, W., Xia, X., Reisenauer, M.R., Hemenway, C.S., and Kone, B.C. (2006). Dot1a-AF9 complex mediates histone H3 Lys-79 hypermethylation and repression of ENaCalpha in an aldosterone-sensitive manner. J Biol Chem *281*, 18059-18068.

Zhang, X., Clark, A.F., and Yorio, T. (2003). Interactions of endothelin-1 with dexamethasone in primary cultured human trabecular meshwork cells. Invest Ophthalmol Vis Sci *44*, 5301-5308.

Zhou, X., Xia, S.L., and Wingo, C.S. (1998). Chloride transport by the rabbit cortical collecting duct: dependence on H,K-ATPase. J Am Soc Nephrol *9*, 2194-2202.

Zoccali, C., Leonardis, D., Parlongo, S., Mallamaci, F., and Postorino, M. (1995). Urinary and plasma endothelin 1 in essential hypertension and in hypertension secondary to renoparenchymal disease. Nephrol Dial Transplant *10*, 1320-1323.

BIOGRAPHICAL SKETCH

Lisa R. Stow was born in Pensacola, Florida in 1983. Lisa left high school in her junior year to attend Emory University for her first year of undergraduate education. During this year she began work on her first research project designing mathematical models of random particle movement under the supervision of Dr. George Hentschel in the Department of Physics. The following summer Lisa interned at the Naval Aerospace Medical Research Laboratory at Pensacola Naval Airstation where she helped to develop software for a tactile awareness system to prevent disorientation of pilots while flying at high speeds. Lisa finished her undergraduate career at the University of Florida. During this time she had the honor of being apart of Dr. Ben Dunn's research laboratory in the Department of Biochemistry and Molecular Biology. Lisa graduated with a Bachelor of Science in integrative biology from the University of Florida in 2004. After entering the Interdisciplinary Program in Biomedical Sciences at the University of Florida, Lisa joined Dr. Charles Wingo's laboratory where she conducted her dissertation work on the Regulation and Function of Aldosterone Induced Endothelin-1. In 2006 the University of Florida Medical Guild presented Lisa with an award for Research Excellence at the annual Department of Medicine Research Competition. The following year Lisa was honored to receive a travel award and an invited oral presentation as the 10^{th} International Meeting on Endothelin in Bergamo, Italy. In 2007 Lisa received a competitive American Heart Association Predoctoral Fellowship, which helped to fund the last two years of her dissertation project. Lisa is also the founder and President of the Collaboration of Scientists for Critical Research in Biomedicine (CSCRB, Inc). CSCRB, Inc is a not-for-profit organization with the mission to support targeted and collaborative research initiatives in areas of medicine that are in critical need of funding or greater scientific interest. Since January 2009 CSCRB has raised over $20,000 for triple negative breast cancer research.

After graduation, Lisa plans on pursuing a career in science. She also plans to continue her work with CSCRB and eventually start a seed grant program for triple negative research at the University of Florida. Her life long goals include completing a marathon and founding a collaborative research institute.